



University of Kentucky
UKnowledge

Theses and Dissertations--Mechanical
Engineering

Mechanical Engineering


2020

SAFETY CONCEPTS FOR EVERY RIDE: A STATISTICAL ENSEMBLE SIMULATION TO MITIGATE ROTATIONAL FALLS IN EVENTING CROSS COUNTRY

Shannon Wood

University of Kentucky, shannon.wood@uky.edu

Author ORCID Identifier:

 <https://orcid.org/0000-0003-1517-5543>

Digital Object Identifier: <https://doi.org/10.13023/etd.2020.173>

[Right click to open a feedback form in a new tab to let us know how this document benefits you.](#)

Recommended Citation

Wood, Shannon, "SAFETY CONCEPTS FOR EVERY RIDE: A STATISTICAL ENSEMBLE SIMULATION TO MITIGATE ROTATIONAL FALLS IN EVENTING CROSS COUNTRY" (2020). *Theses and Dissertations--Mechanical Engineering*. 153.

https://uknowledge.uky.edu/me_etds/153

This Master's Thesis is brought to you for free and open access by the Mechanical Engineering at UKnowledge. It has been accepted for inclusion in Theses and Dissertations--Mechanical Engineering by an authorized administrator of UKnowledge. For more information, please contact UKnowledge@lsv.uky.edu.

STUDENT AGREEMENT:

I represent that my thesis or dissertation and abstract are my original work. Proper attribution has been given to all outside sources. I understand that I am solely responsible for obtaining any needed copyright permissions. I have obtained needed written permission statement(s) from the owner(s) of each third-party copyrighted matter to be included in my work, allowing electronic distribution (if such use is not permitted by the fair use doctrine) which will be submitted to UKnowledge as Additional File.

I hereby grant to The University of Kentucky and its agents the irrevocable, non-exclusive, and royalty-free license to archive and make accessible my work in whole or in part in all forms of media, now or hereafter known. I agree that the document mentioned above may be made available immediately for worldwide access unless an embargo applies.

I retain all other ownership rights to the copyright of my work. I also retain the right to use in future works (such as articles or books) all or part of my work. I understand that I am free to register the copyright to my work.

REVIEW, APPROVAL AND ACCEPTANCE

The document mentioned above has been reviewed and accepted by the student's advisor, on behalf of the advisory committee, and by the Director of Graduate Studies (DGS), on behalf of the program; we verify that this is the final, approved version of the student's thesis including all changes required by the advisory committee. The undersigned agree to abide by the statements above.

Shannon Wood, Student

Dr. Suzanne Weaver Smith, Major Professor

Dr. Alexandre Martin, Director of Graduate Studies

SAFETY CONCEPTS FOR EVERY RIDE:
A STATISTICAL ENSEMBLE SIMULATION TO MITIGATE ROTATIONAL FALLS
IN EVENTING CROSS COUNTRY

THESIS

A thesis submitted in partial fulfillment of the
requirements for the degree of Master of Science in Mechanical Engineering
in the College of Engineering
at the University of Kentucky

By

Shannon Wood

Lexington, Kentucky

Director: Dr. Suzanne Weaver Smith Professor of Mechanical Engineering

Lexington, Kentucky

2020

Copyright © Shannon Wood 2020
<https://orcid.org/0000-0003-1517-5543>

ABSTRACT OF THESIS

SAFETY CONCEPTS FOR EVERY RIDE: A STATISTICAL ENSEMBLE SIMULATION TO MITIGATE ROTATIONAL FALLS IN EVENTING CROSS COUNTRY

Rotational falls are the leading cause of death and serious injury in the equestrian sport of eventing. Previous studies to develop safety devices used physical models representing one or at most several physical situations leading to different designs and no common understanding. In this thesis, a statistical ensemble model is developed and applied to generate and evaluate 10,000 different situations that might potentially lead to rotational falls. For accurate statistical representation of the horse and rider inertia distributions, measurements of over 400 training or competing horses and riders were recorded and incorporated. Video was recorded of 218 total competitors approaching 10 different jumps on cross country courses in competitions ranging from Preliminary to CCI5*, yielding jump configuration angles for different fence types. Combining information for these, among 26 total variables, a statistical ensemble simulation using impulse momentum physics identifies conditions for rotation and defines design criteria for future general and situation-specific jumps and safety devices. A Jump Safety Quality Index is also devised to represent the benefit of an activating fence design for mitigating rotational falls versus the detriment and competition penalties of false activation.

KEYWORDS: Rotational Falls, Statistical Ensemble, Eventing, Horse Inertia,
Cross-Country

Shannon Wood

December 12, 2019

SAFETY CONCEPTS FOR EVERY RIDE: A STATISTICAL ENSEMBLE
SIMULATION TO MITIGATE ROTATIONAL FALLS IN EVENTING CROSS
COUNTRY

By
Shannon Wood

Suzanne Weaver Smith, Ph. D.

Director of Thesis

Alexandre Martin, Ph. D.

Director of Graduate Studies

12/12/2019

Date

DEDICATION

Dedicated to the horses, riders and all those whose lives have been affected by rotational falls.

ACKNOWLEDGMENTS

Dr. Suzanne Weaver Smith has been an incredible leader and mentor throughout this study for myself and all the students working on this problem. From guidance and support through the end of my undergraduate studies throughout graduate school her experience, excellence and example has helped me grow in academic and innumerable other ways. Thank you to my fellow students who contributed: Gregorio Robles Vega, Lange Ledbetter, Sierra Lindeman, and Kylie Schmidt. Thank you to my committee Dr. Smith, Dr. Mick Peterson, and Dr. Martha Grady for your guidance and enthusiasm. Thank you to Dr. Hayley Mojica for the illustrations of the different types of rotational falls and for being one of my first eventer friends.

Thank you to those who have supported me throughout my education. My parents, Janet and Bruce Wood, my sister, Staci Wood, and my grandmother, Loretta Fieser.

The eventing community has been impressive in the support for the project and efforts. Thank you especially to Vanessa Coleman and Anthony Trollope for the support and wealth of knowledge about the sport and willingness to share it with me. Thank you to Dan Michaels, Derek Di Grazia, Mick Costello, Rob Burke, Jon Holling and the Safety Committee and many others in the USEA for your insight and encouragement. Thank you to all who submitted responses to the Safety Survey and allowed me to measure their horses. Thank you to Lauren Gash, Ellen Sadler, Lisa Everett, Ashley Kehoe and all those at Antebellum Farm for teaching me the sport of eventing. Thank you to the Kentucky Three-Day Event and Equestrian Events, Inc, Chattahoochee Hills, and The Event at Rebecca Farm and Sarah Broussard. Ashley Ede and Meriel Moore-Colyer

(Directors, Equine Management Program, Royal Agricultural University), and Jamie MacLeod VMD, PhD (Director of UKY Equine Initiatives).

Thank you to the United States Eventing Association (2017-2018), especially the private donors, and the UKY Department of Mechanical Engineering (2018-2020) for supporting this work.

TABLE OF CONTENTS

ACKNOWLEDGMENTS	iii
TABLE OF CONTENTS	v
LIST OF TABLES	viii
LIST OF FIGURES	ix
CHAPTER 1. Introduction and Motivation.....	1
CHAPTER 2. Background	5
2.1 <i>The Sport of Eventing</i>	5
2.2 <i>Governing Bodies</i>	5
2.3 <i>Level Changes and Equivalencies</i>	6
2.4 <i>Scoring</i>	7
2.4.1 Frangible Fence Penalty Evolution.....	9
2.4.2 Unnecessary Safety Fence False Activations.....	10
2.5 <i>Statistics for Falls, Injuries and Performance</i>	11
2.5.1 Epidemiology Risk Review Studies.....	11
2.5.2 By the Numbers: Frequency of Contact and Rotational Falls.....	13
2.6 <i>Frangible Fence Conception and Progress</i>	15
2.7 <i>Physical Representations of the Horse: Dummies and Inertia</i>	19
2.8 <i>On Course Testing, Frangible Device Testing and FEI Standard</i>	21
CHAPTER 3. Inertia and Survey	24
3.1 <i>Inertia and Center of Gravity</i>	24
3.2 <i>Standing Center of Gravity and Inertia</i>	24
3.2.1 Jumping Center of Gravity and Inertia	31
3.3 <i>Citizen Science Survey and Measurements</i>	33
3.3.1 Levels.....	40
3.3.2 Breeds	41
3.3.3 Horse Heights and Other Dimensions	44
3.3.4 Rider Size	45
3.3.5 Ensemble Parameters from Survey	46
CHAPTER 4. Video Studies	49
4.1 <i>Existing Cross Country Jumping Video and the Importance of Speed</i>	49
4.2 <i>Fence Video Study</i>	51
4.3 <i>Video Recording and Analysis Techniques</i>	52
4.3.1 Details of Fences in Video Study.....	54
4.3.2 Overall Speeds on Course	63
4.3.3 Jumping Speeds.....	65
4.3.4 Jumping Angles.....	72
4.3.5 Take-off Distances	77
4.3.6 Video Contacts	78

4.4	<i>BE Fence Contact Study</i>	81
CHAPTER 5. Rotational Fall Observations		86
5.1	<i>Rotational Fall Situation Categories</i>	86
5.1.1	Rotational Fall Category Identification	92
5.2	<i>Rotational Fall and Close Call Video Catalog</i>	93
5.2.1	Rotational Fall Videos	93
5.2.2	Close Call Videos.....	97
CHAPTER 6. Testing Concepts.....		99
6.1	<i>Physics and Ensemble Methods</i>	99
6.2	<i>Dummies, Pendulums, and Instrumented Sledgehammers</i>	100
CHAPTER 7. Statistical Ensemble Simulations		106
7.1	<i>Equations for Impulse-momentum Collisions and Overturning</i>	106
7.1.1	Collision Energy.....	111
7.2	<i>Map of Variables</i>	112
7.3	<i>Position and Size Variable Distributions for “One Size Fits All” Solutions</i> ..	114
7.4	<i>Contacting a Fixed Fence</i>	118
7.4.1	CG Position Based Fixed-Fence Results	118
7.4.2	Speed’s Relation to Rotation.....	120
7.4.3	Energy Dissipation in Fixed Fence Collisions	122
7.5	<i>Fixed Fence Impulse Ensemble</i>	124
7.6	<i>Activation Criteria Selection</i>	130
7.7	<i>Logic Tree for Possible Outcomes of Contacting a Fence with Safety Device</i> 132	
7.8	<i>Safety Fence Designs and Jump Safety Quality Index</i>	134
7.8.1	Impulse Magnitude Limits	136
7.8.2	Application of Angle Limited Designs.....	142
7.8.3	CG Location Safety Device Improvement	146
7.9	<i>Ensembles for Safety Case Studies Incorporating Video Data</i>	148
7.9.1	2017 Open Oxer Based Ensemble	149
7.9.2	LRK3DE 2018 Vertical in Combination Based Ensemble	155
7.9.3	Current Design Comparison	160
7.9.4	Design Differences for Different Fences: Speeds, Placement, and Fence Type	161
7.9.5	Generalized Categories of Fence Design.....	162
7.10	<i>Expected Improvement and Model Relevancy in Sport</i>	164
7.11	<i>Validation</i>	166
CHAPTER 8. Summary and Future Work		167
8.1	<i>Recommendations for Future Work</i>	169

APPENDICES.....	170
APPENDIX A. ROTATIONAL FALL TYPES	170
APPENDIX B. CODE	172
<i>Uniform Jumping Distributions for Upper Level Competitors</i>	172
<i>Fence Specific: Upper Level RK3DE 2017 Parameters</i>	177
<i>Fence Specific: Upper Level K3DE 2018 Distributions</i>	178
<i>Main Ensemble Function</i>	179
<i>System Mass Function</i>	184
<i>CGcylinders Function</i>	185
<i>COM Function</i>	185
<i>CGcontactCalc Function</i>	186
<i>ICOMseg Function</i>	186
<i>IcontacttoCPT Function</i>	186
<i>Cross2 Function</i>	187
APPENDIX C: Jumping Speed Histograms and QQ Plots	188
APPENDIX D: Impulse Magnitude Histograms for LRK3DE 2018 Fence 4	197
APPENDIX E: Impulse Angle Histograms for LRK3DE 2018	201
REFERENCES	208
VITA	214

LIST OF TABLES

Table 2.1 FEI, USEA and BE levels with corresponding cross country jump heights before and after 2019	7
Table 2.2 Show jumping penalties from FEI rule book [3].....	8
Table 2.3 Cross country penalties from FEI rule book [3].....	8
Table 3.1 Measured Mass of Buchner’s Horse 3 compared to the three cylinder approximations in the measured horse Hugo [33].....	26
Table 3.2 Comparing the CG locations for Horse 3 and Hugo from forehoof	27
Table 3.3 The mass moment of inertia of the horse calculated about the forehoof.....	29
Table 3.4 Eventing competitor inertia component comparison about CG and Forehoof..	30
Table 3.5 Survey Measurements averages and standard deviations in parenthesis.....	48
Table 4.1 Number of video recordings at each event	52
Table 4.2 USEA/USEF Cross Country Speeds and Distances.....	64
Table 4.3 FEI Cross Country Speeds and Distances.....	64
Table 4.4 The average speed overall and in-air jumping for each event captured	67
Table 4.5 A fence wise comparison of p-values for jumping speeds	69
Table 4.6 Average jumping position angles and standard deviations for the events video recorded.	75
Table 4.7 A fence wise comparison of p-values for jumping Body Angles	76
Table 4.8 A fence wise comparison of p-values for jumping Neck Angles.....	77
Table 4.9 A fence wise comparison of p-values for jumping Head Angles.....	77
Table 4.10 Information about the horse’s jumping trajectory.....	78
Table 4.11 The amount of contacts on the fences in all recorded videos.....	80
Table 5.1 A collection of available rotational fall videos.	94
Table 5.2 A table describing the falls and close calls in the list of videos.....	96
Table 5.3 Close call situations that did not result in rotational falls.....	98
Table 7.1 List of outcomes for critical contacts on a safety device fitted fence	134
Table 7.2 Impulse magnitude limits affect the JSQI performance for different	140
Table 7.3 The speed influences the amount of rotations at a fence but can be mitigated by impulse magnitude limits.....	141

LIST OF FIGURES

Figure 1.1 A rotational fall in competition can also be described as a somersault fall [4].	1
Figure 1.2 An adapted “Swiss Cheese Model” illustrating the preventative and mitigative measures to prevent serious injury to competitors in cross country.	3
Figure 2.1 Infographic representation of jump attempts, contacts and rotational falls in a year on FEI courses.	14
Figure 2.2 Show jumping safety cup by Jump For Joy meets FEI requirements [25].	15
Figure 2.3 Drawings of the basic frangible pin show the pin for the rail to sit on and the sheath it is clipped inside. An example of a post and rail jump with a frangible pin is shown on the right [26].	16
Figure 2.4 A reverse pin is installed on a vertical jump. This fence is jumped with the competitor coming from the right side of the photo.	17
Figure 2.5 (A) a broken Prolog has been activated in use [28]. (B) A prolog in use [28]. (C) Dutch poles in use in an oxer [27], [29].	18
Figure 2.6 (A) A MiM Clip holds the rail to the post on a jump. (B) The MiM clip has been activated as seen by the broken circle on the left side of the clip and a released arm as well as a popped out flag. (C) A MiM system with clips and hinges is seen on a post and rail jump [30].	19
Figure 2.7 The Four Cylinder Model captures the horse’s body, neck and head as well as the rider to model mass moment of inertia in the sagittal plane [34].	21
Figure 2.8 USEA kettle bell pendulum suggested test setup [37].	23
Figure 3.1 Horse measurement depictions for Four Cylinder Model Inertia	25
Figure 3.2 Plotting the location of the CGs of the individual segment cylinders show similarities as well as an overall expected CG location for a standing horse.	28
Figure 3.3 Jumping Angle ranges and position for the horse model in the jumping position	32
Figure 3.4 Mobile device view of the survey	35
Figure 3.5 Computer view of the survey	35
Figure 3.6 2015 USEF Horse Falls per Level 2015.	37
Figure 3.7 USEF Percent Horse Falls per Starter by Level in 2015	38
Figure 3.8 Shannon Wood measuring horses at 2018 Rebecca Farm, with Cambalda and Rob Burk (United States Eventing Association CEO) helping.	39
Figure 3.9 Horse Measurement survey responses across the United States.	40
Figure 3.10 A histogram of the 429 total responses across the levels	41
Figure 3.11 Left breed distributions for all levels. (Right Upper) Horse breed distributions for upper levels (Right Lower) Breed distributions for lower level competitors.	43
Figure 3.12 The distribution of heights of horses in upper level competitions.	45
Figure 3.13 The survey response comparison between rider height and weight.	46
Figure 4.1 Camera set up at a T-oxer at Chattahoochee Hills.	53
Figure 4.2 RK3DE 2017’s Fence 14 was an open oxer with MIM Clips on the front and rear rail.	54
Figure 4.3 LRK3DE 2018’s Fence 4 is a vertical with MiM Clips followed by a water complex.	55
Figure 4.4 LRK3DE 2019’s Fence 4 was an open oxer with thin rails and MiM Clips on the front and rear rails.	56

Figure 4.5 The Chattahoochee Hills CCI4*-S T-Oxer was a galloping fence.....	57
Figure 4.6 The Chattahoochee Hills Advanced table was near the beginning of the course.	58
Figure 4.7 Chattahoochee Hills CCI3*-S’s vertical preceded a narrow corner at the bottom of a hill.	59
Figure 4.8 Chattahoochee Hills Intermediate Corner shown prompted runouts from a few competitors.	60
Figure 4.9 Chattahoochee Hills CCI2*-S T-Oxer was after a gallop.	61
Figure 4.10 Chattahoochee Hills Preliminary Tiger Trap prompted big jumps from the competing horses.....	62
Figure 4.11 Chattahoochee Hills Preliminary Vertical was followed by a simpler corner than the one in the CCI3*-S.	63
Figure 4.12 LRK3DE 2018 histogram of speeds and embedded QQ plot demonstrate normal distribution.....	66
Figure 4.13 A box and whisker plot comparison of the three fences filmed during CCI5* competition	70
Figure 4.14 This box and whisker plot presents all of the jumps recorded at the Chattahoochee Hills April 2019 Horse Trials.....	71
Figure 4.15 A sample of a frame from the LRK3DE 2019 CCI5* analyzed in Kinovea with jumping point markers shown at the time the horse’s knees cross the front rail. The trace of the CG represented by the rider’s knee is also shown.	73
Figure 4.16 Examples of (a) lower limb incidental impact; (b) incidental hoof strike or lower leg impact; (c) foreleg contact in the critical range, such as for competitors at the highest risk for a rotational fall (here did not rotate); (d) crash contact with the horse’s chest sliding into the fence (did not clear the obstacle).....	79
Figure 4.17 (a) The 2008 Goodyear instrumented fence was placed on different courses throughout the year and is shown on a downhill approach in this situation [53]. (b) The 2009 British Eventing fence was built with a more upright face than the 2008 jump and was an oxer with two instrumented rails [53].	81
Figure 4.18 (a), (b), and (c). Nearest to forearm critical contacts in the top 20 British Eventing instrumented fence study videos [53].	82
Figure 4.19 Rose Plot of Angle Distribution for Front Rail Front Leg Impacts	84
Figure 4.20 Angle vs. Impulse Scatter Plot for Front Rail Front Leg Impacts	85
Figure 5.1 A horse and rider undergo a one-contact rotational fall	87
Figure 5.2 An illustration of horse and rider having a one-contact rotational fall.....	87
Figure 5.3 Three frames of a rotational fall with the horse in contact with the fence while pushing with its hind legs [54]	88
Figure 5.4 An illustration of a one-contact rotation with the horse’s hind legs pushing...88	
Figure 5.5 A horse and rider undergo a two-contact rotation upon landing fall [55].....	90
Figure 5.6 An illustration of a two-contact rotational fall.....	90
Figure 5.7 A “close call” situation with antebrachium contact but with rebalance upon landing that does not lead to rotation.....	91
Figure 5.8 A horse contacts a fence on an angle and has a torsional fall [56].....	92
Figure 5.9 An illustration of a torsional fall.....	92
Figure 6.1 New Equestrian Dummy (NED) for development of the frangible pin in 2001 [2].....	101

Figure 6.2 (left) Dutch Pole Development Testing 2001 [29]; (middle) MiM Development Testing 2008 [61]; (right) UKY Hinged Gate Testing at the RK3DE Course Builders Display 2010 [35].	101
Figure 6.3 UKY Hinged Gate Frangible Pin Testing: force just under activation compared to slightly higher force causing pin activation [35]	102
Figure 6.4 (left) 2011 Sweden Comparison Testing Using the MiM Pendulum Tester (Right) Collection of used and unused frangible pins and MiM clips.	105
Figure 7.1 The map of variables demonstrates the complexity of identifying causes of rotational falls	113
Figure 7.2 The inertia for 10,000 generated horse and rider critical contact situations forms a normal but skewed distribution.	115
Figure 7.3 (Left) Black circles display the location of the competitor's CG with respect to the antebrachium contact point represented by the red star. (Right) A visualization of the approximation of the competitor's CG is shown to visually represent what the black circles in the left plot look like in real situations.	117
Figure 7.4 Pass (no rotation, 33.2%) and Fail (rotation + irrecoverable, 69.2%) indicated for the CG Positions for a fixed-fence contact at 6 m/s (360 mpm)	119
Figure 7.5 As the speed of the competitor increases, the amount of contacts that do not result in rotations decreases.	121
Figure 7.6 Incoming kinetic energy compared to after collision kinetic energy;	123
Figure 7.7 Percent system energy loss after the collision.	124
Figure 7.8 Impulse magnitude for a fixed fence when the competitor is in any possible position by speed	126
Figure 7.9 Overlaid histogram of rotating and non-rotating impulse magnitude at 6 m/s.	127
Figure 7.10 Impulse angle for a fixed fence when the competitor is in any possible position by speed	128
Figure 7.11 Overlaid histogram of rotating/non-rotating impulse angle, 6 m/s contact speed	129
Figure 7.12 Overlaid polar histogram of rotating/non-rotating impulse angle, 4 m/s contact speed	130
Figure 7.13 A logic tree of possible critical contact outcomes	133
Figure 7.14 An impulse magnitude histogram for fixed-fence probable-rotation contacts that may or may not cause activation with an activation limit of 1000 N-s	137
Figure 7.15 Impulse magnitude histogram for no-rotation contacts that may or may not cause activation with an activation limit of 1000 N-s	138
Figure 7.16 Probable-rotation contacts that have activated a safety fence with a 1000 N-s impulse limit may or may not mitigate a rotational fall.	139
Figure 7.17 Activation or no activation for critical contacts that would not have activated for a fixed-fence	143
Figure 7.18 Overlaid histograms for a safety fence with an impulse magnitude limit of 1000 N-s and an activation window of 10-80 degrees.	145
Figure 7.19 At 6 m/s, (left) Fixed-fence impulse CG location plot about contact point yields 36.9% no-rotation rate; (right) Impulse magnitude limited to 1000 (+/-5%) for impulse angles between 10 and 80 degrees yields 74.2% no-rotation rate	147

Figure 7.20 For similar fixed-fence jumping situations to RK3DE 2017 (above) a histogram of impulse magnitudes and (below) a histogram of impulse angle identify rotation and no-rotation situations150

Figure 7.21 CG location from contact point with speed and jumping positions based on the open oxer filmed at the 2017 RK3DE. The pass/rotate coloring represents (left) a fixed fence and (right) a frangible fence limiting the impulse magnitude to 900 N-s between -10 and 25 degrees.152

Figure 7.22 Impulse angle activation consequences for jump attempts similar to those in RK3DE 2017 with activation impulse criteria of 1000 N-s between -10 and 25 degrees.154

Figure 7.23 For similar fixed-fence jumping situations to LRK3DE 2018 (left) a histogram of impulse magnitudes and (right) a histogram of impulse angle identify rotation and no-rotation situations156

Figure 7.24 CG locations from contact point with speed and jumping positions based on post-and-rail vertical filmed in 2018 LRK3DE. The pass/rotate coloring represents (a) a fixed fence and (b) a frangible fence limiting the impulse magnitude to 700 N-s between 5 and 40 degrees.....158

Figure 7.25 Impulse angle activation consequences for jump attempts similar to those in LRK3DE 2018 with activation impulse criteria of 700 N-s between 5 and 40 degrees..159

Figure 7.26 Illustrations from MiM 2015 Presentation at Maarsbergen Showing Directional Activation of Frangible Designs [31].....161

Figure 7.27 Jane Murray Fence Category Illustrations [1].....163

Figure 7.28 FEI percent rotational falls and serious injuries per starter from 2002 to 2015165

CHAPTER 1. INTRODUCTION AND MOTIVATION

The cross country phase of the equestrian sport of eventing, involving various paces, terrain and types of solid jumping fences, is the most dangerous component of the sport for the horse and rider. The leading cause of eventing serious injury and fatality for horse and rider are rotational falls [1]. A rotational fall is recognized to occur when a horse and rider contacts the fence, usually along their forearm (between the horse's knee and elbow), and rotates over the fence with the horse often landing on their backs and/or the rider [2]. Rotational falls are a subset among horse falls because the shoulder and quarters of the horse have hit the ground [3].



Figure 1.1 A rotational fall in competition can also be described as a somersault fall [4].

Rotational falls are a known risk for all jumping equestrian sports, but have become a critical focus for eventing safety in particular. In 1999, eventing cross country (XC) rotational falls led to five rider fatalities in the United Kingdom [1]. This prompted an international safety summit and the initiation of collecting fall statistics.

Another horse sport, steeplechase racing, experienced a similar change-inciting situation with excessive risk. In 2011 and 2012 at England's Grand National steeplechase races, two horses died each year and a history of horse deaths in preceding decades was recognized. These deaths were not always due to rotational falls specifically. In 2013, there was major redesign of the Grand National fences that included changing the inner components from birch to a softer plastic birch along with adjustments to the beginning of the race and footing quality [5]. After the revisions, there were no more horse deaths until 2019. A notable difference between Grand National races and eventing competitions is that the Grand National follows the same track over essentially the same jumps since 1839, while a new eventing cross country track, consisting of a series of unique jumping questions, is developed for each competition and level.

Reducing risk to competitors is multi-faceted process with numerous fronts for possible improvement. The "Swiss Cheese Model" or system failure model initially described in "Human Error: Models and Management" has been applied to many high-reliability settings such as medicine, nuclear power, and aerospace systems [6]. In Figure 1.2, the model is adapted to represent the layers of safety prevention and mitigation in eventing. A severe injury from a rotational fall is prevented by layers of safety, and only occurs if a number of unusual conditions line up.

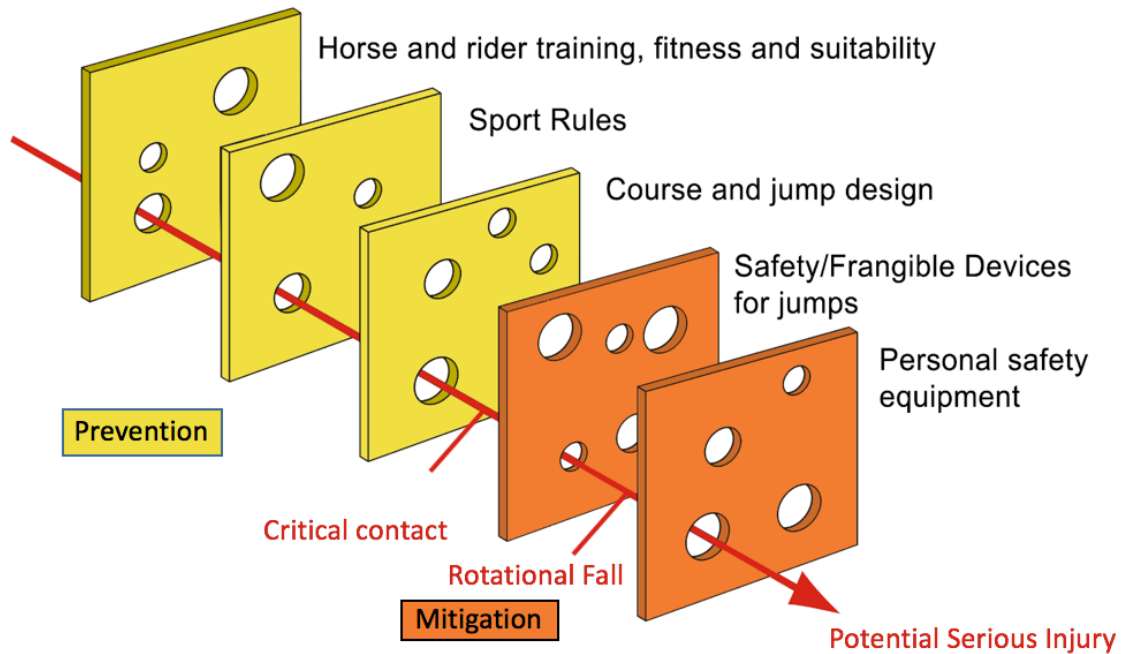


Figure 1.2 An adapted “Swiss Cheese Model” illustrating the preventative and mitigative measures to prevent serious injury to competitors in cross country.

Prevention is accomplished through training, qualifications, sport rules, course and jump design, among others, to prevent what could lead to the horse and rider ending up in a situation where they make contact with the fence in the critical foreleg region associated with rotational falls. If critical contact with the jump does occur, the mitigation layers reduce the risk of a rotational fall through the action of fence safety devices. Finally, if that fails, individual safety technology such as inflatable vests and helmets react to minimize the consequences of a rotational fall.

In this thesis, the mitigation of rotational falls by safety/frangible devices will be addressed. To date, fence safety devices have typically been fuse-like mechanisms

integrated within a fence that yield and break under a specified load, allowing the jump to deform to interrupt and mitigate a rotational fall. These fuses must be replaced after significant wear and after activation. There have been challenges to identify the thresholds for which the fuses yield upon. Different testing and estimation techniques have been used in each device's development and resulting in each type of device having different activation ranges.

A statistical ensemble method is employed to create a population of plausible input situations where a horse and rider contact the fence within the critical forearm region and through impulse-momentum calculations, determine if the competitors would rotate under fixed-fence conditions. This baseline evaluation is then incorporated with impulse limiting values to determine design criteria for the creation of future frangible devices. Expansion and explanation of inputs to the statistical population such as values for competitor inertia through size and position as well as speed are included. This study provides opportunity and evidence for the necessity of the development of more fence safety device options designed conscientiously for the different questions included in eventing cross country courses.

CHAPTER 2. BACKGROUND

2.1 The Sport of Eventing

Eventing is an equestrian triathlon. The first test is Dressage, French for training, which evaluates the horse and rider's performance of the same flatwork test looking for accuracy, correctness, obedience, and relaxation. Next, depending on the competition, is cross country which tests the bravery and fitness of a horse by jumping a course of solid jumps across a variety of terrains in a field. Showjumping is often the final test which evaluates the fitness and precision of the horse and rider team by jumping a course of fences with loose rails in jump cups in an arena setting. Scoring is cumulative so the same horse and rider must complete all three phases to be considered for award.

2.2 Governing Bodies

Eventing has international and national governing bodies. The Fédération Équestre Internationale (FEI) globally governs not only eventing but other equestrian disciplines including dressage, combined driving, endurance, para-equestrian, reining, showjumping and equestrian vaulting. The FEI works with the Olympic committee to maintain equestrian sports, which first debuted in 1900 as a part of the summer Olympics. The FEI has members of 134 National Federations [7].

National Federation governing bodies keep the sports organized internally and sculpt their own levels to educate and promote talent within their jurisdiction. Federations define the sport rules, eligibility requirements, competition operations, and more. United States Eventing Association (USEA) was first created under the name United States Combined Training Association in 1959 to focus on eventing [8]. The USEA works

under the national governing body United States Equestrian Federation (US Equestrian or USEF) which oversees eventing and 17 other disciplines and 11 breeds. British Eventing (BE) governs eventing in Great Britain while the British Equestrian Federation (BEF) performs a role similar to US Equestrian. In addition to the United States and Great Britain, France, Germany, Australia, New Zealand, the Netherlands, Brazil, Ireland, Italy, Canada, Sweden and Russia, among others, have strong eventing programs.

2.3 Level Changes and Equivalencies

In 2018 and before, there were two types of competition: “long” Concours Complet International (CCI) and “short” Concours International Combiné (CIC). The CCI format must take place over three or more days in the order dressage, cross country and show jumping. The CIC competition could be one or more days and must start with dressage. Show jumping and cross country follow in either order, with show jumping leading taking the preference. 1*-3* levels were run in both CCI and CIC format while there was only CCI4* competitions [9].

In 2019, the FEI star system changed. The old CIC format became the CCI-S and the old CCI became CCI-L. An additional CCI1*-Intro level was added that can be run in either long or short format. Levels were shifted downward creating in 2019 a new 1* level while 2*-5* competitions were to be comparable to 1*-4* competitions in 2018 and before [3]. These changes were brought about for reasons of maintaining Olympic status, affordability, and making the sport more accessible to up-and-coming riders, developing nations, and spectators [10].

National governing bodies have levels with similar heights to FEI competitions and lower heights for introductory levels. USEA offers Beginner Novice, Novice, Training, Modified, Preliminary, Intermediate, and Advanced. BE offers BE80, BE90, BE100, BE 105, Novice, Intermediate and Advanced. Despite having similar heights, cross country lengths and expected difficulty differ between the levels across rows in the Table 2.1. In this thesis, levels will be updated to current 2019 FEI levels for ease of future readers. Past competitions will be recognized for their modern level equivalencies.

Table 2.1 FEI, USEA and BE levels with corresponding cross country jump heights before and after 2019

FEI 2019	FEI before 2018	USEA	BE	Cross Country Max Jump Heights (m)
-	-	Beginner Novice	BE80	0.80
-	-	Novice	BE90	0.90
-	-	Training	BE100	1.00
CCI 1* - Intro	-	Modified	BE105	1.05
CCI-L CCI-S 2*	CCI/CIC 1*	Preliminary	Novice	1.10
CCI-L CCI-S 3*	CCI/CIC 2*	Intermediate	Intermediate	1.15
CCI-L CCI-S 4*	CCI/CIC 3*	Advanced	Advanced	1.20
CCI-L CCI-S 5*	CCI/CIC 4*	-	-	1.20

2.4 Scoring

Eventing is run on a penalty score system, so the lowest score wins. In the dressage test, each movement is given a score 0.0-10.0 along with some general

performance points. The dressage percentage is subtracted from 100 and becomes the penalty score. Additional penalty points are added to the penalty score in the jumping and cross country phases. Most commonly seen are time faults where 0.4 faults are added per second over the optimum time in both show jumping and cross country.

Grounds for elimination include, but are not limited to: rider and horse falls, jumping out of order, jumping outside the jump flags, three refusals, dangerous riding, horse welfare, drug and soundness issues evaluated in veterinary inspections, violation of dress and equipment rules, unauthorized assistance, or exceeding time limit as detailed in the respective rulebooks.

Table 2.2 Show jumping penalties from FEI rule book [3]

Fault	Penalty
Knocking down an obstacle	4 penalties
First run-out, refusal or unauthorised circle in the whole test	4 penalties
Second run-out, refusal or unauthorised circle in the whole test	elimination
Fall of Athlete or Horse	elimination

Table 2.3 Cross country penalties from FEI rule book [3]

Fault	Penalty
First refusal, run-out or circle	20 penalties
Second refusal, run-out or circle at the same obstacle	40 penalties
Third refusal, run-out or circle on XC Course	elimination
Fall of Athlete or Horse on Cross Country Course	elimination
Activating a frangible device	11 penalties
Dangerous Riding	25 penalties
Missing a flag as per art. 549.2	15 penalties

2.4.1 Frangible Fence Penalty Evolution

Most eventing competitions whether they are unrecognized, national, or FEI events follow similar rules. One of the differences are the penalty for the activation of frangible fences.

The 2015 FEI rule book placed an automatic, non-appealable 21 penalties when a frangible fence is broken on cross country. This raised contention by FEI riders who were encouraged by the International Eventing Riders Association (ERA International) to voice their disapproval. Reasons for disapproval included course designers resisting inclusion of safety devices to protect the scores of competitors, noting that breaking a jump that is not fitted with a safety device yields no penalties. Possible consequences to safety device activation include unnecessary repetition of the level to acquire a qualifying score and changing the culture of the sport [11]. In response, the FEI changed the penalty to 11 points for an activation and allowing one activation for a Minimum Eligibility Requirement (MER) in March 2015 and then in the 2016 rule book. The competition's ground jury also has the opportunity to remove the 11 penalty points if deemed unnecessary [12].

For the USEF/USEA, activating a frangible device yields no penalties. Riders may be given 25 penalties for Dangerous Riding but this is not attributed to activating frangible fences/safety devices. In US national events above the Training Level, all possible rail fences require a frangible device. This rule was finalized into requirement December 1, 2018 [13]. Notably, US events do not have an approval process for frangible devices, unlike the FEI.

The penalty has caused a lot of discussion within the eventing community. In conversation with riders during this thesis, opinions approaches range from a risky to conservative opinion. The risky approach is that since a fence has a safety device they may be approached more boldly because they would ideally break in a risky situation. The classic opinion is that the jump should be ridden the same way a solid fence would be approached. A conservative view is that frangible fences should be approached with extra caution since they may activate when not warranted and incur penalties. Speculation has included that course designers include more risky questions than would have been chosen if safety devices were not used. These are conversational opinions and not demonstrable or necessarily true, but represent the wide range of uncertainty around the use of frangible safety devices.

2.4.2 Unnecessary Safety Fence False Activations

With the advent of frangible devices and the penalty system, it must be acknowledged that there are three outcome cases: the devices do not activate although the situation would be better if it did, the device activates properly, and a device activates even though it is unnecessary. For this thesis, when a device activates in a situation that would not result in a rotational fall, it would be considered a false activation. A false activation may still include a rider fall or other consequences arising from the fence contact.

In FEI competition, the 11-point activation penalty has a serious impact. Receiving this penalty quickly moves the competitor far down the leaderboard therefore unnecessary activations pose significant cost to the competitor.

2.5 Statistics for Falls, Injuries and Performance

Following the international safety summit in 2000, the FEI began keeping statistics of starters including falls and injuries. Though definitions of injury and serious injury have evolved and sometimes overlapped throughout the years, concussion, broken bones and fatality have all been included as serious injury. Definitions of injuries were clarified in 2010 and in 2018 so that concussions were represented as a subset of both serious and slight injuries [14]. Statistics are kept by national governing bodies like the USEA and BE, but are not publicly available. Before 2000, only a few sports injury studies attempted to monitor fall accounts in specific areas [15]. Therefore it is not possible to verify if more or less rotational falls occurred in “the good old days”.

In 2015, a sports data company for equestrian sports was created by two Irishmen, international event rider Sam Watson and law-trained Diarmuid Byrne. Their data analytics methods provide performance metrics, safety indicators and insights about the influence of different variables on the sport’s scoring [16]. SAP, a software and analytics company, has also expand their brand into new areas of sports and entertainment including the equestrian media space. Their interests include data from sensors carried by riders on course as well as different audience-engaging phone apps [17].

2.5.1 Epidemiology Risk Review Studies

Initially, investigations into rotational falls focused situationally on categorizing causes for prevention of the falls. In 2004, Jane Katherine Murray at the University of Liverpool analyzed epidemiological variables such as rider position awareness, previous

cross-country refusals, rider education levels as they pertained to horse and rider falls. She also investigated jumping conditions such as take-off or landing in water, non-angled fences with a spread of two meters or greater and angled fences and fences with a drop landing [1], [18]. Some improvements were identifiable, but these results did not initiate removal of any type of fence or a single influential cause.

Opinion pieces for methodology and review of the progress of the safety of eventing have been released over the years as well [19], [20].

In 2016, a report for the FEI by Charles Barnett was released covering collection of fall data, qualifications and improvement opportunities for officials. Risk of horse falls increase as the level increases. Barnett calls for video recording of each fence at the 4* and 5* levels for the purpose of post-competition evaluating incidents. Within the report there was a statistical analysis of fall data from 2008-2014, focusing on cross country jumps related to horse falls and rotational falls. It was noted that falls were most likely to occur in the order of decreasing risk at corners, steps, square spreads and post-and-rail jumps. A higher risk was noted at oxers with open fronts and tops, rather than closed tops and open fronts. Fences on downhill approaches as well as downhill landing were noted to have higher rates of rotational falls than uphill or level fences. Fences associated with water —whether into, within or out of water— had more rotational falls than for fences that were not. Ground lines and bends were not indicative of horse falls or rotations, perhaps indicating their already adequate implementation [21].

The Safety for Horses and Riders in Eventing (SHARE) Database is a study from New Zealand and Australian competitions that also analyzed FEI Data. It was noted in this work that rotational falls happen most frequently at post-and-rail fences [22].

2.5.2 By the Numbers: Frequency of Contact and Rotational Falls

It is helpful to understand the numbers of potential rotational fall occurrences each year as we work to prevent and mitigate them. Annual fall and starter statistics from FEI and USEA/USEF can give an idea of the frequency of these situations. In 2016 there were 19,921 starters [23]. Each starter approaches 25-45 jumps per course. If 35 is the average, there would be 697,235 jump attempts/yr. From the 2008/2009 British Eventing (BE) instrumented fence testing on course (over 4,000 approaches) 38.8% made contact . If applicable across all situations, there would be 270,527 contacts/yr. Safety devices must activate when needed, without too many false activations under these conditions. Of the 2008/2009 BE contacts, 3.91% are front hoof/leg contacts. The amount of resulting front leg and front hoof contacts would be 10,578/yr. Of these, most are hoof and lower-leg contacts, but rarely (1 in 66) contact was in the critical forearm range recognized to be associated with rotational falls. Thus, there would be 160 hanging leg contacts per year.

In a year on FEI courses...

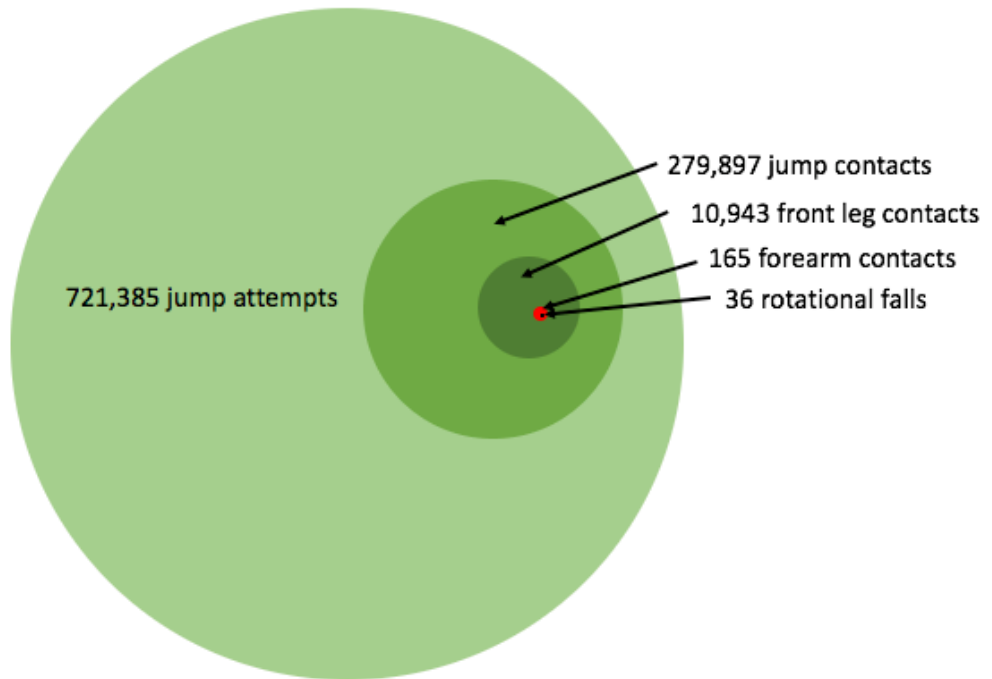


Figure 2.1 Infographic representation of jump attempts, contacts and rotational falls in a year on FEI courses.

The FEI reported about 30 rotational falls in 2016. An important validation of the physics-based simulation comes from considering the number of rotational falls in 2002 before the widespread use of safety devices. For these fixed fences, 0.52% of starters had rotations; for the equivalent number of 2016 starters it would be 104 rotational falls per year. The difference in the number of rotational falls between 2001 and 2016 can be attributed to improvements in course and jump design as well as the inclusion of safety devices. Note that the red and black circles in Figure 2.1 representing forearm contacts and rotational falls are not to scale because if they were, they would be too small to see.

2.6 Frangible Fence Conception and Progress

True rotational falls seldom occur in show jumping (these falls are not documented but have been mentioned anecdotally in conversation with sport members) where the fence's rails fall out of cups when hit or activate a vertically loaded safety cup demonstrated in Figure 2.2. To improve the safety of these jumps, the FEI has established a testing cooperative procedure with Institut für Kraftfahrzeuge Aachen (IKA) where manufactures may submit their designs for review [24].



Figure 2.2 Show jumping safety cup by Jump For Joy meets FEI requirements [25].

With this idea in mind, the sport began to focus on how cross country jumps could deform to reduce the occurrence of rotational falls. Those involved in the sport conversationally report that it is critical that the fences seem to be solid to both encourage competitors to respect the jumps and to maintain the culture of the sport.

British Eventing sponsored the creation of the Frangible Pin made by the Transportation Research Lab (TRL). The pin was placed on the front of a post holding the jumping rail and was intended to shear under vertical impact. The rail was also tied

so if activated the rail wouldn't roll away, which would create a more dangerous situation. A diagram of a frangible pin is shown in Figure 2.3. Frangible pins were first tried in the 2002 season [2].

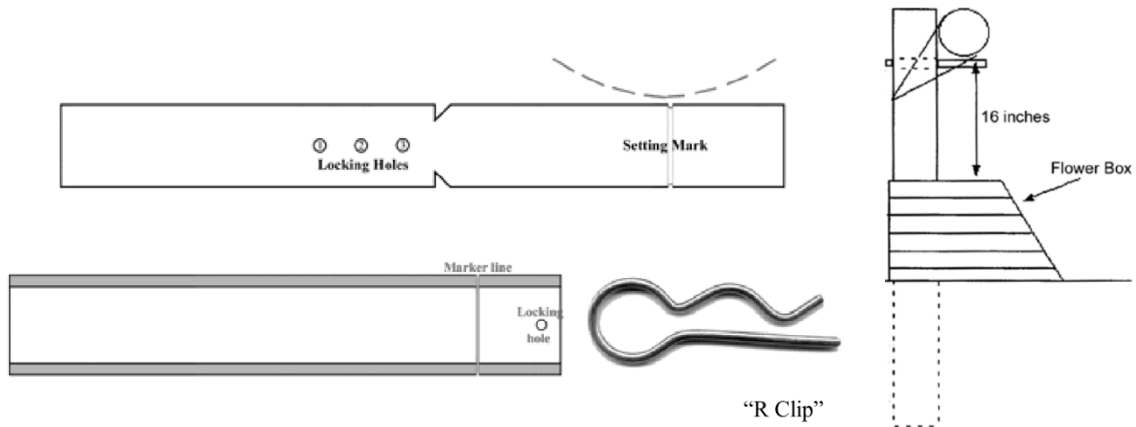


Figure 2.3 Drawings of the basic frangible pin show the pin for the rail to sit on and the sheath it is clipped inside. An example of a post and rail jump with a frangible pin is shown on the right [26].

Later, reverse pin installations were added. This mounted the pin on the back of the post holding that rail and was preloaded with a cable as shown in Figure 2.4. The reverse pin is considered to be more sensitive to horizontal contact components in angle range than the original frangible pin. The reverse pin is secured with a wire chord. Reverse pins are often placed on post and rail oxers and combined with frangible pins to outfit corners.



Figure 2.4 A reverse pin is installed on a vertical jump. This fence is jumped with the competitor coming from the right side of the photo.

Both the frangible pin and the reverse pin share the difficulty of visually identifying material degradation fatigue or partial activation when a pin is bent but not

fractured. In competition, each cross country fence is monitored by volunteer fence judges who range from very experienced to those quickly briefed onsite before the start of competition. Therefore, it can be difficult to ensure the devices are in ideal operating condition for each approach.

Further, in order to replace a pin, the heavy log supported above and a new pin inserted, requiring numerous people to assist and requiring more time, resulting in a hold for the competitors on course [26]. In addition, the jump repair crew must arrive quickly with the replacement from wherever they are on course.

Material solutions where the fence/rail breaks were introduced as well. Prologs by Safer Building Materials, Inc. were polystyrene logs, shown in Figure 2.5, that would crack in the material to decrease impact. Dutch poles similarly would crack. Dutch poles also have a sound that would indicate if they were compromised [27]. These materials solutions found less widespread acceptance and were not approved by the FEI. They were met with disapproval from the sport in cultural aspects such as them appearing to break too easily and not garnering respect [28]. They also take some time to reassemble after activation and require space to store replacement poles.



Figure 2.5 (A) a broken Prolog has been activated in use [28]. (B) A prolog in use [28]. (C) Dutch poles in use in an oxer [27], [29].

MiM Construction AB has created MiMsafe New Era technology, usually called MiM Clips, to prevent rotational falls which have been in use since 2008 [30]–[32]. Shown in Figure 2.6, the MiM hinge system is incorporated into the jump with a red MiM clip being the fuse which breaks when activated, allowing the rail to fall. An activated fence is reset by raising the rail back on its hinge and sliding in a new clip. The clip indicates if it is compromised by a hard contact by having “flags” bend out of the clip. MiM offers post and rail, oxer, gate and wall, and a table kit [31]. Adaptations of MiM have been used on 90 degree and smaller corners as well. It is notable that all current solutions require replacement (like a new pin or clip) after activation and are not purely resettable.



Figure 2.6 (A) A MiM Clip holds the rail to the post on a jump. (B) The MiM clip has been activated as seen by the broken circle on the left side of the clip and a released arm as well as a popped out flag. (C) A MiM system with clips and hinges is seen on a post and rail jump [30].

2.7 Physical Representations of the Horse: Dummies and Inertia

Efforts from the Transportation Research Lab (TRL) in creating the frangible pin included video analysis and some statistical analysis. TRL created a horse dummy called New Equestrian Dummy (NED) with physical characteristics modeling a horse cadaver.

NED was sent on 6 m/s approaches to contact a post-and-rail fence to simulate a rotational fall to understand loading principles [2].

Bristol University engineering students created BESS, a scale-model dummy based on a horse cadaver to simulate rotational falls. BESS impacted jumps at different prescribed speeds.

Competitive Measure Sports Engineering created two instrumented cross country fences: the 2008 Goodyear Safety Research Fence and the 2009 British Eventing Safety Research Fence. The fences were fitted with force gauges in x and y directions, providing on-course force-time history measurements of cross country fence contacts on course. This is the only available observation of its type. The results were not published, but over 250 data sets were shared with University of Kentucky researchers in 2010.

Inertial properties of segments horse were determined empirically by H. H. F. Buchner. Six frozen Dutch Warmblood horse cadavers were dissected into 26 pieces from which inertia was measured. Regression models of the horse were shared [33].

For the purpose of evaluating rotational falls, Gregorio Robles Vega interpreted Buchner's model in combination with a seated pilot model from an aerospace study to create an inertia model for a horse and rider through cylindrical approximation. He titled this inertial model the Four Cylinder Model illustrated in Figure 2.7 [34]. This allowed for measurements of live horses and riders competing in eventing to be modeled and configured into jumping positions.

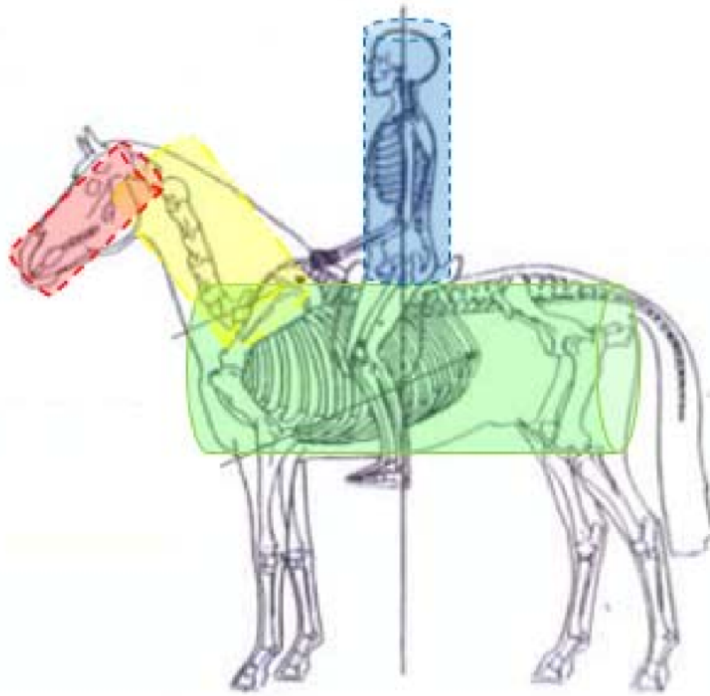


Figure 2.7 The Four Cylinder Model captures the horse's body, neck and head as well as the rider to model mass moment of inertial in the sagittal plane [34].

2.8 On Course Testing, Frangible Device Testing and FEI Standard

At the University of Kentucky, Katie Kahmann's 2009 thesis, largely discussing device design including a gate and a resettable (no fuse replacement) table and testing methods with instrumented sledgehammers.. Specifically, the position of the impact and its relationship to device activation were considered in efforts to promote on course testing for frangible device verification [35].

In 2011, device comparison testing by a team of equestrians, jump builders and engineers, including Dr. Suzanne Weaver Smith, was conducted in Sweden at MiM Construction AB. This testing was done with a pendulum tester developed by MiM.

Participants conducting the tests observed the different design activation thresholds and wondered what the proper activation limit for devices should be mitigate a rotational fall.

In 2012, the FEI Standard for minimum strength of frangible/deformable cross country fences (current, v22) was introduced. The product's function was ultimately decided and declared by the manufacturer. The fence must also pass a test for incidental hits. The manufacturer must provide proper instructions for the user. The strength of the fence is then tested by horizontal impactors in a location where the fence should activate. The fence must also pass a repeatability tests where at 25% less energy than the indicated activation the fence never activates and at the 25% more energy it activates every time [36].

In 2019, the USEA released a DIY kettlebell testing apparatus, illustrated in Figure 2.8, to test frangible fence equipment. The apparatus included a chain and 40 kg kettlebell raised as a pendulum, with performance criteria requiring release/drop heights of 0.41m without activation to 0.51m resulting in activation [37].

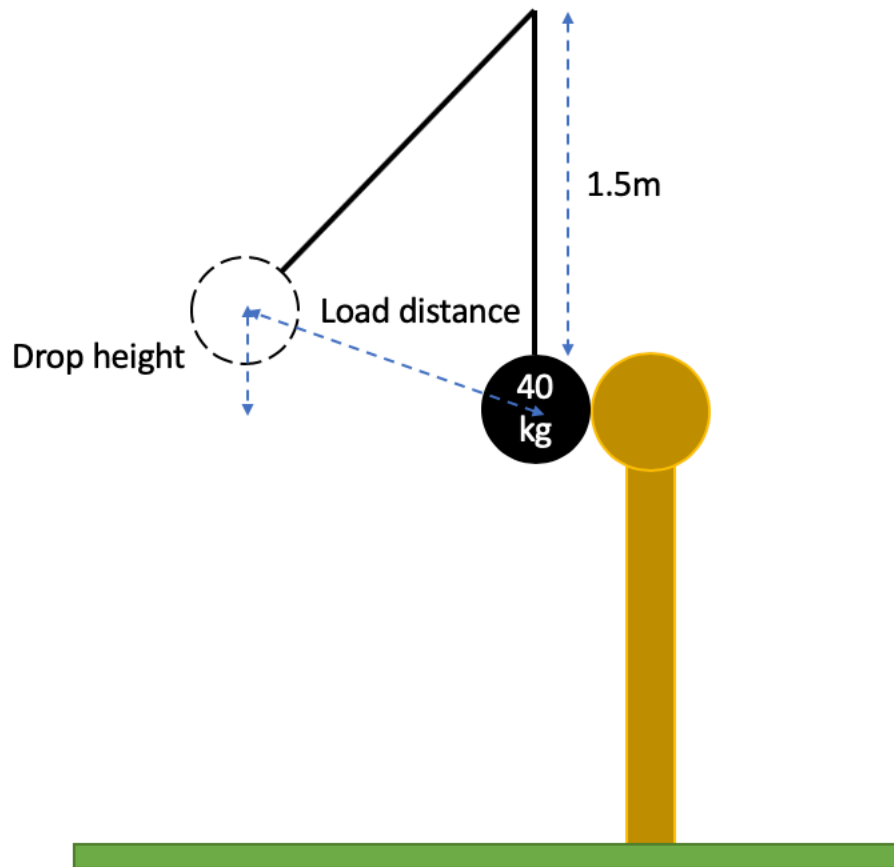


Figure 2.8 USEA kettle bell pendulum suggested test setup [37].

This thesis began in summer 2016 and continued by aid of the USEA through summer 2018. Fall 2018-Winter 2019 was supported by the University of Kentucky.

CHAPTER 3. INERTIA AND SURVEY

3.1 Inertia and Center of Gravity

The inertia model is a vital contributor. It is critical for impulse-momentum physics rotational momentum to model the shape and size of the competitor at the moment the horse contacts the fence. Different horse and rider sizes, and especially positions at contact influence the inertia. However, it is clear from the results that a particular size and shape of a standing horse and rider does not result in a higher likelihood of rotation. The position of a competitor at the time of contact is one of the most sensitive parameters, identified by Robles Vega [34]. Inertia of the horse had been measured for individual segments of a small sample size of dissected horses, first six Dutch Warmbloods and 38 horses of different breeds and types [38] , [33]. The horses's fitness levels and ages were not seen to be suitable to the population of horses competing in eventing. Densities and masses of thoroughbred limbs have been used to make weight approximations [39].

3.2 Standing Center of Gravity and Inertia

Few studies have investigated overall inertia of the horse. Often the focus is on particular limbs. For this rotation problem, the full body inertia about the axes perpendicular to the sagittal plane is needed. While determining key parameters was largely the focus of Robles Vega's thesis, subsequent refinement was developed and is included here [34].

The Four Cylinder Model (FCM) for inertia represents a standing horse and rider by approximating cylinders as the horse's head, neck and body, along with the rider. The

Body cylinder of the horse also represents the four legs. Cylinders have been used as an appropriate method of estimating horse inertia in the past [40]. The head, neck and body (incorporating the thigh) contain most of the mass and inertia of the horse so the model was simplified to those features [33]. Though simple cylinders are an approximation, the model provides enough of a frustum measurement to represent the majority of the mass distribution and inertia. The model is validated by comparison to Buchner and a technical report from the US Air Force for the rider [33], [34], [41]. For validation of the Four Cylinder Model, measurements of an available horse, Hugo a Dutch Warmblood of similar size to Horse 3 in Buchner's data, were taken as shown in Figure 3.1. Note: the horse shown is not Hugo. Bruchner's data does not include comparable measurements, so the Hugo comparison was devised.

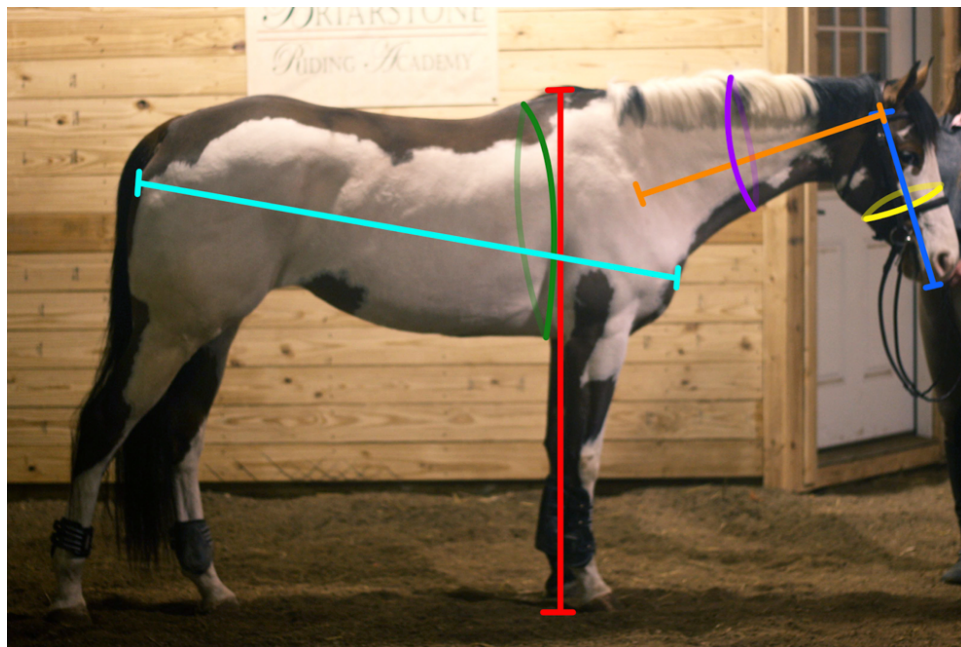


Figure 3.1 Horse measurement depictions for Four Cylinder Model Inertia

In Robles Vega’s thesis, other mass approximations methods were considered such as dividing a total mass by the volume of the cylinders, using segment percentage of mass numbers but using published densities had the lowest percent error from Buchner’s empirical measurements [34].

Therefore, the mass of the horse for the Four Cylinder Model is found by density approximation. For the head and neck cylinders, the Dutch Warmblood head and neck densities in Buchner were multiplied by the cylindrical volume from measurements taken in Figure 3.1 [33]. To account for the extreme tapering shape, half of the neck volume was used for the mass approximation. The body cylinder incorporates the horse’s legs so the overall horse density was used for the approximation.

Table 3.1 Measured Mass of Buchner’s Horse 3 compared to the three cylinder approximations in the measured horse Hugo [33].

	Horse 3 (kg)	Hugo Standing Model (kg)	Percent Difference
Head	21.6	22.7	5.1%
Neck	28.4	31.3	10.2%
Body	472.77	489.0	3.4%
Total Mass	522.77	543.14	3.9%

Table 3.1 shows the mass of the segments recorded for Buchner’s published Horse 3, next to the approximation using the published densities and cylindrical approximation measurements recorded of Hugo in this study. Note that the mass comparisons show similar numbers, with some difference as expected for two different animals. This result validates the measurement process and the density approximation method. This is important because by using this measurement process and density

method, it is possible to expand the pool of data to include live and competing horses by taking unintrusive measurements.

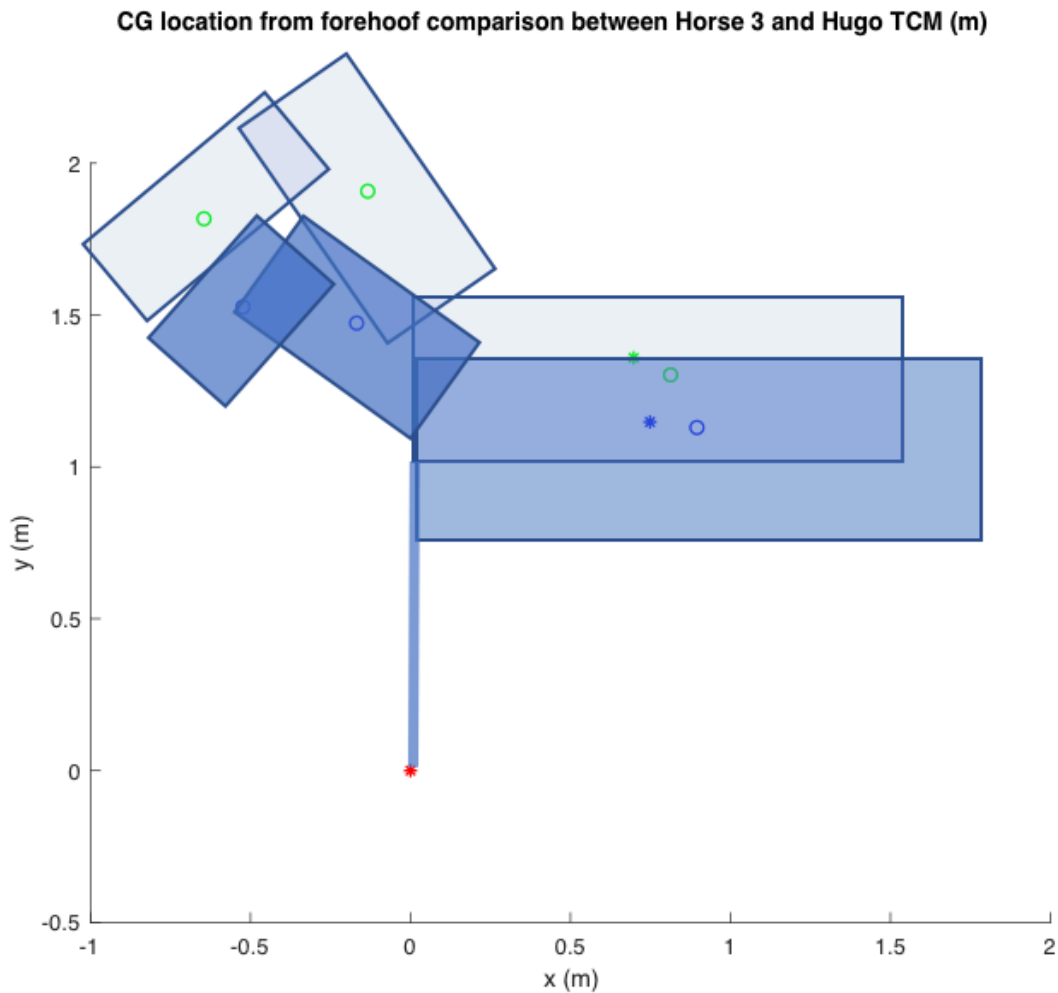
Similarities in CG location are also noted in Table 3.2. For simple comparison, the head neck and body cylinders were located into a standing position with the datum at the front foot. \bar{x} and \bar{y} represent the distance of the CG from the datum at the forehoof. This shows that the weight distribution approximation is correct. Geometry comparisons showed similar center of gravity locations.

Table 3.2 Comparing the CG locations for Horse 3 and Hugo from forehoof

	Horse 3 \bar{x} (m)	Horse 3 \bar{y} (m)	Hugo \bar{x} (m)	Hugo \bar{y} (m)
Head	-0.52	1.53	-0.65	1.82
Neck	-0.17	1.47	-0.13	1.91
Body	**0.90	**1.13	0.81	1.30
Overall	0.75	1.15	0.70	1.36

**TCM considers the limbs as a part of the body cylinder while Horse 3 only has coordinates for the trunk here

Cylinder locations may be visualized as well, by imagining Horse 3 and Hugo standing side by side as shown in Figure 3.2. Individual cylinder CGs are shown by circles and the overall CG locations are noted by stars. These points are plotted with respect to the forehoof as a common datum. Some postural differences may account for the slightly different positions in CG location as well. Comparable CG locations are found between Horse 3 and Hugo for segment cylinders and overall CG.



Red Star- origin at forehoof
Green- Hugo TCM
Blue- Horse 3
Blue and Green Stars- overall CG

Figure 3.2 Plotting the location of the CGs of the individual segment cylinders show similarities as well as an overall expected CG location for a standing horse.

Standing inertia in comparison to Buchner's previous works is the next verification of the TCM. First inertia was found about the CG of each segment cylinder and then combined using parallel axis theorem about a common point at the forehoof for comparison purposes. For jumping situations, the inertia can be translated from the inertia

about an axis through the combined CG to the contact point on the foreleg using parallel axis theorem. Table 3.3 presents that this is an accurate (<5% difference except for the head) representation. This model is intended to be expanded into simulations over large statistical ensemble populations.

Table 3.3 The mass moment of inertia of the horse calculated about the forehoof

	Horse 3 (kg*m ²)	Hugo Standing Model (kg*m ²)	Percent difference
Head	56.24	66.16	17.6%
Neck	62.56	59.86	-4.3%
Body	1224.22	1269.70	3.7%
Total Inertia	1430.10	1475.30	3.2%

Rider inertia is added as the fourth cylinder in the Four Cylinder Model (FCM). It has been shown that there is a significant effect on the horse's angular momentum by added rider mass to the system. However, it has been recognized and further explained that the behavioral components of the rider's effect on the horse may exceed the inertial effects in jumping situations [42]. The rider makes up an average of 11.5% of the competitor's mass and contributes significantly to the inertia in jumping contact situations. For these reasons, the rider was included in the statistical ensemble. Historically in dummies and pendulum testers only mass and size values for the horse had been included in testing.

The method used to calculate riders' inertia was obtained from a study for a seated human pilot with outstretched arms for aerospace applications [43]. This model uses rider height and weight as inputs for calculating the inertia. For the rotation axis

perpendicular to the sagittal plane, the horse may rotate around the competitor's CG or about the contact point. From the inertia parallel axis theorem, the distance squared is significant and magnifies a rider's importance. As shown in Table 3.4, the rider's CG is close to the overall CG so the rider's inertia is the lowest contributor out of the four cylinders to the overall moment of inertia about the CG axis. However, if the inertia is calculated about the forehoof, the rider becomes the second largest contributor to the overall inertia. For this reason it is important to include the rider. The inertia and the percentage of contribution of each cylinder will change again as the inertia is calculated for a jumping position about an antebrachium contact point. Chapter 7 presents more detail on this with simulation results.

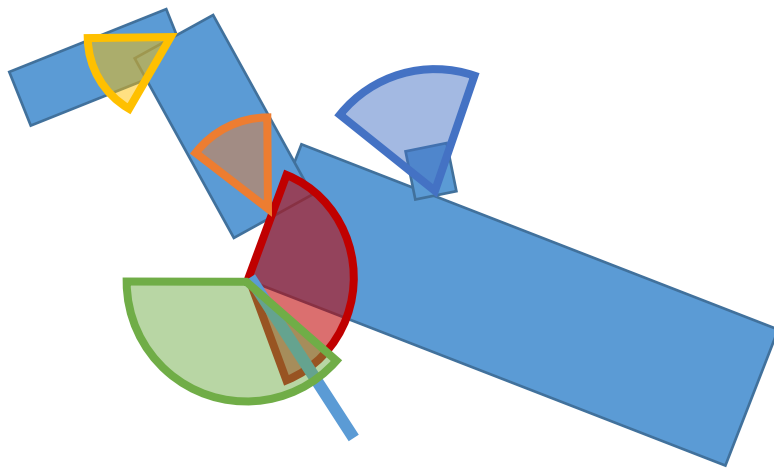
Table 3.4 Eventing competitor inertia component comparison about CG and Forehoof

	I about CG (kg*m ²)	% of total	I about Forehoof (kg*m ²)	% of total
Head	33.1	17%	69.2	4%
Neck	25.9	13%	107.4	6%
Body	129.5	66%	1288.4	76%
Rider	7.6	4%	221.5	13%
Total	196	100%	1686.5	100%

The jump performance influence of riding a proper approach exceeds the rider's physical influence at the time of contact [42]. It has been theorized that the rider could throw their body into a position to prevent a rotational fall. Robles Vega showed that rotation is insensitive to the rider position. Further, rider reaction time is too slow compared to rotational falls to provide any mitigation [44],[34].

3.2.1 Jumping Center of Gravity and Inertia

The FCM is geometrically arranged into jumping position at the time of contact by varying the jumping angles shown in Figure 3.3. The five jumping angles include the angle of the horse's body from the horizontal, with the origin of measurement at the shoulder. The other position angles reference to the body angle and are added on. The neck, head and rider angles are positioned from unique origins at the midpoint of the base of the cylinders where they connect to other pieces. The antebrachium angle models the position of the horse's foreleg at the time of contact with the position approximated from the front lower point of the body cylinder.



Angle	Variable	Range
Body angle	Alpha (α)	-45° to 45° (range 90°)
Neck angle	Beta (β)	$\alpha+110^\circ$ to $\alpha+190^\circ$ (range 80°)
Head angle	Phi (φ)	$\alpha+200^\circ$ to $\alpha+260^\circ$ (range 60°)
Ante brachium angle	Nu (ν)	$\alpha+200^\circ$ to $\alpha+260^\circ$ (range 60°)
Rider angle	Lambda (λ)	$\alpha+80^\circ$ - $\alpha+160^\circ$ (range 80°)

Figure 3.3 Jumping Angle ranges and position for the horse model in the jumping position

For general “any jump on course, any situation” simulations, full angles ranges are used from Figure 3.3 with uniform distributions. The range of these angles can be modified to suit the expected represented body angles when relating to terrain, spread, and face of the jump for a clearer picture of the expected result at a particular fence where normal distributions are more appropriate. The expected jumping position angles can be based on video studies over similar jumping situations. The body angle of the horse, α , is the most sensitive parameter to the result of the competitor rotation [34].

The contact point of the horse with the fence associated with rotational falls also varies along the foreleg region. The geometric arrangements of the FCM including the carriable length along the foreleg allows the contact point to be closer to the chest or knee of the horse, which has been shown to be a sensitive parameter because it changes the moment arm.

In observation, the competitor’s body shape sometimes changes throughout the time of contact by the extension of the legs and neck. This change in position is accounted for by adopting the statistical ensemble approach for the problem. Other position cases resemble the different degrees of the difference in shape, incorporating the physics for each in turn.

3.3 Citizen Science Survey and Measurements

At first, a citizen science survey approach was adopted to widely gather data not available in the literature or through other sources. The FCM allowed straightforward, repeatable, quick measurements of horses in order to acquire a large sample size of live,

current competitors in eventing. An online survey was distributed. Riders and owners measured and submitted data for their own horses. Advantages of this type of survey include the following: open to submissions anywhere in the world, open to a greater number of submissions, and participants could feel pride in contributing to rotational fall prevention.

The survey asked that the participants safely take the measurements of the horse as pictured. A soft measuring tape at least 7' in length was needed (one used to measure jump heights or lines may be handy); a horse height measuring stick and a second person were helpful but not required. If there were any unknown measurements, such as the horse's scale weight, participants were instructed to skip and complete the rest of the survey. Demographic information including breed, competition level and home location were also collected [45].

Google Forms was used to create the survey because it automatically feeds the data into a spreadsheet, has high reliability, and is functional for both computer and mobile devices as seen in Figure 3.4 and 3.5. The survey was published in July 2016 and remained open for entries until March 2019. Overall 155 entries were submitted.

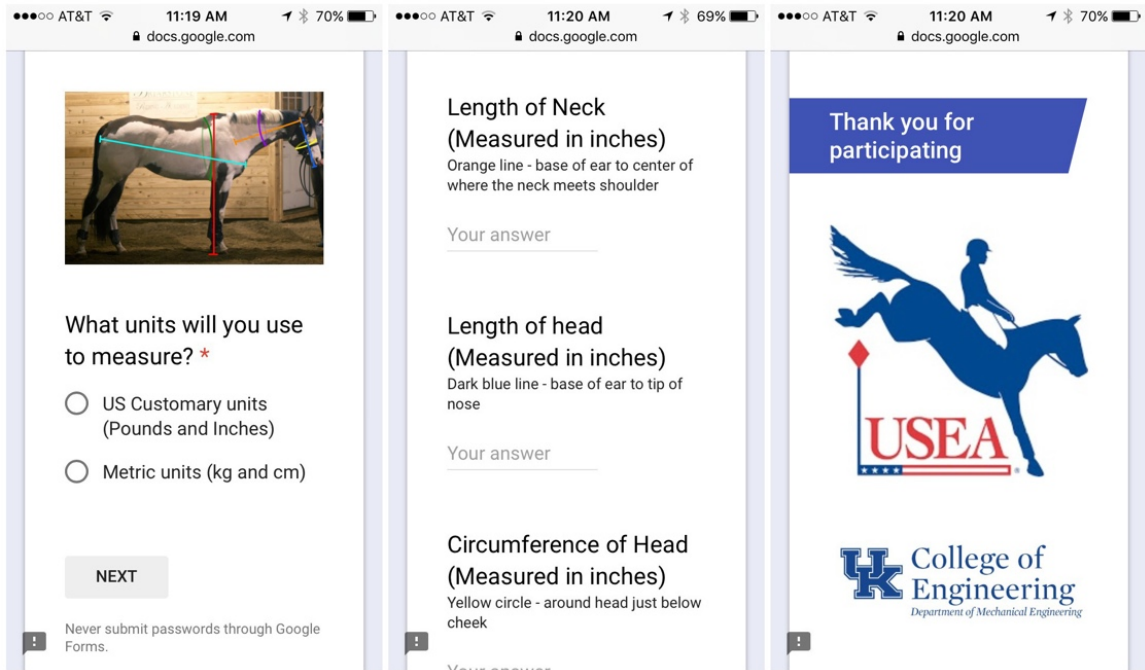


Figure 3.4 Mobile device view of the survey

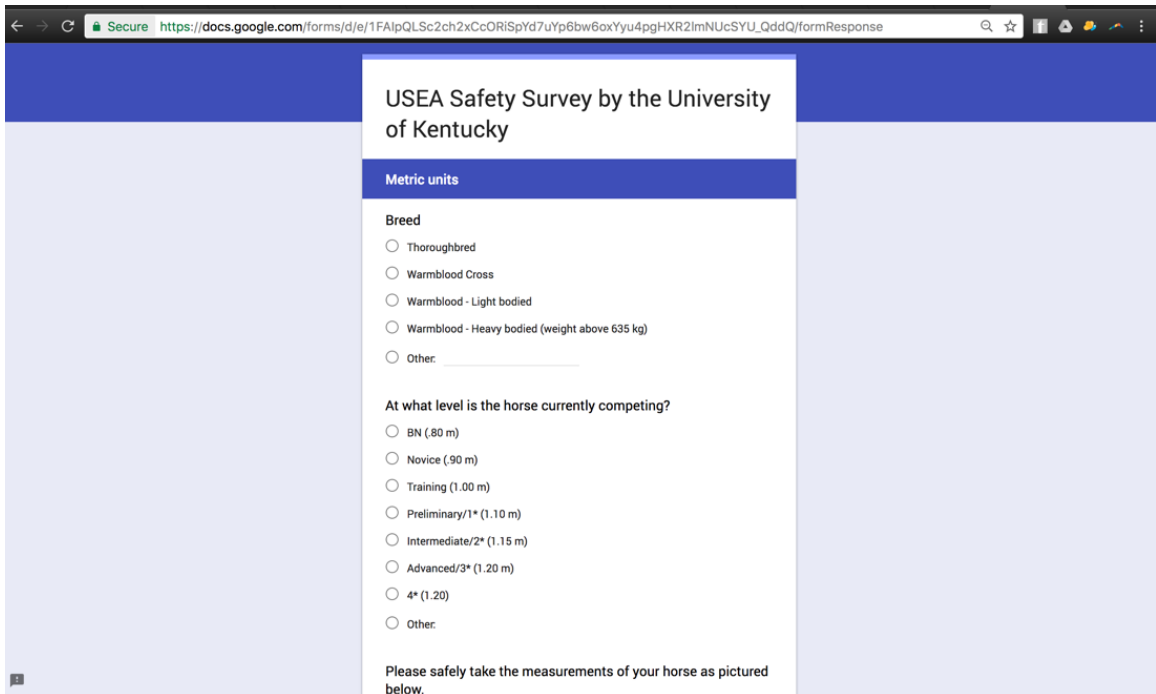


Figure 3.5 Computer view of the survey

Disadvantages of a citizen-science survey include the possibility of incorrect information, difficulty of widespread communication, and inadequate response to the survey for the intended purpose. Criteria were developed for quality control of the submitted data, and many submissions had some values identified and not used further based on these criteria. To have sufficient numbers to be a representative sample, more measurements were needed than were submitted. Additionally, most of the responses were from lower level competitors. Because risk for rotational falls increase with levels, it is important to adequately represent upper level competitors.

The inertia survey should represent the starters on course as well as the starters most at risk. The inertia survey was conducted prior to the 2019 FEI level shift, but will be presented in the new star system for future use. “Lower Levels” used herein will refer to Training Level and below, including ‘other’ responses. “Upper Level” herein will refer to Preliminary/1* to 5* levels.

In 2015, the number of horses and riders that competed in Beginner/Novice was approximately 24 times the number in Advanced and 5* levels according to statistics from the USEF and FEI. Conversely, the total number of horse falls are greatest for Preliminary and Intermediate/2* competitors as seen in the left plot of Figure 3.6 which shows a histogram of the number of occurrences on the vertical axis and Competitor Level on the horizontal. These statistics include both rotational and non-rotational falls, even though rotational falls have greater risk of injury for horse and rider.

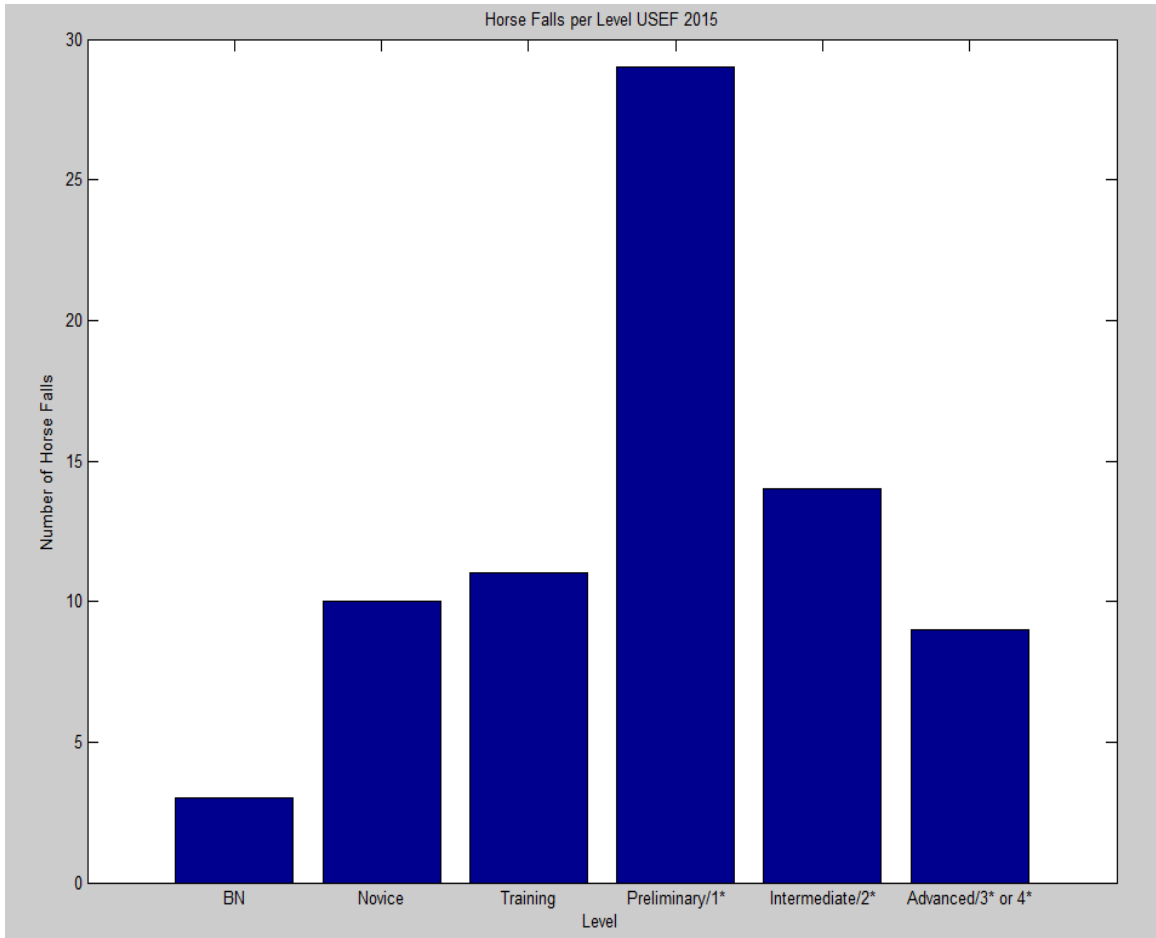


Figure 3.6 2015 USEF Horse Falls per Level 2015.

The number of horse falls *per starter* dramatically increases at the upper levels as seen in Figure 3.7. Even though there are fewer competitors in the upper levels than at the lower levels, they are exposed to more risk. For that reason it is important that the models represent all situations, but can also be focused on conditions expected for upper level competitors.

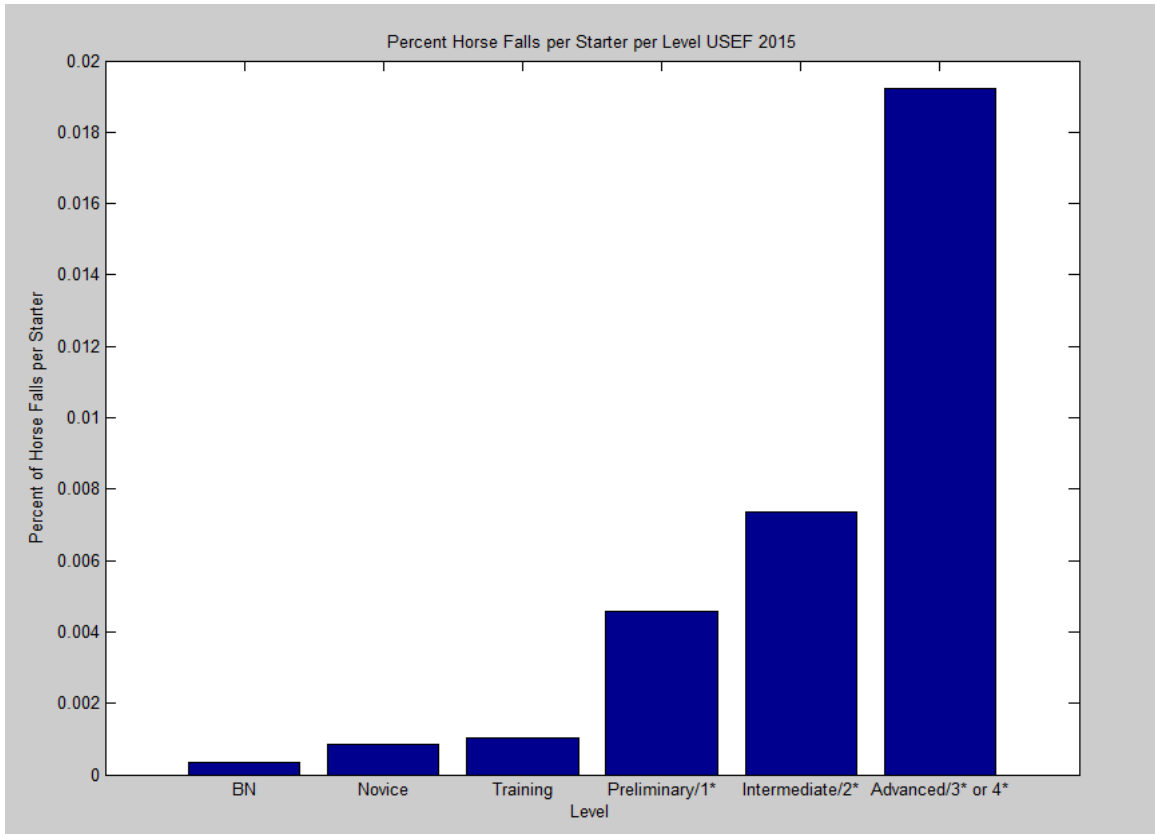


Figure 3.7 USEF Percent Horse Falls per Starter by Level in 2015

In order to represent the US population of event horses, first consider that the United States Eventing Association has nearly 12,000 members. For a 95% confidence interval and a 5% margin of error, the minimum population measured should be 384 horses based on the student t distribution in Statistics. An Institutional Animal Care and Use Committee (IACUC) protocol titled Horse Measurements for Inertia Approximation 2017-2691 was developed so UKY researchers could measure horses themselves to contribute to the study. The protocol was approved May 16, 2018.

Measurements were taken at Midsouth Horse Trials, Champagne Run Horse Trials, Dauntless Sport Horses, Clearview Equestrian Center, Montgomery Equestrian, LLG Eventing and Antebellum Farm. Travel to the Event at Rebecca Farm 2018 pictured

in Figure 3.8, and the Instructor Certification Program Clinic 2019 allowed additional access to more difficult-to-find upper level horses.

A scale was not practical to be transported and few-to-no competitors knew a measured weight of their horse besides estimation so that question was ultimately eliminated. Based on these researcher interactions, it is expected that that few online submissions were measured weights, but rather guesses. Therefore, in creating the model, more systematic approximations for masses are obtained with densities available from literature. With both UKY measured and citizen science survey submissions, 429 total competitor measurements were gathered.



Figure 3.8 Shannon Wood measuring horses at 2018 Rebecca Farm, with Cambalda and Rob Burk (United States Eventing Association CEO) helping.

Overall, 34 states are represented in the data from survey submissions and UKY measurements as displayed in Figure 3.9. The top 3 states from which data was received was Kentucky, California and Washington. International submissions are included from Canada, United Kingdom, and Australia.

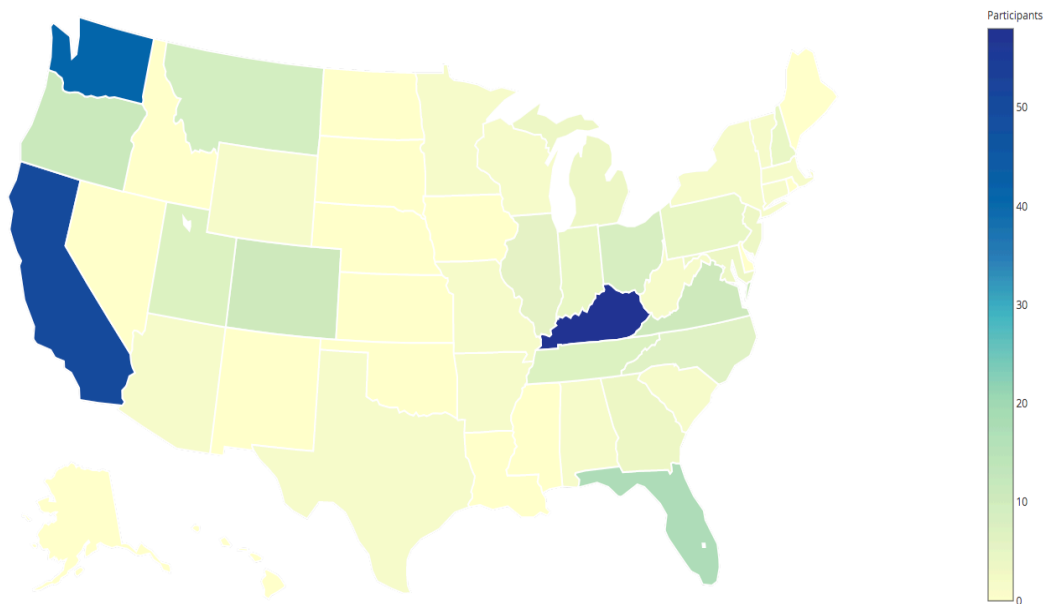


Figure 3.9 Horse Measurement survey responses across the United States.

3.3.1 Levels

The survey gathered 429 total data submissions over a variety of levels as seen in Figure 3.10. 175 upper level competitors submitted to the survey. This does provide an adequate basis for those more at risk for rotational falls. Horses in the ‘other’ competition level included horses who have not yet competed, competed in Starter level competitions, dressage and, most commonly, Hunter/Jumper horses.

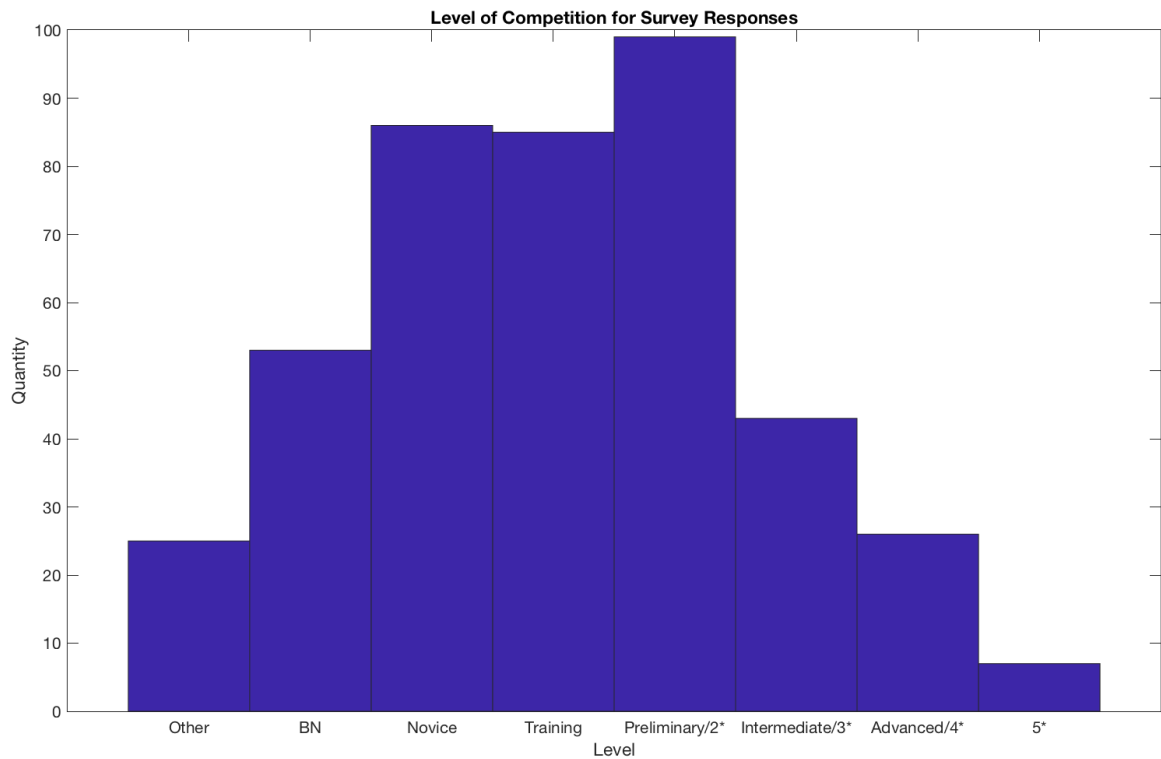


Figure 3.10 A histogram of the 429 total responses across the levels

3.3.2 Breeds

Breed categories included in the survey were Thoroughbred, Warmblood – Light Bodied, Warmblood Cross, Warmblood – Heavy Bodied and Other with a write-in option. Many of the write-in responses included Irish Sport Horses with a few submissions of sport horses from other countries, so an additional ‘Sport Horse’ category was eventually included in the breed analysis. The distribution of the breeds are shown in the pie charts in Figure 3.11.

The largest plurality of horses competing in eventing were thoroughbreds. Nearly half of lower level horses competing were thoroughbreds. The next largest category was

Light Bodied Warmbloods. This was probably the broadest category as it included breeds such as Dutch Warmbloods, Swedish Warmbloods, Holsteiners, Hanoverians, Selle Francis, and more. Horses of other breeds mostly competed in the lower levels including Quarter Horses, Paint horses, Appaloosas, and Appendixes while large numbers of sport horses competed in the upper levels. Warmblood cross horses were often crossed with Thoroughbreds. Few heavy bodied warmblood horses competed, which occasionally were truly draft horse crosses. This justifies the use of Dutch Warmblood densities for use in the model.

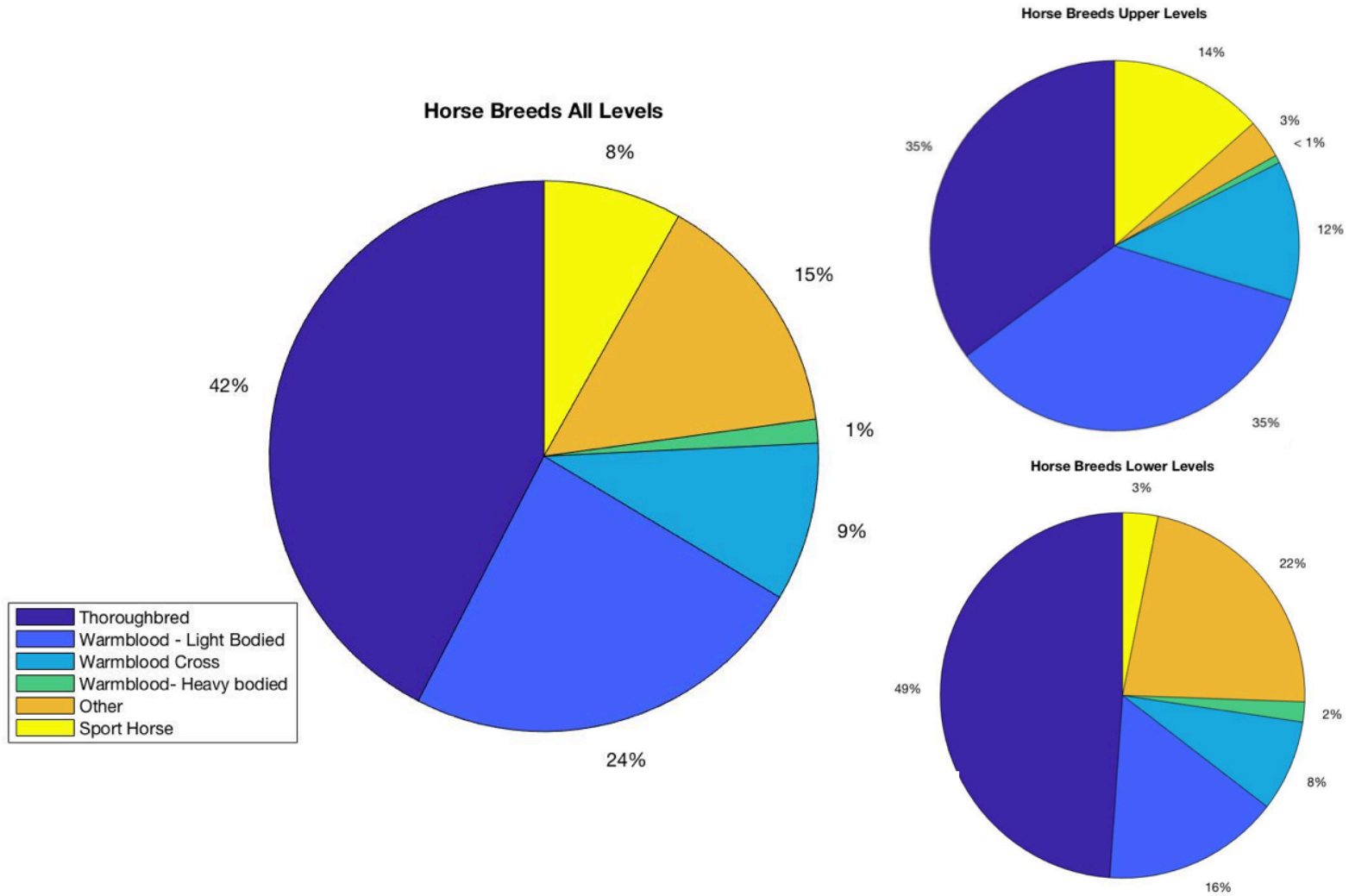


Figure 3.11 Left breed distributions for all levels. (Right Upper) Horse breed distributions for upper levels (Right Lower) Breed distributions for lower level competitors.

3.3.3 Horse Heights and Other Dimensions

Measured heights and sizes of the horses formed normal distributions, but didn't yield a predictive relationship between lengths and circumferences. Some outlier points include ponies which are rare in upper level competition. Upper level measurements are most clearly represented by normal distributions. The histogram in Figure 3.12 shows a tightly grouped height distribution, aside from the outlier 13hh pony competing in Preliminary. The inscribed QQ plot is a measure of how "normal" the distribution is. Since the points on the QQ plot are grouped tightly to the 45 degree line, this indicates consistency with a normal distribution.

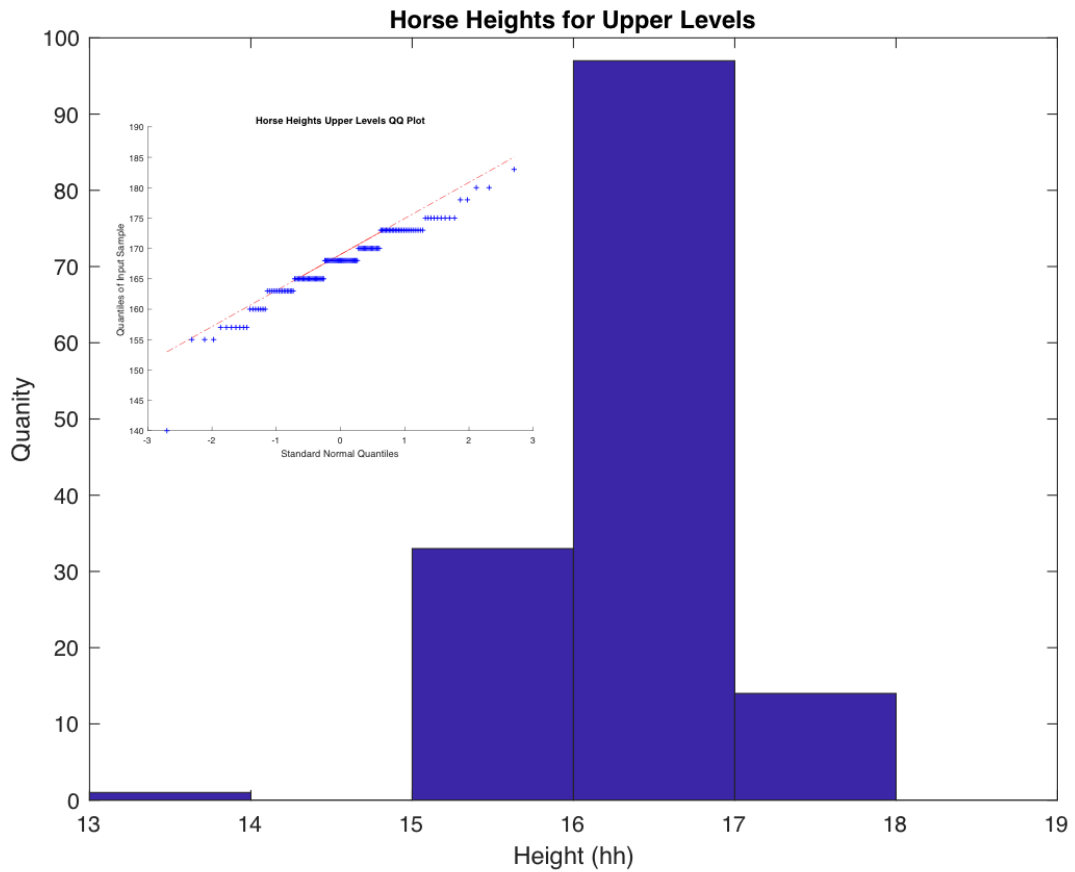


Figure 3.12 The distribution of heights of horses in upper level competitions

Using these values as realistic guides for the statistical ensemble models, a horse with randomly generated measurements along the normal distributions from the survey would be a realistic representation of an eventing horse.

3.3.4 Rider Size

Rider heights and weights were requested in the survey. There is no distinction between men and women in eventing, though in population less men compete in all but

are seen more frequently in upper levels of competition. Gender was not requested in the survey, though. Figure 3.13 provides insight into the height and weight distribution.

Generally riders were of healthy BMI based on their height and weight.



Figure 3.13 The survey response comparison between rider height and weight.

3.3.5 Ensemble Parameters from Survey

In order to generate the population for the statistical ensemble, the average and standard deviation for each parameter is used to create an appropriate normal distribution.

Table 3.5 shows the survey measurement averages and standard deviations for each parameter. Lower level measurements were slightly different than upper level

measurements, but but with this a device would not expected to act much differently at different levels.

Table 3.5 Survey Measurements averages and standard deviations in parenthesis

Average (stdev)	Withers height (hh)	Withers height (cm)	Length of body (cm)	Heart Girth (cm)	Length of neck (cm)	Circumference of Neck (cm)	Length of head (cm)	Cicumference of head (cm)	Rider Height (cm)	Rider Weight (kg)
All Levels	16.1 (1)	166 (8)	173 (14)	193 (9)	71 (6)	97 (9)	57 (4)	65 (5)	169 (9)	63 (10)
Upper Levels	16.3 (1)	168 (6)	170 (10)	194 (7)	71 (5)	98 (6)	57 (4)	65 (4)	172 (8)	64 (10)
Lower Levels	16 (1)	164 (8)	175 (17)	192 (10)	71 (8)	97 (11)	57 (5)	64 (4)	167 (9)	63 (10)

CHAPTER 4. VIDEO STUDIES

4.1 Existing Cross Country Jumping Video and the Importance of Speed

For all stages of the development of a model and a frangible device it is important to know variety of cross country jumping situations in the field. This includes understanding the nature of competitor-fence contacts including the direction, magnitude, position and the speed of the competitor, as well as the outcome of the situation which may be a rotational fall, a horse or rider fall, stumbling or no effect.

Few research studies exist, but for those that do methods of evaluating these field situations include force gauges and more commonly video recording. Video is helpful for understanding and to some extent quantifying physical scenarios, especially for rotational fall situations for which little is known.

There is still relatively little video information available about rotational falls. Existing videos of rotational falls were typically taken for spectator purposes and pan to follow the competitors across the course. Therefore, data on speeds and angles could not be determined from them. Even so, rotation time and qualitative impressions can be extracted to guide this and future study. During a rotational fall, the forces exerted on the ground at takeoff are unknown as well as the reaction of the fence contact.

Speed is the primary contributor to forward momentum and was recognized as a key parameter for determining rotation after a critical forearm contact to a fence. The incoming speed for the simulation calculation must be the jumping speed at the moment of contact. Although cross country courses have an assigned optimum time appropriate for each level, actual on-course speeds vary. Jumps closer together or on turns require the competitor to slow down and many competitor pairs finish above or below the optimum

time. Speeds at cross country jumps have been rarely studied. The USEA supported a GPS Speed Study focused between the fences, but the results have not been published and are not available for fence contact speeds. Speeds in show jumping scenarios have been studied [46], [47], [48]. Speed and take off distance information acquired by video has been found for show jumping situations of different heights and widths, some exceeding dimensions for eventing applications [49].

Jumping position in terms of the body angles listed in Chapter 3 were also largely unavailable in existing literature. This is also a key parameter identified in the sensitivity study in Robles Vega's thesis. As part of the study that led to elimination of the rule that the rider must weigh 75 kg or additional weight would be added, body angle information was included [50]. The jumping position is key to determining the inertia of the horse and rider well as the position of the CG with respect to the contact point. Little existing information was found about distances, jumping angles or instantaneous speeds at the potential time of contact for cross country fences especially on varied terrain slopes or banks but existing methodology for acquiring this information exists [51], [49]. With expansion to more cameras, in other sports information about locating the CG can be learned from video recordings [52]. One such study is considering situations on cross country skiing courses for accelerations from pushing with poles and skis. This expands the possibilities for future studies within eventing. Because of the limited availability of information, a targeted video study was deemed necessary using stationary video recordings set perpendicular to the fence.

Impulses on the fence are important for understanding the activation range and resilient range for the creation of frangible devices. British Eventing supported a study

with force gauges mounted on cross country fences. No rotational fall contacts were measured but it provides other insights on the nature of horse fence contacts.

All preexisting data and data collected for this study are combined to gather an understanding of jumping situations on a cross country course to give insight into the important characteristics of rotational falls.

4.2 Fence Video Study

A video study was added as a part of this project in 2017, with the objectives to understand the variety in speed, jump arc, jumping position and take off distance within Kentucky 3-Day Event competition cross country courses. In April 2019, it was expanded at Chattahoochee Hills Horse Trials to include more situational variety in level and fence type. Though capturing a rotational fall on video would allow detailed study of the circumstance, no one would ever want a dangerous, life-threatening rotational fall to occur. Recording a rotational fall was not the aim of the video study, but instead to capture the nature of a cross country competition as a statistical range of situations.

Videos of a single fence were recorded for three years at Land Rover/RoLEX Kentucky Three-Day Event CCI5*. Video was also recorded at Chattahoochee Hills April 2019 which featured six divisions of competition: Preliminary, CCI2*-S, Intermediate, CCI-3*, Advanced, and CCI4*-S. The number of videos recorded at each competition is shown in Table 4.1 totaling to 218 videos. The greater number of riders competing in a single division at K3DE results in a better, larger sample size.

Table 4.1 Number of video recordings at each event

Competition	Number of Videos
CH CCI4*-S	25
CH Advanced	16
CH CCI3*-S	20
CH Intermediate	5
CH CCI2*-S	16
CH Prelim Vert	7
CH Prelim Tiger Trap	6
RK3DE 2017	47
LRK3DE 2018	40
LRK3DE 2019	36
Total	218

4.3 Video Recording and Analysis Techniques

The RK3DE 2017 videos were recorded using a GoPro Hero 3 and the rest of the videos were recorded using a GoPro Hero 4 Silver set on a tripod as perpendicular as possible to the fence and the plane of motion of the jump as shown in Figure 4.1. The cameras were selected for the function of one button push to both turn the camera on and record and a second button push to cease recording and power off to save battery for all day use. GoPros are durable and in a waterproof case, suitable for changing weather conditions. The GoPro also has a wide field of view useful for capturing video from the narrow galloping lane. Disadvantages of the GoPro include fisheye distortion, which was mitigated by using the narrow field-of-view setting and lack of zoom.



Figure 4.1 Camera set up at a T-oxer at Chattahoochee Hills

Videos were analyzed using free and open source Kinovea software (beta version 8.27). Kinovea was developed for sports motion tracking purposes. Useful features include point tracking and marking.

There are some limitations in the video tracking technique. Typical video tracking methods include planar movements with a designated approach and trackable white or reflective markers for key points. However, these videos were taken during sanctioned events where competitors approach the fence from different angles and positions along

the length of the fence and wore no special markers on tracked points. These decrease the accuracy of the measurements, but are still suitable for these statistical ranges.

4.3.1 Details of Fences in Video Study

Rolex Kentucky Three-Day Event 2017 Fence 14 was an open oxer fitted with MiM Clips on the front and rear rails is shown in Figure 4.2. The fence was on a slight downhill after a long gallop. The competition was a CCI4* (now 5*) competition. There were no problems at this fence. During the competition it rained, giving a difference in footing among competitors. Videos were recorded at 60 frames per second (fps) and at a resolution of 1280x720p. The competitor comes from the left to right in this video frame.



Figure 4.2 RK3DE 2017's Fence 14 was an open oxer with MIM Clips on the front and rear rail.

Land Rover Kentucky Three-Day Event 2018 Fence 4a was a vertical fitted with MiM Clips which landed on a downhill quickly followed by a water jump and bending to another jump on an uphill approach as shown in 4.3. The competition was a CCI4* (now 5*) competition. Videos were shot at 120 fps and 1280x720p. The competitor comes from the left to right in this video frame.



Figure 4.3 LRK3DE 2018's Fence 4 is a vertical with MiM Clips followed by a water complex.

Land Rover Kentucky Three-Day Event 2019 Fence 4 was an open oxer fitted with MiM Clips on the front and rear rails as shown in Figure 4.4. The fence was the second jump situated on a line bending right from an open oxer 6-7 strides away, also fitted with MiM on both rails. Several problems and falls occurred at the preceding fence on course but not at the fence filmed. The timber rails on Fence 4 were fairly small. The competition was a CCI5*. Videos were shot at 120 fps and 1280x720p. The competitor comes from the left to right in this video frame.



Figure 4.4 LRK3DE 2019's Fence 4 was an open oxer with thin rails and MiM Clips on the front and rear rails.

Chattahoochee Hills (CH) CCI4*-S Fence 11 was a “T-oxer” table type jump with a long gallop before and a long turn to a water complex afterwards as shown in Figure 4.5. Videos were shot at 60 fps and 1920x1080p. The competitor comes from the left to right in this video frame.



Figure 4.5 The Chattahoochee Hills CCI4*-S T-Oxer was a galloping fence.

Chattahoochee Hills Advanced Fence 3b was a table on a downhill “S” curve combination including Fence 3a open oxer right turn to the 3b table and left turn to an identical 3c table as shown in Figure 4.6. Videos were shot at 60 fps and 1920x1080p. The competitor comes from the left to right in this video frame.



Figure 4.6 The Chattahoochee Hills Advanced table was near the beginning of the course.

Chattahoochee Hills CCI3*-S Fence 16a was a vertical log after a turning gallop, that landed on a downhill to approach a corner as shown in Figure 4.7. Though there were not many problems at 16a, at the corner there were many run outs due to the angle of approach and tight jumping space. Videos were shot at 60 fps and 1920x1080p. The competitor comes from the right to left in this video frame.



Figure 4.7 Chattahoochee Hills CCI3*-S's vertical preceded a narrow corner at the bottom of a hill.

Chattahoochee Hills Intermediate Fence 9b was a brush corner after a table bending left followed by a gallop on flat terrain as shown in Figure 4.8. This video was shot as an experiment on how to video corners for due to their geometry and invitation for varying approach angles. Videos were shot at 60 fps and 1920x1080p. The competitor comes from the right to left in this video frame.



Figure 4.8 Chattahoochee Hills Intermediate Corner shown prompted runouts from a few competitors.

Chattahoochee Hills CCI2*-S Fence 10 was a galloping “T-oxer”, as shown in Figure 4.9, similar to the CCI4*-S T-Oxer. This fence was chosen to compare the speeds and positions at different levels of competition. Videos were shot at 60 fps and 1920x1080p. The competitor comes from the left to right in this video frame.



Figure 4.9 Chattahoochee Hills CCI2*-S T-Oxer was after a gallop.

Chattahoochee Hills Preliminary Fence 16 was a “Tiger Trap” ramped fence with MiM on the upper rail as shown in Figure 4.10. This fence was activated once and a similar fence beside it in another division was also activated. It had rained fairly heavily the night before this competition. Videos were shot at 60 fps and 1920x1080p. The competitor comes from the left to right in this video frame.



Figure 4.10 Chattahoochee Hills Preliminary Tiger Trap prompted big jumps from the competing horses.

Chattahoochee Hills Preliminary Fence 14a was a vertical, as shown in Figure 4.11, to a corner similar to the one recorded in the CCI3*-S. The corner following 14a was placed on a more straight forward approach and there were few problems for competitors. It had rained fairly heavily the night before this competition. Videos were shot at 60 fps and 1920x1080p. The competitor comes from the left to the right in this video frame.



Figure 4.11 Chattahoochee Hills Preliminary Vertical was followed by a simpler corner than the one in the CCI3*-S.

4.3.2 Overall Speeds on Course

Cross country courses are assigned an average speed by the level of competition as shown for USEF/USEA Events in Table 4.2 and Table 4.3. The speed and distance of

the track increases as the level increases. The optimum time to complete is unique to each course and is calculated by the distance of the track divided by the optimum speed [13].

Table 4.2 USEA/USEF Cross Country Speeds and Distances

	Beginner Novice	Novice	Training	Modified	Preliminary	Intermediate	Advanced
Track distance (m)	1400- 2000	1600- 2200	2000- 2600	2200- 3000	2200- 3120	2600- 3575	3200- 3990
Optimum speed, mpm (m/s)	300-350 (5-5.8)	350-400 (5.8- 6.7)	420- 470 (7-7.8)	490 (8.2)	520 (8.7)	550 (9.2)	570 (9.5)

Table 4.3 FEI Cross Country Speeds and Distances

	CCI 1*	CCI 2*-S	CCI 2*-L	CCI 3*-S	CCI 3*-L	CCI 4*-S	CCI 4*-L	CCI 5*
Track Distance (m)	2000- 3000	2600- 3120	3640- 4680	3025- 3575	4400- 5500	3420	5700- 6270	6270- 6840
Optimum speed, mpm (m/s)	500 (8.3)	520 (8.7)	520 (8.7)	550 (9.2)	550 (9.2)	570 (9.5)	570 (9.5)	570 (9.5)

Despite the average optimum speed on course, the instantaneous speed of the horse fluctuates so the average optimum speed is most likely not the jumping speed. Horse and rider approach jumps at different speeds due to difference in competitor preference as well as the type of jump and its placement. Often as the level increases, fewer competitors achieve the optimum time, for example in LRK3DE 2019 only 4 pairs completed the course within the time allowed while 31 completed the course with time penalties and 6 competitors were eliminated or retired on course. While a very rough

estimate of speed could be estimated from these numbers, it is more useful to know the speed of the competitor at the time of jumping.

4.3.3 Jumping Speeds

The jumping speeds are determined from the videos by tracking the rider's knee as an estimate of the horse and rider's CG. For example, the trace of the CG path throughout the entire video can be seen in Figure 4.12, which is a video frame at the takeoff of the jump.

For a particular jump, the average speeds for each attempt form a normal distribution. The normality is verified through a histogram resembling a normal distribution and a nearly linear QQ plot. An example of a histogram and embedded QQ plot is shown in Figure, histogram and QQ plot combinations for the rest of the jumps are included in Appendix C.

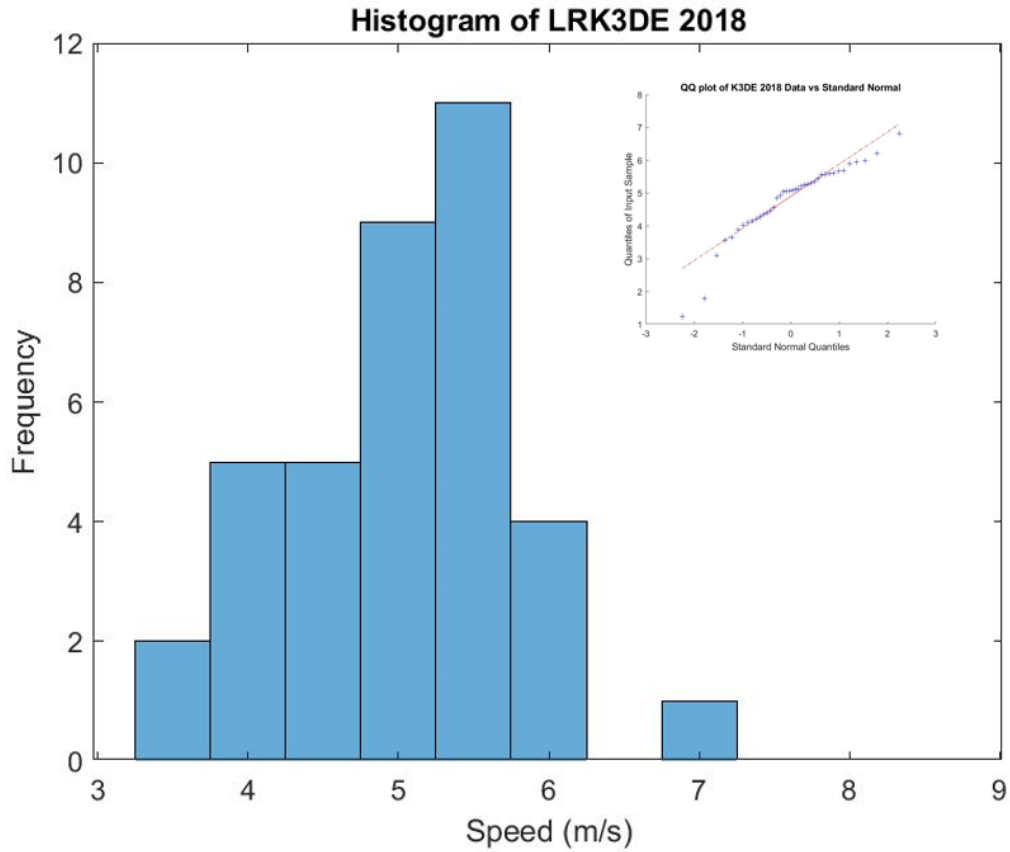


Figure 4.12 LRK3DE 2018 histogram of speeds and embedded QQ plot demonstrate normal distribution.

The mean filmed speed and standard deviation, shown in Table 4.4, was found for the overall duration of the video and the jumping speed calculated from the time the horse's hind legs left the ground until the front legs touched the ground.

Table 4.4 The average speed overall and in-air jumping for each event captured

Event/Level	Overall Speed		In Air Jumping Speed		
	Mean (m/s)	Stdev	Speed (m/s)	Stdev	Optimum Speed
RK3DE 2017 CCI5*	5.60	0.72	6.12	0.33	9.5 m/s
LRK3DE 2018 CCI5*	4.73	0.71	4.81	0.33	9.5 m/s
LRK3DE 2019 CCI5*	5.64	0.73	6.28	0.31	9.5 m/s
CCI4*-S	6.51	0.79	7.24	0.34	9.5 m/s
Advanced	6.30	0.87	7.10	0.29	9.5 m/s
CCI3*-S	4.77	0.57	5.18	0.33	9.2 m/s
Intermediate	7.88	0.61	---	---	9.2 m/s
CCI2*-S	6.29	0.72	6.95	0.30	8.7 m/s
Preliminary (TT)	6.34	1.04	7.25	0.22	8.7 m/s
Preliminary (Vert)	5.52	0.77	5.86	0.45	8.7 m/s

In every case recorded, the mean jump speed was higher than the overall speed. It is notable that all of the speeds recorded are lower than the optimum speeds for each level in the USEA/USEF and FEI in Table 4.2 and 4.3. This makes sense that gallops between fences would have competitors “making up time” at higher speeds than while jumping.

Fences can be grouped according to fence type for identifying commonalities. Fences can be compared by the average and standard deviation of speeds and because the speed distributions have been proven to be normal through the QQ plots can also be compared through Student’s t-test at a 95% confidence interval.

Three vertical jumps were LRK3DE 2018 Fence 4, CH CCI3*-S Fence 16a, and CH Preliminary Vertical 14a. These fences were jumped at the lowest average speeds from 4.81 to 5.86 m/s. This may be because they require precision and were a part of a combination of fences. Opposite of the optimum speed, the jumping speed trended inverse to the level, with the Preliminary fence jumping at the highest speed. This could be a testament to the wide variety of speeds seen at higher levels and the difficulty of the

following fences in the combination or the limited number of videos recorded at CH. Using Student's t-test at a 95% confidence interval, if two jumps were taken at distinct speed distributions, the p value would be less than 0.05. T-test comparisons are shown in Table 4.5. This is what is seen when comparing the other two verticals to CH Prelim Fence 14a. However, the P-value for the LRK3DE 2018 Fence 4 and CH CCI-3*-S Fence 14a was 0.179. This alludes to the fences being jumped at speeds that are not distinct from one another and present an opportunity to share similar conditions for frangible devices. More videos would increase the quality of this result.

Oxer jumps included the RK3DE 2017, LRK3DE 2019, CH CCI4*-S, and CH CCI2*-S which ranged in speeds from 6.1 to 7.5 m/s. The only fence in a somewhat related distance to another fence was the LRK3DE 2019 oxer, but it was jumped at similar speeds to the other galloping oxers in the open. Jumping speeds could not be proven distinct for both CCI5* open oxers RK3DE 2017 Fence14 and LRK3DE 2019 Fence 4 and the similarly designed CH CCI4*-S and CH CCI2*-S T-oxers. This presents an opportunity for some fence groupings for similar approach speeds.

The following tables presents t-test comparisons for all fences recorded in this thesis with each other fence. Dark borders surround the comparisons of similar jump types. Note that 64% of the jump approach speed comparisons suggest very distinct jumping situations with very low p-values, which indicates the need for different safety device sensitivities between the fences. These very distinct populations are colored in red. There were three situations (8%) marked in pink which involve preliminary fences (which had low sample sizes and should be considered for more data collection) being indistinct within a 90% confidence interval. Perhaps with more sampling these would

prove to be indistinct populations and candidates for using the same safety device. Fence comparisons marked in blue did not demonstrate distinctive populations with p values less than 0.05, making them possible candidates for using the same safety device activation threshold. 28% of the comparisons showed similarities.

Table 4.5 A fence wise comparison of p-values for jumping speeds

Jumping Speed p-value		Verticals			Oxers			Table	Other	
		KY CCI5* 2018	CH CCI3*-S	CH Prelim	KY CCI5* 2017	KY CCI5* 2019	CH CCI4*-S	CH CCI2*-S	CH Adv	CH Prelim
		Fence 4	Fence 16a	Fence 14a	Fence 14	Fence 4	Fence 11	Fence 10	Fence 3b	Fence 16
KY CCI5* 2018	Fence 4		0.179	0.0196	7.54E-09	5.06E-10	1.34E-14	9.27E-09	2.65E-10	9.87E-06
CH CCI3*-S	Fence 16a			0.0246	1.59E-05	3.10E-08	2.26E-13	5.87E-08	4.84E-10	1.28E-05
CH Prelim	Fence 14a				0.3904	0.0798	1.92E-05	0.0057	3.55E-04	0.021
KY CCI5* 2017	Fence 14					0.2994	5.91E-08	9.01E-04	4.03E-05	0.0033
KY CCI5* 2019	Fence 4						1.44E-07	0.0022	5.51E-05	0.0033
CH CCI4*-S	Fence 11							0.2358	0.4995	0.9868
CH CCI2*-S	Fence 10								0.6039	0.5349
CH Adv	Fence 3b									0.7145
CH Prelim	Fence 16									

Figure 4.13 is a box and whisker plot comparing the in-air jumping speeds of three fences recorded in CCI5* competitions during the Kentucky 3-Day Event. The “whiskers” of the plot display the range while the box displays the inner-quartile range. The line within the box shows the median and the plus signs display any outliers. Outliers are usually points where the competitor had a refusal or ran into the fence. Higher speeds were seen in the two oxer jumps. The 2017 Fence 14 was placed on a gallop and had a wider range of speed while the 2019 Fence 4 followed another jump and had a smaller range. In combination with Table 4.5, Figure 4.13 demonstrates the differences in jump speed between oxers and verticals and the similarity in speeds between the two CCI5* Oxers.

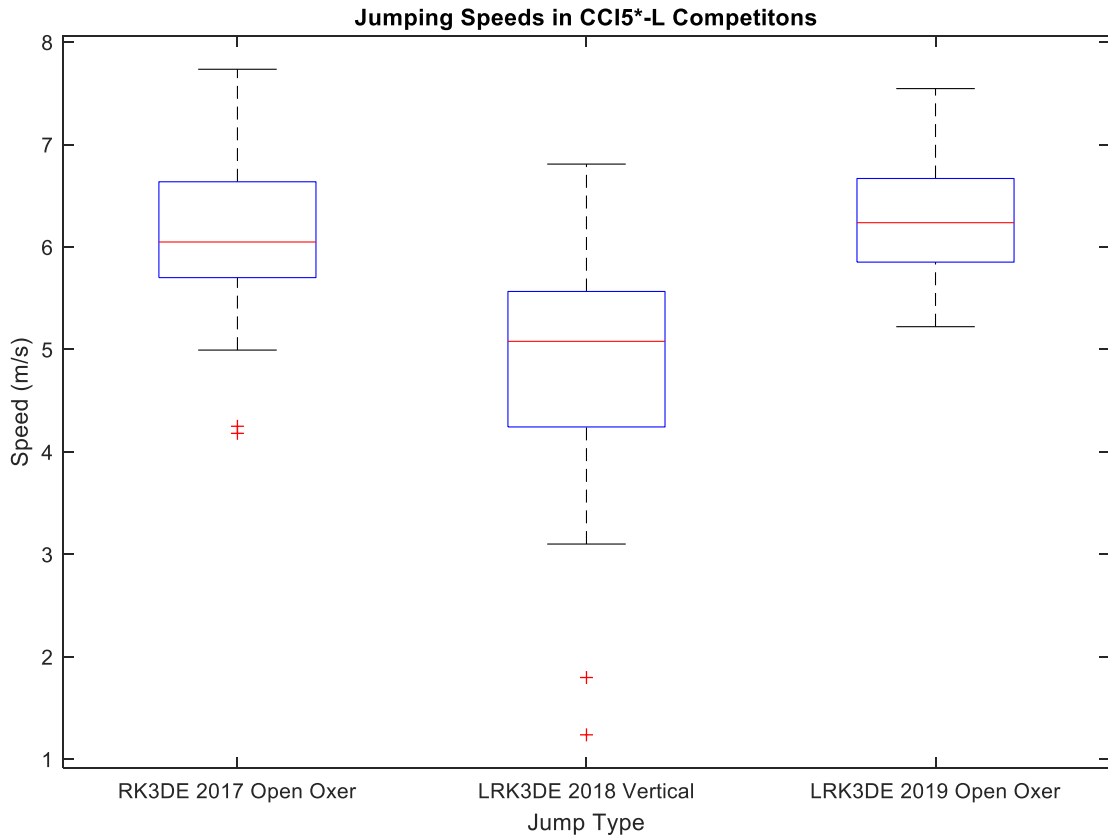


Figure 4.13 A box and whisker plot comparison of the three fences filmed during CCI5* competition

The results from the Chattahoochee Hills Horse Trials display a wider range of speeds than the CCI5* videos as seen in Figure 4.14. The Preliminary Tiger Trap has speeds at the top of the range nearing 9 m/s while the more technical 3* Vertical is at the bottom of the range near 4 m/s. Higher speeds do not indicate a higher level for every jump, which is further exemplified by the t-tests in Table 4.5.

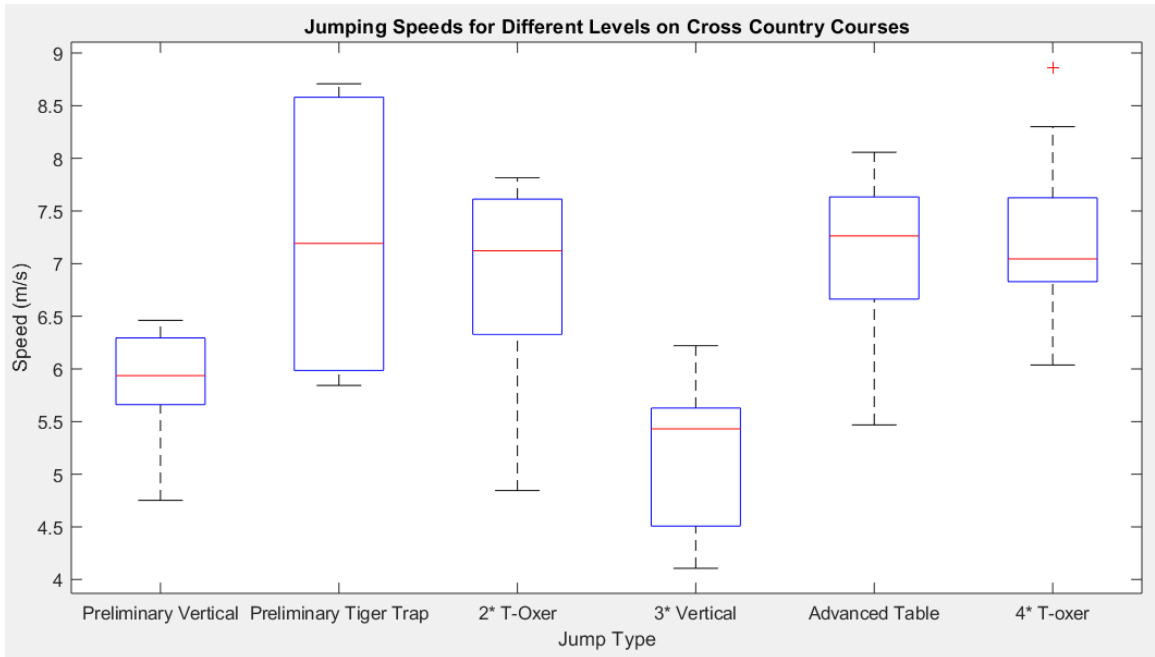


Figure 4.14 This box and whisker plot presents all of the jumps recorded at the Chattahoochee Hills April 2019 Horse Trials.

Due to the small sample size of jumps particularly at CH, final conclusions about the speeds of all oxer, vertical and other fence types may not be drawn. However this study does demonstrate differences in speeds between optimum course speed and jump speed in cross country competition. It also verifies that jumping speeds are different for different fences, through there may be opportunity to group fences with indistinct jumping speed distributions together for the purposes of using and designing safety devices. Further video data on speed populations over cross country and their would be useful for device development and proper selection on course.

4.3.4 Jumping Angles

The jumping angles describe the jumping position of a horse. These jumping angles correspond to transforming the FCM from a standing position to a jumping position. The five jumping angles detailed in Chapter 3 and Figure 3.3 include the body, neck, head and antebrachium angle of the horse, and the rider angle.

From the video analysis in Kinovea, points were plotted at the time the horse's front leg is crossing the front rail to extract the jumping angles. Points plotted on the frame are shown on Figure 4.15 and include the horse's nostril, the base of ear, midpoint along the horse's base of neck, the lower of the front knee, the elbow, stifle, hind foot, and the rider's knee which represents the combined horse and rider CG. Using these points, the body angles can be determined for typical jumping positions in the field and along with their variability.



Figure 4.15 A sample of a frame from the LRK3DE 2019 CCI5* analyzed in Kinovea with jumping point markers shown at the time the horse's knees cross the front rail. The trace of the CG represented by the rider's knee is also shown.

The average and the standard deviation of the jumping angles are shown below in Table 4.6. Note that these fall within the ranges developed in Chapter 3 except for the antebrachium angle. Most of the videos recorded were of the horses jumping successfully, with their knees above their shoulder instead of pointing downward, which is a characteristic of a forearm contact which may lead to a rotational fall. That means the antebrachium angles listed below would be different for critical contacts, though the Body, Neck, and Head angles should be similar. Due to parallax error from the positioning of the camera, the angles measured in the videos may have some difference from the actual angles. Another reason for differences between determined body angle and the actual angle is the location of the marker for the stifle, which was difficult to keep consistent in the video software without physical markers placed directly on the horse.

Similarities are seen between the body angle and the fence type. LRK3DE 2018, CH CCI3*-S, and CH Prelim Vert were all vertical jumps with body angles of approximately -24° to -25° . RK3DE 2017 and LRK3DE 2019 were open oxers of similar sizes and had angles of about -32° . Due to the limited data set, no conclusions may be drawn for other fence types, similarities could establish a baseline corresponding to these fence types. For simulation purposes angle ranges, maximums, and minimums are useful if uniform angle ranges are to be considered.

Table 4.6 Average jumping position angles and standard deviations for the events video recorded.

Angle (degrees)	RK3DE 2017	LRK3DE 2018	LRK3DE 2019	CH CCI4*-S	CH Advanced	CH CCI3*-S	CH CCI2*-S	CH Prelim TT	CH Prelim Vert
Body	-32.3 (5.5)	-24.0 (5.1)	-31.5 (9.3)	-36.9 (2.4)	-20.2 (4.4)	-25.2 (7.1)	-19.6 (4.1)	-17.9 (5.3)	-24.2 (33.1)
Neck	153.3 (11.1)	158.0 (15.5)	153.1 (15.8)	151.7 (7.6)	149.6 (18.3)	154.5 (10.3)	155.2 (9.7)	158.8 (7.8)	154.3 (13.3)
Head	238.6 (9.3)	242.5 (42.8)	239.5 (11.4)	248.6 (8.4)	244.8 (14.6)	243.3 (35.3)	248.7 (6.0)	245.8 (7.7)	250.7 (10.6)
Antebrachium	177.2 (21.1)	174.7 (15.3)	177.1 (23.4)	161.8 (4.9)	172.6 (29.1)	191.5 (38.5)	173.0 (17.9)	161.0 (15.1)	193.7 (33.1)

Jumping position angles can also be compared using Student’s t-test at a 95% and 90% confidence. The body angle is most sensitive parameter to the overturning analysis and are compared fence-wise in Table 4.7. Similarities in position can be used for commonalities in device use and development. Body angles that are very distinct with a p-value less than 0.05 include 67% of the comparisons. Distinct comparisons, with a p value greater than 0.10 or a 90% confidence level accounted for 14% of the comparisons. Indistinct comparisons represent 19% of the comparisons made, which would be an opportunity for using similar conditions for creating and implementing frangible devices. Notably, the body angles for all three vertical jumps are indistinct and possible candidates for sharing the same device under this criteria.

Table 4.7 A fence wise comparison of p-values for jumping Body Angles

Body Angle p-value		Verticals			Oxers				Table	Other
		KY CCI5* 2018	CH CCI3*-S	CH Prelim	KY CCI5* 2017	KY CCI5* 2019	CH CCI4*-S	CH CCI2*-S	CH Adv	CH Prelim
		Fence 4	Fence 16a	Fence 14a	Fence 14	Fence 4	Fence 11	Fence 10	Fence 3b	Fence 16
KY CCI5* 2018	Fence 4		0.442	0.918	1.53E-10	1.48E-09	1.08E-17	0.003	0.012	0.004
CH CCI3*-S	Fence 16a			0.723	3.99E-05	1.30E-04	1.36E-09	0.008	0.019	0.016
CH Prelim	Fence 14a				4.29E-04	9.56E-05	8.20E-12	0.021	0.050	0.004
KY CCI5* 2017	Fence 14					0.490	1.48E-04	5.93E-12	4.12E-11	3.09E-08
KY CCI5* 2019	Fence 4						2.09E-07	8.52E-13	8.03E-12	7.56E-10
CH CCI4*-S	Fence 11							1.00E-19	1.25E-18	3.20E-17
CH CCI2*-S	Fence 10								0.681	0.258
CH Adv	Fence 3b									0.167
CH Prelim	Fence 16									

Table 4.8, demonstrates that all of the comparisons made with neck angles during different jumps are indistinct. In Table 4.9, the majority, 81%, of fences compared by Head Angle have p-values more than 0.05 and are indistinct. There are 8% distinct values and 11% very distinct values when comparing the Head Angle. This demonstrates opportunities to share values.

Table 4.8 A fence wise comparison of p-values for jumping Neck Angles

Neck Angle p-value		Verticals			Oxers				Table	Other
		KY CCI5* 2018	CH CCI3*-S	CH Prelim	KY CCI5* 2017	KY CCI5* 2019	CH CCI4*-S	CH CCI2*-S	CH Adv	CH Prelim
		Fence 4	Fence 16a	Fence 14a	Fence 14	Fence 4	Fence 11	Fence 10	Fence 3b	Fence 16
KY CCI5* 2018	Fence 4		0.364	0.579	0.105	0.177	0.064	0.516	0.087	0.923
CH CCI3*-S	Fence 16a			0.965	0.690	0.724	0.304	0.841	0.320	0.444
CH Prelim	Fence 14a				0.850	0.865	0.532	0.861	0.579	0.564
KY CCI5* 2017	Fence 14					0.937	0.522	0.564	0.339	0.346
KY CCI5* 2019	Fence 4						0.690	0.637	0.493	0.488
CH CCI4*-S	Fence 11							0.215	0.612	0.097
CH CCI2*-S	Fence 10								0.304	0.508
CH Adv	Fence 3b									0.350
CH Prelim	Fence 16									

Table 4.9 A fence wise comparison of p-values for jumping Head Angles

Head Angle p-value		Verticals			Oxers				Table	Other
		KY CCI5* 2018	CH CCI3*-S	CH Prelim	KY CCI5* 2017	KY CCI5* 2019	CH CCI4*-S	CH CCI2*-S	CH Adv	CH Prelim
		Fence 4	Fence 16a	Fence 14a	Fence 14	Fence 4	Fence 11	Fence 10	Fence 3b	Fence 16
KY CCI5* 2018	Fence 4		0.945	0.620	0.541	0.689	0.487	0.624	0.832	0.851
CH CCI3*-S	Fence 16a			0.593	0.396	0.562	0.470	0.605	0.867	0.863
CH Prelim	Fence 14a				0.003	0.021	0.583	0.599	0.353	0.373
KY CCI5* 2017	Fence 14					0.684	2.66E-05	7.30E-04	0.049	0.072
KY CCI5* 2019	Fence 4						0.001	0.011	0.160	0.199
CH CCI4*-S	Fence 11							0.975	0.305	0.474
CH CCI2*-S	Fence 10								0.403	0.403
CH Adv	Fence 3b									0.877
CH Prelim	Fence 16									

Using the Student's t-test to compare values and identify distinct and indistinct fence conditions can be used for identifying placement and development opportunities for safety devices as well as for simplification of inputs to the computer impulse momentum ensemble.

4.3.5 Take-off Distances

Riders and others in the sport often refer to the take-off distance as having a major influence on the horse's jump of the fence. Table 4.10 presents the take-off distance as the distance from the base of the jump to the horse's hind feet just before takeoff. The jump arc range is both the horizontal range of the jump (x) and the change in elevation

(y) from take-off to landing. Here the take-off is where the hind legs leave the ground and the landing is where the front legs meet the ground.

Table 4.10 Information about the horse's jumping trajectory

Event and Level	Jump Height (m)	Angle of fence (degrees)	Take off distance (m)	Jump Arc Range (m)		Take off Distance to Jump Height
				x	y	
RK3DE 2017	1.03	62	0.71 (0.23)	3.87 (0.45)	0.16 (0.08)	0.69
LRK3DE 2018	1.34	80	1.35(0.28)	2.93 (0.53)	0.16 (0.06)	1
LRK3DE 2019	1.16	65	0.65 (0.25)	2.70 (0.45)	0.95 (0.41)	0.6
CH CC14*-S	0.7	54	0.67 (0.03)	3.60 (0.28)	0.12 (0.04)	0.96
CH Advanced	0.81	55	1.47 (0.45)	4.67 (0.59)	0.22 (0.06)	1.8
CH CC13*-S	0.94	79	1.02 (0.26)	2.94 (0.45)	0.29 (0.06)	0.86
CH CC12*-S	0.86	49	0.54 (.30)	4.21 (0.53)	0.06 (0.08)	0.62
CH Prelim Vertical	1.04	62	1.04 (0.39)	3.56 (0.63)	0.17 (0.09)	1
CH Prelim Tiger Trap	0.91	47	0.97 (0.43)	4.53 (0.75)	0.31 (0.11)	1.07

4.3.6 Video Contacts

Cross country jumps are often contacted incidentally. Minor collisions can be hoof strikes, lower front leg contacts, rear leg strikes and sometimes more major contacts like the horses crashing, scraping across the tops of jumps, or body contacts such as the horse's chest or stomach. Though these contacts do not necessarily bring penalty to competitors, it is important that a jump withstand these incidental contacts, especially if it is a frangible fence so that competitors are not penalized without necessity. Examples of different incidental contacts are shown below in Figure 4.16. Figure 4.16 (a) shows a lower front limb contact and (b) shows a front hoof strike. Neither of these situations present a danger to the competitor and the jump must be able to withstand these in typical use. Figure 4.16 (c) displays a critical forearm contact, what people in the sport would call a hung leg. Though this contact did not result in a rotational fall these sorts of

contacts should be assessed carefully. Figure 4.16 (d) shows a crashing body contact where the horse's chest is in contact with the fence. In this video the competitor did not clear the fence and did not rotate. The jump was fitted with MiM Clips and they did not activate.



Figure 4.16 Examples of (a) lower limb incidental impact; (b) incidental hoof strike or lower leg impact; (c) foreleg contact in the critical range, such as for competitors at the highest risk for a rotational fall (here did not rotate); (d) crash contact with the horse's chest sliding into the fence (did not clear the obstacle).

Understanding of the occurrence of jump attempts, incidental contacts and critical contacts is useful. Table 4.11 details the number of front and rear leg/hoof strikes that are incidental to the competition as well as the critical antebrachium contacts. Most jumps

incurred significant numbers of incidental contacts and scrapes, indicating the requirement for resilient cross country jumps with the CH Advanced table enduring the most contacts for 69% of jump attempts. Two vertical jumps, LRK3DE 2018 and CH CCI3*-S, had critical contacts in the forearm range (no rotations occurred) but the CH Prelim Vertical did not. These results indicate the environment for the wear and fatigue of a device.

Table 4.11 The amount of contacts on the fences in all recorded videos.

Event and Level	Number of Videos	Front Leg Strike	Rear Leg Strike	Crashing contact	Antebrachium Contact	Incidental Contact %	Critical Contact %
RK3DE 2017	47	4	6	0	0	21%	0%
LRK3DE 2018	40	12	10	3	2	55%	5%
LRK3DE 2019	36	9	8	0	0	47%	0%
CH CCI4*-S	25	1	0	0	0	4%	0%
CH Advanced	16	7	4	0	0	69%	0%
CH CCI3*-S	20	3	0	0	3	15%	15%
CH CCI2*-S	16	0	0	0	0	0%	0%
CH Prelim Vertical	7	0	1	0	0	14%	0%
CH Prelim Tiger Trap	6	1	2	0	0	50%	0%

Though it was not recorded as a part of the study, the CH Prelim Tiger Trap and a similar fence in a higher level were fitted with MiM devices and each activated once during competition by landing on the rail with the horse's hind legs. This activation may have prevented injury to the horse and rider but were not conditions for the rotational falls studied in this thesis.

4.4 BE Fence Contact Study

Collisions with cross country fences were comprehensively studied in a 2008 and 2009 British Eventing (BE) research project. There were two instrumented fences: one significantly ramped to a rail and the other a table with front and rear rails protruding from the table top as shown in Figure 4.17 (a) and (b). The rails were instrumented with force gauges below and behind the rails to measure force time histories in the x and y directions. In 2008, 60 impacts were recorded and in 2009, 229 front or rear rail impacts were measured. Video for the top 20 force magnitudes were shared for each year. No rotational falls occurred. From this study, the idea of incidental hoof strikes and lower leg impacts was identified, and additionally noted were higher magnitude body impacts and a horse pushing off the fence itself for support.

Unlike the jumps recorded in this thesis, the BE instrumented fences were placed on multiple courses in different positions.

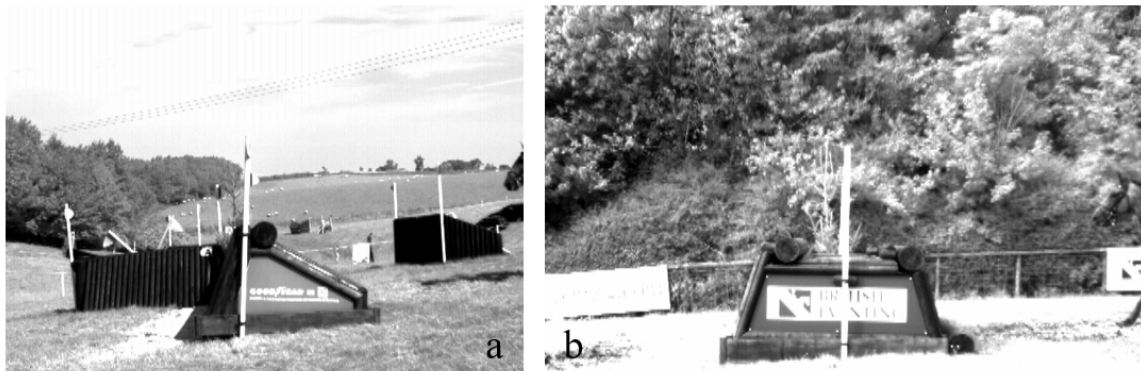


Figure 4.17 (a) The 2008 Goodyear instrumented fence was placed on different courses throughout the year and is shown on a downhill approach in this situation [53]. (b) The 2009 British Eventing fence was built with a more upright face than the 2008 jump and was an oxer with two instrumented rails [53].

Video recordings from the BE instrumented fence study were shared for the top 20 fence impacts for each year. Many of these high magnitude contacts were rear leg collisions or body contacts. Sometimes the horse appeared to be pushing off the jump like a spring board. Of the 20 top contacts in 2008, only one approached being a critical contact, but the contact was on the lower knee as shown in Figure 4.18 (a). Similarly in 2009 there were two knee contacts shown in Figure 4.18 (b) and (c). These contacts were just below the critical antebrachium region, setting up similarities in geometry to a rotational fall case but the impulse measurement would likely be different.

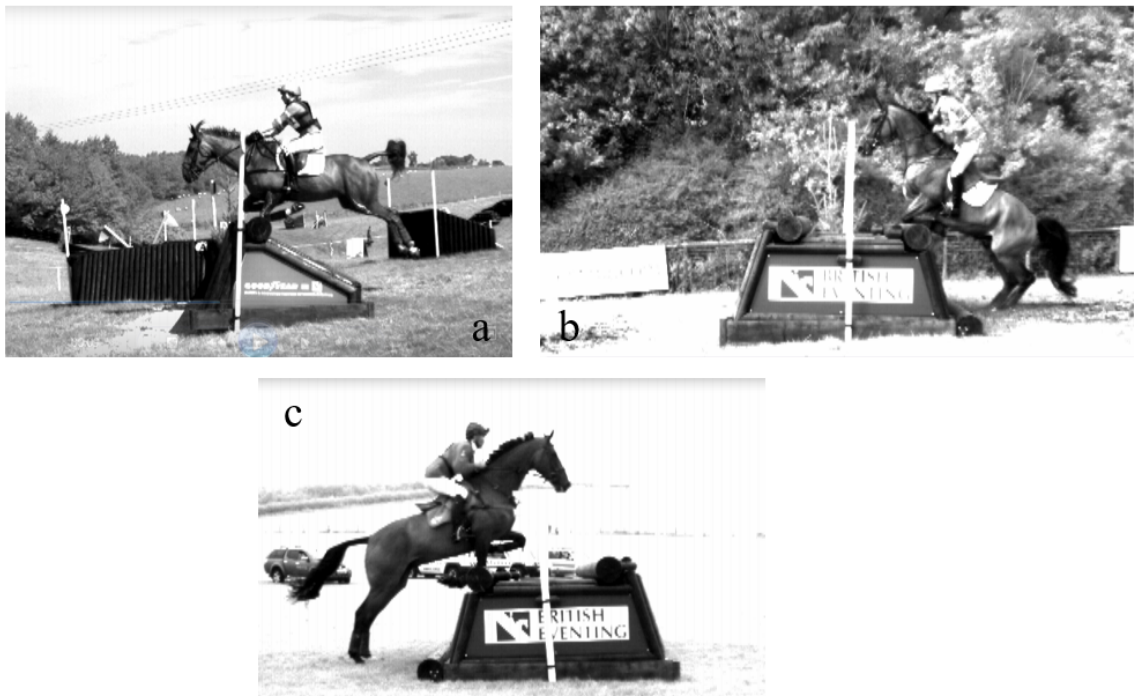


Figure 4.18 (a), (b), and (c). Nearest to forearm critical contacts in the top 20 British Eventing instrumented fence study videos [53].

Information from these contacts could be interpreted in a variety of ways. Since no rotational falls occurred, some may think that fences should be resistant to the forces presented. A better way would be to consider that the fences need to be resistant to hoof

strikes and lower limb contacts, but consider body collisions more carefully along with critical forearm contacts. There is not enough information in these videos to determine an expected force range for rotational falls or critical contacts because they either did not occur or were not identified.

This BE study captured the reaction forces on the fence revealing information about the types of contacts a fence should expect. The rose plot in Figure 4.19 shows the 35 impact angles from the 2009 BE Fence's front leg, front rail contacts. The direction of approach of the horse presented is right to left. From this plot it is noted that the impacts mostly align with the x axis, but also have some contacts with negative angles, meaning the horse is contacting the fence from below the front rail. This gives an idea of the proposed activation range for fences with frangible devices.

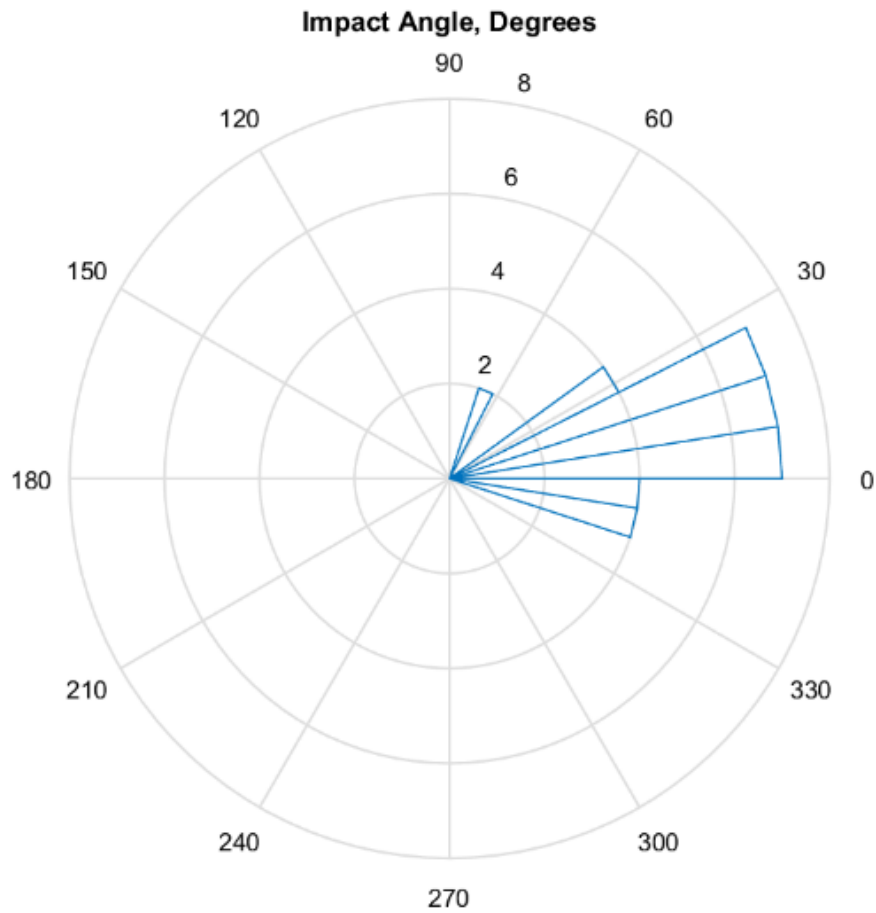


Figure 4.19 Rose Plot of Angle Distribution for Front Rail Front Leg Impacts

In Figure 4.20, the angles presented in Figure 4.19 are presented along the x axis corresponding to calculated impulse values on the y axis. The axis range are wide enough to include all of the maximum impulse values for the 2008 and 2009 data, which displays the idea that these front leg front rail contact magnitudes may be less than some of the hind leg contacts. This introduces the idea of the necessity of tailoring the safety device's activation range to particular angles.

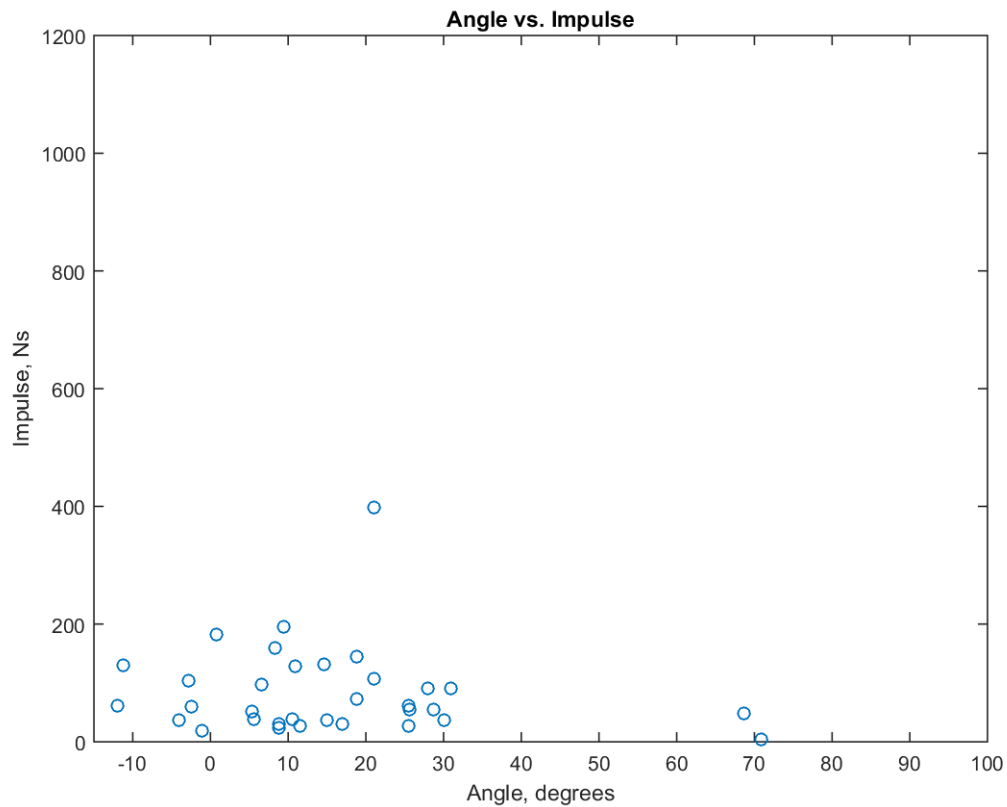


Figure 4.20 Angle vs. Impulse Scatter Plot for Front Rail Front Leg Impacts

Despite having no rotational falls recorded with the camera arrangement that allows scientific observation, the British Eventing instrumented fences and the videos recorded for this study help to define elements of problem. The Goodyear 2008 and British Eventing 2009 instrumented fences characterized the impulses a fence should withstand in normal competition use. The videos recorded for this study also helped to identify speed, position, the frequency of contacts and characteristics of different fence types. British Eventing on-course force measurement results suggest an impulse lower limit of 500 N-s for triggered safety devices to withstand normal on-course contact such as hoof strikes.

CHAPTER 5. ROTATIONAL FALL OBSERVATIONS

5.1 Rotational Fall Situation Categories

Evaluation of 35 rotational fall videos lead to a refined understanding of the contact situations. Rotational falls may occur with one or a combination of four situations: antebrachium rotational falls, pushing during contact, rotation upon landing, and torsional rotational falls. Despite these falls all having similar results with the horse eventually landing on its back, the physics of the situations are different and would affect the loading on the fence and safety devices.

The simplest rotational fall from a physics standpoint is the antebrachium contact rotational fall or “one-contact rotational fall”, which was first identified in 2000 and is modeled in this thesis. In this situation the competitor has already pushed off the ground with all four legs when the horse’s antebrachium comes in contact with the fence. The horse then rotates about the contact point with the fence. The motion all occurs in what is essentially a 2-D plane.

A video still example of a one-contact rotational fall can be seen in the frames of Figure 5.1 and an illustration version is shown in Figure 5.2. In the first frame, the horse has left the ground and is in contact with the fence with its antebrachium. The second frame shows the rotation of the horse about the contact point at the fence. The third frame shows the results which is the horse landing on its back. The horse is in air for the contact and for the rotation with only the impulse from the fence causing the rotation. The one-contact rotational fall is modeled by the simulation of this thesis and can be initiated with the position and speed information.



Figure 5.1 A horse and rider undergo a one-contact rotational fall

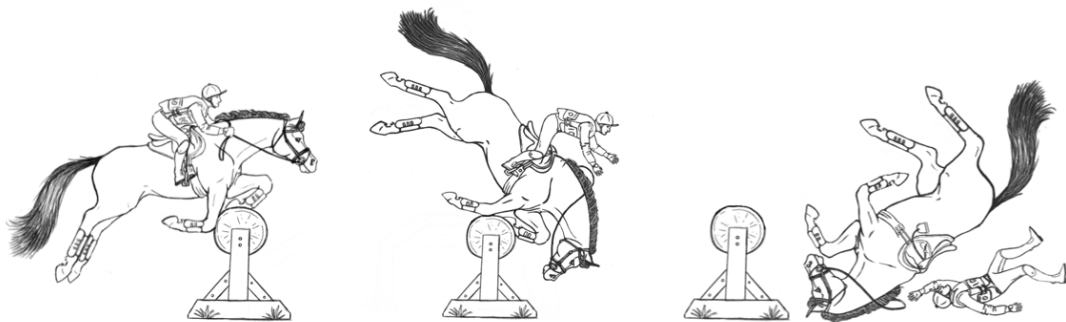


Figure 5.2 An illustration of horse and rider having a one-contact rotational fall

Another situation of rotational falls occurs when the horse makes contact with the fence before the hind legs take off. Consequently, the horse is pushing with its hind legs while being in antebrachium contact with the fence. This additional force can contribute to the rotation, so a rotation can occur even with the competitor approaching the fence slowly. Three stages of the fall can be seen in the video still frames of Figure 5.3 and in an illustration in Figure 5.4. In the first frame the horse is in contact with the fence on its antebrachium. Note that the horse may have contacted the fence on both front legs as shown in Figure 5.3 or with one front leg as in Figure 5.4. Notice that the horse's hind legs are still on the ground with hocks flexed, indicating that it is still pushing. The second frame shows rotation over the contact point at the fence with the hind legs high

and the horse's head very low. The third frame displays signs of a true rotational fall with the horse landing on its back.



Figure 5.3 Three frames of a rotational fall with the horse in contact with the fence while pushing with its hind legs [54]



Figure 5.4 An illustration of a one-contact rotation with the horse's hind legs pushing

The rotational fall with the horse's hind legs pushing during contact is not included in current simulations but could be easily added by including the effect of the moment generated by the legs pushing as an additional angular impulse. Little information is known about the impulse applied by the hind legs in cross country situations regards to force magnitude, direction and duration, let alone for rotational falls.

A reliable estimate or data from a force jumping plate study would be necessary to evaluate this scenario.

Another type of rotational fall situation is rotation upon landing or a “two-contact rotation”. The distinction between the one-contact rotational fall and rotating upon landing is that after the rotation has been initiated by the horse first contacting the fence with their antebrachium, one or both of the horse’s front feet contact the ground before the horse completely rotates over and back hits the ground. This type of fall has some general plane motion, as the horse is not purely rotating over the point of contact. This rotation is in a 2-D plane.

An example of this fall is shown in the video frames of Figure 5.5 and in an illustrated version in Figure 5.6. In the first frame the horse is contacting the fence. It is also notable that the horse’s hind legs are still on the ground in the video frame, and should be accounted for if modeling this specific situation. This contact initiates the rotation but the horse is not fully rotated before landing. The second frame shows the landing where the horse’s front leg contacts the ground before the horse fully rotates. Here the force of the ground on the front contact adds additional rotational momentum. The final frame shows the resulting rotation of the horse rolling across its neck before landing on its back.



Figure 5.5 A horse and rider undergo a two-contact rotation upon landing fall [55].

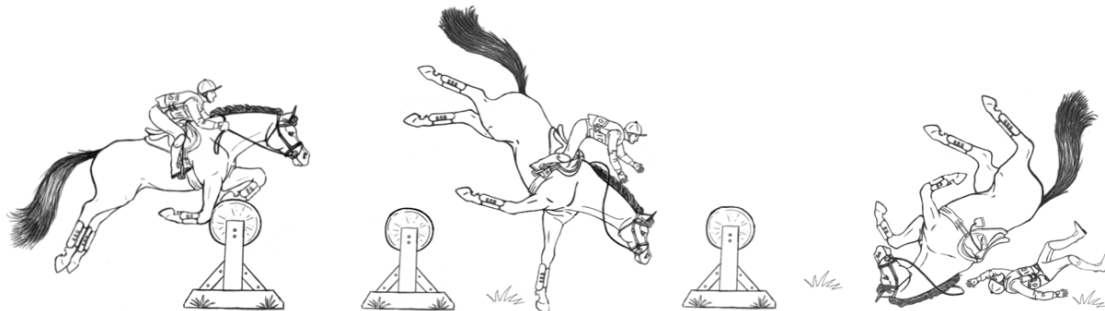


Figure 5.6 An illustration of a two-contact rotational fall

This type of fall has many additional variables. Factors for this type of fall include the reaction from the horse, ground conditions, and the landing leg’s position and ability to collapse at the time of contact. Evaluating these falls requires more insight on the second impulse arising from the front leg hitting the ground. One way it could be adapted from the existing model by first calculating the rotational velocity due to the contact with the fence, and then adding a second representation of the new physics for the landing contact.

Situations resulting in rotating upon landing are often similar to many of the “close calls.” Sometimes the horse is able to stumble and regain balance, or may slide into the ground on its belly without rolling over to its back. This idea is illustrated by the frames in Figure 5.7. In the first frame a critical antebrachium contact is shown. The

horse's hind end goes higher than it normally would on the landing shown in the second frame due to rotational momentum from the first contact. The landing is the second contact for potential rotation, but as seen in the third frame, the horse was able to rebalance and continue on with no issues.



Figure 5.7 A “close call” situation with antebrachium contact but with rebalance upon landing that does not lead to rotation

The final type of rotational fall identified is a torsional fall where the horse twists over the fence rather than somersaults. Unlike the other situations discussed, this rotation does not occur in a 2-D plane, but is 3-D. This would require 3-D adaptation of the inertia model, which is possible, but adds a much higher level of complexity beyond the scope of this thesis. These falls often occur when the fences are jumped on an angle.

Examples of a torsional fall are shown by video frames in Figure 5.8 and in an illustrated version in Figure 5.9. The horse and rider attempt this fence on an angle over a ditch. In the first frame, the horse has left the ground and is in antebrachium contact with the fence. The safety device does activate in the video, but the horse swings to the side and rotates torsionally. The horse lands on its side while rolling to its back.



Figure 5.8 A horse contacts a fence on an angle and has a torsional fall [56].

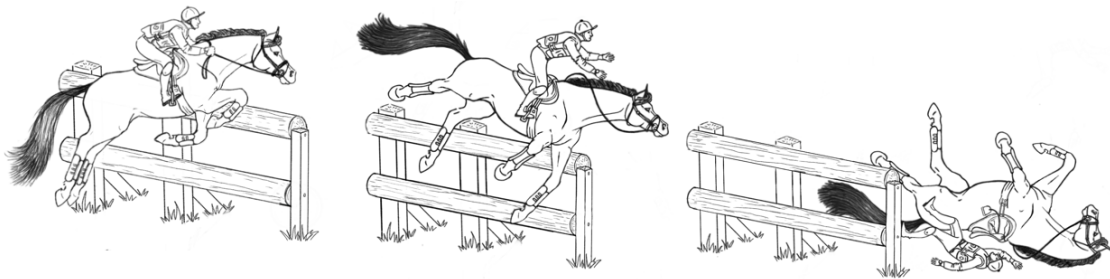


Figure 5.9 An illustration of a torsional fall

In a report describing torsional falls, fences jumped on angles and corners were noted to be potential situations for rotational falls. However the report also states that there is not data to confirm this idea [57].

5.1.1 Rotational Fall Category Identification

Currently, categorical rotational fall situations are not recorded. A randomly selected amount of videos are used in the next section to estimate the frequency of each type of fall, but it is relatively unknown. Identification of the category of rotational falls could be useful for improving course design and study.

In FEI and USEA/USEF competitions, statistics and falls are reported as discussed in Chapter 2. USEF has reports for Equine Accident/Injury/Collapse and

Eventing Human Accident/Injury [58], [59]. There are yes/no boxes to be marked by Frangible Fence and Rotational Fall. There is no distinction between collapse and horse fall. USEF does not release injury report statistics online annually. The 2019 FEI Fall Report form requests more details about the fence, if the frangible device broke, did the horse hit the fence on the way up or down, did horse hit fence hard, did the fence break or tip over, if the horse somersaulted, and a horse drawing to indicate where the horse hit the fence [60].

Adding a question to identifying rotational fall situations is present by providing illustration examples shown in the previous section in order to identify the frequency of the rotational fall types.

5.2 Rotational Fall and Close Call Video Catalog

A collection of 35 rotational fall and “close call” videos have been gathered, evaluated and categorized in Table 5.1. The sample size and quality of these videos is insufficient to make to make quantitative, conclusions but is still useful. These videos were recorded for sports and spectator reasons so the camera pans and they may not be used for speeds or positions.

5.2.1 Rotational Fall Videos

The gathered videos are useful for limited qualitative evaluation for the different types of rotational falls and contributing factors. These evaluations are subjective and the camera angle can limit the visibility for contacts and hind-legs pushing while taking off. In Table 5.1 the videos are described by the event or video title and their time stamp

within the video. Rotations are noted and 2nd is included if the rotation is upon the second contact, or 2+ for more stumbling steps after landing. The nature of the contact is described along with the fence type and further scenario characteristics. These descriptions help categorize the many situations and factors that contribute and cause rotational falls and provided qualitative validation for the thesis simulations.

Table 5.1 A collection of available rotational fall videos.

Video Description	Time	Rotation	Activation	Type of contact	Fence Type	Key Characteristic
Torsional						
Badminton 2016 (Boyd Martin)		Yes	Yes	Antebrachium	Vertical Over a ditch	Hung leg, Torsional fall
Burghley Horse Trials 2019	3:40	Yes (2nd)	No	Antebrachium, and 2nd contact rotation	Vertical Gate (MiM Wall Kit)	Jumped on angle, Torsional fall, 2nd contact, pushing hind
Burghley Horse Trials 2019	9:08	Yes (2nd)	No	Antebrachium, and 2nd contact rotation	Vertical Gate (MiM Wall Kit)	Jumped on angle, Torsional fall, pushing hind legs, (2nd contact not contributing?)

One Contact						
Burghley Horse Trials 2019	11:20	Yes	No	Antebrachium	Vertical Gate (MiM Wall Kit)	1 contact rotation
Badminton 2017	5:37	Yes	No	Antebrachium	Log	1 contact rotation
Badminton 2017	7:43	Yes	No	Lower Front legs	Brush narrow corner, no ground line	Appears to "kneel" on fence, downward body angle
CCI*** de Saumur (Clayton)	0:14	Yes	No	Antebrachium	Brush Vertical jumped on angle	Hung leg, somewhat torsional
Clayton Fredericks 2011	2:50	Yes	No	Antebrachium	Brush on a log? On a hill	Downward body angle and direction
European Championships 2011 (Mary Kinf)		Yes	No	Antebrachium	Table	Hung legs
Luhmuhlen 2013 (Opposition Buzz)		Yes	No	Antebrachium	Boat table	Hung leg, difficult camera angle
Boekelo (Coral Keen)		Yes	No	Antebrachium	Log table	Hung leg, difficult camera angle
Bramham 2009 (Victoria Thirlby)		Yes	No	Antebrachium	Log after downhill	Hung leg, difficult camera angle
European Championships 2010? (Karim Florent)		Yes	No	Antebrachium, Pushing hind legs	Vertical (?)	Hung leg, pushing upward at contact for rotation
Glanusk Junior Championships CCI*		Yes	No	Antebrachium, Pushing hind legs	Vertical log	Hung legs while pushing
Luhmuhlen 2018		Yes	No	Antebrachium	Vertical (MiM)	Hung leg, difficult camera angle
Russian Fall		Yes	No	Antebrachium	Table	Hung leg
Two Contact						
Badminton 2017	9:30	Yes (2+)	No	Antebrachium	Vertical plank (Mim)	Hung leg, 2 or 3 stumbling steps before horse rolling
Burghley Horse Trials 2017	0:19	Yes (2nd)	No	Antebrachium Hind leg (Pushing)	Log	Possible pushing hind legs, rotation about front legs hitting the ground
Rolex Kentucky 2006	All	Yes (2nd)	No	Antebrachium, 2nd contact landing in water	Log drop to water	Hung leg, second contact in water after large drop
Rolex Kentucky 2010	0:09	Yes (2nd)	No	Antebrachium, pushing hind legs, 2nd contact	Vertical log	Hung leg hind legs pushing at take off, second contact same level rotation
Rolex Kentucky 2010	1:10	Yes (2+)	No	Antebrachium, pushing hind legs, 2nd contact +	Vertical log	Hung leg hind legs pushing at take off, second contact same level landing and then rotation rolling off a bank
Rolex Kentucky 2010	1:43	Yes (2+)	No	Antebrachium, pushing hind legs, 2nd contact +	Vertical log	Hung leg hind legs pushing at take off, second contact same level landing and then rotation rolling off a bank while pushing a second time
Benjamin Winter		Yes (2nd)	No	Antebrachium, 2nd contact	Table	Hung leg, high speed, 2nd contact rotation upon landing
Badminton 2014 (Mark Kyle)		Yes (2nd)	No	Antebrachium, 2nd contact	Log	Hung leg, rotation on second contact down hill

A subjective breakdown of the videos is shown in Table 5.2. The majority of the rotational falls are one-contact rotations in the 2-D plane which are represented by the simulation. The next subset of rotational falls is the two-contact rotation which has a wide variety of physical situations: the horse's feet touching the ground did not seem to contribute to the rotation as the horse was already nearly completely rotating; where the landing impulse was the extra contributing factor to cause the full rotation; where the horse took two or more stumbling steps before rolling over onto its back sometimes contributed by a downward hill or bank. Some falls have the hind legs pushing, a contributing factor for a portion of the falls of each variety. A small minority of the fences were fitted with frangible devices, the only rotational fall that still occurred was a one-sided frangible pin activation during a torsional fall.

Table 5.2 A table describing the falls and close calls in the list of videos

One Contact	13	54%
Pushing Hind Legs	3	13%
Frangible Device?	2	8%
Activation?	0	0%
Two Contact	8	33%
Pushing Hind Legs	4	50%
Frangible Device?	1	13%
Activation?	0	0%
Torsional	3	13%
Pushing Hind Legs	2	67%
Frangible Device?	3	100%
Activation?	1	33%
Second Contact?	2	67%
Rotational Falls Total	24	
Close Calls	12	
Pushing Hind Legs	4	33%
Frangible Device?	7	58%
Activation?	2	17%
Total Videos	35	

5.2.2 Close Call Videos

There are many recorded “close calls” and a number of them are documented in Table 5.3. Three of the close calls were contacts on the back rail of an oxer or corner. One of the close calls was still a horse fall where the horse contacted the fence with its hind end and rolled after being on the ground. This hind end and heavy ground contact is not captured in the thesis model. The other two were front end contacts and are captured in the thesis model with downward body angle contacts. Many of the other close calls were antebrachium contacts that look like potential two-contact falls but the horse regained its balance upon landing. It is not simple to conclude what caused the horses to rebalance rather than rotate. Many times the rider will fall but the horse will not, which decreases risk of injury. For one case, the horse contacted the fence, rotated up and then rotated down on the same side of the fence. The rider fell off but the horse returned to its feet. This case is also ideal for avoiding serious injury of the horse and rider.

Table 5.3 Close call situations that did not result in rotational falls.

Close Calls						
Downward Rear Rail						
Burghley Horse Trials 2019	3:24	No	Rear Rail Reverse Pin	Front lower legs, rear rail	Open Oxer (MiM Front rail, Reverse Pin Rear rail)	Downward body angle and direction
Burghley Horse Trials 2019	8:07	No	Rear Rail Reverse Pin	Front lower legs, rear rail	Open Oxer (MiM Front rail, Reverse Pin Rear rail)	Downward body angle and direction
Brazil Olympics (Padraig McCarthy)		No	No	Hind leg on back rail	Pinned rail corner	corner, horse sliding/stumbling on landing and then rolls over
Front Rail						
Burghley Horse Trials 2019	8:10	No	No	Antebrachium	Vertical post & rail (MiM)	Hung leg, rebalanced on landing, No fall
Badminton 2017	3:50	No	No	Antebrachium	Log	Hung leg, rebalanced on landing, rider fall
Badminton 2017	4:06	No	No	Antebrachium	Vertical plank (Mim)	Hung leg, rebalanced on landing, rider fall
Badminton 2017	6:25	No	No	Antebrachium	Table	Hung leg, rebalanced on landing, rider fall
Badminton 2017	8:40	No	No	Antebrachium	Vertical plank (Mim)	Hung leg, rebalanced on landing, rider fall. Looks like start of a torsional fall
Rolex Kentucky 2010	2:20	No	No	Antebrachium, pushing hind legs	Vertical log	Hung leg, hind legs pushing at take off, regain balance on landing
Burghley Horse Trials 2000 (Andrew Nicholson)		No	No	Antebrachium, Pushing hind legs	Log vertical	Hung leg, hing legs pushing, Regain balance on landing
Badminton 2011	0:12	No	No	Antebrachium	Vertical Gate (A pin?)	Hung leg, pushing at contact slightly, horse and rider stumble and fall
"Near rotation"		No	No	Antebrachium	Vertical before drop into water	Hung legs, hind legs pushing, horse rotates up but not over. Rider falls

The number of close calls seen in this compilation demonstrates the potential for safety device activations in times where no rotational fall would occur. For example, at Burghley Horse Trials 2000, there was a serious critical contact where both horse and rider recovered to continue on to win the event. This was before the advent of frangible devices, but being a timber vertical today it would have been a candidate for adding the frangible device. Had it activated, the competitor would have been awarded 11 penalties under current FEI rules and wouldn't have won the event. It is for this reason that caution must be used in creating frangible devices to resist changing the culture of the sport.

CHAPTER 6. TESTING CONCEPTS

6.1 Physics and Ensemble Methods

The physics principles of momentum and impulse are of particular importance when acting forces vary over time, such as when objects impact each other. The term “linear impulse” is the cumulative effect of a force acting over time. Impulse will alter the linear momentum, the mass times the velocity. Similarly, when an object in forward motion experiences an offset contact with a fixed or movable object, its motion can change into rotation. Note that in impacts, the initial kinetic energy changes significantly, typically losing a significant percentage during the collision.

Previously, physical simulations, such as dummies and pendulum testing, were used as means to develop and evaluate frangible devices. The dummies modeled the horse size and weight but did not include the mass of the rider. Pendulum tests typically have not been done with horse and rider mass, and the speeds are often lower than on-course jumping speeds. Using a statistical ensemble computer simulation it is possible to model a wide variety of realistic horse and rider masses, jumping velocities and positions.

Physical analysis of rotational falls can be considered in the 2-D plane because they are somewhat symmetric and in the plane. For future analysis of torsional falls or impulses outside of the plane, the current inertia model may be rotated to consider 3-D scenarios.

In the statistical ensemble, each key variable in the next section is modeled with 10,000 random values from an appropriate statistical distribution determined from published studies - if available, from data such as the inertia survey or on-course measurements, or from subject matter experts. The variables are then combined random-

value-by-random-value in a validated physics-based model to examine 10,000 realistic cases in which the horse and rider contact the fence in the dangerous ante brachium region of the foreleg. To provide insight and results for policy decisions and design guidance, each physics-based simulation looks at 10,000 cases of competitors with critical contacts, which is the equivalent of more than 62.5 years of “very bad days” based on the statistics in Chapter 2.

6.2 Dummies, Pendulums, and Instrumented Sledgehammers

Testing efforts have been conducted for nearly two decades to aid in the development of specifications and designs for safety devices for use on course, and to evaluate their performance. When contacted by the horse in the critical ante brachium region, any fence or safety design that interrupts the reaction of the fence and reduces the impulse compared to a fixed fence improves safety.

In 2001, the Transportation Research Laboratory (TRL) in Wokingham, Berkshire, UK studied videos of rotational falls, and developed an equestrian crash test dummy (NED) to aid in the development of the original frangible pin. The approximate CG is denoted by a triangle and the ante brachium is simulated by the blue leg. The fence shown is fixed. NED’s incoming speed and direction were defined by the height and incline of the line it slid along, so NED’s results can be thought of as one competitor’s approach. NED was 470 kg, the approximate weight of a horse not including the rider [2].



Figure 6.1 New Equestrian Dummy (NED) for development of the frangible pin in 2001 [2].

NED is representative of one horse cadaver and is configured with the same “jumping position” for each trial. This provides one particular inertia value for a competitor.

From 2001-2008, after two horse deaths in 1997, the Netherlands Equestrian Sports Federation (KNHS) developed, tested, and required on-course use of Dutch Poles for all national Events [29]. From the KNHS 2008 presentation, an average of 5000 starters were competing each year, with about four (4) pole activations (0.08%) [27].



Figure 6.2 (left) Dutch Pole Development Testing 2001 [29]; (middle) MiM Development Testing 2008 [61]; (right) UKY Hinged Gate Testing at the RK3DE Course Builders Display 2010 [35].

MiM development testing in 2008 used an instrumented pendulum tester to evaluate force and impulse results. For the fixed fence, peak force was 20kN with contact duration of 0.2 seconds. The impulse for the fixed contact is 2445 N-s. When tape or a force-limiting device is added to the MiM hinged gate, the force peaks at 9 kN, with an impulse of 262 N-s. For a table prototype, the force peaks at 13 kN, with an impulse of 536 N-s. The force-time curves obtained in these contacts are similar to those in the UKY Hinged Gate Frangible prototype.

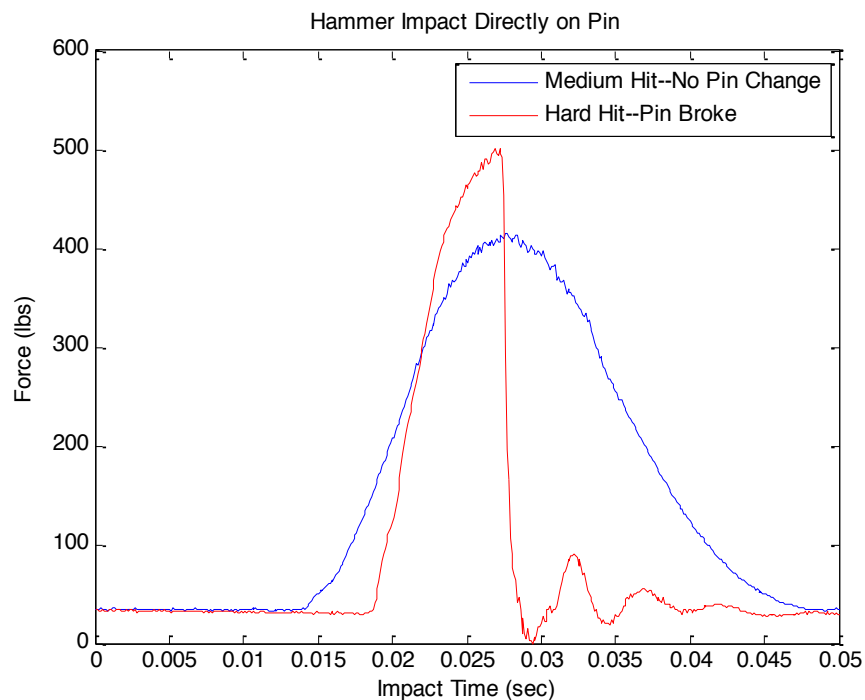


Figure 6.3 UKY Hinged Gate Frangible Pin Testing: force just under activation compared to slightly higher force causing pin activation [35]

University of Kentucky safety device testing in 2009-2011 included testing of a full-scale hinged gate held in place by a small horizontal frangible pin to determine what size, strength and placement of frangible pins yield the desired performance.

Instrumented sledgehammers, particularly PCB Piezotronics Impulse Force Hammer Model Number 086B50, were used to measure the contact. In Figure 6.3 the force-time history of the unbroken pin peaks at 400 lbs (1780 N) with an impulse (the force-time reaction) of 53.4 N-s. When hit slightly harder, the horizontal force peaks at 500 lbs (2,225 N) with impulse of 11.1 N-s, reducing the impulse to 20% by interrupting the reaction [35].

Bristol University capstone design teams built a laboratory scale model, BESS, with 1/3 of the mass of a competing horse. They also built and tested different mitigating designs. Their results indicated that reducing the friction between the surface and the horse's leg may help to reduce rotation. Further, a rail that was allowed to rotate freely effectively reduced the friction and rotation, but is difficult to implement on course.

Hints of the magnitude and direction of appropriate limiting impulses can be gained by considering the combined results of side-by-side testing of multiple safety devices in a post-and-rail configuration. Each of the four devices available in 2011 were developed independently by teams including engineers following different logical processes. Consequently, each design functions differently, with different performance criteria [36].

Typically video of rotational falls were watched to key on an aspect of the motion. The TRL team focused on vertical activation and the ante brachium contact position. TRL built a test apparatus that represented one cadaver horse and one direction of contact motion. The MiM device was developed through a sequence of testing, gradually increasing the activation force of the device until on-course performance satisfied sport experts that there were not excessive false activations. The Dutch Poles

team also focused on activation in any direction, testing several materials combinations until finding one that had the desired breaking strength. The PROLOGS team focused on activation in any direction, absorbing and reducing the contact speed to one that does not have enough momentum for rotation. The PROLOGS product was tested by a transportation laboratory in the U.S. and on course.

Therefore looking at the performance of these devices as a set offered “wisdom of the crowd” insight. KNHS statistics averaged 4 activations for 5,000 starters (0.08%). In 2010, MiM on-course statistics included 15 indicator flag replacements and 6 activations for 1,300 approaches (1.2% flags; 0.46% activations). PROLOGS used on course in 14 competitions saw 8 activations for 2300 competitor approaches (0.35% activations). Between 2002 and 2008, the rate of rotational falls trended downward from 0.5% to 0.3%, so the number of activations of these devices on course was consistent with preventing what would have been rotational falls, providing a sense of validation of their respective design criteria.

NED’s mass was 470 kg, with speed of 6 m/s (360 mpm). Initial MiM testing was accomplished with a 300 kg mass, and speeds of 3.9 – 4.8 m/s (234-288 mpm). Laboratory tests of the PROLOG were with 753kg mass at 3.22 m/s (193 mpm). The 2011 comparison testing in Sweden was accomplished using the MiM pendulum tester seen in Figure 6.4 with either 118 or 202 kg mass, at speeds varying from 1.1-5.1 m/s (66-306 mpm). The pendulum was fitted with a rubber impactor to approximate the effects of horse anatomy.



Figure 6.4 (left) 2011 Sweden Comparison Testing Using the MiM Pendulum Tester (Right) Collection of used and unused frangible pins and MiM clips.

It is important to note that most of the safety device testing is not done using realistic horse and rider mass, or speeds that are realistic for competition. A gap in current understanding is how to best translate results from these tests to relevant on-course performance in different jumps with different moving masses.

As the FEI Standard was being developed in 2011, a comparison test was organized. The MiM tester was used for a comparison test of six (6) different devices that included all available designs at the time, as well as ideas that were tested spontaneously. Side-by-side comparisons for activation performance are useful, even though tested at lower momentum and energy due to the lower mass and speeds. However, the information from this testing is proprietary.

7.1 Equations for Impulse-momentum Collisions and Overturning

In the rotational fall situation, when a horse and rider are moving forward and contact a jump with the horse's forearm, the contact impulse changes the forward momentum into rotational motion. The simulation developed for this thesis, implements 2-dimensional equations that represent angular impulse-momentum physics for the instant that the competitor is first in contact with the fence. In Eq. (1), three possibilities for incoming initial momentum or impulses are envisioned contributors: initial forward linear momentum acting offset from the fence contact location, initial rotational momentum of the horse and rider associated with the jump arc, and the horse continuing to push off the ground with its hind legs while in contact with the fence.

The simulation in this thesis only includes initial offset linear momentum. The other two conditions, initial rotational velocity and hind leg take off may be incorporated later with more information from video studies and force plate measurements. First, contacts with fixed (stationary, with no safety device) fences are computed to serve as a baseline for comparison. Initial angular momentum from normal jump arc contributes little to the angular momentum that would be required for rotation.

Angular momentum perpendicular to the plane of motion about the fixed point of contact, CP, is conserved. In Eq. (1), the distance from the contact point to the center of gravity is $\vec{r}_{CG/CP}$, the linear momentum at the instant immediately before the contact is $m\vec{v}_1$, the angular impulse arising from contact forces at the contact point is zero, the inertia about the contact point is I_{CP} , and the resulting angular velocity is ω_2 . Initial angular velocity related to the jump arc motion, ω_1 is neglected. The impulse of the hind

legs pushing off at point A on the ground while in contact with the fence, the scenario illustrated in Figure 5.4 is not included in this scenario.

$$I_{CP}\omega_1 + \vec{r}_{CG/CP} \times m\vec{v}_1 + \int_{t_1}^{t_2} \sum \vec{r}_{CP/A} \times F_{hind} dt = I_{CP}\omega_2 \quad (1)$$

Resulting angular velocity is therefore determined from the incoming velocity and the competitor position at the instant immediately preceding contact, which determines the CG location and inertia.

$$\vec{r}_{CG/CP} \times m\vec{v}_{CG1} = I_{CP}\omega_2 \quad (2)$$

An indication of overturning (rotation), or not, is accomplished by comparing the energy of two critical states: 1) the state when the horse first collides with the fence and is rotating about the contact point, it has kinetic energy, and 2) the state in which the horse has rotated so that the CG is directly above the point it had contacted, where it has maximum potential energy and minimum kinetic energy. Note that this criteria also allows for general plane motion, meaning the horse may translate as well as rotating vertically. This means the moment the competitor's CG is above the contact point may be above the jump or later in the jump arc.

$$\frac{1}{2}I_{CP}\omega_{contact}^2 = \frac{1}{2}I_{CP}\omega_{90}^2 + mg(h_2 - h_1) \quad (3)$$

Identify that if the angular velocity when the CG is directly above the contact point is nonzero that it will overturn. Therefore we can simplify (3) into an overturning test.

$$0 > \frac{1}{2} I_{CP} \omega_{contact}^2 - mg(h_2 - h_1) \quad (4)$$

If (4) is satisfied, then the competitor does not rotate past a vertical horse body position.

The design challenge for this problem then becomes limiting the impulse with which the horse contacts the fence by the action of a safety device. Note that a safety fence is one that incorporates any design to reduce the contact impulse: frangible, resettable, angled face, brush, friction-reducing, etc. Consideration of the linear impulse-momentum allows analysis and fence impulse manipulation to determine design criteria.

The two component momentum equations are now considered. The mass and CG velocity of the competitor at the time of contact along with the impulse of contacting the fence is equal to the following instant's momentum of the competitor's CG.

$$m\vec{v}_1 + \int f_x dt = m\vec{v}_2 \quad (5)$$

Where \vec{v}_1 is the incoming CG velocity and \vec{v}_2 is the velocity of the CG at the instant after contact (not after rotating 90 degrees).

$$\vec{v}_2 = \vec{r}_{CG/CP} \times \omega_{contact} \quad (6)$$

Eq. 6 is then solved for the impulse of the fence.

As a first evaluation of conditions that lead to an overturned horse as noted in (4), a mitigation response is sought. A reduced fence impulse is created by a fixed impulse response, which would be physically implemented by a release or give in the fence.

Using the reduced fence impulse and the incoming CG velocity the new CG velocity for the reduced fence is found. The new angular velocity is found by equation 7.

$$\vec{r}_{CP/CG} \times \int_{t_1}^{t_2} \sum \vec{F}_{Reduced} dt = I_{CG} \omega_{2Reduced} \quad (7)$$

Returning to the energy equation, which is adapted from (4)

$$\frac{1}{2} I_{CG} \omega_{90}^2 + mg(h_2 - h_1) = \frac{1}{2} I_{CG} \omega_{2Reduced}^2 \quad (8)$$

yielding,

$$0 > \frac{1}{2} I_{CG} \omega_{2Reduced}^2 - mg(h_2 - h_1) \quad (9)$$

In order to create an evidence-based model, all variables must be considered. In overview, given the wide ranges of speeds and configurations defined by consultation with sport professionals and practitioners, the simulation computes results as follows:

Initial Set-Up

- All distances involved from the geometry and contact point
- Horse and rider mass and Center of Gravity (CG)
- Horse and rider inertias about the fixed contact point and the CG
- Intermediate plots of results distributions as validation

Fixed-fence Simulations

- Rotational velocity of the horse and rider after contact with a fixed fence
- Whether horse and rider would rotate past vertical for a fixed fence (if no: pass, green; if yes: rotation past vertical, i.e. a rotational fall, red)
- CG plot of results for specific contact speeds
- Magnitude and angle of force-time reaction (Impulse) at the contact point for a fixed fence
- Histogram plots of results for specific contact speeds
- Parameter map plots of magnitude vs speed, among others

Safety-fence Simulations with Design Criteria

- Rotational velocity of the horse and rider after contact with an impulse-limited fence
- Whether horse and rider would rotate past vertical (if no: pass, green; if yes: fall, red)

- CG plot of results for specific contact speeds

Safety Fence Simulation for Case Studies

- Incorporate values and ranges from on-course videos for contact speed and prior safety device tests for limited impulse
- Rotational velocity of the horse and rider after contact with an impulse-limited fence
- CG plot of results

7.1.1 Collision Energy

Energy and impulse-momentum are two lenses from which to view motion. Impulse-momentum is the appropriate physics for describing these collisions because momentum is conserved, while system kinetic energy is not conserved as energy is dissipated in other forms. Horse-fence collisions are an inelastic collision, meaning all incoming kinetic energy is not outgoing kinetic energy, even with a fixed fence. Energy “loss” or dissipation can include energy converted to heat or sound. Energy is also consumed by elastic and inelastic deformation of materials in the horse’s leg and the fence in contact. These sources of loss may be higher in the field than in simulations due to factors including absorption through fence or horse leg deflection or material give, etc.

Further, energy is not a vector quantity like impulse momentum, so the design element of reaction direction is also lost.

7.2 Map of Variables

The overturning analysis can be subdivided in three parts as seen in the illustration of the variables in Figure 7.1: 1) the inertia and CG of the competitor in the contact position, 2) the incoming momentum of the competitor, and 3) the fence reaction of the jump which could result from safety device action.

The green boxes along the top of the variable map contain the input measurements related to the inertia and overall CG location to model the size, weight and the position that define the evidence-based overturning model of the competitor at the time of contact. Among these are the angles for the jumping position of the horse and rider at the moment of contact, previously described in Section 4.3.4. This encapsulates where the horse is along the jump arc (ascending, suspension, or descending), and the degree to which they “hang a leg” which is the angle of the foreleg to the body and the distance along the foreleg where the horse hits the jump. Each of these variables are randomly selected from the normal distributions found from video studies or direct measurements or sport professionals.

Overall, there are 18 input variables. Horse and rider size measurements, which accounts for 9 or half of the input variables, are somewhat fixed distributions as they would not vary by fence type. The horse and rider density is a constant value from literature. The contact angles, contact point, and the CG velocity account for 8 variables and vary by jump type and situationally. There are two design variables, the fence deformation speed/impulse and the deformation angle.



created with www.bubbl.us

Figure 7.1 The map of variables demonstrates the complexity of identifying causes of rotational falls.

From an equestrian perspective, the variable body position angles create any possible jumping position within a range of values accounting for fences of different heights, terrain changes, spreads, and fence shapes, as well as different takeoff distances, positions along the jump arc at contact, and jumping techniques. These factors result in the inertia and CG values used in the model. The body position and the speeds also account for the results of variation of footing, jump placement, and sequence.

7.3 Position and Size Variable Distributions for “One Size Fits All” Solutions

In using the statistical ensemble for 10,000 different competitors from normally distributed sizes and uniformly distributed jumping positions, the inertia forms a distribution that not only represents examples like NED or Buchner’s Dutch Warmbloods adjusted for jumping, but expands the possibilities for horses of other sizes and in different position situations.

The jumping competitor inertia about the CG, shown in Figure 7.2, is right skewed normal distribution compared to the normal distribution outline also included. Statisticians consider a skew to be in the direction of the “tail” of the distribution. This accurately represents the population of competitors on cross country. Intermediate inertia results from the model for the rider and horse cylinders can also be used with forward CG momentum to validate the assumption of primarily 2-dimensional motion (i.e., rotation in one vertical plane) without significant 3-dimensional aspects.

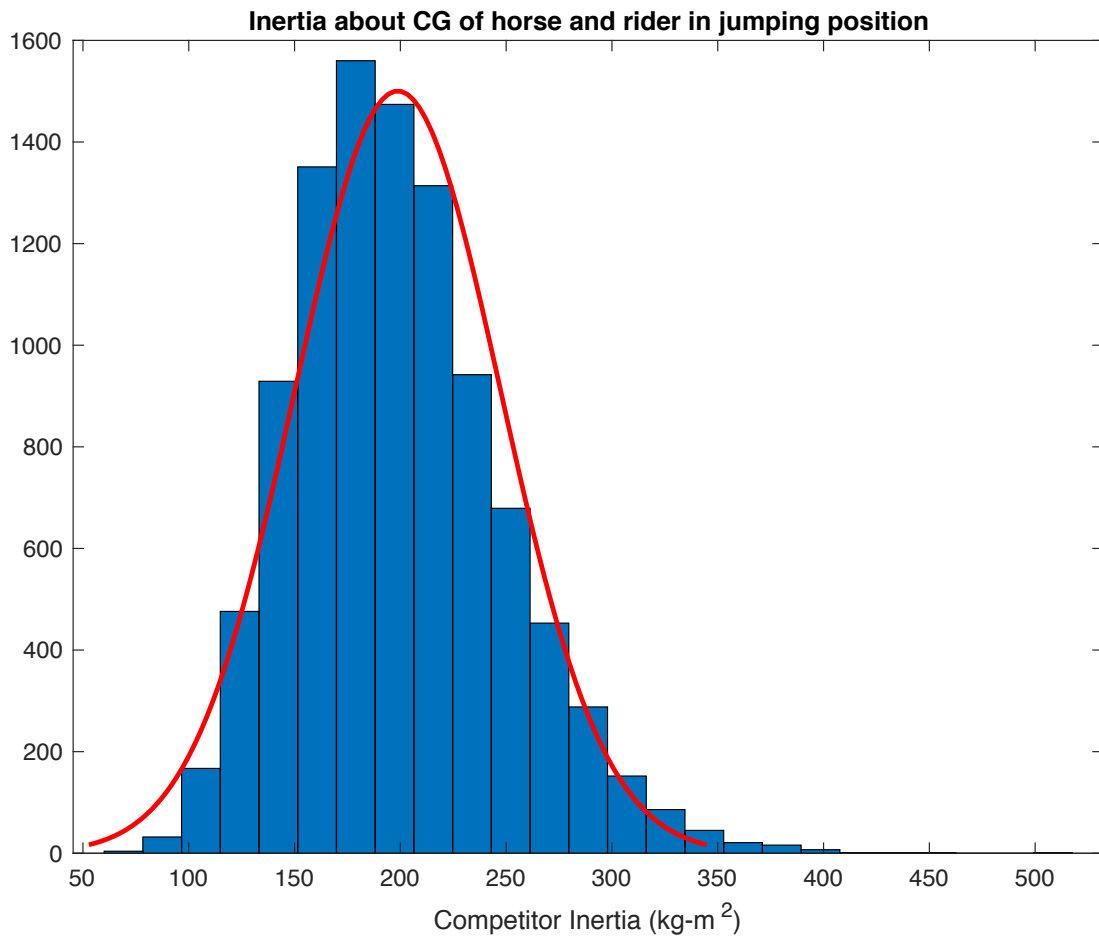


Figure 7.2 The inertia for 10,000 generated horse and rider critical contact situations forms a normal but skewed distribution.

The ensemble generates intermediate results, such as CG location and inertia along with the final rotation/no-rotation results for each of the 10,000 contacts. A variety of plots and ways to present the results have been used to communicate and differentiate among the many variables, though there is a lot of overlap.

The position of 10,000 centers of gravity at the moment of contact is an important intermediate result. Each CG position is shown in Figure 7.3 as a black circle, plotted with respect to the red star representing the horse-fence contact point on the

antebrachium. The red triangle approximates the CG corresponding to the NED. Each position generated in the model is in antebrachium or critical contact to the fence. Jump attempts with no contact, lower limb or hind limb contacts are not considered critical contact for rotational falls and therefore are not represented in the simulation.

The distribution in Figure 7.3 represents the complete variety jumping positions of the competitor along the jump arc, along with the complete range of contact on the antebrachium. The model addresses more than 60 years of dangerous contact situations, incorporating the most extreme situations that could be experienced, and many more than would be practical to replicate with physical testing.

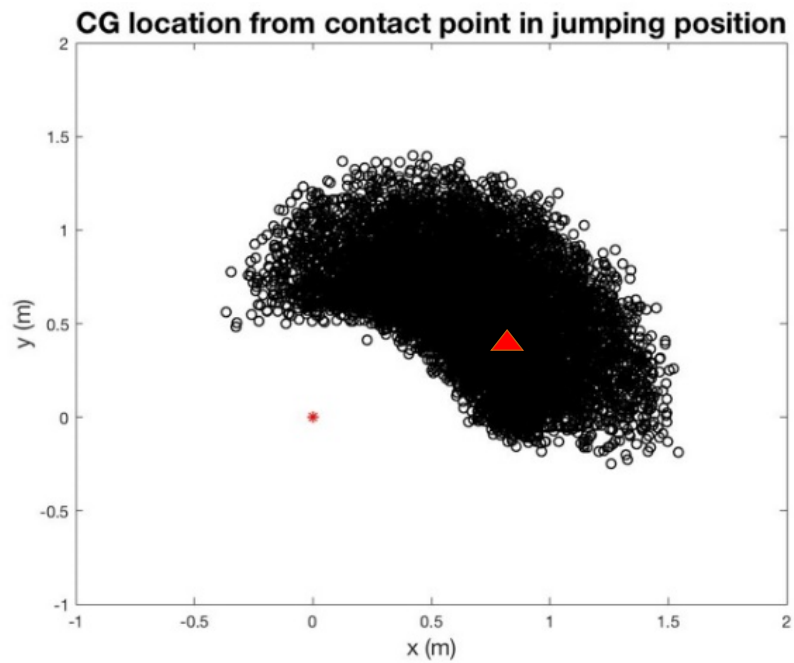


Figure 7.3 (Left) Black circles display the location of the competitor's CG with respect to the antibrachium contact point represented by the red star. (Right) A visualization of the approximation of the competitor's CG is shown to visually represent what the black circles in the left plot look like in real situations.

7.4 Contacting a Fixed Fence

A fixed fence, or a fence that does not have a safety device, is the control situation for assessing rotational falls. With a fixed fence, the risk of rotation primarily depends on speed and position factors. A sensitivity study was conducted following the approach of Robles Vega and revealed that the most influential variables are body angle, antebrachium angle, speed and direction of the competitor's motion, and the fence reaction [34].

From the distributions formed in Chapter 4, an estimated range of jumping positions was formed in combination with sport expert opinion. Each body position is considered equally likely for a one size fits all solution, because there are no rotational fall video observations, so uniform distributions are used for the initial understanding. In the field, horses and riders approach the fence at a variety of speeds and distances. This causes a lot of overlap in both situations and result representation. For visualization purposes, the simulations in this section are shown at a particular speed, but the position factors and size of the competitors are varied for a "one size fits all" jump perspective.

The antebrachium angle in a critical contact for a possible rotational fall situation is different than what is observed in a successful jump (most results from the video study) and is called a "hanging leg". A hanging leg angle is expected to point down and forward or down and back while a "good" jumping form would have the foreleg pointed upward.

7.4.1 CG Position Based Fixed-Fence Results

Figure 7.4 shows the results for contact speed of 6 m/s (360 mpm) with a fixed fence (control), with CG positions as circles with respect to the contact point on the ante

brachium denoted by the black star. The blue points represent the irrecoverable contacts which occur when the CG is past the contact point and impulses of even low magnitudes will cause rotations and are not able to be mitigated by safety devices. This represents 2.4% of the contacts. The red points represent rotations, 66.8% of the contacts. These red points provide the opportunity for mitigation with a safety fence. The no-rotation contacts are marked in green and represent about 1/3 of the contacts.

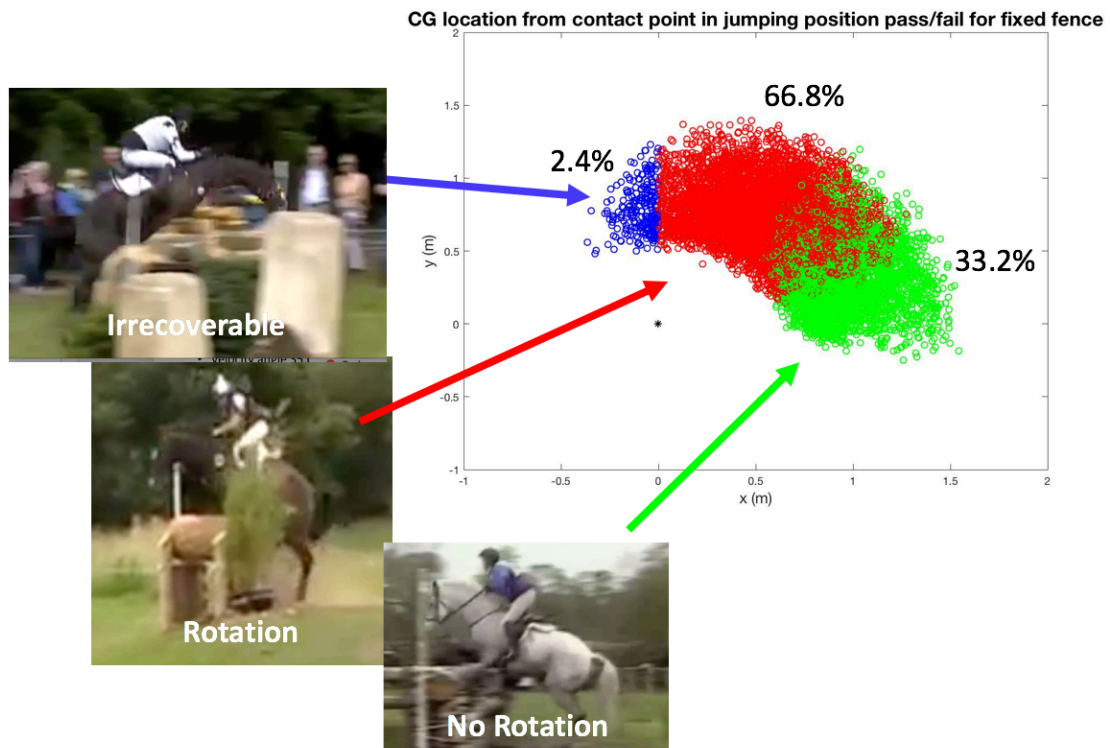


Figure 7.4 Pass (no rotation, 33.2%) and Fail (rotation + irrecoverable, 69.2%) indicated for the CG Positions for a fixed-fence contact at 6 m/s (360 mpm)

If the CG of the combined horse and rider (approximately near the rider's knee) crosses the vertical plane above the contact point, a rotational fall will occur. The geometry can be used to understand the results of the physics-based simulations.

Geometrically, the CG points further from the vertical plane do not have enough momentum to carry them over past it in a rotational fall. Green CG points show horses that will not rotate under these conditions despite contacting the fence with the forearm. CGs closer to the vertical plane at contact have momentum that rotated them past vertical and are indicated in red. Points denoted in blue represent CGs of competitors that are already past the vertical plane at the time of contact. These also result in rotational falls, but are not preventable by incorporation of safety devices. Positions shown in blue must be mitigated through personal safety devices, or prevented by other means such as reducing approach speed or considering course incline. Red CG points show competitors that will rotate if they contact a fixed fence. The red CG points are sought to be mitigated by safety devices.

7.4.2 Speed's Relation to Rotation

Figure 7.5 is a plot of the “no-rotation” percentage for a fixed jump over a range of contact speeds from 1 m/s (60 mpm) to 9 m/s (540 mpm). The no-rotation percentage decreases from 76% at 3 m/s (180 mpm) to 18% at 8 m/s (480 mpm). Despite speed representation outside of a practical jumping range, it is useful to identify the relationship of more rotations with increased speed.

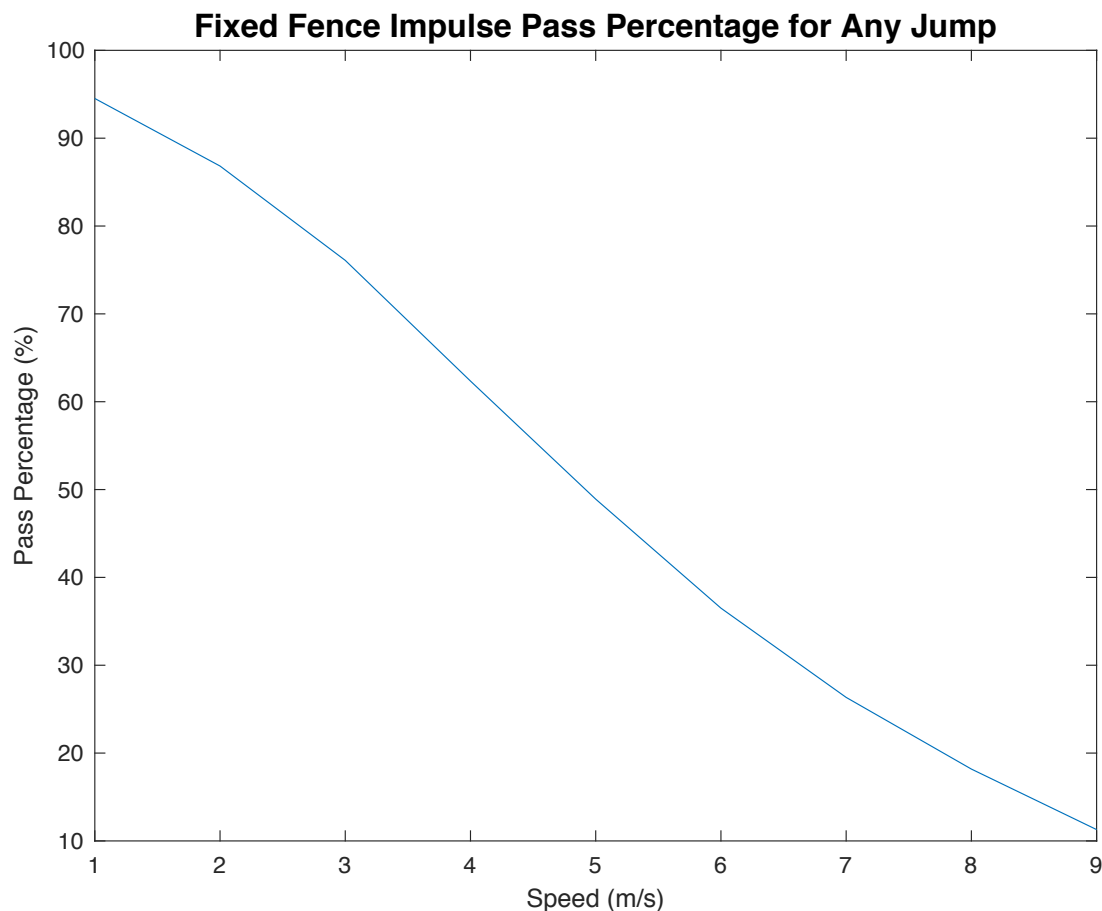


Figure 7.5 As the speed of the competitor increases, the amount of contacts that do not result in rotations decreases.

The good news is that many dangerous contact situations that occur for fixed fences will not result in a rotational fall. Conversely, that presents a challenge for the sport and safety device designers, as these no-rotation contacts may be of significant force and likely to trigger safety devices – even when the device is functioning as designed and is not compromised by prior contacts.

Fences that are approached at the highest speeds are candidates for incorporating safety devices and other approaches should be considered carefully for prevention as well. Reducing the approach speed, and therefore the momentum, at which a competitor

hits a fixed fence decreases the percentage of horses who overturn, suggesting that course design to reduce speed is an option where safety devices are not able to be included. This mitigation approach is impractical in some cases. Higher speeds at higher levels are an important aspect of the culture of the sport and necessary to clear large jumps.

Additionally, low speeds also increase the likelihood that the horse's hind legs would remain on the ground adding jump force, and adding rotational momentum, at the time of contact (not included in the current simulation). Further, there is an understanding in the sport that low-speed approaches result in "slow-rotations" in which the rider is more likely to end up on the ground underneath the horse, while "high-speed rotation" is more likely to throw the rider clear of the horse.

Note again that in Figure 7.5 there are competitors that contact the fence with their CG already past the contact point when rotations are irrecoverable, even with a safety device included in the fence.

7.4.3 Energy Dissipation in Fixed Fence Collisions

Energy and impulse-momentum are two lenses from which to view motion. Impulse-momentum is the appropriate physics for describing these collisions because momentum is conserved, while system kinetic energy is not conserved. Horse-fence collisions are an inelastic collision, meaning all incoming kinetic energy is not outgoing kinetic energy, even with a fixed fence. Energy "loss" or dissipation can include energy converted to heat or sound, energy is also consumed by elastic and inelastic deformation of materials in the horse's leg and the fence in contact. These sources of loss may be

higher in the field including absorption through fence or horse leg deflection or material give, etc.

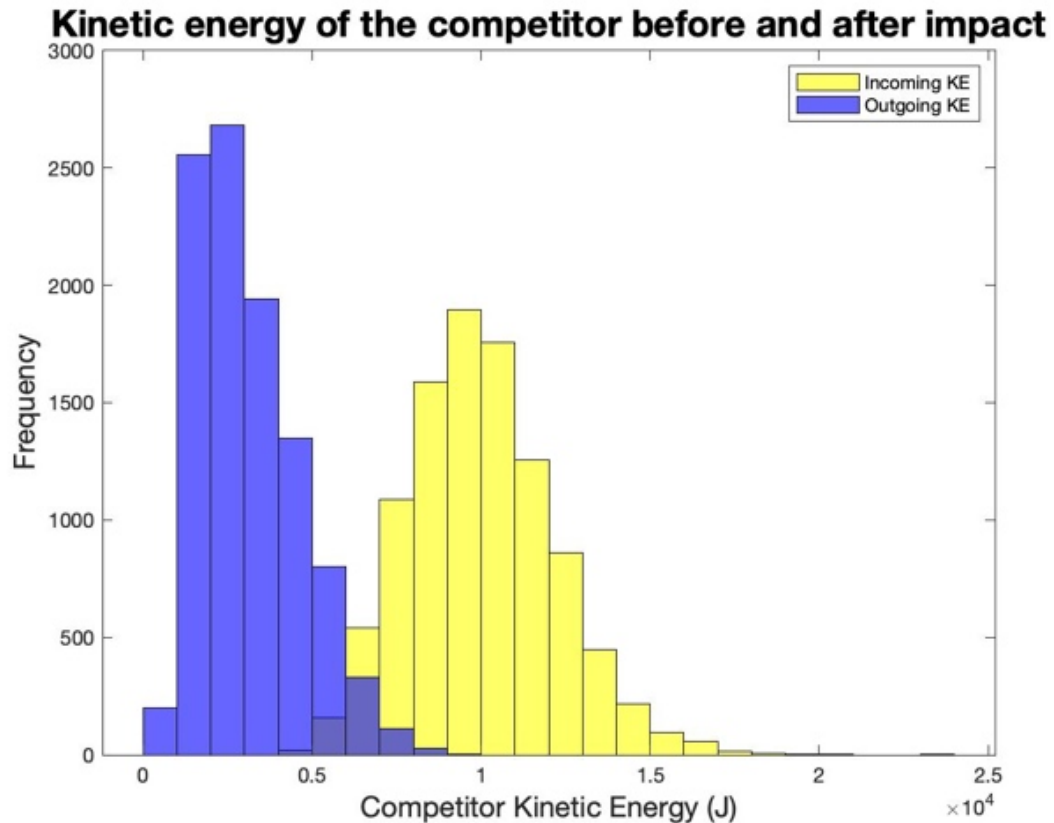


Figure 7.6 Incoming kinetic energy compared to after collision kinetic energy;

Figure 7.6 shows the incoming kinetic energy from mass and velocity with higher values than the kinetic energy of rotational velocity and inertia immediately after the contact. For this ensemble, a speed of 6 m/s (360 mpm) was used and the generated competitors for any possible position contacted a fixed fence. Figure 7.7 has two histograms one of the incoming and outgoing competitor kinetic energy illustrating the difference and the other of the energy loss or dissipation shown ranging from 30% to

90%. Surprisingly, contact often results with a high percentage of the energy being lost. The average energy loss from the simulation results is 68.5%. Impulse is therefore used to present and discuss the simulation results. Many standards including ASTM impact testing standards, and the FEI testing standard for safety devices reference energy due to the ease of pendulum impact testing approach [36].

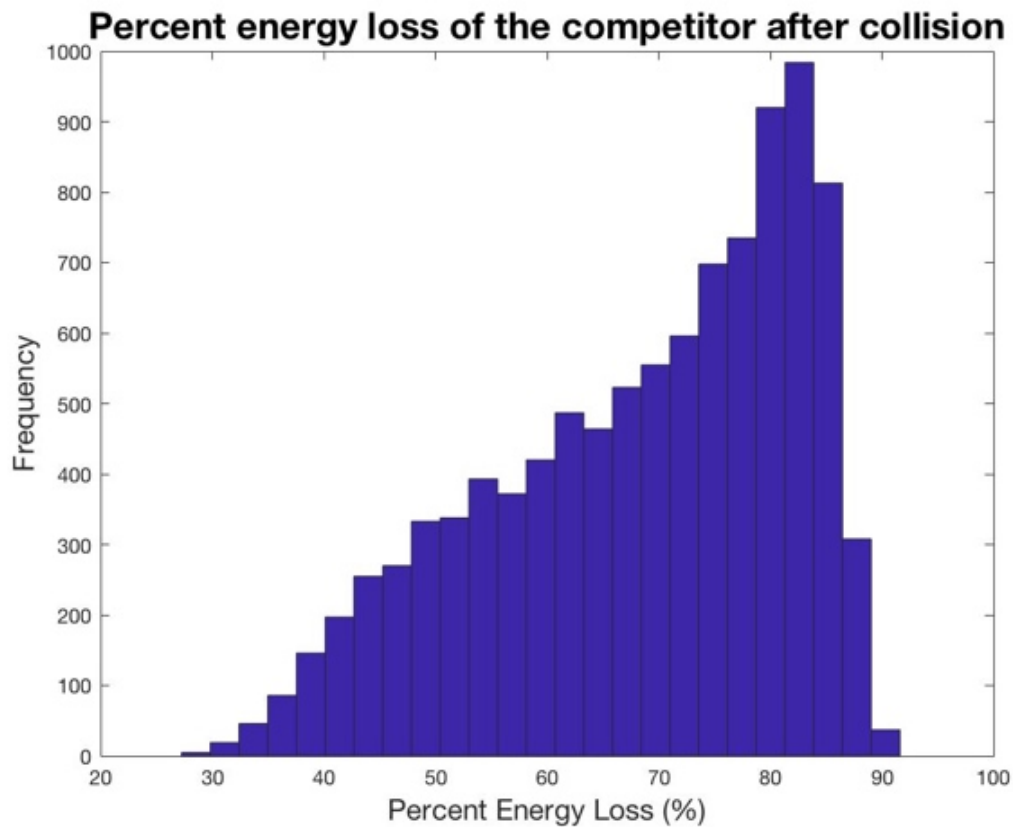


Figure 7.7 Percent system energy loss after the collision.

7.5 Fixed Fence Impulse Ensemble

The fence impulse is the key design parameter for safety fences. It has two components: the magnitude of the impulse of the fence on the horse and the direction of that impulse. Fixed-fence impulse results provide the domain of impulse reaction seeking

improvement (i.e. reduction). As identified in Section 7.4.2, speed is an influential variable for rotation and is used to further separate overlapping impulse results in this section. For added context, a canter pace is considered to be between 4.5 m/s (270 mpm) and the overall gallop course pace for 5* cross country is 9.5 m/s (570 mpm).

Fixed-fence impulse comparisons between rotating and no-rotation contacts are plotted by speed in Figure 7.8 and Figure 7.9 for fixed-fence results, with all angle range jumping positions. For each contact speed with a fixed fence, the average impulse magnitude of the passing situations is plotted (green) compared to the rotations (red), including irrecoverable ones. Error bars represent one standard deviation from the mean.

The key result from Figure 7.8 is that at all speeds the fence reactions in non-rotating foreleg contacts have larger magnitudes on average than those for rotations. This means it would be ideal for devices to activate at lower magnitudes, but not higher magnitudes which is impractical. It also shows significant overlap in impulse magnitude results with the average values for rotations and no-rotation contacts lying within one standard deviation of each other. This makes design criteria of an impulse limit only difficult to separate the two situations. Consequently, safety devices designed to prevent rotational falls will likely have activations by contacts of the same or similar magnitudes by competitors that would not rotate with contact with a fixed fence.

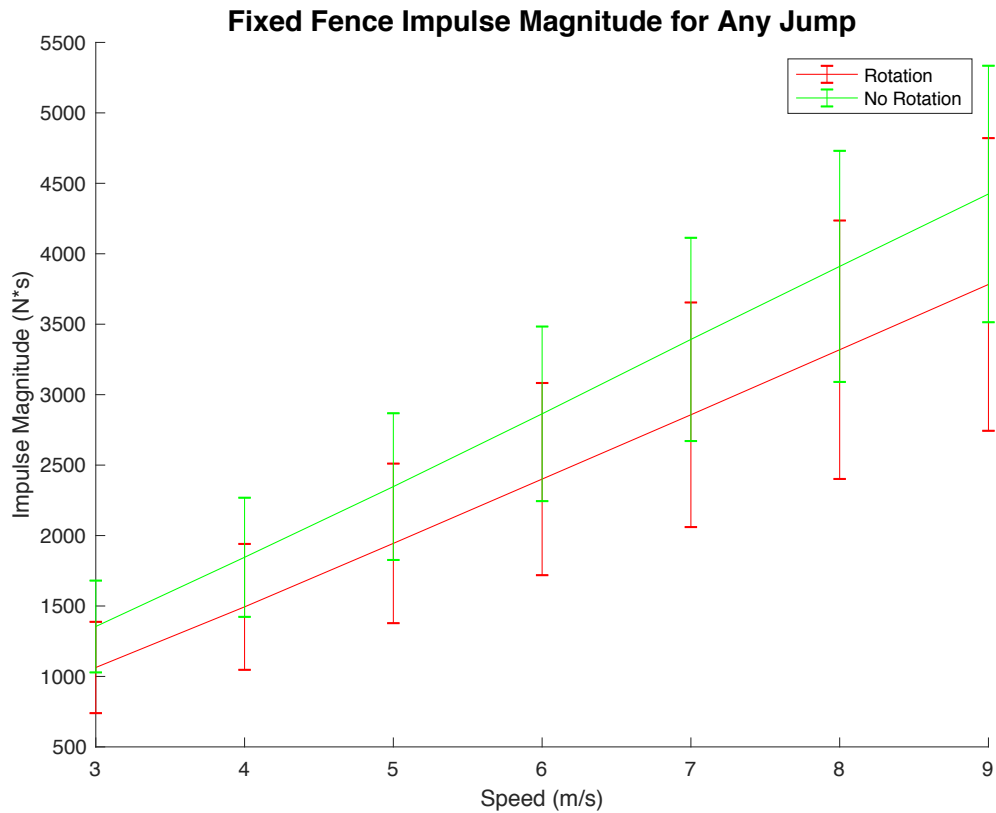


Figure 7.8 Impulse magnitude for a fixed fence when the competitor is in any possible position by speed

To further illustrate the overlap, a histogram can be seen as a piece of the line plot in Figure 7.8, where the line plot points would be the peaks of the red rotation curve and the green no-rotation curve shown in Figure 7.9. The distributions provide more insight to the overlap of the error bars. The white curve shows the magnitude of all critical contacts on the fence, the sum of all rotation and non-rotation results. Note in this presentation, the x-axis is the impulse magnitude, increasing to the right.

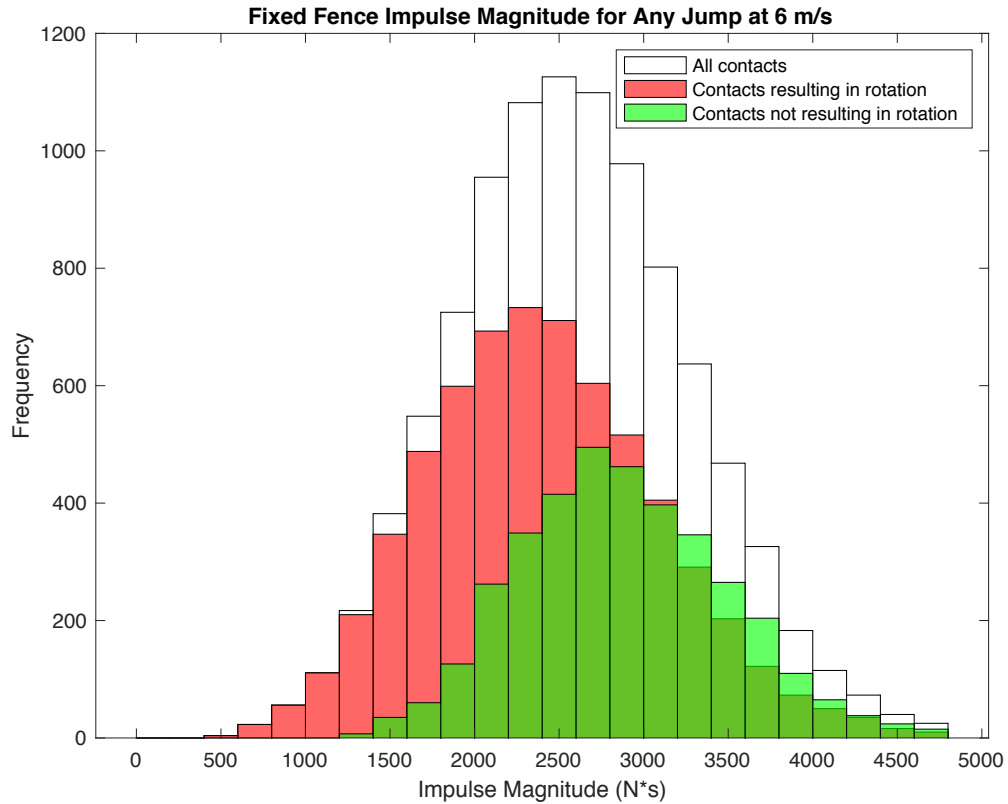


Figure 7.9 Overlaid histogram of rotating and non-rotating impulse magnitude at 6 m/s.

In Figure 7.10, a plot of similar fashion to Figure 7.8 presents the contact reaction angle or impulse angle average and standard deviation for the passing (green) and rotating (red) results with error bars representing one standard deviation. The impulse angle is on the vertical axis and the speed is on the horizontal axis. Here the impulse angles for rotation and no-rotation contacts have less overlap of the results than the impulse magnitude results because the means are not within one standard deviation of each other. The angle ranges overlap even less at higher speeds greater than 7 m/s (420 mpm).

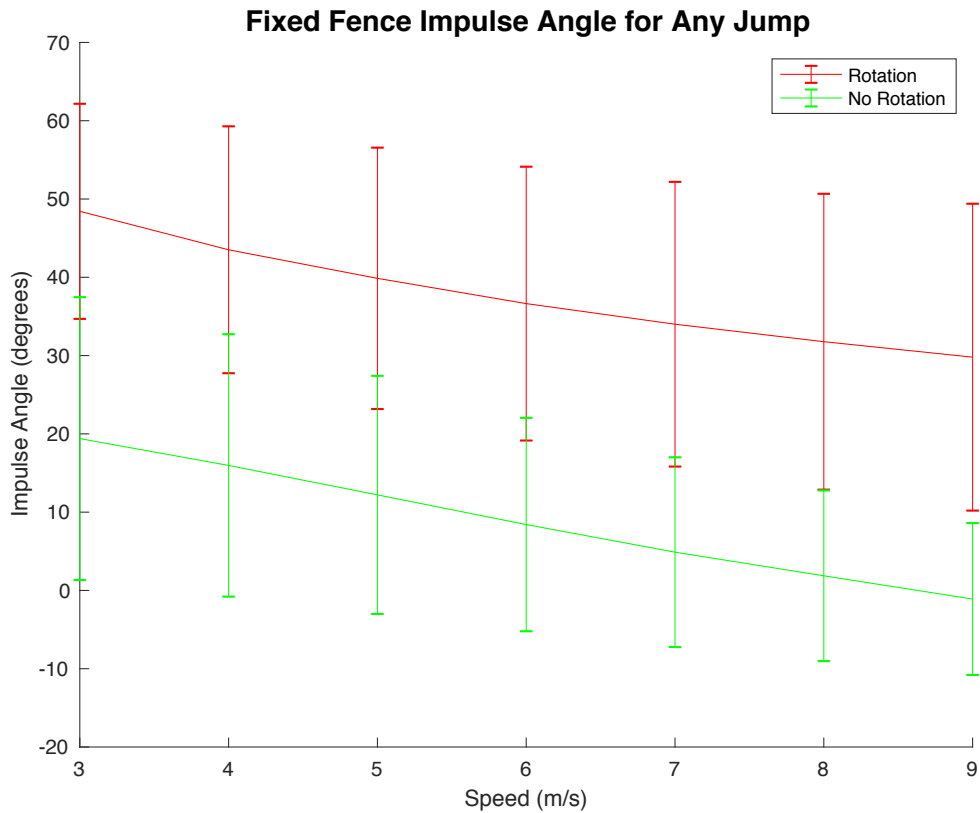


Figure 7.10 Impulse angle for a fixed fence when the competitor is in any possible position by speed

A closer look at the overlap of impulse angles at 6 m/s is shown as a histogram in Figure 7.11. The angle distributions do not show standard normal distribution for all of the critical contacts on the fence (white), no-rotation contacts (green) and rotation contacts (red). Larger segments indicate more contacts in that range. The rotation and no-rotation curves are skewed toward each other.

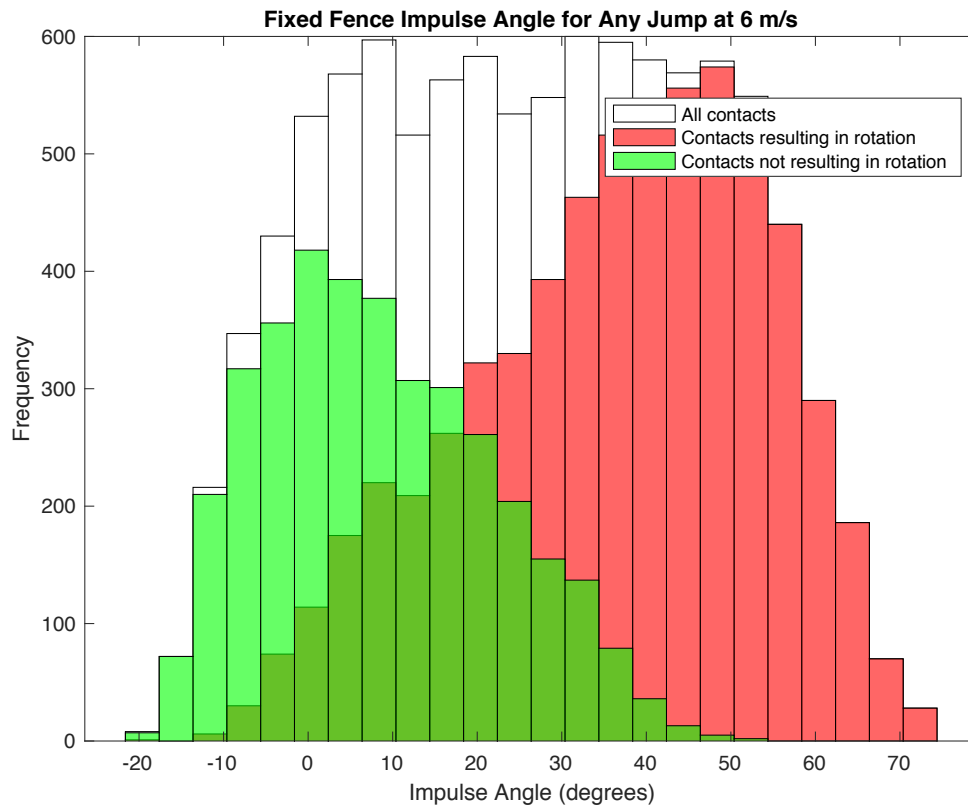


Figure 7.11 Overlaid histogram of rotating/non-rotating impulse angle, 6 m/s contact speed

The impulse histogram in Figure 7.11 can also be shown in a polar format in Figure 7.12 which helps to visualize the impulse of the horse's leg on the rail or jump. The picture can be visualized as an impulse direction vector with the arrow pointed into the center. Rotating contacts tend to mostly come from above, but are not straight down. The direction of potential movement for a safety device may also be informed by this figure.

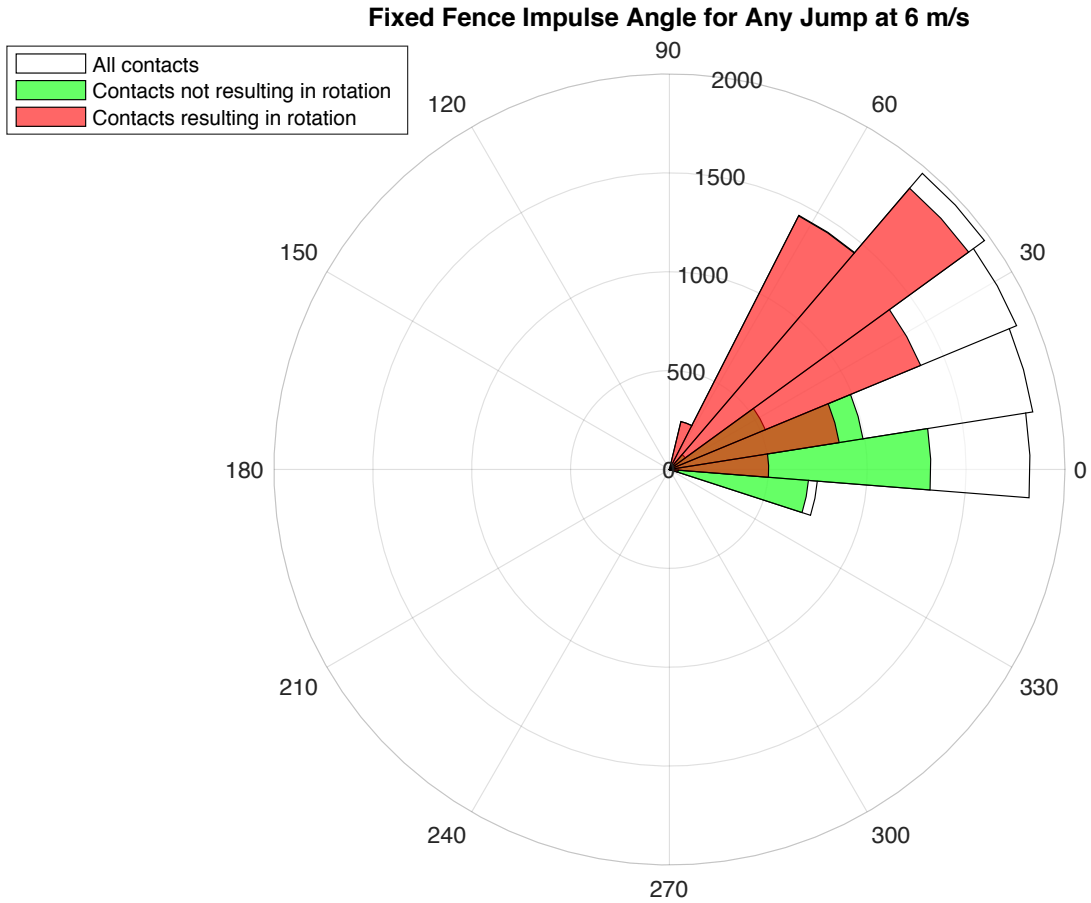


Figure 7.12 Overlaid polar histogram of rotating/non-rotating impulse angle, 4 m/s contact speed

7.6 Activation Criteria Selection

The fixed-fence criteria laid out in the previous section should inform decisions for activation criteria for a safety fence. Ideally, the activation criteria line should be drawn so that a fence activates for as many as possible fixed-fence situations which are probable rotations for safety fences. However, it should also seek to reduce the number of activations for contacts that would not have rotated for a fixed fence, or no-probable-rotation contacts.

Cross country fences should be insensitive to incidental contacts like the incidental hoof strikes from the BE Instrumented fence. Remember that the simulation only models forearm contacts, not incidental hind leg, lower leg, hoof strikes or other contacts. 97% of the incidental contacts for the BE Instrumented fence were below 500 N-s impulse magnitude and generally, that is less than the impulse magnitude of most critical forearm contacts. Designers and competitors can be confident about setting the impulse limit above 500 N-s to prevent false activations from incidental contacts without missing activations for probable rotational falls.

Drawing an impulse-magnitude activation line in Figures 7.8 and 7.9 is difficult due to the overlap between rotation and no-rotation contacts and the higher magnitudes of no-rotation contacts. In Figure 7.8 an activation line can be drawn horizontally with the expectation that the fence would activate for that magnitude and greater. The same activation line would be visualized as a vertical line in Figure 7.9 where all contacts to the right of the line would activate the device. Consequences of this activation will be shown in later sections. Unfortunately, with the average rotation contact being a lower mean than the no-rotation contact, many false activations are likely by using only the impulse magnitude limit.

Impulse angle based designs offer opportunities for more control in preventing false activations. Designers have the opportunity to create an activation window with an upper and lower bound. From this one-contact rotation ensemble the impulse angle is generally larger for rotation cases. Therefore, the upper bound of the activation window may be as high as 75-80 degrees. The lower bound of the angle limit must appropriately balance the amount of mitigating activations for probable rotational falls and false

activations for contacts leading to no probable rotational fall. A potential safety device would ideally activate for all contacts meeting the impulse limit within the activation angle window. Activations outside the window may also activate if the projection of their impulse magnitude inside the angle window is great enough to exceed the impulse magnitude activation threshold.

7.7 Logic Tree for Possible Outcomes of Contacting a Fence with Safety Device

In the safety fence ensemble, there are three intermediate yes-or-no situations and five possible outcomes that describe the effectiveness of the device, and that ultimately indicate the competitor's rotation or non-rotation. First, the simulation indicates if the horse would overturn or not when contacting a fixed fence. This is the baseline understanding of the situation explained in the previous section. Next, contacts are evaluated for meeting safety device activation criteria. If the safety device activates, the resulting collision is re-evaluated for rotation or no rotation.

The process of the outcome situations are shown in a logic tree in Figure 7.13. The right side of the tree examines the consequence of adding frangible fences to the course for competitors that wouldn't have rotated. Despite a critical antebrachium contact, often no rotation would have occurred if the fence was fixed. However if the fence is fitted with a frangible device, the contact may or may not meet the activation criteria even if it would not have resulted in a rotational fall. The left side of the tree is the mitigation side, where there would have been a rotational fall had the fence been fixed. If the critical contact doesn't activate the safety device, there will still be a

rotational fall. If the safety device does activate, some falls will be successfully mitigated. Sometimes the competitor will rotate despite activation.

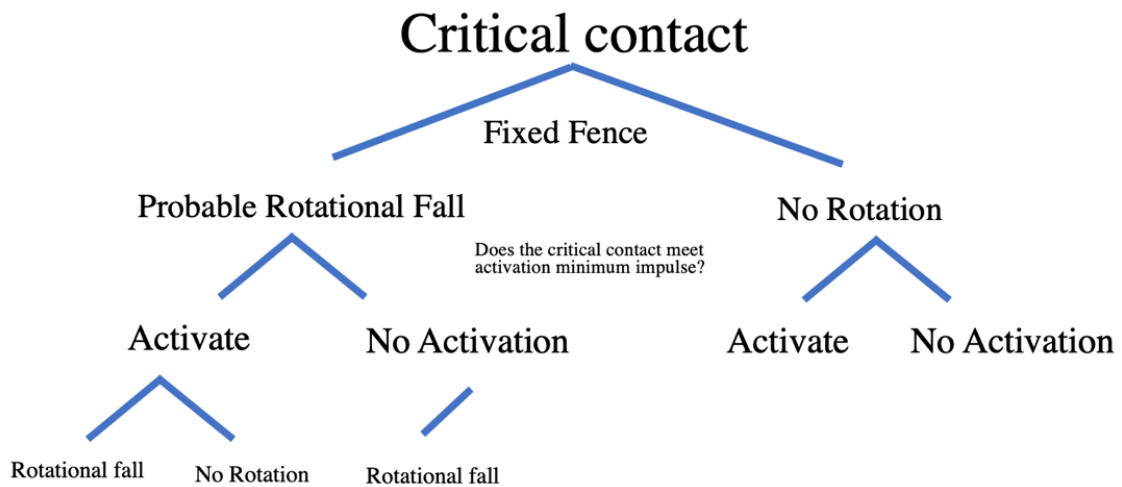


Figure 7.13 A logic tree of possible critical contact outcomes

Therefore, there are 5 total outcomes from a safety device fitted fence. Table 7.1 is an adaptation of the logic tree in Figure 7.13. The negative results are no activation, rotations (in red) and activation, but still rotation (in pink). The successful results include activation successfully mitigates rotation (in light green) and no predicted rotation, no activation which would score as a clean attempt (in green). A potential problem is a false activation, where the contact with a fixed fence would not have rotated, however the fence activates (in orange). Under FEI rules if the fence activates, the competitor is awarded 11 penalties. This “false activation” should be sought to be minimized, though it is a tradeoff with preventing other rotational falls.

Table 7.1 List of outcomes for critical contacts on a safety device fitted fence

Possible Fixed Fence Rotation	Device Activation	Safety Device Rotation	Result
Yes	No	Yes	No activation, rotation
Yes	Yes	Yes	Activates, but still rotation
Yes	Yes	No	Activation produces no rotation (Successful mitigation)
No	No	X	No predicted rotation, no activation (“Clear” attempt)
No	Yes	X	No predicted rotation, but activation (False activation)

7.8 Safety Fence Designs and Jump Safety Quality Index

A device activates if it is struck with an impulse greater than its designed impulse limit and if it is within the activation angle window. In the following sections, the impulse magnitude limit for any direction is described first and then adding an angle activation window follows. Examples of impulse-limiting frangible device reactions were presented in the test results of MiM and UKY pinned-gate safety fences. Other safety designs act to limit the impulse reaction that the horse experiences. Force measurements to confirm the degree that a reaction is limited for various speeds and angles is not currently available and would be difficult to determine experimentally on course. With the results herein, new laboratory and on-course experiments can address this knowledge gap for non-frangible safety concepts.

A Jump Safety Quality Index (JSQI), explained in Eq. (9), is a way to evaluate a design criteria’s effectiveness. The baseline of the JSQI is the number of no-rotation critical contacts for a fixed fence, $n_{FFNoRotation}$. Then the number of rotational falls

mitigated by safety device activation, $n_{MitigatedRotation}$, is added. The unwanted number of false activations is subtracted. Due to the large amount of overlap and likelihood of false activations, a percentage of importance, w , can be used to weigh the effect of false activations, $n_{FalseActivation}$, on the JSQI. With different weighting factors, the false activations may be 100%, 50% or 25% as influential as activation effective rotational fall mitigating. These percentages are chosen and may be altered to suit designer and sport preferences. The false activation number and weight represent the importance of the FEI 11-point activation penalty and the culture of the sport against obstacles collapsing “too easily”. If the jump activating under any critical contact is most important and there is no penalty, the false activation importance may be set at 0%, and removed. The sum of those criteria are divided by the number of critical contacts generated by the ensemble, N , to result in a percentage for the JSQI.

$$(n_{FFNoRotation} + n_{MitigatedRotation} - w * n_{FalseActivation})/N = JSQI \quad (9)$$

Fixed fences have a JSQI, purely based on the number of no-rotations for a fixed-fence contact. Sometimes the amount of false activations brings the JSQI lower than that of a fixed fence. Variables influencing the JSQI include the activation magnitude and angle criteria as well as the speed and position factors. This means a jump with different expected geometries and speeds due to placement on course should have a different JSQI. JSQI allows for jump-specific designs and comparison for quality if the same device is used on different jumps.

7.8.1 Impulse Magnitude Limits

As a recommended process, first implement a fence with an impulse magnitude limit, with activation in any direction. The simulation in this section is considering a fence approached at 6 m/s with the general, one-size-fits-all jumping angle distributions. Figure 7.14 shows the impulse magnitude histograms for contacts resulting in rotation or no rotation for fixed fences. From fixed-fence analysis the mean impulse magnitude for rotation is 2,400 N-s with a standard deviation of 700 N-s. From z-score statistics, it is known that setting the activation impulse limit at the mean would activate for about half of the rotation contacts. Setting the limit at 1700 N-s would activate for 84% of contacts, and at 1000 N-s for 97.7% of rotation contacts. For this reason 1000 N-s is chosen for the impulse magnitude limit. Figure 7.14 shows a histogram of impulse magnitudes for contacts that would have rotated with a fixed fence. The distribution of contacts that meet the impulse magnitude limit and would activate are shown in light green and the probable-rotation contacts that would not cause activation are in red. The device activates for most of the contacts that would cause rotation with a fixed fence. Note that the activation cases, shaded in light green, do not necessarily prevent the competitor from rotating.

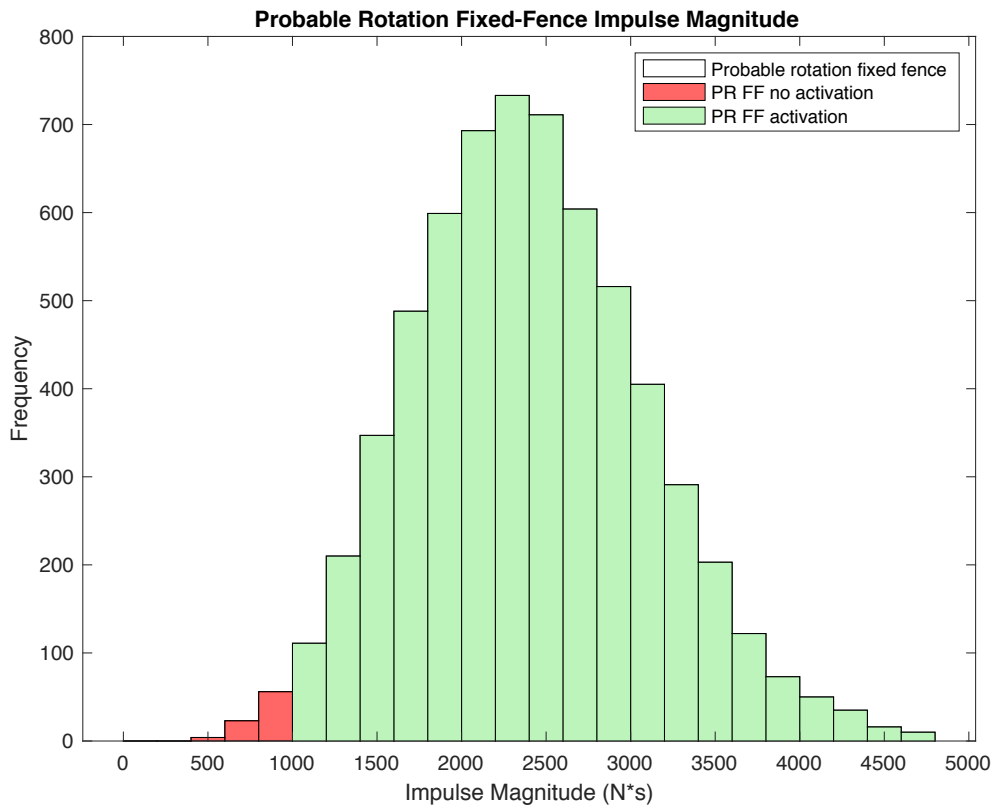


Figure 7.14 An impulse magnitude histogram for fixed-fence probable-rotation contacts that may or may not cause activation with an activation limit of 1000 N-s

The consequence of false activations are shown in Figure 7.15 with a histogram of no-rotation critical contacts. Since all of the no-rotation contacts have a higher magnitude than the activation limit, all no-rotation contacts cause the fence to activate. These would all be considered false activations.

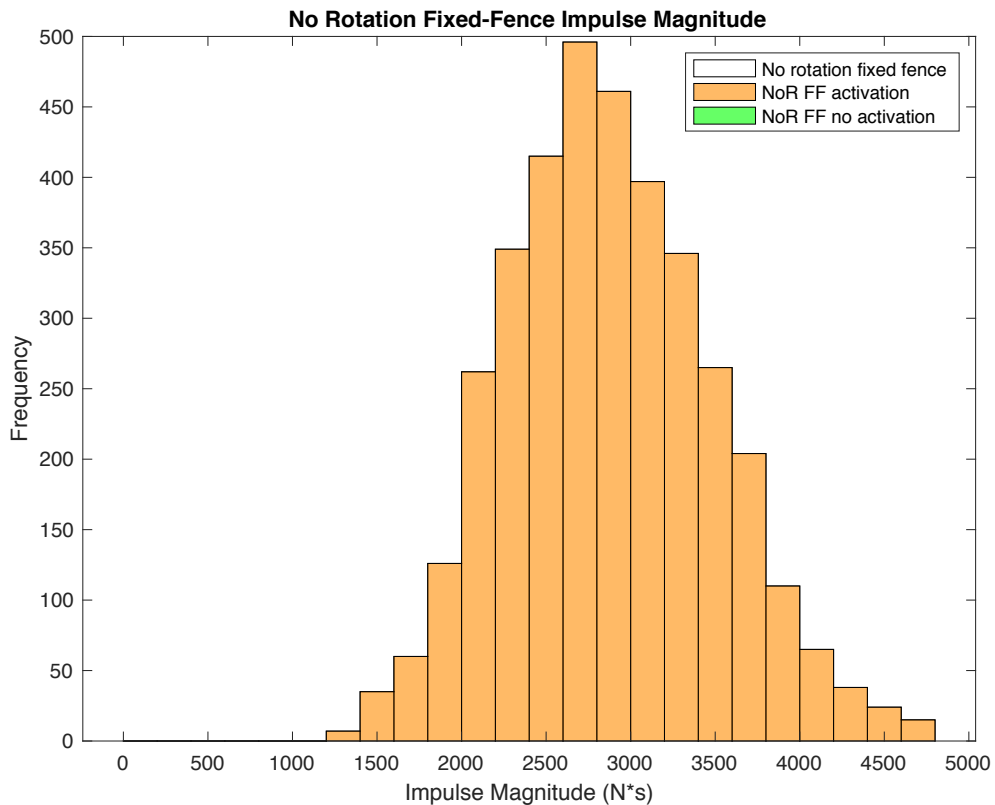


Figure 7.15 Impulse magnitude histogram for no-rotation contacts that may or may not cause activation with an activation limit of 1000 N-s

Of the probable rotations, most will cause activation. However, the device may or may not mitigate these rotations. At an impulse limit of 1000 N-s about 33% of the activations will still rotate, while 66% of mitigated probable-rotation contacts will not rotate. No videos or conversational anecdotes about this phenomena have been shared with UKY researchers. This situation is one indicated by the wide variety and large number of critical contacts evaluated through the simulation. They may have not been observed in practice yet or be additionally explained for. Perhaps more of these do not rotate due to the moving mass of the rails in safety jumps.

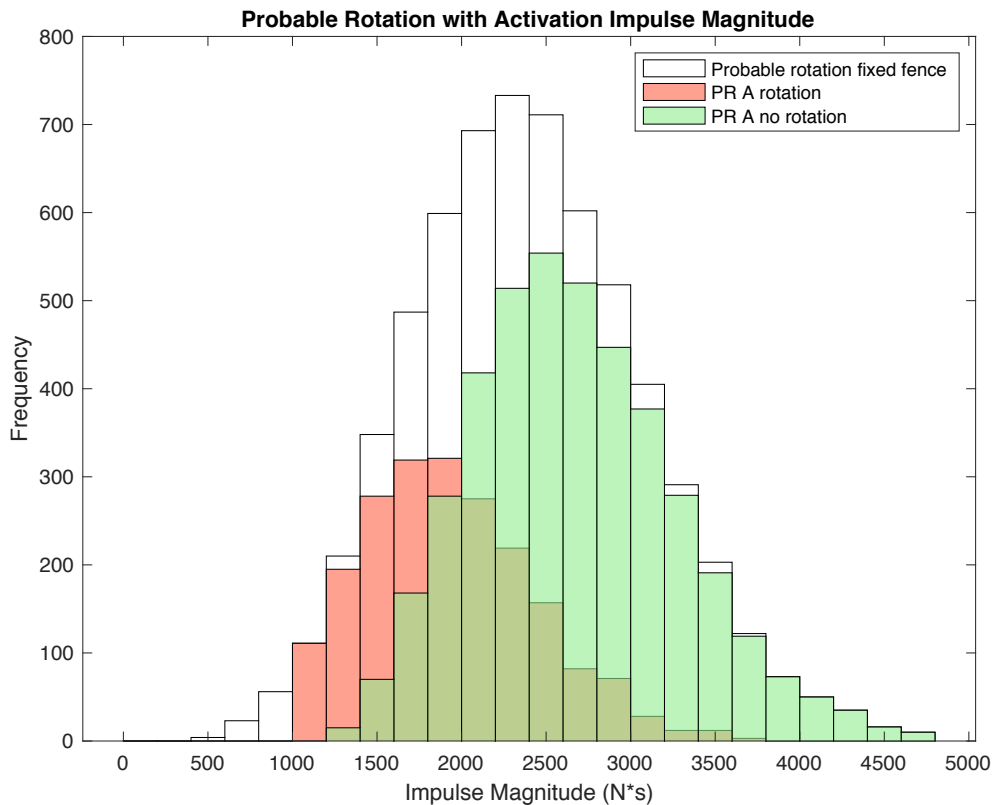


Figure 7.16 Probable-rotation contacts that have activated a safety fence with a 1000 N-s impulse limit may or may not mitigate a rotational fall.

JSQI demonstrates the difference in performance (for any jumping position) between a fixed fence and a safety fence with an impulse limit added for any direction. The JSQI for a fixed fence is 37%. The JSQI is better than that of a fixed fence — regardless of false activation importance weight— for a safety fence at an impulse limit of 1000 N-s. Table 7.2 shows the how the impulse magnitude limit affects the intermediate outcomes shown in the logic tree and the JSQI. For fences with an impulse limit of over 1500 N-s, the JSQI starts to be lower than that of the fixed fence (highlighted in orange) as the number of activations decrease and thus mitigated rotations decrease. As the importance of false activations decreases, the JSQI increases.

Table 7.2 Impulse magnitude limits affect the JSQI performance for different

Impulse magnitude limit for all jumping position angles at 6 m/s	Probable Rotation	No Probable Rotation	Probable Rotation No Activation	Probable Rotation Activation Rotation	Probable Rotation Activation No Rotation	No Probable Rotation No Activation	No Probable Rotation Activation	JSQI 100	JSQI 50	JSQI 25
250 NS	6314	3686	0	487	5827	0	3686	58%	77%	86%
500 NS	6314	3686	0	1004	5310	0	3686	53%	72%	81%
1000 NS	6314	3686	83	2066	4165	0	3686	42%	60%	69%
1500 NS	6314	3686	539	2912	2863	19	3667	29%	47%	56%
2000 NS	6314	3686	1838	2829	1647	228	3458	19%	36%	45%
2500 NS	6314	3686	3612	1937	765	1042	2644	18%	31%	38%
3000 NS	6314	3686	5095	952	267	2211	1475	25%	32%	36%
Fixed	6314	3686	--	--	--	--	--	37%	37%	37%

Different impulse limits and speeds affect the number of rotations and no-rotation situations. Table 7.2 compares impulse limits from 2000 to 100 N-s and their influence on the percent of critical contacts that do not rotate. The leftmost column organizes the results by contact speed. Note that this is not the approach speed, but the magnitude of the horse velocity at the instant of contact. The second column is the fixed-fence pass rate previously plotted in Figure 7.5, highlighting the relationship between higher speed and reduction of the pass (no-rotate) rate. For contact speeds of 4 m/s (240 mpm) or less, the majority of critical fixed-fence contact situations do not result in rotational falls. Impulse magnitude limits of 2000 N-s to 100 N-s reduce rotations (i.e., increase the no-rotation percentage) in all cases. Considering the potential for false activations from hoof strikes revealed by the BE on-course measurements, 500 N-s is recommended as the minimum impulse to achieve 88% passing safety mitigation for all speeds. For higher contact speeds, the safety improvement is dramatic by including an impulse-limiting safety design.

Table 7.3 The speed influences the amount of rotations at a fence but can be mitigated by impulse magnitude limits

Speed, m/s (mpm)	Fixed	Impulse Magnitude Limit (N*s)						Irrecoverable
		2000	1500	1000	500	300	100	
0 (0)	97.78%	97.78%	97.78%	97.78%	97.78%	97.78%	97.78%	2.22%
1 (60)	92.55%	92.55%	92.55%	92.55%	92.56%	93.26%	96.01%	2.23%
2 (120)	84.70%	84.70%	84.70%	84.87%	88.96%	92.59%	96.55%	2.18%
3 (180)	71.44%	71.47%	72.06%	76.25%	87.58%	92.02%	96.47%	2.23%
4 (240)	58.76%	59.90%	64.81%	75.17%	88.24%	92.76%	96.36%	2.25%
5 (300)	45.08%	52.02%	62.62%	75.21%	87.65%	92.17%	96.29%	2.21%
6 (360)	34.41%	50.11%	62.11%	75.26%	88.25%	92.74%	96.31%	2.18%
7 (420)	23.61%	49.49%	61.73%	74.49%	87.63%	92.20%	96.18%	2.22%
8 (480)	15.37%	49.03%	61.42%	74.41%	87.38%	92.21%	96.32%	2.19%
9 (540)	9.87%	49.91%	62.61%	75.42%	88.45%	92.66%	96.18%	2.23%
10 (600)	5.61%	49.79%	62.66%	75.26%	88.20%	92.58%	96.32%	2.25%
11 (660)	2.64%	49.98%	62.07%	74.95%	87.72%	92.43%	96.26%	2.22%

Table 7.2 summarizes the pass-rate results for the widest range of contact situations. Pass rates (i.e., competitors that do not rotate past vertical after dangerous foreleg contacts) are determined through the simulation by analyzing 10,000 random situations for each result presented, more than 780,000 dangerous foreleg fence contact situations total. Table 7.2 therefore represents the conservative approach by using a uniform distribution of random jumping configurations and positions, and an impulse magnitude limit for all impulse angles.

Limiting the impulse magnitude is effective in preventing rotational falls, especially at higher speeds. The table above abides by the device tolerance of +/-5% as specified by the FEI in the current safety device standard. This table can be used to estimate the percentage improvement from a fixed-fence to a safety fence when defining design criteria. Note that a safety fence is one that incorporates any design to reduce the contact impulse: frangible, resettable, angled face, brush, friction-reducing, etc.

7.8.2 Application of Angle Limited Designs

It was recognized in Figure 7.10 that separation of rotation and no-rotation contacts is more possible by using a window of activation based on impulse angle than by a criteria based on impulse magnitude. The impulse angles for probable-rotation and no-probable-rotation contacts do not follow a normal distribution. Choosing a 10 degree to 80 degree angle window will limit some false activations. Figure 7.17 shows the curve of no-probable-rotation for a fixed-fence with no activation in green and false activations in orange. In this example, the peak of the no-rotation critical contact curve is outside of the activation angle window

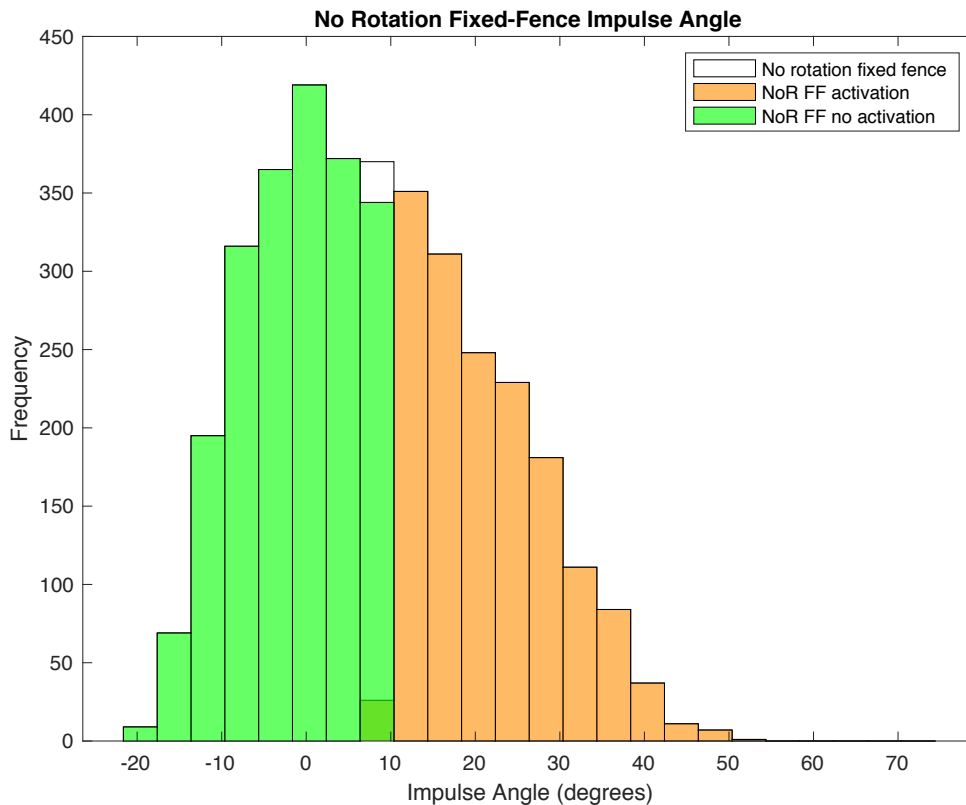


Figure 7.17 Activation or no activation for critical contacts that would not have activated for a fixed-fence

As a result of angle range (10 to 80 degrees) activation and a 1000 N-s impulse magnitude limit, 16% of probable rotations do not activate, while without the angle window there would be 2% of probable rotations that would not activate. With only the impulse magnitude limit of 1000 N-s, 100% of critical contacts with no probable rotation would activate the fence. If the 10-80 degree angle window is added, then the false activation rate is 43%.

The overlaying histograms in Figure 7.18 visualizes all the categories of outcomes together. Critical contacts left of the 10 degree impulse angle limit do not activate. No probable rotation, no activation contacts (green) make up 21% of critical contacts. This

population is an improvement to the impulse limit activation only which results in the fence activating for all critical contacts. No activation, rotation contacts (red) are 6% of critical contacts which are primarily to the left of the activation angle lower bound also bridge into the activation window for contacts less than 1000 N-s. This is 5% more than the probable rotation, no activation rate for only 1000 N-s limit. The activation angle window starts at 10 degrees and activates for the rest of the contacts that meet the 1000 N-s limit. False activations, or no-probable-rotation activations (orange) are 16% of contacts, which is 21% lower than with no activation angle window. Probable-rotation contacts that activate the safety fence and then still rotate are 20% of all critical contacts. The result of adding the safety device is that 37% of all contacts are activations that mitigate rotational falls.

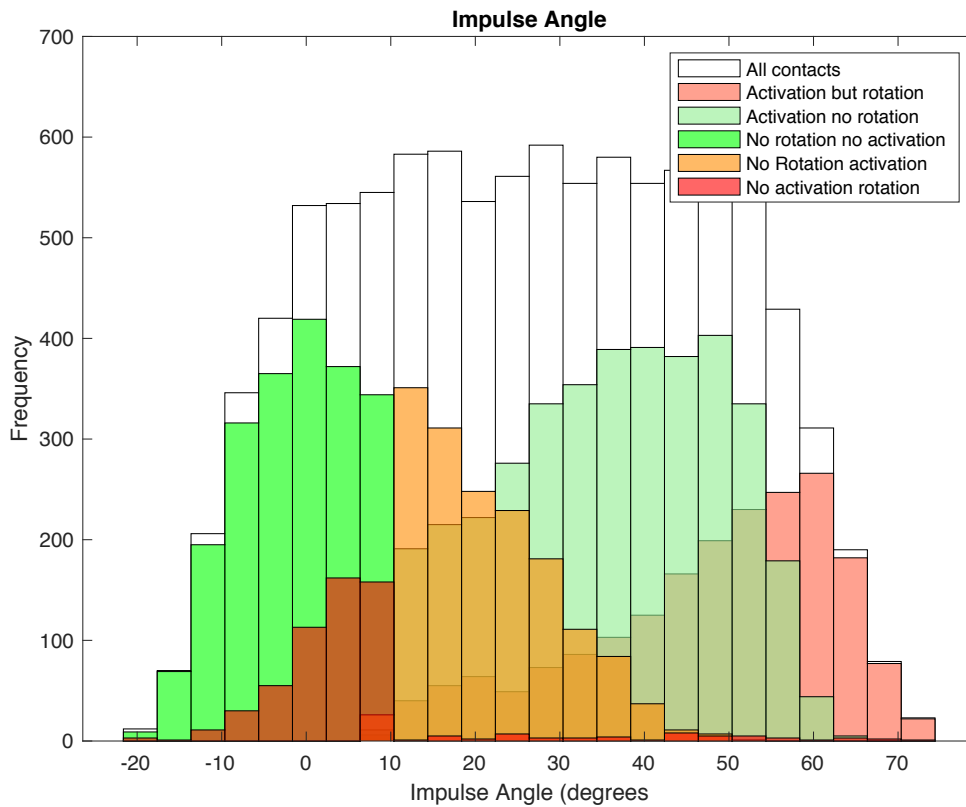


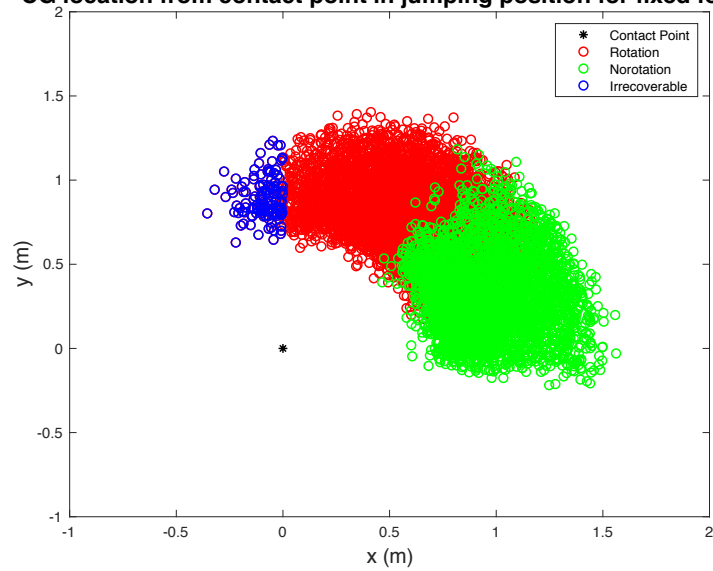
Figure 7.18 Overlaid histograms for a safety fence with an impulse magnitude limit of 1000 N-s and an activation window of 10-80 degrees.

The complexity of the in-the-field results are seen in the simulation. This explains the source of conflicting observations when rotational falls do happen, of cases where devices activate when riders feel they shouldn't, and when rotations happen even though devices activate. Federations and competitors must acknowledge the range of possible outcomes and how safety devices may affect them.

7.8.3 CG Location Safety Device Improvement

In Figure 7.19, to geometrically illustrate the improvement of an impulse-magnitude limiting safety design, the circumstances for a 6 m/s speed at the time of contact for any jumping position are repeated with CG plots for a fixed-fence (left) and with safety design (right). Many rotation and no-rotation CG points overlap. The safety design employed is a 1000 N-s impulse magnitude limit within a 10 to 80 degree impulse angle window. Competitors in situations closest to irrecoverable remain at risk, but 37.3% additional competitors do not rotate with the safety design.

CG location from contact point in jumping position for fixed fence



CG location from contact point in jumping position for Safety Fence

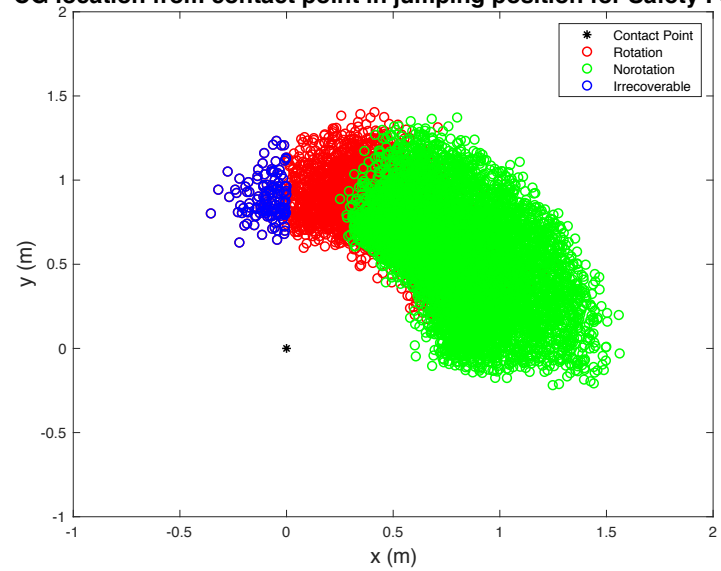


Figure 7.19 At 6 m/s, (left) Fixed-fence impulse CG location plot about contact point yields 36.9% no-rotation rate; (right) Impulse magnitude limited to 1000 (+/-5%) for impulse angles between 10 and 80 degrees yields 74.2% no-rotation rate

In general, as fence impulse magnitude limits are implemented in the simulation, competitors in previously overturning positions do not overturn, progressing from CGs near the vertical plane above the contact to CGs corresponding primarily to upward and forward jump arc positions. Recall that the points in blue are irrecoverable scenarios, therefore achieving a 100% pass rate is only possible if the fence is positioned so that is it impossible to have the CG near the top of the fence at the time of contact. This reiterates the course designer/builder collective wisdom for avoiding upright or square jumps with minimal ground lines, especially at high speeds.

7.9 Ensembles for Safety Case Studies Incorporating Video Data

It is generally recognized that a variety of the cross country questions are ridden differently. For example, an approach to an open oxer is different than to a vertical into a combination. This causes a set of different response expectations for safety devices based on their application. Two simulations based on recent video data with contact speeds will be considered, followed by a discussion of how design requirements can be both tailored to custom questions and generalized for sports safety.

The following simulations are based on a jumping situations similar to jumps in 2017 RK3DE pictured in 4.2 and 2018 LRK3DE pictured in Figure 4.3, but do not recreate the real events that occurred because no rotational falls happened. Recall that the simulation models all competitors as having contact on the foreleg, and only one of the competitors in 2018 and none of the horses in 2017 contacted the fence on their foreleg. The situations modeled can be thought of as a horse jumping the fence in a similar manner (speed and position angles) to those seen on course, but then each competitor

contacts the fence on their antebrachium. Normal distributions are created about the jumping positions and the speeds measured from the video to generate this scenario-specific simulation for these two case studies with critical contacts with 270 ± 20 degree antebrachium angle.

7.9.1 2017 Open Oxer Based Ensemble

At RK3DE 2017, Fence 14 was an open oxer after a long gallop on a slight downhill. The average speed at a potential time of contact was 6.12 m/s with a standard deviation of 0.33 m/s and the body angle was -32.3 degrees with a standard deviation of 5.5 degrees. None of the horses contacted the fence in the critical forearm zone, but this ensemble considers the consequence of 10,000 forearm contacts in similar situations.

Consider the baseline fixed-fence situation in order to understand the situation and select a reasonable impulse magnitude limit and angle activation window. Figure 7.20 shows the fixed-fence histograms for impulse magnitude and angle. The overall no-rotation rate and JSQI is 64.9%, which is better than the no-rotation rate seen for jumps in any jumping position as seen in previous sections. The mean impulse magnitude for rotation contacts is 2075 N-s and the standard deviation is 553 N-s. Setting the impulse limit at 900 N-s would capture about 97.7% of critical rotation contacts. In this case, the impulse angle distribution for no-rotations is approximately normal, and the mean is -7.4 degrees, so a minimum limit of -10 degrees may be chosen. The maximum impulse angle is 23.3 degrees so an upper bound may be 25 degrees to capture all critical contacts, and make the device less sensitive to incidental contacts.

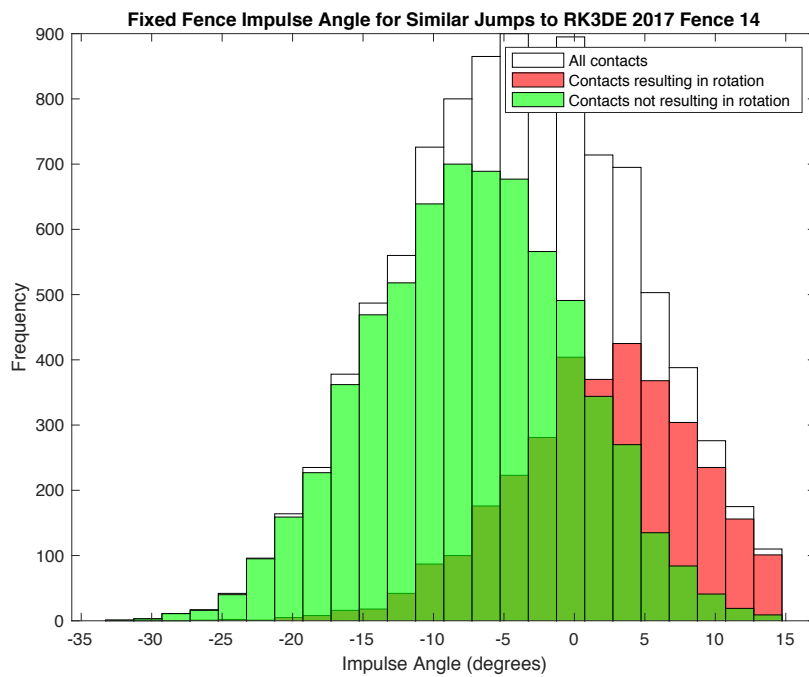
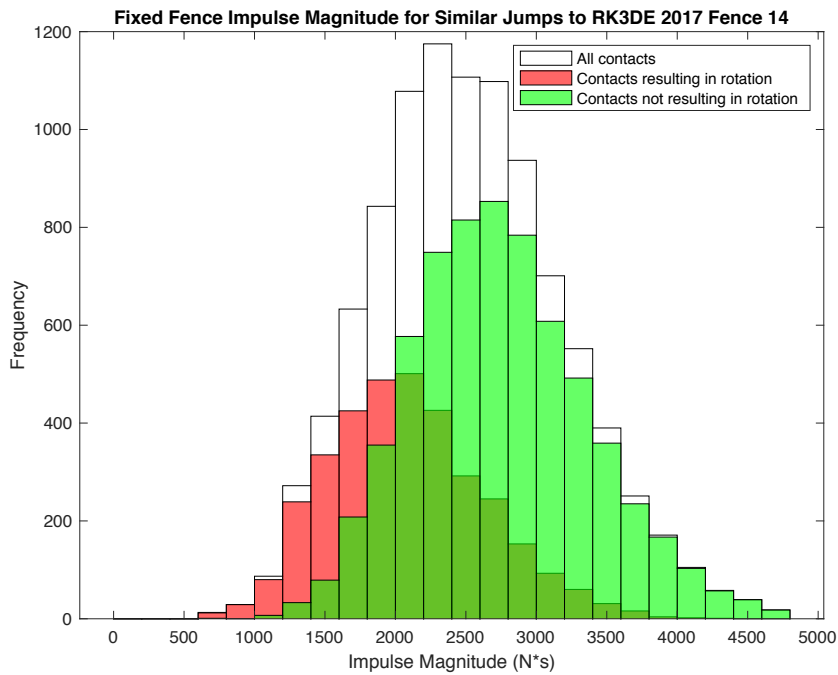
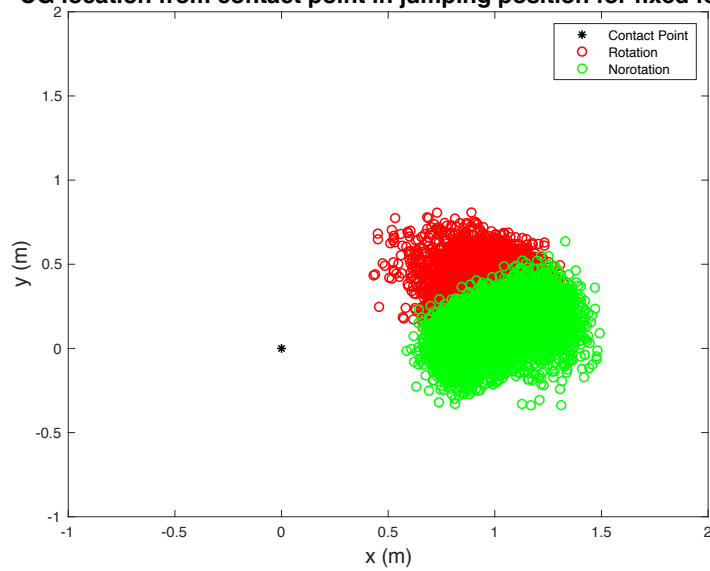


Figure 7.20 For similar fixed-fence jumping situations to RK3DE 2017 (above) a histogram of impulse magnitudes and (below) a histogram of impulse angle identify rotation and no-rotation situations

Adding the safety device reduces the number of rotational falls that would have occurred with a fixed fence. For comparison purposes, Figure 7.21 (above) represents the fixed-fence scenario, with a 64.9% pass rate. For the same population, 96.4% of competitors do not rotate if the fence is impulse-magnitude limited from -10 to 25 degrees. Note that there is overlap of no-rotation contacts (green) and rotation contacts (red). It is also notable that there are no irrecoverable cases (which would have been shown in blue) in this ensemble developed by using the distributions from the video study, unlike the previous distributions using wider ranges of configuration possibilities to represent multiple jump situations. This demonstrates that the fence was well placed by course designers.

CG location from contact point in jumping position for fixed fence



CG location from contact point in jumping position for Safety Fence

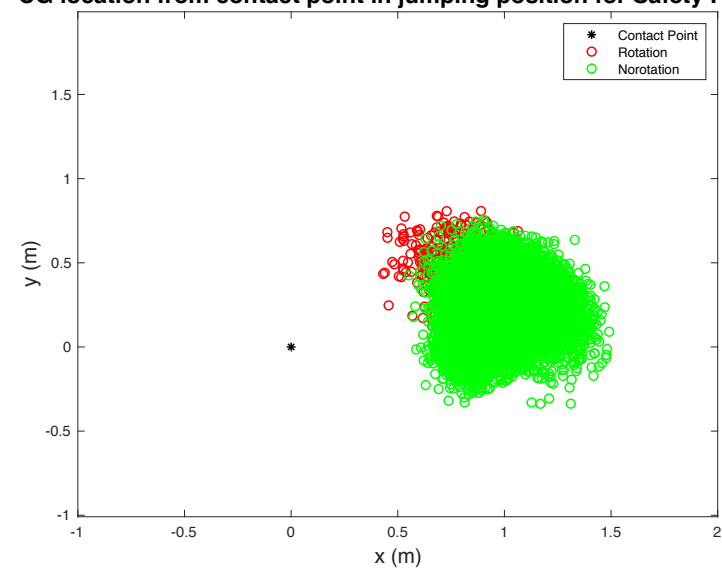


Figure 7.21 CG location from contact point with speed and jumping positions based on the open oxer filmed at the 2017 RK3DE. The pass/rotate coloring represents (left) a fixed fence and (right) a frangible fence limiting the impulse magnitude to 900 N-s between -10 and 25 degrees.

Adding a safety device by the specified limits increases the no-rotation rate by 31.5%, but also introduces false activations. Figure 7.22 demonstrates the various outcomes of the safety device criteria. Critical contacts left of the -10 degree impulse angle limit do not activate. No probable rotation, no activation contacts (green) make up 23.6% of critical contacts. No activation, rotation contacts (red) are only 1.4% of critical contacts. This means the device does a very good job of activating for probable rotations. False activations, or no-probable-rotation activations (orange) are 41.3% of all critical contacts. Probable-rotation contacts that activate the safety fence and then still rotate are 2.2% of all critical contacts. The result of adding the safety device is that 31.5% of all contacts are activations that mitigate rotational falls, while 41.3% are activations providing no mitigation (false activation).

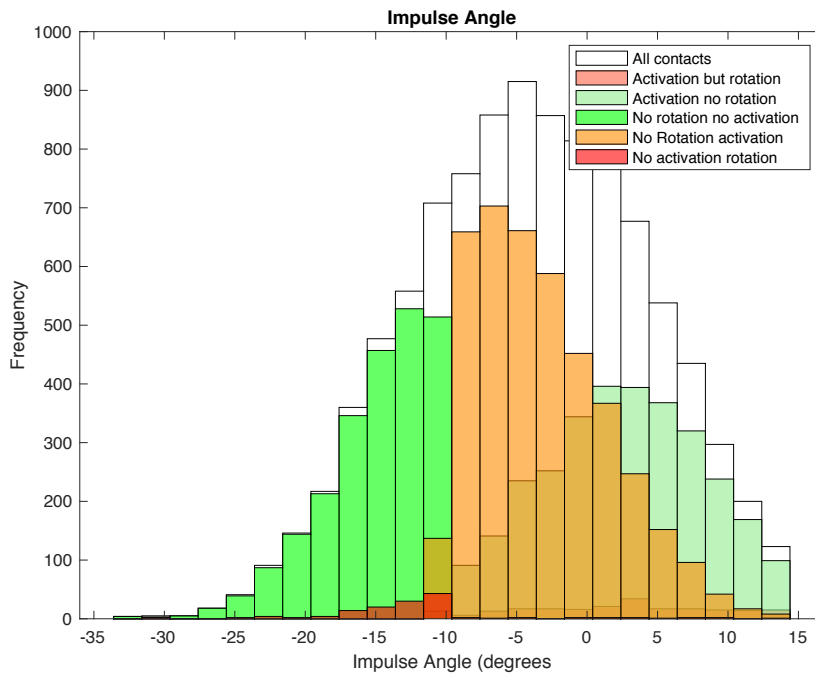


Figure 7.22 Impulse angle activation consequences for jump attempts similar to those in RK3DE 2017 with activation impulse criteria of 1000 N-s between -10 and 25 degrees.

The JSQI for this situation is important for understanding the trade-offs for preventing rotational falls and false activations. A fixed-fence JSQI is 64.9%. The no-rotation percentage for this safety device is 96.4%, but if the false activations are taken into account, the device quality changes. JSQI 100 is 55.1% which is less than the quality of a fixed fence. JSQI 50 is 75.7% and JSQI 25 is 86.1% which is better than that of a fixed fence. Decreasing the angle range reduces the overall no-rotation percentage but reduces the number of false activations. Understanding this should influence sport rules on the degree of penalty for fence activation, since the occurrence of false activations is recognized through the JSQI.

7.9.2 LRK3DE 2018 Vertical in Combination Based Ensemble

At LRK3DE 2018, fence 4 was a vertical into a three-jump bending combination with water was video recorded. The average speed was 4.81 m/s with a standard deviation of 0.33 m/s and the body angle was -24.0 degrees with a standard deviation of 5.1 degrees. None of the horses contacted the fence in the critical forearm zone, but this ensemble considers the consequence of 10,000 forearm contacts in similar situations.

Consider the baseline fixed-fence situation in order to understand the situation and select a reasonable impulse magnitude limit and angle activation window. Figure 7.23 shows the fixed-fence histograms for impulse magnitude and angle. The overall no-rotation rate and JSQI is 80.1%, which is better than the no-rotation rate seen for jumps in any jumping position as seen in section 7.5. The mean impulse magnitude for rotation contacts is 1510 N-s and the standard deviation is 431 N-s. Setting the impulse limit at 700 N-s would capture about 97.7% of critical rotation contacts. In this case, the impulse angle distributions are very overlapped so a minimum limit of 5 degrees can be proposed and adjusted to a designer's preferences. The maximum impulse angle is 34.7 degrees so an upper bound may be 40 degrees to capture all critical contacts, and make the device less sensitive to incidental contacts.

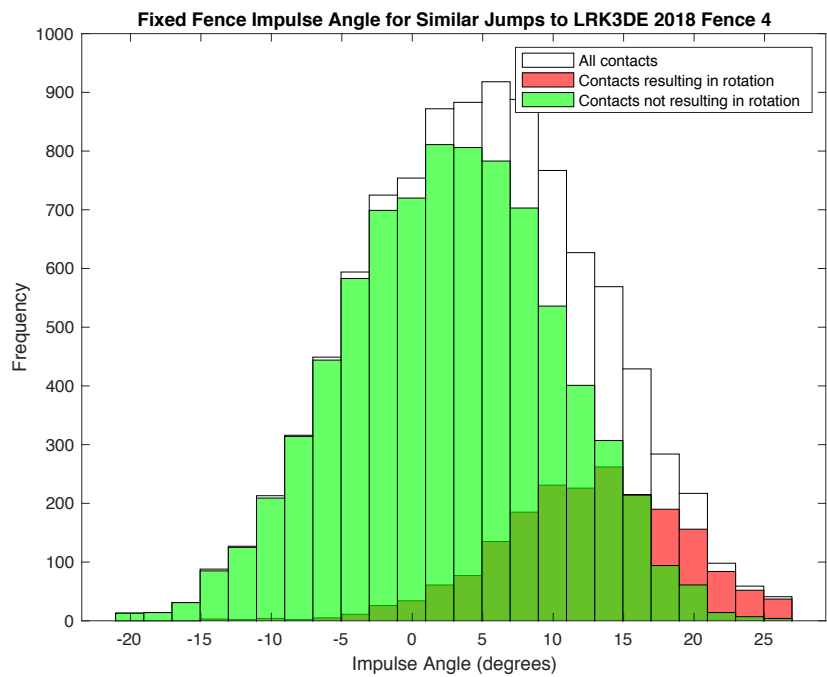
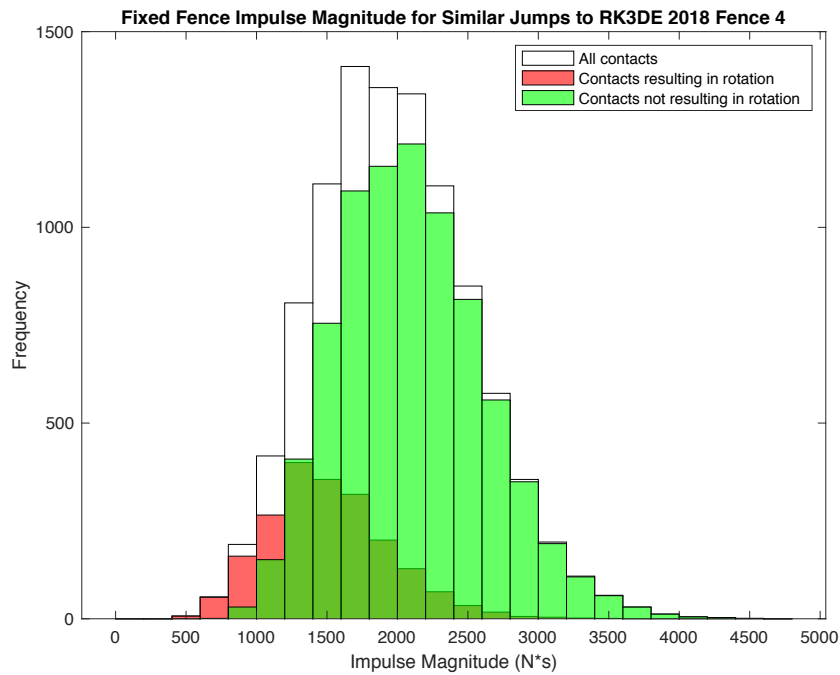
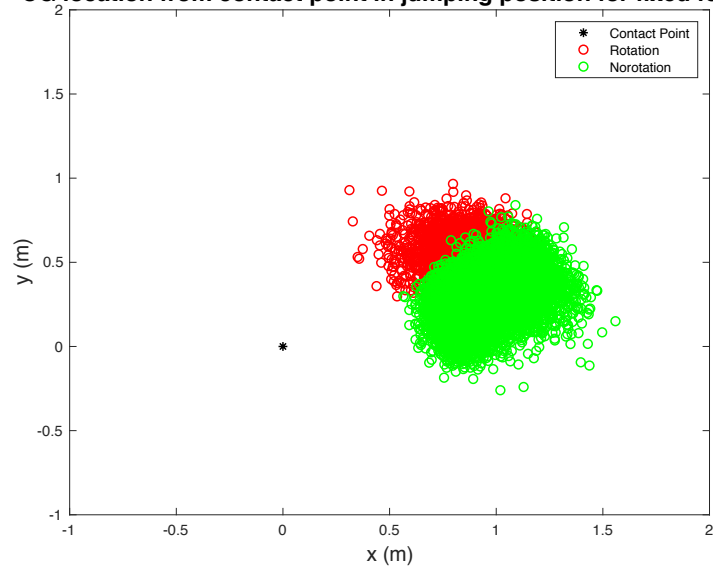


Figure 7.23 For similar fixed-fence jumping situations to LRK3DE 2018 (left) a histogram of impulse magnitudes and (right) a histogram of impulse angle identify rotation and no-rotation situations

Adding the safety device reduces the number of rotational falls that would have occurred with a fixed fence. For comparison purposes, Figure 7.24 (above) represents the fixed-fence scenario, with a 80.1% pass rate. For the same population, 96.1% of competitors do not rotate if the fence is impulse-magnitude limited to 700 N-s from 5 to 40 degrees. Note that there is overlap of no-rotation contacts (green) and rotation contacts (red). It is also notable that there are no irrecoverable cases (which would have been shown in blue) in this ensemble developed by using the distributions from the video study, unlike the distributions for all jumping situations and angles. This demonstrates that the fence was well placed by course designers.

CG location from contact point in jumping position for fixed fence



CG location from contact point in jumping position for Safety Fence

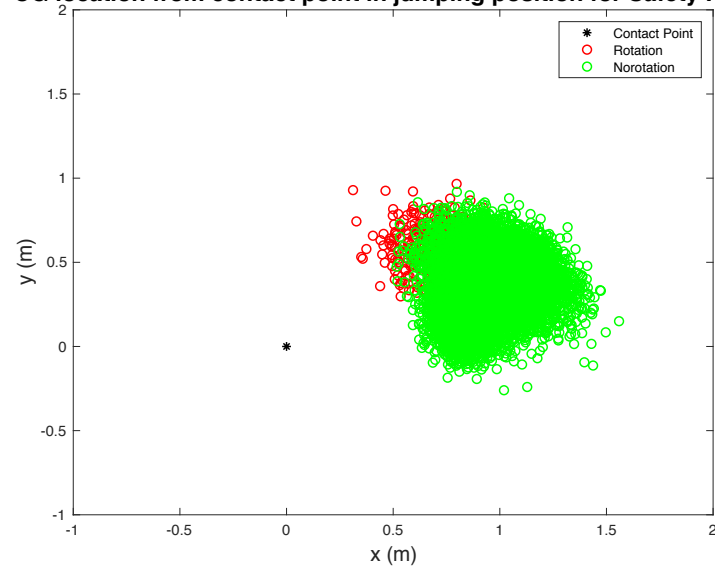


Figure 7.24 CG locations from contact point with speed and jumping positions based on post-and-rail vertical filmed in 2018 LRK3DE. The pass/rotate coloring represents (a) a fixed fence and (b) a frangible fence limiting the impulse magnitude to 700 N-s between 5 and 40 degrees.

Adding a safety device by the specified limits increases the no-rotation rate by 16.0%, but also introduces false activations. The various outcomes of the safety device criteria are shown in Figure 7.25. Critical contacts left of the 5 degree impulse angle limit do not activate. For this population, the number of rotation contacts are already low at 19.9% compared to wider jumping position distributions. No probable rotation, no activation contacts (green) are 48.7% of critical contacts. No activation, rotation contacts (red) are 2.6% of critical contacts. False activations, or no-probable-rotation activations (orange) are 32.5% of all critical contacts. Probable-rotation contacts that activate the safety fence and then still rotate are 1.2% of all critical contacts. The result of adding the safety device is that 16.0% of all contacts are activations that mitigate rotational falls.

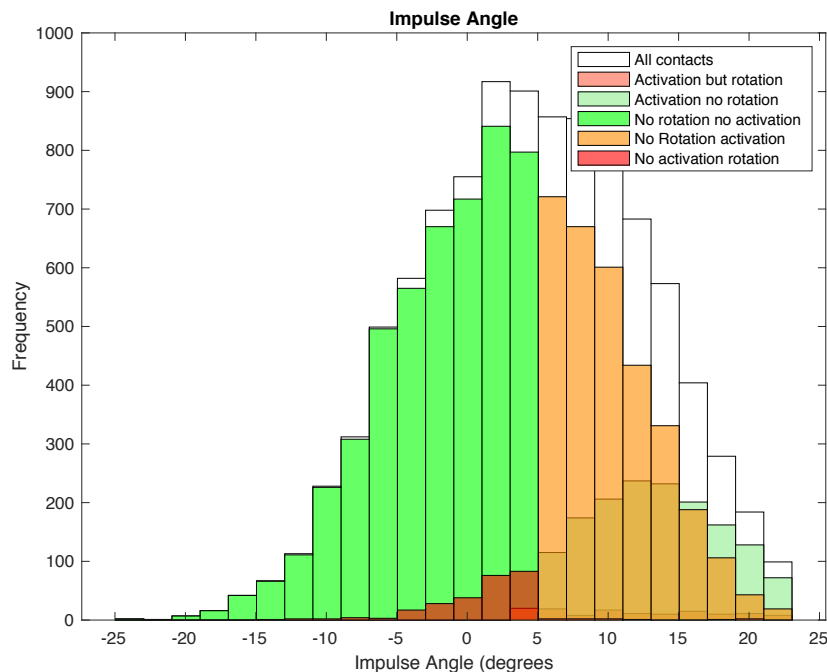


Figure 7.25 Impulse angle activation consequences for jump attempts similar to those in LRK3DE 2018 with activation impulse criteria of 700 N-s between 5 and 40 degrees.

The no-rotation percentage for the fixed-fence results in a very high JSQI percentage of 80.1%. The likelihood false activations is high for this many no-rotation opportunities. The no-rotation percentage for this safety device is 96.1%, but if the false activations are taken into account, the device quality changes. JSQI 100 is 64.7% which is less than the quality of a fixed fence. JSQI 50 is a small improvement of 80.4% and JSQI 25 is 88.3% which is better than that of a fixed fence. Decreasing the angle range reduces the overall no-rotation percentage but also reduces the number of false activations.

For this design, it is important to recall the horse's hind legs pushing scenario which is not modeled in this thesis but is expected to be influential to the number of rotational falls in low speed, vertical fences.

7.9.3 Current Design Comparison

Current designs used in the field have designed inherent angle limitations. First the device may not be sensitive to impulses in the direction of the post holding the rail. Designs for directionally activated safety devices such as original pins (vertical activation) and MiM clips (horizontal activation) activate for contacts over a range of angles as seen in MiM illustrations (Figure 7.26). Some of these concepts such as the MiM table implementation where activation by vertical contact is not desired and therefore prevented, are angle-limited by design. As illustrated, activations for the table occur between -15° and $+45^\circ$, with 0° as the incoming approach is parallel to the ground (here, horizontal).

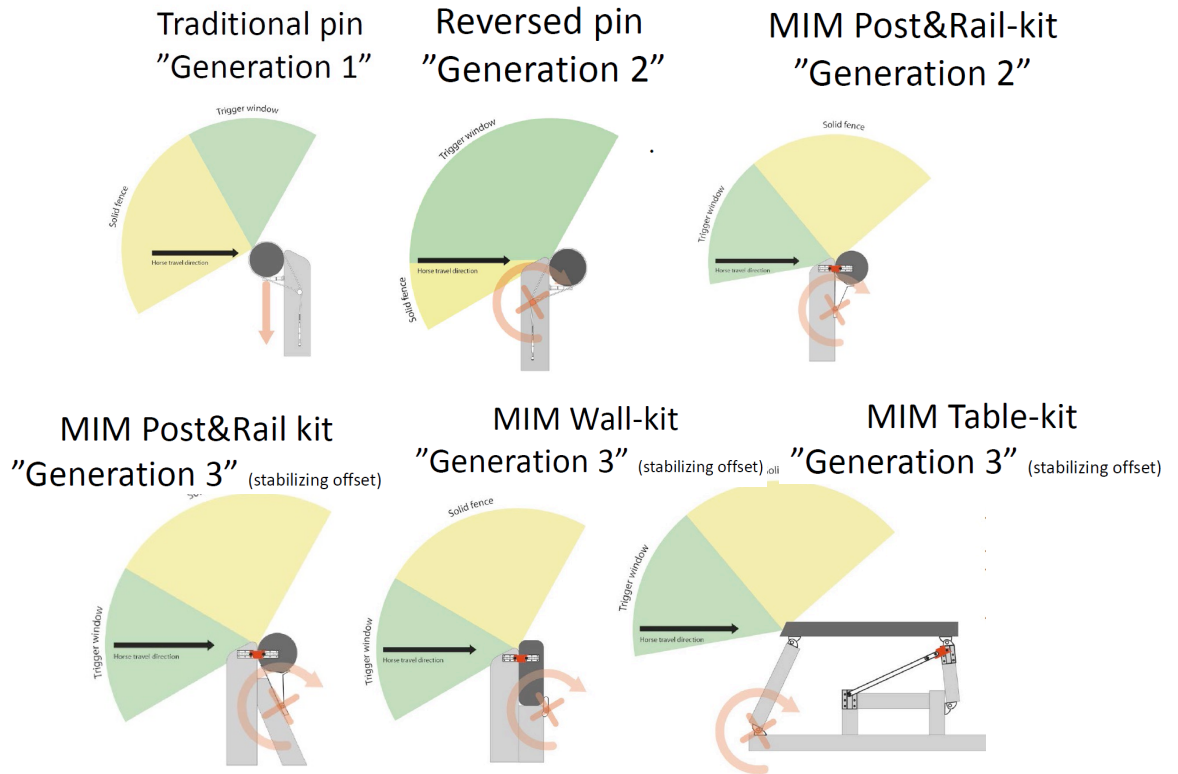


Figure 7.26 Illustrations from MiM 2015 Presentation at Maarsbergen Showing Directional Activation of Frangible Designs [31]

7.9.4 Design Differences for Different Fences: Speeds, Placement, and Fence Type

The plausible range of speeds for cross country jumping contact is 4 m/s (240 mpm) to 9 m/s (540 mpm). From simulation results, competitor rotations are recognized as sensitive to expected contact speeds. For this reason, the safety device appropriate for a galloping fence would be more sensitive, and could be a different model or have different activation criteria, than that for a fence jumped at slower speeds such as a combination.

The impulsive reaction of the moving mass of the fence safety design must also be taken into account. During the impulse-limited reaction, the moving mass will start at

rest and increase until moving at the same speed as the horse at the contact point. This will be less than the contact speed, but if the contact speed is assumed the estimated moving-mass impulse will be slightly high, and therefore a conservative estimate. For a 550-lb rail (250 kg, the maximum with a frangible pin) contacted at 4 m/s, the reaction impulse is 1000 N-s.

Any design that limits the reaction of the contact with the fence, whether frangible mechanisms, friction-reducing surfaces, angled front faces, resettable moving subparts, or new concepts will reduce rotations for all cases, and are most effective for high-speed contact. More research is needed to understand the impulsive reactions across diverse classes of designs

7.9.5 Generalized Categories of Fence Design

Fences may be grouped in a variety of ways. Charles Barnett and Jane Murray grouped fences into categories while identifying fall risk factors based on fall reports from 2008-2014 [21]. The eleven categories included the following: post-and-rail, palisade, square spread, ascending spread, brush, round, corner, Trakahner, step, water and ditch. Illustrations for the first four are included in Figure 7.27. In the USEA Cross Country Obstacle Design Guidelines, 35 different fence types are identified [63]. Placement affects the way fences are approached in terms of speed and jumping position, but some grouping consolidation must be made so that 11 or 35 different frangible devices are not required.

From the Barnett and Murray report, a total of 274 rotational falls occurred of the 1739 fall reports representing 3,212,036 jumping efforts over 113,354 fences including

1*-4* CCI and CIC (levels from before the 2019 rule change) competitions. Of these, only a few fence-related factors showed statistical association with rotational falls, although post-and-rail and palisade categories presented a slightly greater likelihood of rotational falls than others. Murray also noted influential factors for all horse falls, including non-angled fences with a spread of two meters or more, landing in water and drop landings.

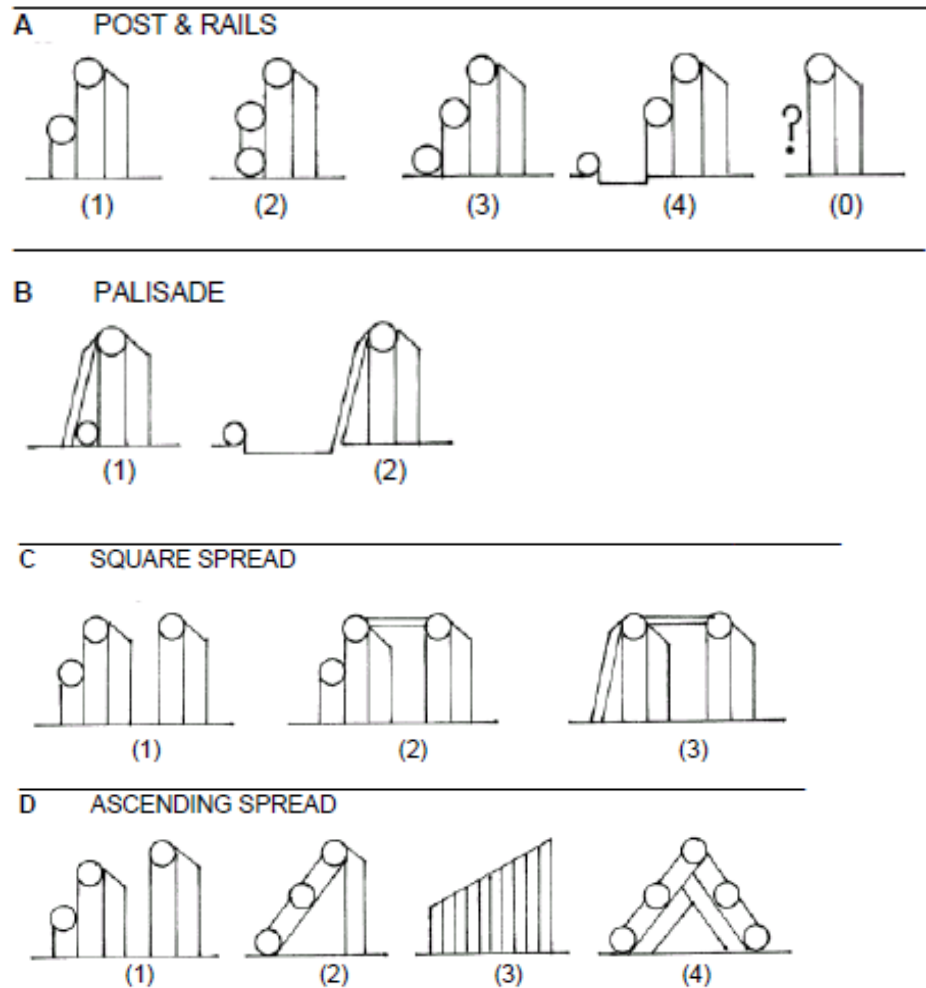


Figure 7.27 Jane Murray Fence Category Illustrations [1]

Murray's categories of fence types can form a framework for safety fence design recommendations, although course designers and builders may prefer a different grouping. The case studies of the previous section used contact velocity magnitude and direction distributions based on video analysis in Chapter 4. Further expansion of this study would provide insight to possible obstacle grouping.

- Galloping spreads such as oxers, tables, coops, some corners may be grouped together due to the similarity in approach speed and jumping position. This would be similar to the open oxer case study simulation.
- Combination fences such as verticals, coffins, steps, and some corners may be grouped together due to the similarity in approach speed and jumping position resembling the combination vertical case study simulation.
- Other groupings may be of interest based on how course designers think of questions, how course builders think of geometry, or how the safety committee frame policy.

Any fence type can be modeled by the simulation by using the expected speed and direction of the horse's contact. Because the direction of the contact velocity is modeled with respect to the ground, inclined fence installations are accounted for in the results.

7.10 Expected Improvement and Model Relevancy in Sport

To provide insight and results for policy decisions and design guidance, each physics-based simulation looks at 10,000 cases of competitors with critical contacts, which is the equivalent of more than 62.5 years of "very bad days." Reducing the

occurrence of rotational falls to 19/yr or less is achievable without changing the culture of the sport. This represents 1 in 1048 starters (0.095%), half the rate of 2015.

Not all rotational falls can be eliminated, though, even with safety device/designs for irrecoverable contacts and low impulse magnitude contacts that would change the culture of the sport and eliminate all effects of jump contact on horse motion. Simulation results show 2.2% of the critical-contact situations for one size fits all cases can't be mitigated by jump safety devices or designs. Prevention of rider injury in these cases would rely on personal safety protection for 3-4/yr.

Data from different sport organizations differ as to what is included, so comparisons are more challenging for rotational fall statistics. However, as seen in Figure 7.28, FEI data continues to confirm that rider serious injury is correlated to rotational falls. In 2015, only 1 in 536 (0.19%) starters on cross-country in an FEI Event had a rotational fall.

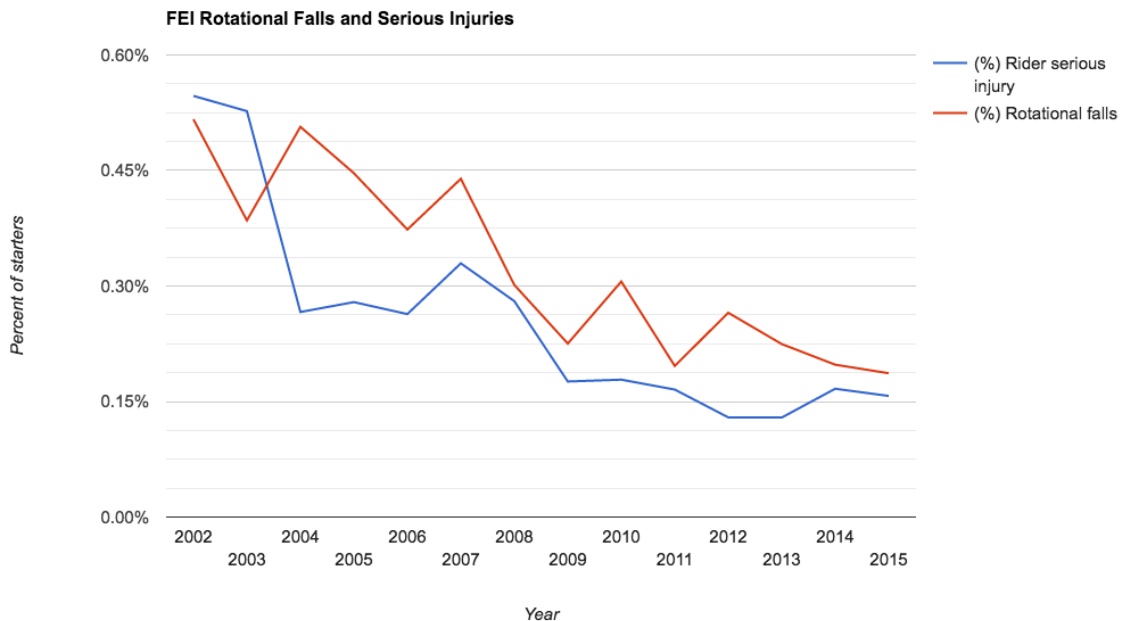


Figure 7.28 FEI percent rotational falls and serious injuries per starter from 2002 to 2015

7.11 Validation

Analysis of available rotational fall videos showed rotation rates from 100-220 deg/s. Simulation results for 4 m/s (240 mpm) primarily occur 100-170 deg/s, and for 7 m/s (420 mpm) 190-250 deg/s, signifying validation of the physics models. British Eventing on-course force measurement results suggest an impulse lower limit of 500 N-s for triggered safety devices to withstand normal on-course contact such as hoof strikes.

CHAPTER 8. SUMMARY AND FUTURE WORK

The overall objective of this thesis was to create a statistical ensemble method for evaluating the physics of potential rotational fall situations. This provides an alternative to physical testing dummies for determining indicators of rotation. The study was motivated by the continued occurrence of rotational falls after implementing some safety devices into cross country eventing jumps and the lack of evidence based methods for safety device testing criteria.

A comprehensive physics-based, data-driven simulation was developed to understand the occurrence and mitigation methods of rotational falls in eventing, and to produce design requirements for safety devices to reduce the incidence and consequences of the most-dangerous situations a competitor can encounter. Each ensemble simulation examines ten thousand (10,000) cases in which different competitors make contact with the fence in the dangerous ante brachium range of the horse's foreleg.

The physics of this contact and the resulting motion involves more than 20 variables that are modeled based on available literature, direct measurement, prior efforts by the sport and individuals/companies, subject matter expert inputs, video analysis, and textbook dynamics. Validation of the simulation was accomplished through comparison to federation reported fall statistics and published physical studies, confirming the accuracy of the models and computations.

Important additional information was obtained to fill missing pieces in the background information for physical analysis including inertia, CG and jumping speeds and positions. This was accomplished through comparison to published literature, a

survey for horse and rider size and a video study to capture speeds and positions on course.

Design opportunities were identified by limiting the impulse imparted by the fence to the horse, false activations of safety devices may be limited by the device angle activation range. Different designs and design criteria are suggested for different categories of on-course situations based on fence type, approach speed, and likely contact position. to allow for the creation of new varieties of designs. Note that a safety fence is one that incorporates any design to reduce the contact impulse: frangible, resettable, angled face, brush, friction-reducing, etc. For a design floor, false activations from hoof strikes and incidental contact will be minimized with an impulse limit set greater than 500 N-s. However, false activations remain likely in most situations from ante brachium contacts that would not rotate past vertical on a fixed fence.

Designs with the largest range of reaction angles will be the most effective, and are recommended. For angle-limited designs, activation for the range of 30° to 80° above a 0° datum aligned with the ground incline will address the most critical downward-arc contact situations and may reduce false activations.

Opportunities were identified for the creation of new safety devices for specific fence types and placement on course. Grouping appropriate fences together i.e. high speed oxers, combination verticals, etc. should be identified through empirical evaluation of competitor speed and position for possible device innovation or alteration to provide more options for course designers and builders. This idea should be guided by using the Jump Safety Quality Index to evaluate the necessity and the mitigative benefits of adding a safety device.

8.1 Recommendations for Future Work

Device testing methods were reviewed for appropriateness and effectiveness. Currently, primarily energy based tests are used to evaluate devices. This method must be used conscientiously or be altered due to high energy dissipation in inelastic collisions such as rotational fall situations. Future work should focus on how to test using impulse measurements that account for the specific reaction of the fence and how to adapt that testing to “garage” or workshop testing possibilities.

Additional rotational fall types must be addressed. In this thesis, one-contact rotations are evaluated. One-contact rotations should be considered with the additional hind legs pushing impulse while in contact with the fence. Force plate jumping take-off studies should be created from cross country situations or adapt numbers from showjumping research. The two-contact case should also be considered. The physical model may be adapted to the second impulse on landing. Torsional falls may be modeled by using advanced dynamics concepts to rotate the inertia and reactions outside of the 2-D plane. The statistical ensemble method can be adapted to include the additional fall types and factors as empirical studies are conducted.

Additionally, the rotational fall problem should continue to be addressed from a course designer and builders perspective as far as jump arc design, ground lines, and decorations to increase horse perception and understanding of the question as well as placement on terrain and proper footing.

APPENDICES

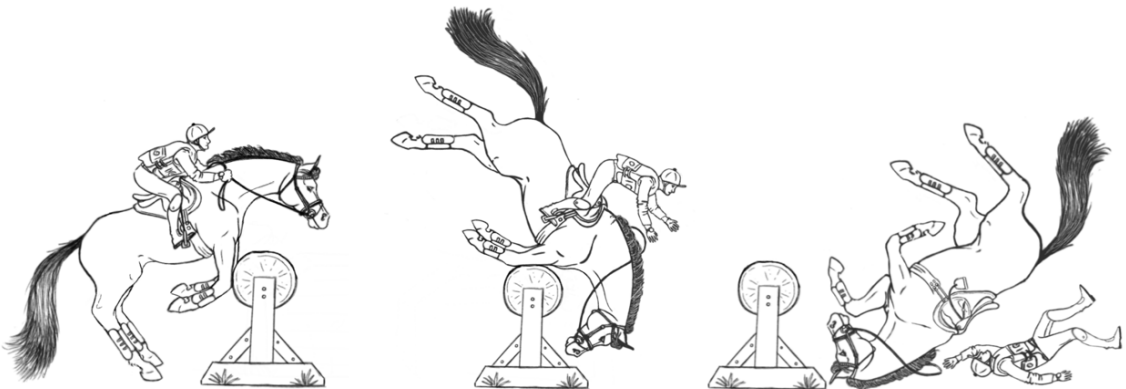
APPENDIX A. ROTATIONAL FALL TYPES



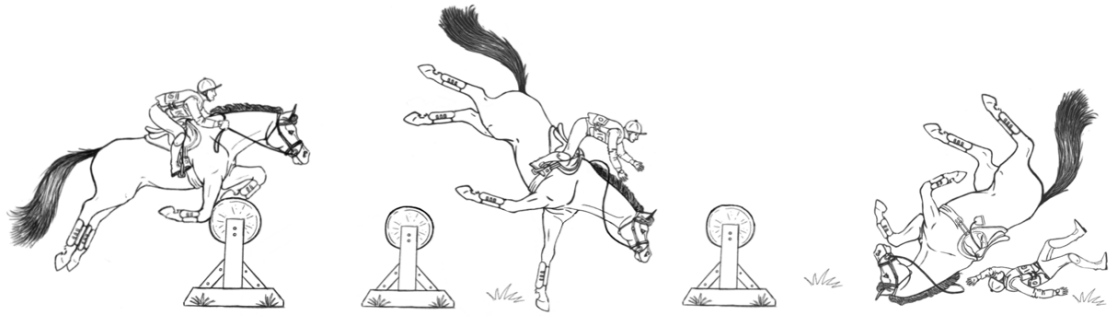
One-contact rotational fall



One-contact rotational fall with hind legs pushing off the ground



One-contact rotation with two front legs in contact with the fence and hind legs pushing off the ground



Two-contact rotational fall

APPENDIX B. CODE

Uniform Jumping Distributions for Upper Level Competitors

```
%%%%%Analysis for impulse problem

%%%Parameter library (select one)
%%Conservative case- All angle ranges
% [N, alpha, beta, phi, lamda, BL, BR, NL, NR, HL, HD, RH, mrider, HH,
nu, contactpct, rCGtoHind, Fhind,
deltathind,BD,ND,HR,AB,antebrachiumContactL, wi, vCGimag, vCGiDir,
ImpulseReductpct, ReductCode, ImpulseReductpctRange,
ImpulseReductFixed, ImpulseReductFixedRange,
ImpulseReductAngleRange]=JumpAlluniformSgroupUpperLevelA();
%%Video cases
%%2017
% [N, alpha, beta, phi, lamda, BL, BR, NL, NR, HL, HD, RH, mrider, HH,
nu, contactpct, rCGtoHind, Fhind,
deltathind,BD,ND,HR,AB,antebrachiumContactL, wi, vCGimag, vCGiDir,
ImpulseReductpct, ReductCode, ImpulseReductpctRange,
ImpulseReductFixed, ImpulseReductFixedRange,
ImpulseReductAngleRange]=UpperLevel2017VideoSgroupA();
%%2018
% [N, alpha, beta, phi, lamda, BL, BR, NL, NR, HL, HD, RH, mrider,
HH, nu, contactpct, rCGtoHind, Fhind,
deltathind,BD,ND,HR,AB,antebrachiumContactL, wi, vCGimag, vCGiDir,
ImpulseReductpct, ReductCode, ImpulseReductpctRange,
ImpulseReductFixed, ImpulseReductFixedRange,
ImpulseReductAngleRange]=UpperLevel2018VideoSgroupA();

%%Standing Upper Level Horse & Rider
% [N, alpha, beta, phi, lamda, BL, BR, NL, NR, HL, HD, RH, mrider, HH,
nu, contactpct, Fcontactcomp, deltatfence, rCGtoHindvect, Fhindcomp,
deltathind,BD,ND,HR,AB,antebrachiumContactL]=StandingUpperLevel();

%%Mass
[M, mbody, mneck, mhead]= SystemMass(HL,HD,BL,BR,NL,NR,mrider,N);
%function for mass by density

%%CG
[CGbodycoor, CGneckcoor, CGheadcoor, CGridercoor]=
CGcylinders(BL,BD,alpha,NL,ND,beta,HL,phi,RH,lamda);%CG coors of
individual cylinders, origin at pt of shoulder (m)
CGoverall=COM(mbody,mneck,mhead,mrider, CGbodycoor, CGneckcoor,
CGheadcoor, CGridercoor); %Overall CG coordinate (m) origin at pt of
shoulder
[CGcontact,CGcontactH,CGcontactN,CGcontactB,CGcontactR,gamma]=CGcontact
Calc(CGoverall,CGheadcoor, CGneckcoor,CGbodycoor,
CGridercoor,antebrachiumContactL); %Location of CGs origin contact
point (m)

%%Moment of Inertias
%Moment of Inertia about center in segments
[ICOMbody, ICOMneck, ICOMhead,
ICOMrider]=ICOMseg(mbody, BR, BL, mneck, NL, NR, mhead, HR, HL, RH, mrider);
```

```

    %MOI about Overall CG and about Contact point
    [ICGtotal,ICPtotal,dCG_contact,dCG_contactvect,Ishoulderttotal,
    IOCGbody,IOCGneck, IOCGhead,IOCGrider,IOCPbody,
    IOCPneck,IOCPhead,IOCPrider]=IcontacttoCPT(CGbodycoor,CGoverall,CGheadc
    oor,CGneckcoor,CGridercoor,ICOMbody,mbody,ICOMneck,mneck,ICOMhead,mhead
    ,ICOMrider,mrider,antebrachiumContactL,M);

%% Dynamic Analysis%%

g=9.81; %gravitational constant (m/s^2)
vCGi=[vCGimag.*cosd(vCGiDir) vCGimag.*sind(vCGiDir)]; % Incoming
velocity of CG instant before contact (m/s) positive x is to the right

%%%Conservation of Impulse momentum
wcontact=(ICGtotal.*wi+cross2(CGcontact,M.*vCGi)+cross2(rCGtoHind,
M.*deltathind.*Fhind))./ICPtotal; %rotational velocity after contact
(rad/s)

    %Change in CG height when horse rotates
h1= CGcontact(:,2); %height of CG after initial contact (m)
h2= dCG_contact; %height of CG at rotation, CG is directly above
contact point (m)
deltah=h2-h1; %change in height from contact to CG over CP (m)

%%% Is CG past vertical at time of contact, change PE=0 for CG past
vertical (m)
for i=1:N
if CGcontact(i,1)<0
    CGpastvertical(i,1)=-1; %CG is past the vertical
    deltah(i)=0;
else
    CGpastvertical(i,1)=0; %CG is not past vertical
end
end
indexCGpastvertical=find(CGcontact(:,1)<0);
pctCGpastVertical=sum(CGpastvertical)/N*-100; %%%pct past vertical

%% Fence Impulse
vCGf=[wcontact.*-dCG_contactvect(:,2) wcontact.*dCG_contactvect(:,1)];
%velocity after contact (m/s)
FenceImpulse= M.*(vCGf-vCGi); %Fixed fence impulse in x&y (N*s)
FenceImpulseMag=mag(FenceImpulse); %Fixed fence impulse mag (N*s)
FenceImpulseAngle=atand(FenceImpulse(:,2)./FenceImpulse(:,1)); %angle
of fence impulse (degrees)
    for i=1:N
        if FenceImpulse(i,1)<0
            FenceImpulseAngle(i)=180+FenceImpulseAngle(i); %Angle range
correction for atan in Q2 & Q3
        end
    end

%% Overturning Conservation of Energy
E1= .5*ICPtotal.*wcontact.^2-M.*9.81.*(deltah); %initial Kinetic energy
minus after potential energy CG over CP (J)

%%%loop calculate pass rate
for i=1:N

```

```

if E1(i)<0
    solidFenceRotate(i,1)=1; %does not overturn

else
    solidFenceRotate(i,1)=0; %overturns
end
end

% Find index ("i" value) for Rotation and No Rotate cases
indexProbRotate=find(solidFenceRotate(:,1)==1);
indexNoRotate=find(solidFenceRotate(:,1)==0);

%% Reduce impulse magnitude by four methods
%1=Reductpct, 2=ReductpctRange, 3=ReductFixed, 4=ReductFixedRange input
%conditions in parameter file

%count activations
DidActivate=zeros(N,1);
if ReductCode==1 %Reduce by one percentage
    ImpulseReductmag=FenceImpulseMag*ImpulseReductpct; %Magnitude of
the fence impulse if reduced (N*s)
    FenceImpluseRed=[ ImpulseReductmag.*cosd(FenceImpulseAngle)
ImpulseReductmag.*sind(FenceImpulseAngle)];

elseif ReductCode==2 %Reduce by range of percentages
    ImpulseReductmag=cat(3,
FenceImpulseMag*ImpulseReductpctRange(:,1),FenceImpulseMag*ImpulseReduc
tpctRange(:,2), FenceImpulseMag*ImpulseReductpctRange(:,3),
FenceImpulseMag*ImpulseReductpctRange(:,4),
FenceImpulseMag*ImpulseReductpctRange(:,5)); %Magnitude of the fence
impulse if reduced (N*s)
    FenceImpluseRed=[ ImpulseReductmag.*cosd(FenceImpulseAngle)
ImpulseReductmag.*sind(FenceImpulseAngle)];

elseif ReductCode==3 % Reduce to fixed value if above?
    for i=1:N
        if FenceImpulseMag(i)>ImpulseReductFixed

ImpulseReductmag(i,1)=ImpulseReductFixed+ImpulseReductFixed*.05*randn()
;
            DidActivate(i,1)=1; % Mark activations as 1
        else
            ImpulseReductmag(i,1)=FenceImpulseMag(i);
        end
    end
    FenceImpluseRed=[ ImpulseReductmag.*cosd(FenceImpulseAngle)
ImpulseReductmag.*sind(FenceImpulseAngle)];

elseif ReductCode==4 %Reduce to range of fixed values
    RangeLength=size(ImpulseReductFixedRange); %Number of values in
ImpulseReductFixedRange (for loop counter)
    for j=1:RangeLength(1,2)
        %loop limits impulse to greatest value in range
        for i=1:N
            if FenceImpulseMag(i,1)>ImpulseReductFixedRange(1,j)

```

```

ImpulseReductmagH(i,1)=ImpulseReductFixedRange(1,j)+ImpulseReductFixedR
ange(1,j)*.05*randn();
    DidActivate(i,1,j)=1; % Mark activations as 1
else
    ImpulseReductmagH(i,1)=FenceImpulseMag(i);
end
end
ImpulseReductmag(:,:,j)=ImpulseReductmagH; %store in 3dim array
end
FenceImpluseRed=[ ImpulseReductmag.*cosd(FenceImpulseAngle)
ImpulseReductmag.*sind(FenceImpulseAngle)];

elseif ReductCode==5 %Reduce to range of fixed values within range of
angles
    %loop limits impulse to greatest value in range
    for i=1:N
        if FenceImpulseMag(i,1)>ImpulseReductFixed
            if (FenceImpulseAngle(i)>ImpulseReductAngleRange(1,1) &
FenceImpulseAngle(i)<ImpulseReductAngleRange(1,2))
                ImpulseReductmag(i,1)=ImpulseReductFixed;
                DidActivate(i,1)=1; % Mark activations as 1
            else
                ImpulseReductmag(i,1)=FenceImpulseMag(i);
            end
        else
            ImpulseReductmag(i,1)=FenceImpulseMag(i);
        end
    end

    FenceImpluseRed=[ ImpulseReductmag.*cosd(FenceImpulseAngle)
ImpulseReductmag.*sind(FenceImpulseAngle)];
end

%% Check overturning for Impulse Reduced Fence
%% Select failures
wcontactRed= (FenceImpluseRed(:,2).*-dCG_contactvect(:,1)-
FenceImpluseRed(:,1).*-dCG_contactvect(:,2))./ICGtotal; % angular
velocity after contacting impulse reduced fence (rad/s)

%%Overturning Conservation of Energy after reduced impulse
ElRed(:,1)=.5*ICPtotal.*wcontactRed(:,1).^2-M.*9.81.*(deltah); %initial
Kinetic energy minus after potential energy CG over CP (J)
%%loop calculate pass rate
RotateAfterRed=zeros(N,1);
for i=1:N
    if solidFenceRotate(i,1)==1
        RotateAfterRed(i,1)=NaN; % Initial no rotate cases, which Red limit
doesn't affect
    elseif ElRed(i,1)<0
        RotateAfterRed(i,1)=1; % If Red changes to No Rotation
    else
        RotateAfterRed(i,1)=0; % With Red Still Rotates
    end
end
end

```

```

%%%Simple Pass/Fail analytics
NFpass=sum(solidFenceRotate);
NFfail=N-NFpass;
NFpasspct=(NFpass/N)*100
NFfailpct=(NFfail/N)*100;

%% Energy
label_fs = 14; % fontsize for the figures
title_fs = 18; % title fontsize for figures

InKE=1/2*M.*vCGimag.^2; %J
OutKE=.5*ICPtotal.*wcontact.^2; %J
Energylosspct=(InKE-OutKE)./InKE.*100; % pct energy loss
Energyloss=(InKE-OutKE);
    InKEavg=mean(InKE);
    OutKEavg= mean(OutKE);
    Energylossavg= mean(Energyloss);

%% Solid Rotation/Activation/RedRotation and Indexes
SolidActivateRedRotation=[ solidFenceRotate DidActivate
RotateAfterRed]; %concat

%Indexes
indexNoRotate=find(solidFenceRotate(:,1)==1); %index of solid fence no
rotations
indexProbRotate=find(solidFenceRotate(:,1)==0); %index of solid fence
rotations
indexNoRotateActivation=find((SolidActivateRedRotation(:,1)==1) &
(SolidActivateRedRotation(:,2)==1)); %index of solid fence no rotations
indexNoRotateNoActivation=find((SolidActivateRedRotation(:,1)==1) &
(SolidActivateRedRotation(:,2)==0)); %index of solid fence rotations
indexProbRotateActiv=find((SolidActivateRedRotation(:,1)==0) &
(SolidActivateRedRotation(:,2)==1)); %index of solid fence rotations
w/activate
indexProbRotateNoActiv=find((SolidActivateRedRotation(:,1)==0) &
(SolidActivateRedRotation(:,2)==0)); %index of solid fence no activate
indexProbRotateActivRot=find((SolidActivateRedRotation(:,1)==0) &
(SolidActivateRedRotation(:,2)==1)&
(SolidActivateRedRotation(:,3)==0)); %index of solid fence rotations
w/activate
indexProbRotateActivNoRot=find((SolidActivateRedRotation(:,1)==0) &
(SolidActivateRedRotation(:,2)==1)&
(SolidActivateRedRotation(:,3)==1)); %index of solid fence no activate

%sums and percentages
    CountProbRotateActivRot=length(indexProbRotateActivRot)
    CountProbRotateActivNoRot=length(indexProbRotateActivNoRot)
    CountProbRotateActiv=length(indexProbRotateActiv)
    CountProbRotateNoActiv=length(indexProbRotateNoActiv)
    CountNoRotateActivation=length(indexNoRotateActivation)
    CountNoRotateNoActivation=length(indexNoRotateNoActivation)
    %sums and percentages
    PctNoRotate=sum(solidFenceRotate)/N*100
    PctRotate=100-PctNoRotate

```


Fence Specific: Upper Level RK3DE 2017 Parameters

```
function [N, alpha, beta, phi, lamda, BL, BR, NL, NR, HL, HD, RH,
mrrider, HH, nu, contactpct, rCGtoHind, Fhind,
deltathind,BD,ND,HR,AB,antebrachiumContactL, wi, vCGimag, vCGiDir,
ImpulseReductpct, ReductCode, ImpulseReductpctRange,
ImpulseReductFixed, ImpulseReductFixedRange,
ImpulseReductAngleRange]=UpperLevel2017VideoSgroupA()
```

```
N=10000; %Number of Random Variables
```

```
%%%Approach Properties%%%
```

```
%formulate by lowerbound+range*rand distribution
```

```
alpha= -32.3+5.5.*randn(N,1); %Body Contact Angle for positive x-
axis (degrees)
```

```
beta=alpha+153+11.1.*randn(N,1); % Neck Contact Angle from alpha
(degrees)
```

```
phi=alpha+238.6+9.3.*randn(N,1); %Head Contact Angle from alpha
(degrees)
```

```
lamda=alpha+120+5.*randn(N,1);%Rider Contact Angle from positive
x-axis (degrees)
```

```
nu=alpha+300+8.*randn(N,1); %Angle from X-axis (origin at point
of shoulder) to Antebrachium (degrees)
```

```
%%%Geometric Parameters%%%
```

```
%Body
```

```
BL=1.70+.10*randn(N,1); %Body Length (m)
```

```
BR=(0.293398+0.03845*randn(N,1)); %Body Radius (m)
```

```
BD=BR.*2; %Body Diameter (m)
```

```
%Neck
```

```
NL=0.71+0.05*randn(N,1); %Neck Length (m)
```

```
NR=0.1552+0.016225*randn(N,1); %Neck Radius (m)
```

```
ND=NR.*2; %Neck Diameter (m)
```

```
%Head
```

```
HL=0.57+0.04*randn(N,1); %Head Length (m)
```

```
HD=0.2006+0.0255*randn(N,1); %Head Diameter (m)
```

```
HR=HD./2; %Head Radius (m)
```

```
%Antebrachium
```

```
HH=1.68+0.06*randn(N,1); %Horse Height to Withers (m)
```

```
contactpct=rand(N,1); %pct distance of antebrachium where contact
took place (%)%Rider
```

```
AB=(HH-BD).*(0.6); %Antebrachium Length (m) ***consider
elongating
```

```
antebrachiumContactL=-1.*[((AB.*contactpct).*cosd(nu))
((AB.*contactpct).*sind(nu))]; % vector from contact point on
antebrachium to point of shoulder
```

```
%Rider
```

```
RH=1.72+0.08*randn(N,1); %Rider height (m)
```

```
mrrider=64+10*randn(N,1); %Mass of Rider (kg)
```

```
%%%Dynamic Analysis%%%
```

```
wi=0; % Incoming angular velocity instant before contact(rad/s)
```

```
vCGimag=6.12+.33*randn(N,1); % incoming velocity (m/s)
```

```

vCGiDir= 180+alpha; %180-35; % angle of approach velocity
(degrees)

%%%Fence Impulse reduction options
ReductCode=3; %1=Reductpct, 2=ReductpctRange, 3=ReductFixed,
4=ReductFixedRange, 5=ReductFixedRange and angle
ImpulseReductpct=.7; %percent of fixed fence impulse
ImpulseReductpctRange= [.9 .8 .7 .6 .5]; %percent of fixed fence
impulse over range
ImpulseReductFixed=1000; %Impulse reduced to fixed amount (N*s)
ImpulseReductFixedRange= [1500 1000 300]; %[2000 1500 1000 500
300 100]; %Impulse reduced to fixed amount (N*s)
ImpulseReductAngleRange=[30 80];

%%%Hind Leg Pushing Impulse parameters- For future use
rCGtoHind= [0 0]; %distance from hind takeoff to CG
Fhindmag=0; %force of takeoff with hind legs (N/kg)
HindAngle=0; % angle of force of takeoff (degrees)
Fhind=[Fhindmag.*cosd(HindAngle) Fhindmag.*sind(HindAngle)];
deltathind= .0; %duration of takeoff impulse (s)

```

Fence Specific: Upper Level K3DE 2018 Distributions

```

function [N, alpha, beta, phi, lamda, BL, BR, NL, NR, HL, HD, RH,
m rider, HH, nu, contactpct, rCGtoHind, Fhind,
deltathind, BD, ND, HR, AB, antibrachiumContactL, wi, vCGimag, vCGiDir,
ImpulseReductpct, ReductCode, ImpulseReductpctRange,
ImpulseReductFixed, ImpulseReductFixedRange,
ImpulseReductAngleRange]=UpperLevel2018VideoSgroupA()

N=10000; %Number of Random Variables

%%%Approach Properties%%%
%formulate by lowerbound+range*rand distribution
alpha= -24.0+5.1.*randn(N,1); %-35 to +35 Body Contact Angle for
positive x-axis (degrees)
beta=alpha+158+15.5.*randn(N,1); %110 to 190 % Neck Contact Angle
from alpha (degrees)
phi=alpha+242+60.*randn(N,1); %+13.42895*randn(N,1); %Head Contact
Angle from alpha (degrees)
lamda=alpha+80+80.*randn(N,1); % from 80 to 160 %Rider Contact
Angle from positive x-axis (degrees)
nu=alpha+300+8.*randn(N,1); %*randn(N,1); %+13.5*randn(N,1); %Angle
from X-axis (origin at point of shoulder) to Antebrachium (degrees)

%%%Geometric Parameters%%%
%Body
BL=1.70+.10*randn(N,1); %Body Length (m)
BR=(0.293398+0.03845*randn(N,1)); %Body Radius (m)
BD=BR.*2; %Body Diameter (m)
%Neck
NL=0.71+0.05*randn(N,1); %Neck Length (m)
NR=0.1552+0.016225*randn(N,1); %Neck Radius (m)
ND=NR.*2; %Neck Diameter (m)

```

```

%Head
HL=0.57+0.04*randn(N,1); %Head Length (m)
HD=0.2006+0.0255*randn(N,1); %Head Diameter (m)
HR=HD./2; %Head Radius (m)

%Antebrachium
HH=1.68+0.06*randn(N,1); %Horse Height to Withers (m)
contactpct=rand(N,1); %pct distance of antebrachium where contact
took place (%)%Rider
AB=(HH-BD).*(0.6); %Antebrachium Length (m) ***consider
elongating
antebrachiumContactL=-1.*[((AB.*contactpct).*cosd(nu))
((AB.*contactpct).*sind(nu))]; % vector from contact point on
antebrachium to point of shoulder

%Rider
RH=1.72+0.08*randn(N,1); %Rider height (m)
m rider=64+10*randn(N,1); %Mass of Rider (kg)

%%%Dynamic Analysis%%%
wi=0; % Incoming angular velocity instant before contact(rad/s)
vCGimag=4.81+.33*randn(N,1); % incoming velocity (m/s)
vCGiDir= 180+alpha; %180-35; % angle of approach velocity
(degrees)

%%%Fence Impulse reduction options
ReductCode=3; %1=Reductpct, 2=ReductpctRange, 3=ReductFixed,
4=ReductFixedRange, 5=ReductFixedRange and angle
ImpulseReductpct=.7; %percent of fixed fence impulse
ImpulseReductpctRange= [.9 .8 .7 .6 .5]; %percent of fixed fence
impulse over range
ImpulseReductFixed=1000; %Impulse reduced to fixed amount (N*s)
ImpulseReductFixedRange= [1500 1000 300];%[2000 1500 1000 500
300 100]; %Impulse reduced to fixed amount (N*s)
ImpulseReductAngleRange=[30 80];

%%%Hind Leg Pushing Impulse parameters- For future use
rCGtoHind= [0 0]; %distance from hind takeoff to CG
Fhindmag=0; %force of takeoff with hind legs (N/kg)
HindAngle=0; % angle of force of takeoff (degrees)
Fhind=[Fhindmag.*cosd(HindAngle) Fhindmag.*sind(HindAngle)];
deltathind= .0; %duration of takeoff impulse (s)

```

Main Ensemble Function

```

%%%%%%%%Analysis for impulse problem

%%%Parameter library%%% Select One
%%%Conservative case- All angle ranges
%[N, alpha, beta, phi, lamda, BL, BR, NL, NR, HL, HD, RH, m rider,
HH, nu, contactpct, rCGtoHind, Fhind,
deltathind,BD,ND,HR,AB,antebrachiumContactL, wi, vCGimag, vCGiDir,
ImpulseReductpct, ReductCode, ImpulseReductpctRange,

```

```

ImpulseReductFixed, ImpulseReductFixedRange,
ImpulseReductAngleRange]=JumpAlluniformSgroupUpperLevelA());

%%%Video cases
%%%2017
%[N, alpha, beta, phi, lamda, BL, BR, NL, NR, HL, HD, RH, mrider,
HH, nu, contactpct, rCGtoHind, Fhind,
deltathind,BD,ND,HR,AB,antebrachiumContactL, wi, vCGimag, vCGiDir,
ImpulseReductpct, ReductCode, ImpulseReductpctRange,
ImpulseReductFixed, ImpulseReductFixedRange,
ImpulseReductAngleRange]=UpperLevel2017VideoSgroupA();
%%%2018
%[N, alpha, beta, phi, lamda, BL, BR, NL, NR, HL, HD, RH, mrider,
HH, nu, contactpct, rCGtoHind, Fhind,
deltathind,BD,ND,HR,AB,antebrachiumContactL, wi, vCGimag, vCGiDir,
ImpulseReductpct, ReductCode, ImpulseReductpctRange,
ImpulseReductFixed, ImpulseReductFixedRange,
ImpulseReductAngleRange]=UpperLevel2018VideoSgroupA();

%%%Mass
[M, mbody, mneck, mhead]= SystemMass(HL,HD,BL,BR,NL,NR,mrider,N);
%function for mass by density

%%%CG
[CGbodycoor, CGneckcoor, CGheadcoor, CGridercoor]=
CGcylinders(BL,BD,alpha,NL,ND,beta,HL,phi,RH,lamda);%CG coors of
individual cylinders, origin at pt of shoulder (m)
CGoverall=COM(mbody,mneck,mhead,mrider, CGbodycoor, CGneckcoor,
CGheadcoor, CGridercoor); %Overall CG coordinate (m) origin at pt of
shoulder
[CGcontact,CGcontactH,CGcontactN,CGcontactB,CGcontactR,gamma]=CGc
ontactCalc(CGoverall,CGheadcoor, CGneckcoor,CGbodycoor,
CGridercoor,antebrachiumContactL); %Location of CGs origin contact
point (m)

%%%Moment of Inertias
%Moment of Inertia about center in segments
[ICOMbody, ICOMneck, ICOMhead,
ICOMrider]=ICOMseg(mbody,BR,BL,mneck,NL,NR,mhead,HR,HL,RH,mrider);
%MOI about Overall CG and about Contact point
[ICGtotal,ICPtotal,dCG_contact,dCG_contactvect,Ishouldertotal]=Ic
ontacttoCPT(CGbodycoor,CGoverall,CGheadcoor,CGneckcoor,CGridercoor,ICOM
body,mbody,ICOMneck,mneck,ICOMhead,mhead,ICOMrider,mrider,antebrachiumC
ontactL,M);

%%%Dynamic Analysis%%%
g=9.81; %gravitational constant (m/s^2)
vCGi=[vCGimag.*cosd(vCGiDir) vCGimag.*sind(vCGiDir)]; % Incoming
velocity of CG instant before contact (m/s) positive x is to the right

%%%Conservation of Impulse momentum
wcontact=(ICGtotal.*wi+cross2(CGcontact,M.*vCGi)+cross2(rCGtoHind
, M.*deltathind.*Fhind))./ICPtotal; %rotational velocity after contact
(rad/s)

```

```

        %Change in height when horse rotates
        h1= CGcontact(:,2); %height of CG after initial contact (m)
        h2= dCG_contact; %height of CG at rotation, CG is directly above
contact point (m)
        deltah=h2-h1; %change in height from contact to CG over CP (m)
        %%%count if CG is past vertical at time of contact, change
PE=0 for
        %%%CG past vertical (m)
        for i=1:N
        if CGcontact(i,1)<0
            CGpastvertical(i,1)=-1; %CG is past the vertical
            deltah(i)=0;
        else
            CGpastvertical(i,1)=0; %CG is not past vertical
        end
        end
        pctCGpastVertical=sum(CGpastvertical)/N*-100; %%%pct past
vertical

        %% Overturning Conservation of Energy
        E1= .5*ICPtotal.*wcontact.^2-M.*9.81.*(deltah); %initial Kinetic
energy minus after potential energy CG over CP (J)

        wcontactPass=[];%initialize
        wcontactFail=[];%initialize

        %%%loop calculate pass rate
        for i=1:N
        if E1(i)<0
            b(i,1)=1; %does not overturn

        else
            b(i,1)=0; %overturns
            wcontactFail= [wcontactFail; wcontact(i)];
        end
        end

        %% Fence Impluse
        vCGf=[wcontact.*-dCG_contactvect(:,2)
wcontact.*dCG_contactvect(:,1)]; %velocity after contact (m/s)
        FenceImpulse= M.*(vCGf-vCGi); %Fixed fence impulse in x&y (N*s)
        FenceImpulseMag=mag(FenceImpulse); %Fixed fence impulse mag (N*s)

        %%%Identify failures and reduct impulse by pct
        %find impulse angle
        FenceImpulseAngle=atand(FenceImpulse(:,2)./FenceImpulse(:,1));
%angle of fence impulse (degrees)
        for i=1:N
            if FenceImpulse(i,1)<0
                FenceImpulseAngle(i)=180+FenceImpulseAngle(i); %Range
correction for atan in Q2 & Q3
            end
        end

        %% reduce impulse magnitude by four methods

```

```

%1=Reductpct, 2=ReductpctRange, 3=ReductFixed, 4=ReductFixedRange
imput
%conditions in parameter file

if ReductCode==1 %Reduce by one percentage
    ImpulseReductmag=FenceImpulseMag*ImpulseReductpct; %Magnitude
of the fence impulse if reduced (N*s)
    FenceImpluseRed=[ImpulseReductmag.*cosd(FenceImpulseAngle)
ImpulseReductmag.*sind(FenceImpulseAngle)];

    elseif ReductCode==2 %Reduce by range of percentages
        ImpulseReductmag=cat(3,
FenceImpulseMag*ImpulseReductpctRange(:,1),FenceImpulseMag*ImpulseReduc
tpctRange(:,2), FenceImpulseMag*ImpulseReductpctRange(:,3),
FenceImpulseMag*ImpulseReductpctRange(:,4),
FenceImpulseMag*ImpulseReductpctRange(:,5)); %Magnitude of the fence
impulse if reduced (N*s)
        FenceImpluseRed=[ImpulseReductmag.*cosd(FenceImpulseAngle)
ImpulseReductmag.*sind(FenceImpulseAngle)];

    elseif ReductCode==3 % Reduce to fixed value if above?
        for i=1:N
            if FenceImpulseMag(i)>ImpulseReductFixed

ImpulseReductmag(i,1)=ImpulseReductFixed+ImpulseReductFixed*.05*randn()
;
                else
                    ImpulseReductmag(i,1)=FenceImpulseMag(i);
                end
            end
            FenceImpluseRed=[ImpulseReductmag.*cosd(FenceImpulseAngle)
ImpulseReductmag.*sind(FenceImpulseAngle)];

    elseif ReductCode==4 %Reduce to range of fixed values
        RangeLength=size(ImpulseReductFixedRange); %Number of values
in ImpulseReductFixedRange (for loop counter)
        for j=1:RangeLength(1,2)
            %loop limits impulse to greatest value in range
            for i=1:N
                if FenceImpulseMag(i,1)>ImpulseReductFixedRange(1,j);

ImpulseReductmagH(i,1)=ImpulseReductFixedRange(1,j)+ImpulseReductFixedR
ange(1,j)*.05*randn();
                    else
                        ImpulseReductmagH(i,1)=FenceImpulseMag(i);
                    end
                end
                ImpulseReductmag(:,j)=ImpulseReductmagH; %store in 3dim
array
            end
            FenceImpluseRed=[ImpulseReductmag.*cosd(FenceImpulseAngle)
ImpulseReductmag.*sind(FenceImpulseAngle)];

    elseif ReductCode==5 %Reduce to range of fixed values within
range of angles
        RangeLength=size(ImpulseReductFixedRange); %Number of values
in ImpulseReductFixedRange (for loop counter)

```

```

        for j=1:RangeLength(1,2)
            %loop limits impulse to greatest value in range
            for i=1:N
                if FenceImpulseMag(i,1)>ImpulseReductFixedRange(1,j);
                    if (FenceImpulseAngle(i)>ImpulseReductAngleRange(1,1) &
FenceImpulseAngle(i)<ImpulseReductAngleRange(1,2))
                        ImpulseReductmagH(i,1)=ImpulseReductFixedRange(1,j)+ImpulseReductFixedR
ange(1,j)*.05*randn();
                    elseif FenceImpulseAngle(i)>ImpulseReductAngleRange(1,2)
& (FenceImpulseMag(i,1)*cosd(FenceImpulseAngle(i)-
ImpulseReductAngleRange(1,2)) >ImpulseReductFixedRange(1,j))
                        ImpulseReductmagH(i,1)=ImpulseReductFixedRange(1,j)+ImpulseReductFixedR
ange(1,j)*.05*randn();
                    elseif FenceImpulseAngle(i)<ImpulseReductAngleRange(1,1)
& (FenceImpulseMag(i,1)*cosd(ImpulseReductAngleRange(1,1)-
FenceImpulseAngle(i)) >ImpulseReductFixedRange(1,j))
                        ImpulseReductmagH(i,1)=ImpulseReductFixedRange(1,j)+ImpulseReductFixedR
ange(1,j)*.05*randn();
                    else
                        ImpulseReductmagH(i,1)=FenceImpulseMag(i);
                    end
                else
                    ImpulseReductmagH(i,1)=FenceImpulseMag(i);
                end
                end
                ImpulseReductmag(:, :, j)=ImpulseReductmagH; %store in 3dim
array
            end
            FenceImpulseRed=[ ImpulseReductmag.*cosd(FenceImpulseAngle)
ImpulseReductmag.*sind(FenceImpulseAngle)];

        end

        if ReductCode==1 || ReductCode==3
            NumRanges=1;
        else
            R=size(ImpulseReductmag);
            NumRanges=R(3);
        end

        for j=1:NumRanges
            %%%Select failures
            wcontactRed(:, :, j)= (FenceImpulseRed(:, 2, j).*-
dCG_contactvect(:, 1)-FenceImpulseRed(:, 1, j).*-
dCG_contactvect(:, 2))./ICGtotal; % angular velocity after contacting
impulse reduced fence (rad/s)

            %%%Overturning Conservation of Energy after reduced impulse
            ElRed(:, 1, j)=.5*ICPtotal.*wcontactRed(:, 1, j).^2-
M.*9.81.*(deltah); %initial Kinetic energy minus after potential energy
CG over CP (J)
            %%%loop calculate pass rate
            for i=1:N
                if b(i,1)==1

```

```

        bRed(i,1,j)=1; %still count passes from solid fence
        bRed(i,2,j)=0; %Red value did not cause change to passing
elseif ElRed(i,1,j)<0
        bRed(i,2,j)=2; %Red value caused change to passing
        bRed(i,1,j)=1; %does not overturn
else
        bRed(i,1,j)=0; %overturns
        bRed(i,2,j)=0; %Red value did not cause change to passing
end
end

end

%%%Simple Pass/Fail analytics
NFpass=sum(b);
NFfail=N-NFpass;
NFpasspct=(NFpass/N)*100
NFfailpct=(NFfail/N)*100;

Redpass = sum(bRed(:,1,1));
if NumRanges>1
for i = 2:NumRanges
        Redpass = horzcat(Redpass, sum(bRed(:,1,i)));
end
end
RedpassChange=((sum(bRed(:,2)))/2)/NFfail)*100;
Redpasspct=(Redpass/N)*100;
differenceinpass=Redpass-NFpass;
Diffpct=Redpasspct-NFpasspct
PctDiff=Diffpct./(Redpasspct+NFpasspct)/2;

Fimpmagavg=mean(FenceImpulseMag)

%% Energy
InKE=1/2*M.*vCGimag.^2; %J
OutKE=.5*ICPtotal.*wcontact.^2; %J
Energyloss=(InKE-OutKE)./InKE.*100; % pct energy loss

```

System Mass Function

```

%%%Function finds the total mass of the system and each
cylinder's mass in
%%%the Four Cylinder Model
function [M, mbody, mneck, mhead]=
SystemMass(HL,HD,BL,BR,NL,NR,mrider,N)

%%%Densities%%% constants
rhodwbody= 950+0.05*rand(N,1); %DWB body density (kg/m^3)
rhodwneck= 1038+0.002*randn(N,1); %DWB neck density (kg/m^3)
rhodwhead= 1031+0.01*randn(N,1); %DWB head density (kg/m^3)
rhotbbody=1192.6+0.054*randn(N,1); %TB body density (kg/m^3)
rhotbneck=1019+0.015*randn(N,1); %TB neck density (kg/m^3)
rhotbhead=1031+0.045*randn(N,1); %TB head density (kg/m^3)

```



```

%%%Cylinder Masses%%%
%Body
BV=pi.*(BR).^2.*BL; %Body Cylinder Volume (m^3)
mbody=BV.*rhodwbbody; %Body Mass (kg)
%Neck
NV=pi.*(NR).^2.*NL; %Neck Cylinder Volume (m^3)
mneck=(1/2).*rhodwbneck.*NV; %Neck Mass (kg)
%(1/2).*rhodwbneck.*NV; %Neck Mass (kg)
%Head
HR=HD./2; %Head Radius (m)
HV=pi.*(HR).^2.*HL; %Head Cylinder Volume (m^3)
mhead=rhodwbhead.*HV; %Head Mass (kg)

M=mbody+mneck+mhead+mrider; %FCM total Mass (kg)

```

CGcylinders Function

```

%Function to calculate CG coordinates of the cylinders with
origin at point
%of shoulder
function [CGbodycoor, CGneckcoor, CGheadcoor, CGridercoor]=
CGcylinders(BL,BD,alpha,NL,ND,beta,HL,phi,RH,lamda)
%%%Physical Properties%%%
%Body
r=.5.*sqrt(BL.^2+BD.^2); %Distance from Body COM to shoulder (m)
GammaBody= atand(BD./BL); %angle
CGbodycoor=[r.*cosd(alpha+GammaBody) r.*sind(alpha+GammaBody)];
%Body CG coordinates origin at shoulder (m)
%Neck
hyp=((ND./2)./cosd(45)); %Hypotenuse Distance (m)
CGneckcoor=[BD.*cosd(alpha+90)+((NL./2)-hyp).*cosd(beta)
BD.*sind(alpha+90)+((NL./2).*sind(beta))]; %Neck CG coordinate origin
at shoulder(m)
%Head
CGheadcoor=[BD.*cosd(alpha+90)+((NL)-
hyp).*cosd(beta)+(HL./2).*cosd(phi) BD.*sind(alpha+90)+((NL)-
hyp).*sind(beta)+(HL./2).*sind(phi)]; %Head CG coordinate origin at
shoulder(m)
%Rider
RR=((0.54.*RH)./(2*pi));
RPH=0.1.*RH; %Rider pseudo height (m)
CGridercoor=[BD.*cosd(alpha+90)+(1/3).*BL.*cosd(alpha)+(1/2).*RPH
.*cosd(lamda)
BD.*sind(alpha+90)+(1/3).*BL.*sind(alpha)+(1/2).*RPH.*sind(lamda)];
%Rider CG coordinate at shoulder(m)

```

COM Function

```

%%%Overall Center of Mass Location
function y=COM(m1,m2,m3,m4,x1,x2,x3,x4)

y(:,1)=[(x1(:,1).*m1+x2(:,1).*m2+x3(:,1).*m3+x4(:,1).*m4)./(m1+m2
+m3+m4)]; %Over All XCG location (m)
y(:,2)=[(x1(:,2).*m1+x2(:,2).*m2+x3(:,2).*m3+x4(:,2).*m4)./(m1+m2
+m3+m4)]; %Over All YCG location (m)

```

CGcontactCalc Function

```
%%Locate CG wrt contact point (CP)
function
[CGcontact,CGcontactH,CGcontactN,CGcontactB,CGcontactR,gamma]=CGcontact
Calc(CGoverall,CGheadcoor, CGneckcoor,CGbodycoor,
CGridercoor,antebrachiumContactL)

CGcontact=CGoverall+antebrachiumContactL; %Location of CG
competitor from contact point
CGcontactH=CGheadcoor+antebrachiumContactL; %CG coor of cylinder
from contact point
CGcontactN=CGneckcoor+antebrachiumContactL; %CG coor of cylinder
from contact point
CGcontactB=CGbodycoor+antebrachiumContactL; %CG coor of cylinder
from contact point
CGcontactR=CGridercoor+antebrachiumContactL; %CG coor of cylinder
from contact point
gamma=atand(CGcontact(:,2)./CGcontact(:,1)); %Angle to overall CG
origin at contact point
```

ICOMseg Function

```
%%MOI for each cylinder about center
function [ICOMbody, ICOMneck, ICOMhead,
ICOMrider]=ICOMseg(mbody,BR,BL,mneck,NL,NR,mhead,HR,HL,RH,mrider)
%Body
ICOMbody=(1/12).*mbody.*((3.*(BR).^2+(BL).^2)); %Body Segment
Inertia about Segment COM (kg m^2)
%Neck
ICOMneck=(1/12).*mneck.*((3.*(NR).^2+(NL).^2)); %Neck Segment
Inertia about Segment COM (kg m^2)
%Head
ICOMhead=(1/12).*mhead.*((3.*(HR).^2+(HL).^2)); %Head Segment
Inertia about Segment COM (kg m^2)
%Rider
RR=((0.54.*RH)/(2*pi));
RPH=0.1.*RH; %Rider pseudo height (m)
ICOMrider=(1/12).*mbody.*((3.*(RR).^2)+(RPH).^2); %Inertia of
rider about its CG (kg m^2)
```

IcontacttoCPT Function

```
%%MOI to Contact point
function
[ICGtotal,ICPtotal,dCG_contact,dCG_contactvect,Ishouldertotal]=Icontact
toCPT(CGbodycoor,CGoverall,CGheadcoor,CGneckcoor,CGridercoor,ICOMbody,m
body,ICOMneck,mneck,ICOMhead,mhead,ICOMrider,mrider,antebrachiumContact
L,M)
%Over All MOI about system CG
dB_CG=dist(CGbodycoor, CGoverall); %Distance between Body CG to
CG overall (m)
dN_CG=dist(CGneckcoor, CGoverall); %Distance between Neck CG to
CG overall (m)
```

```

    dH_CG=dist(CGheadcoor,CGoverall); %Distance between Head CG to CG
overall (m)
    dR_CG=dist(CGridercoor, CGoverall); %Distance between Rider CG to
CG overall (m)
    IOCGbody=ICOMbody+mbody.*(dB_CG).^2; %Component of overall ICG
contributed by body (kg m^2)
    IOCGneck=ICOMneck+mneck.*(dN_CG).^2; %Component of overall ICG
contributed by neck (kg m^2)
    IOCGhead=ICOMhead+mhead.*(dH_CG).^2; %Component of overall ICG
contributed by head (kg m^2)
    IOCGrider=ICOMrider+mrider.*(dR_CG).^2; %Component of overall ICG
contributed by rider (kg m^2)
    ICGtotal=IOCGbody+IOCGneck+IOCGhead+IOCGrider; %Overall Inertia
of TCM about total CG (kg m^2)

    %Contact Point
    dCG_contactvect=[CGoverall(:,1)+antebrachiumContactL(:,1)
CGoverall(:,2)+antebrachiumContactL(:,2)]; %Distance between Contact
Point and CG overall (m)
    dCG_contact=sqrt(dCG_contactvect(:,1).^2+dCG_contactvect(:,2).^2)
;

    %Overall MOI about contact point
    ICPTtotal=ICGtotal+M.*(dCG_contact).^2;
    Ishoulderttotal=ICGtotal+M.*sqrt(CGoverall(:,1).^2+CGoverall(:,1).
^2);

```

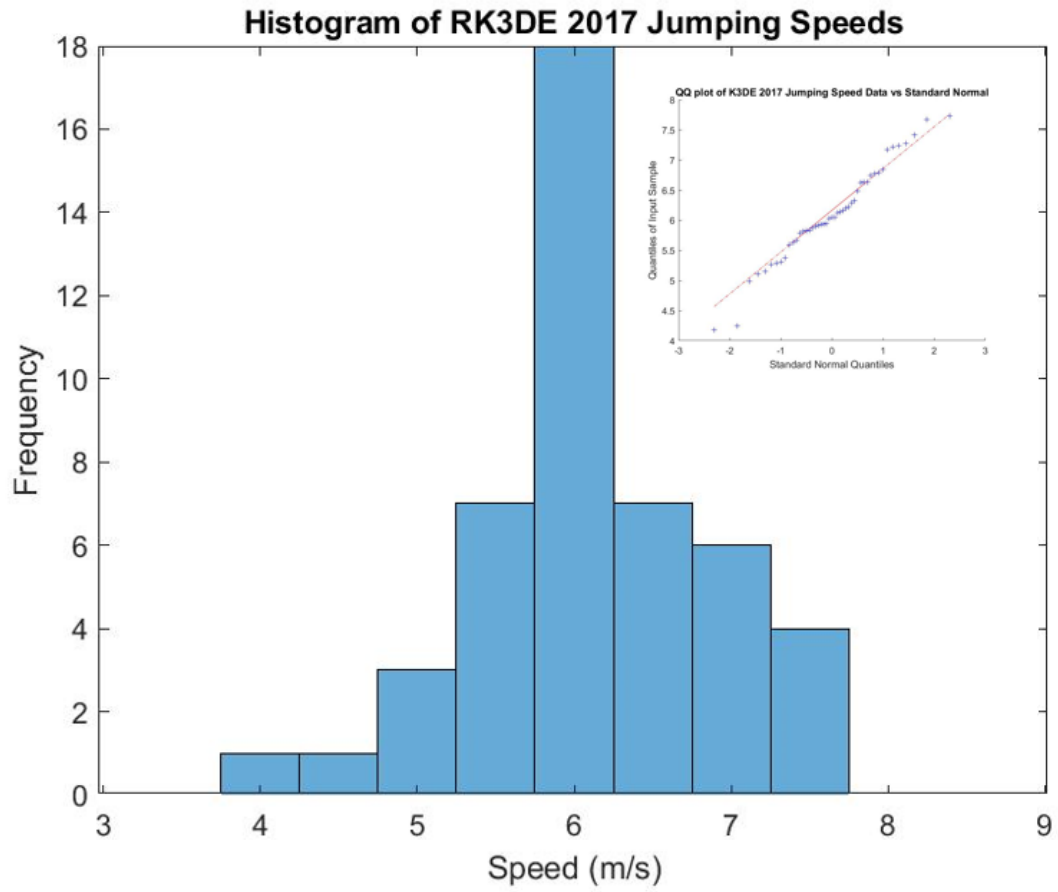
Cross2 Function

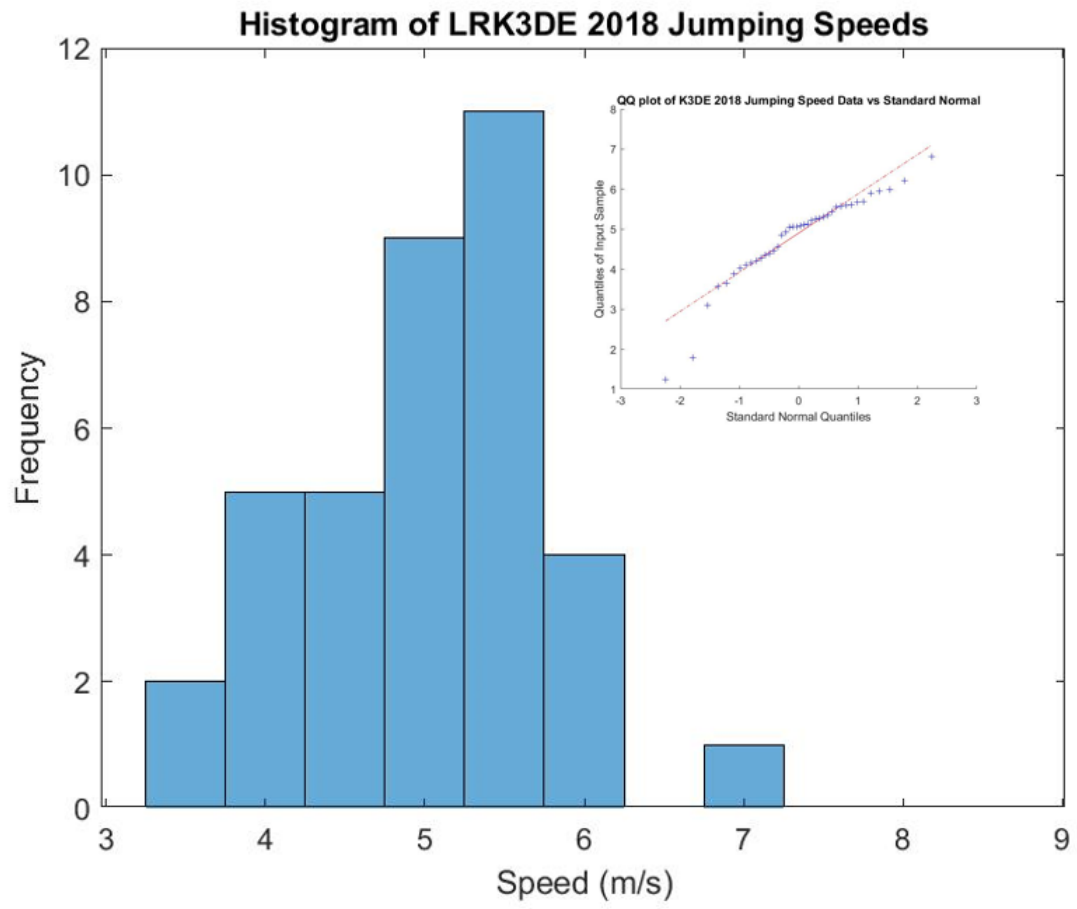
```

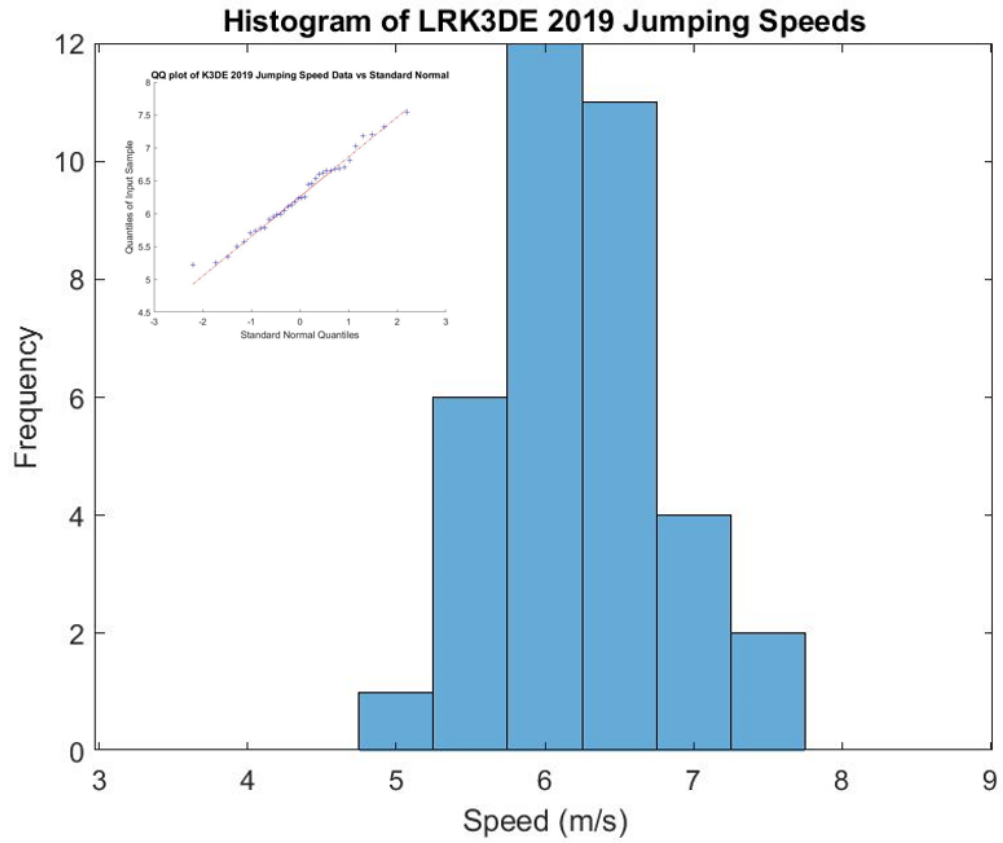
%%Cross product
function k=cross2(v1, v2)
k=v1(:,1).*v2(:,2)-v2(:,1).*v1(:,2);

```

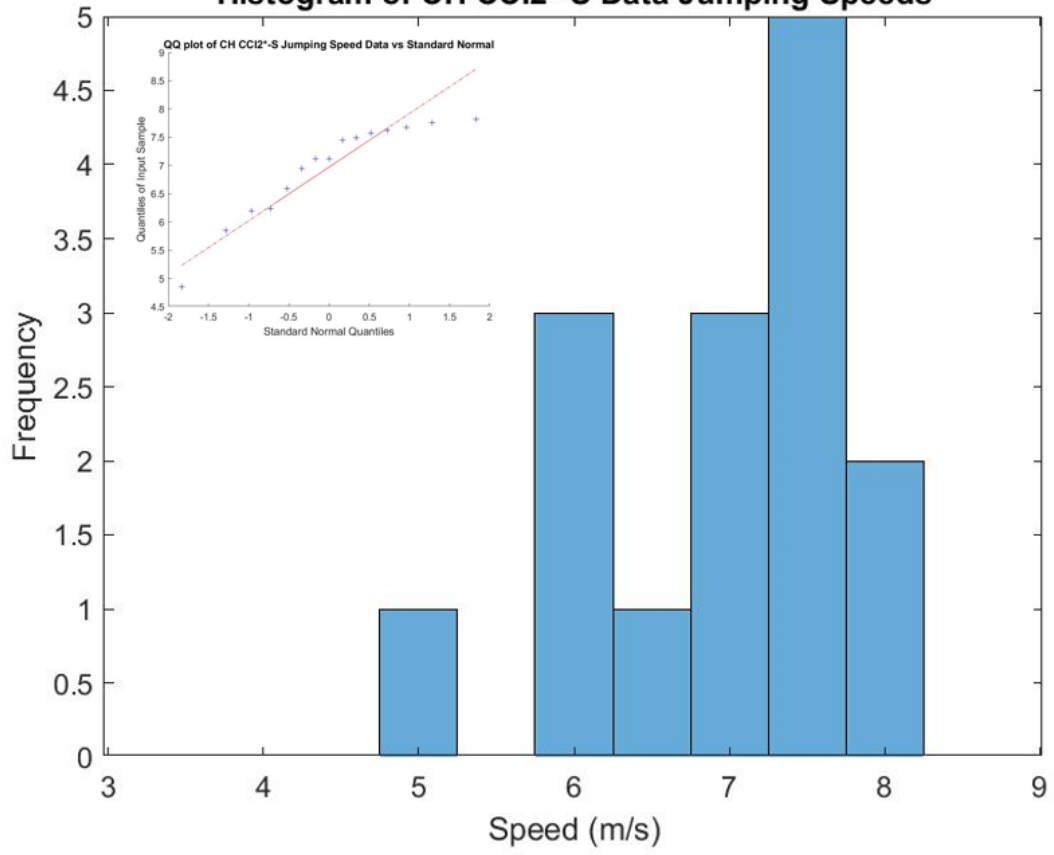
APPENDIX C: JUMPING SPEED HISTOGRAMS AND QQ PLOTS

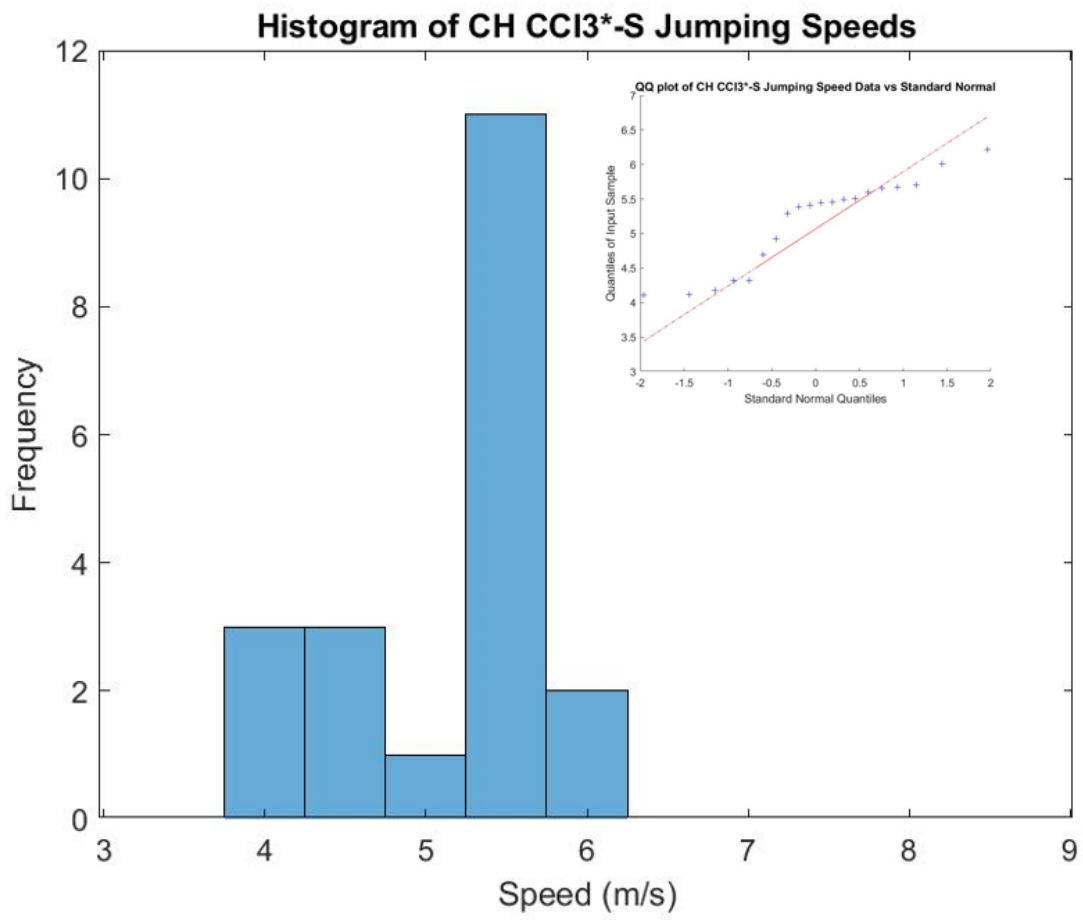




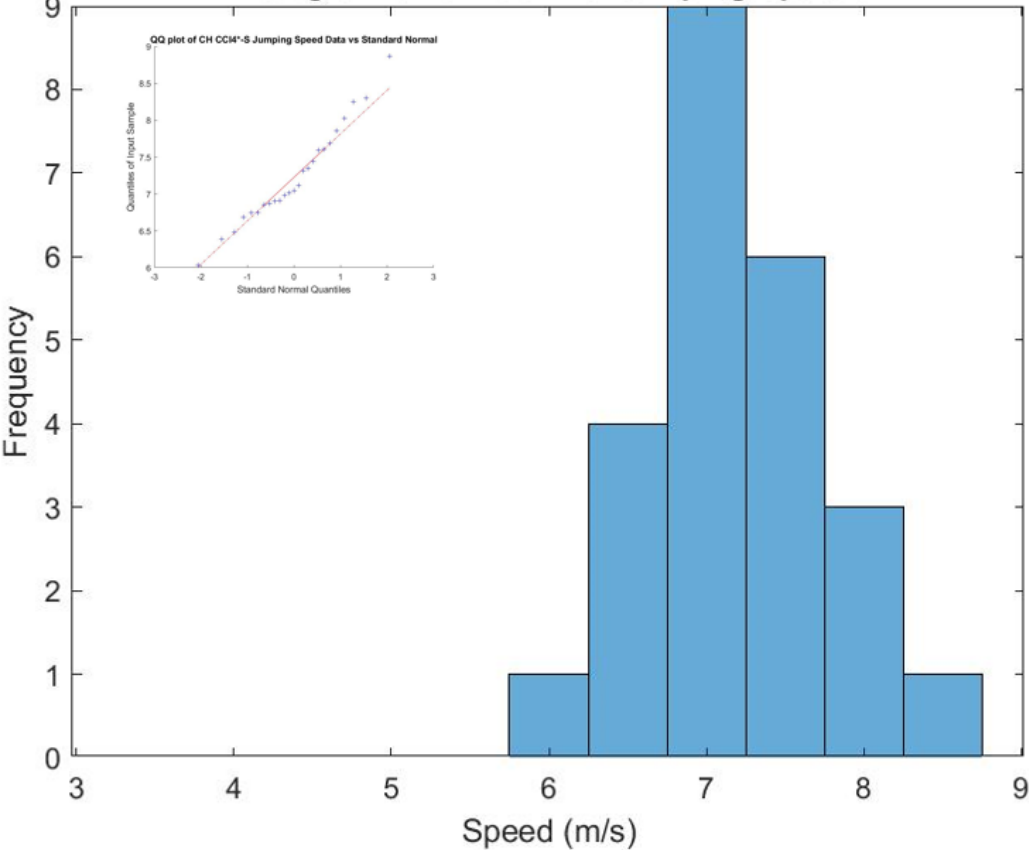


Histogram of CH CCI2*-S Data Jumping Speeds

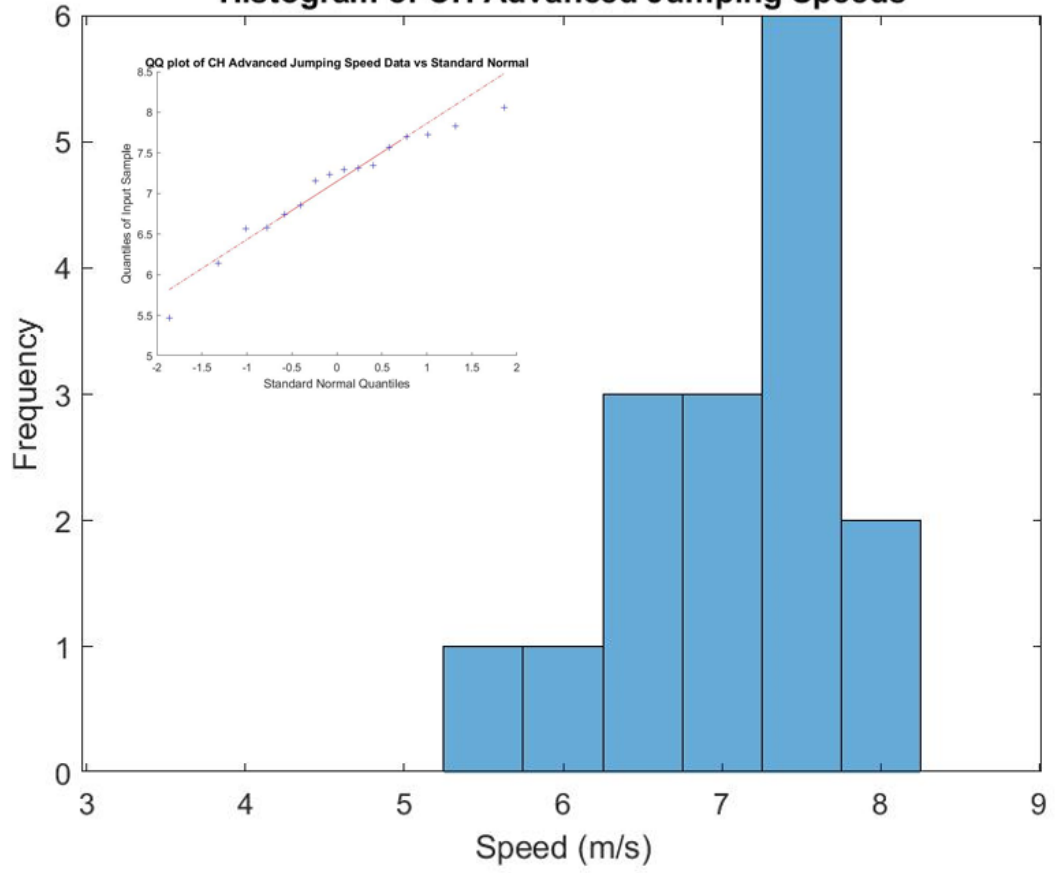


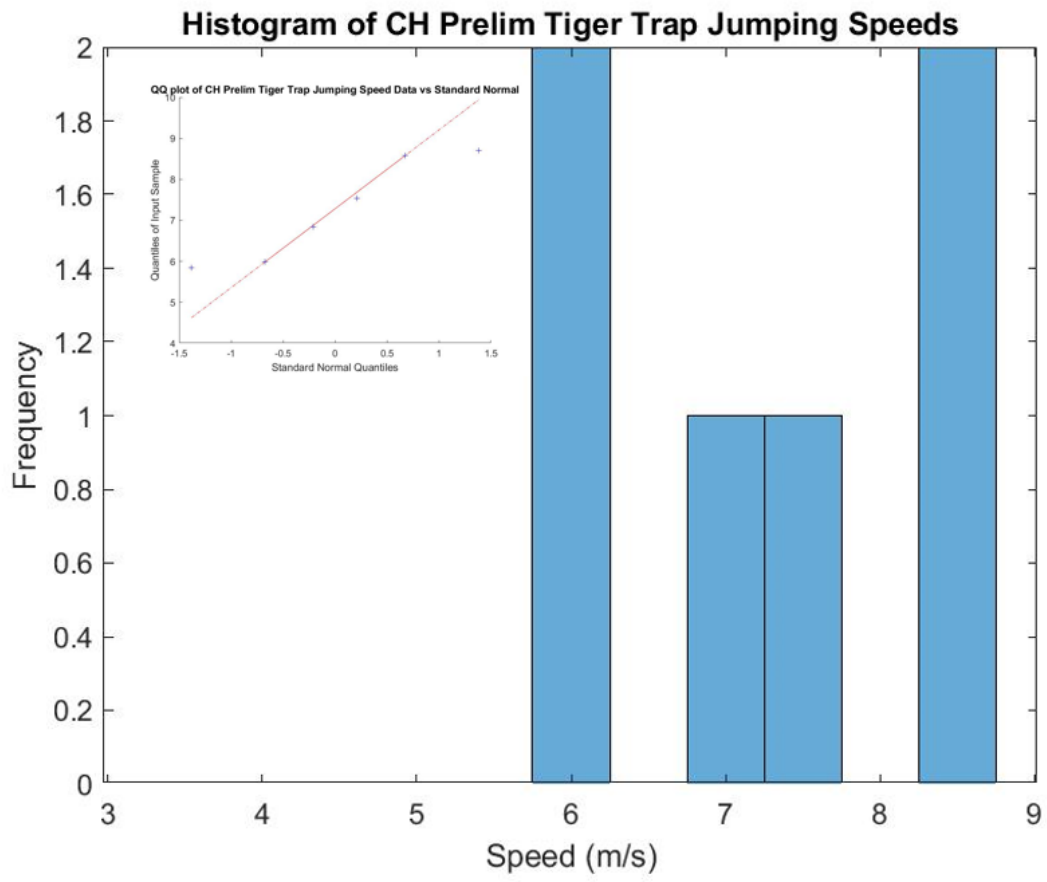


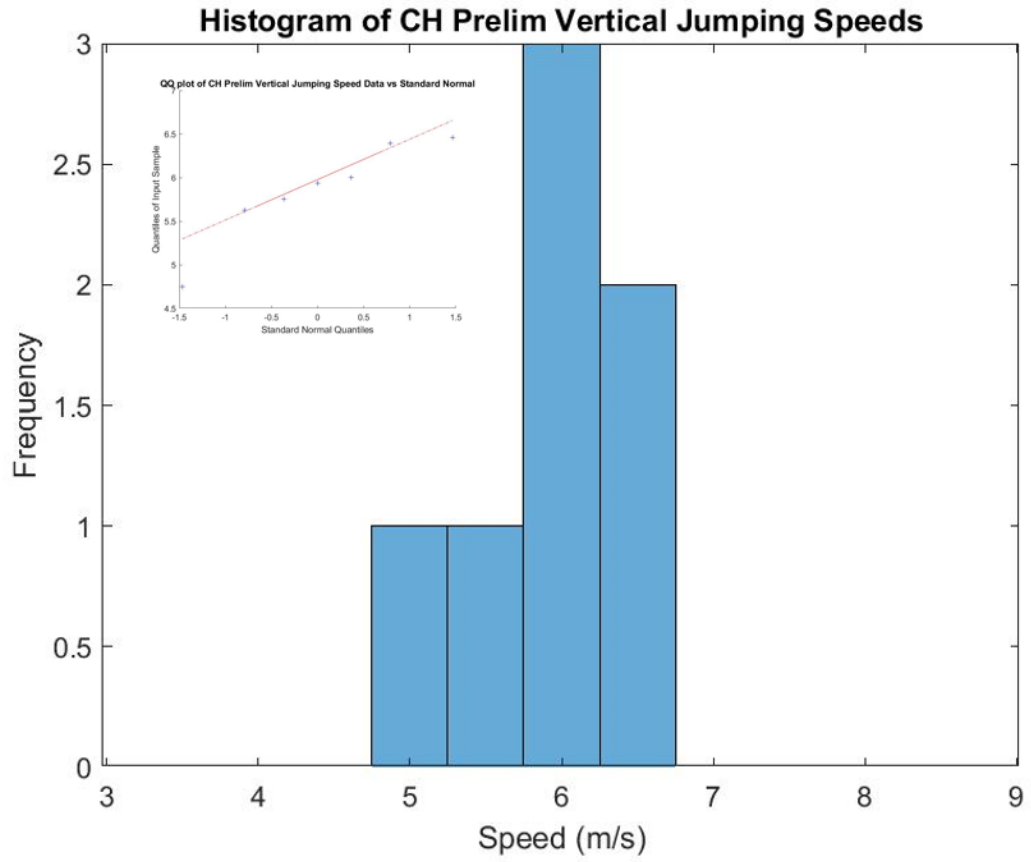
Histogram of CH CCI4*-S Jumping Speeds



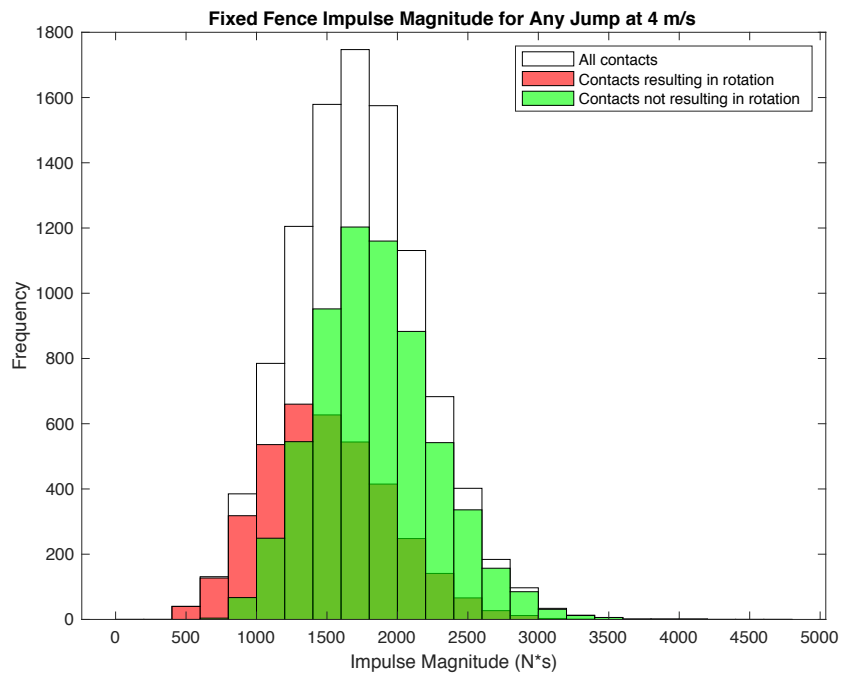
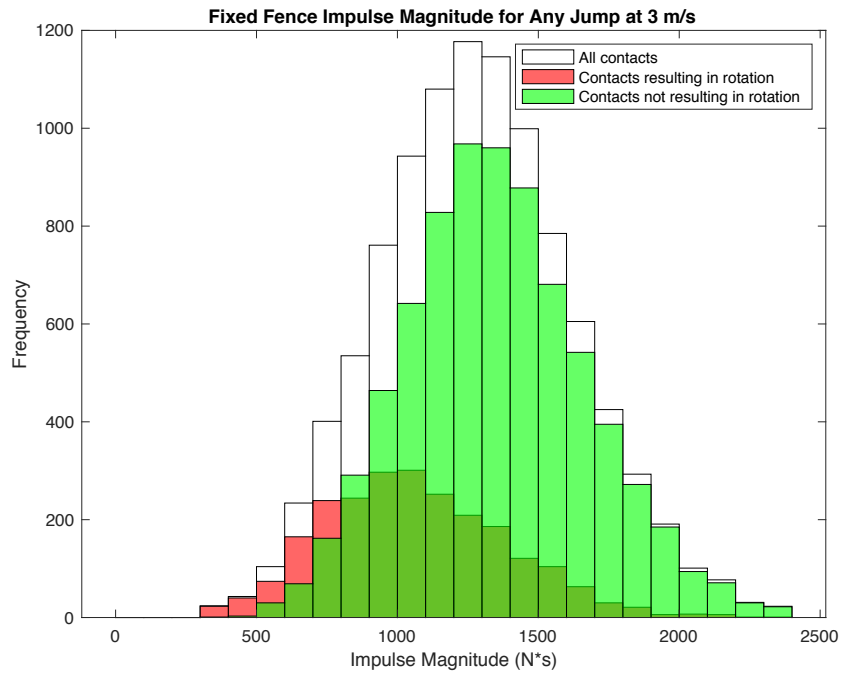
Histogram of CH Advanced Jumping Speeds

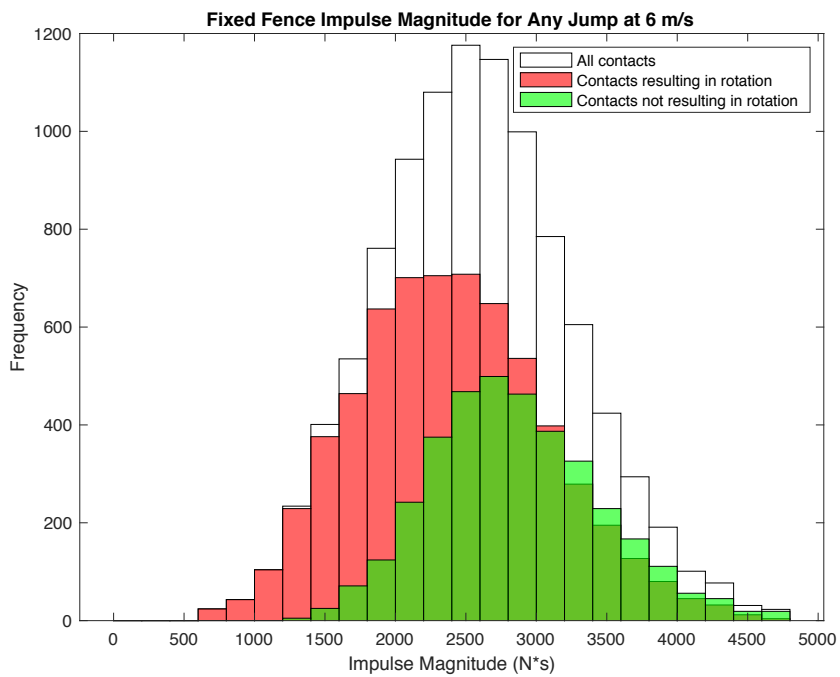
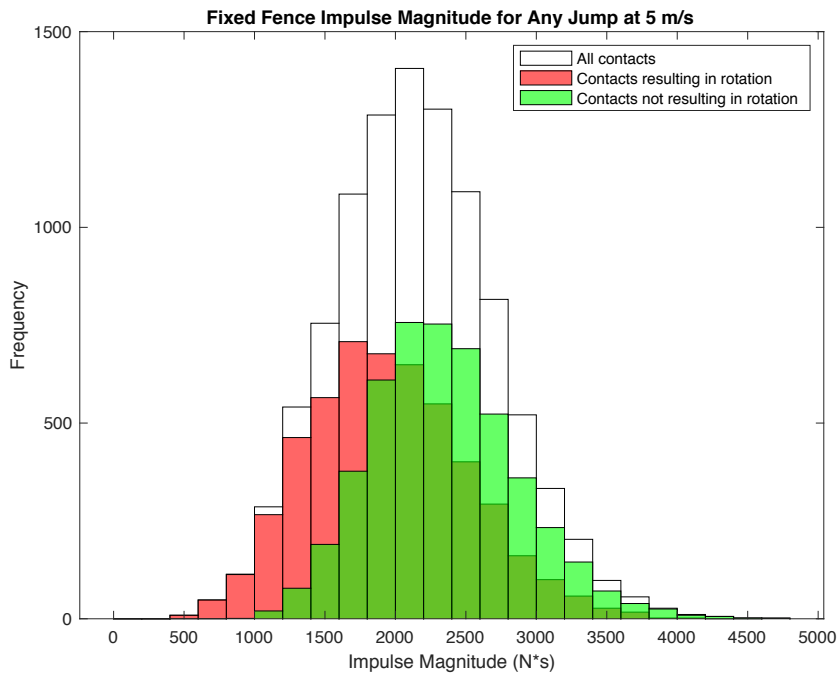


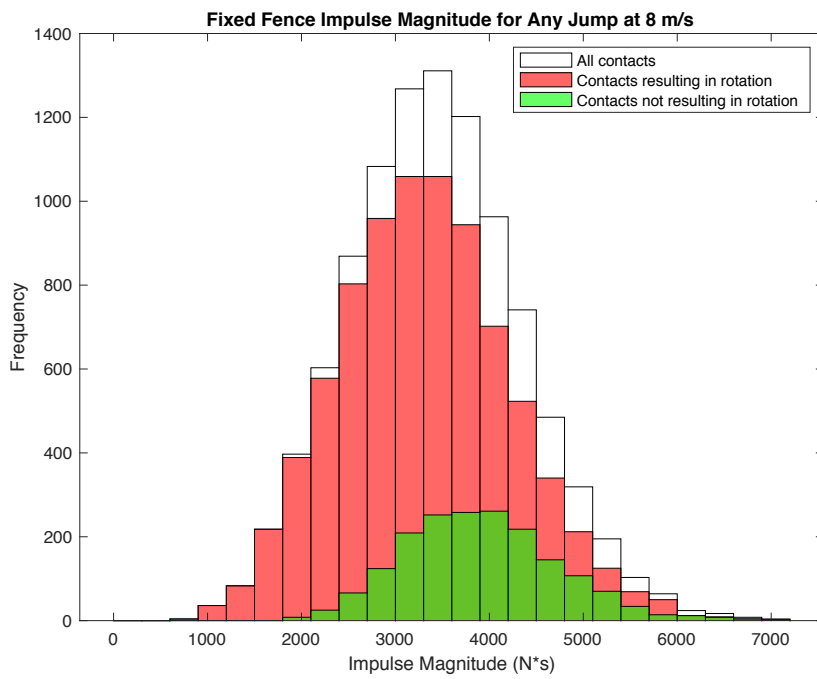
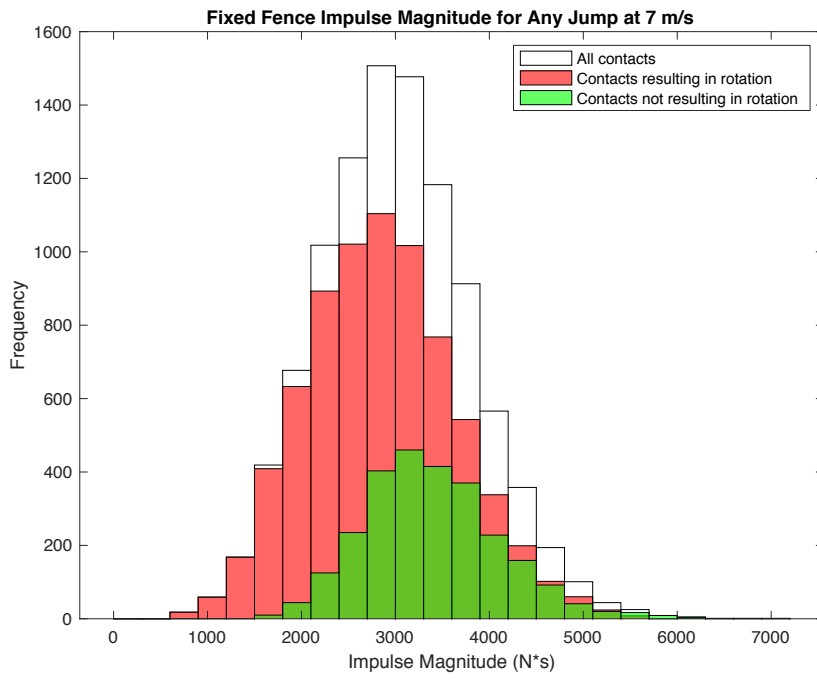


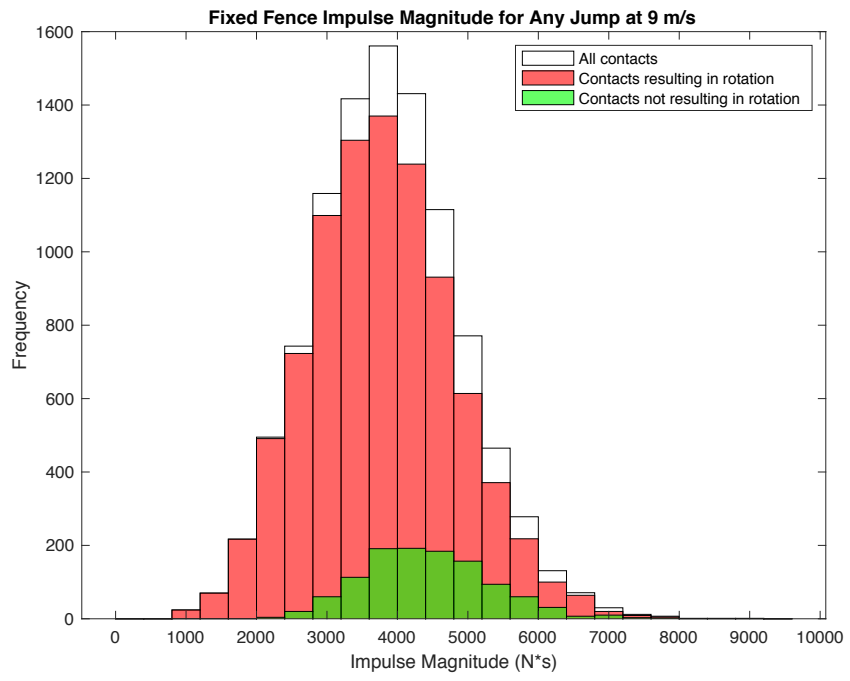


APPENDIX D: IMPULSE MAGNITUDE HISTOGRAMS FOR LRK3DE 2018 FENCE 4

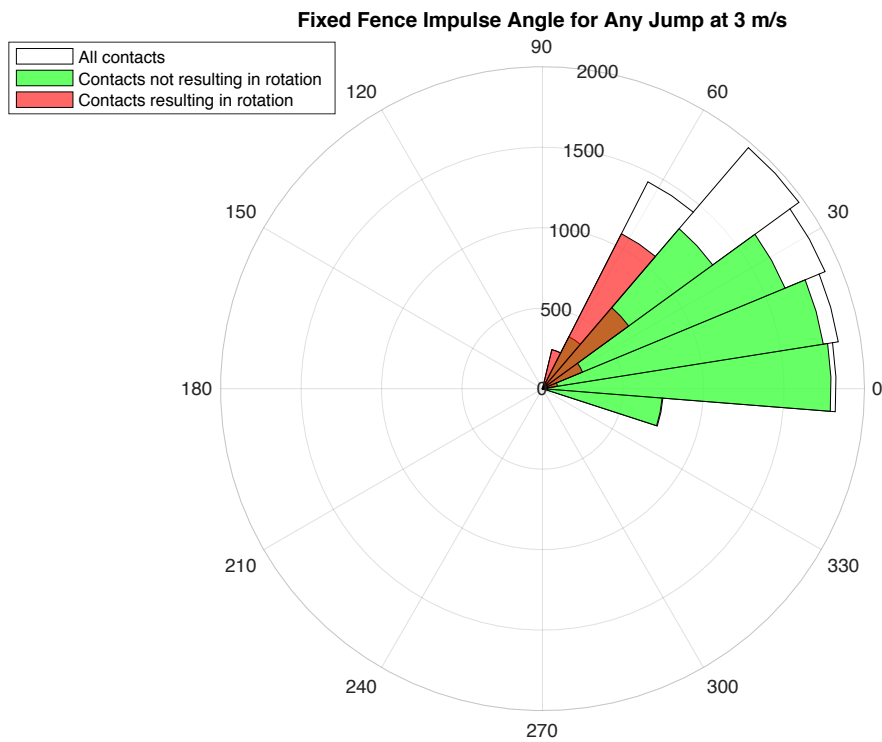
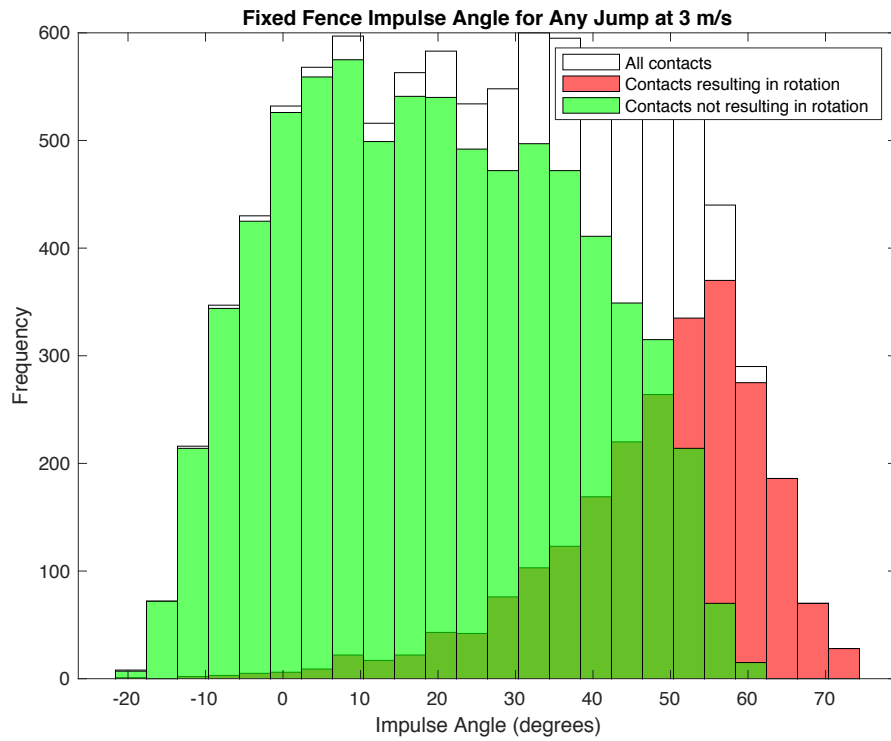


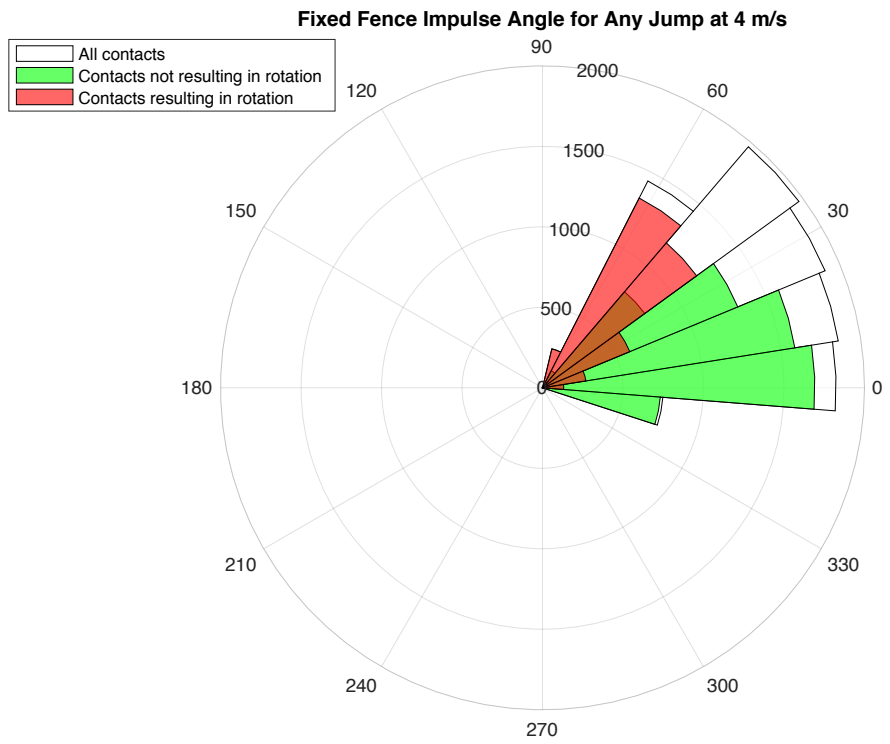
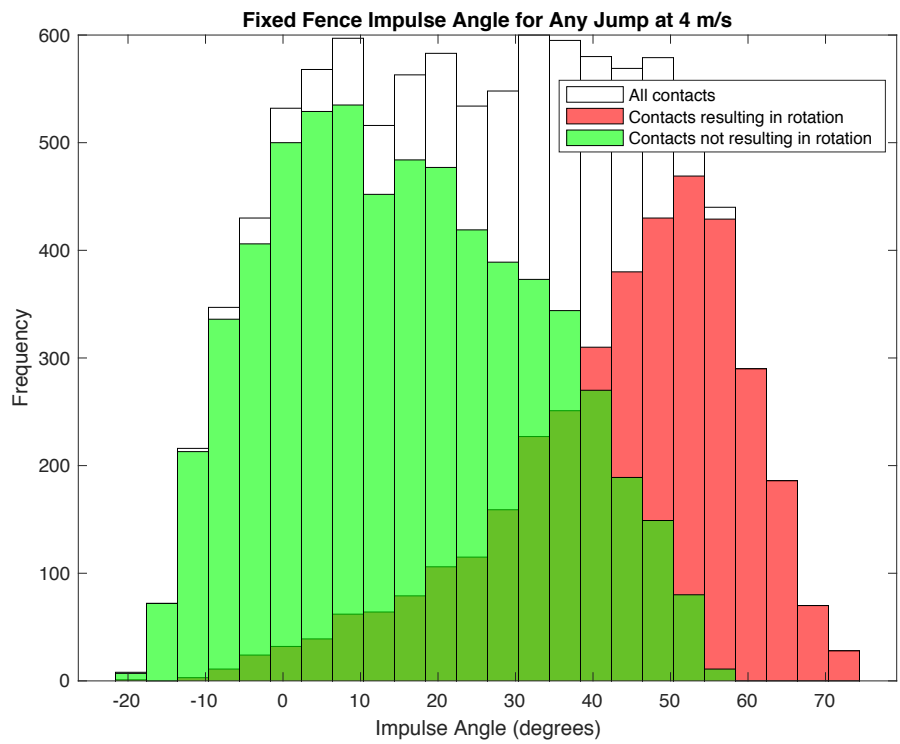


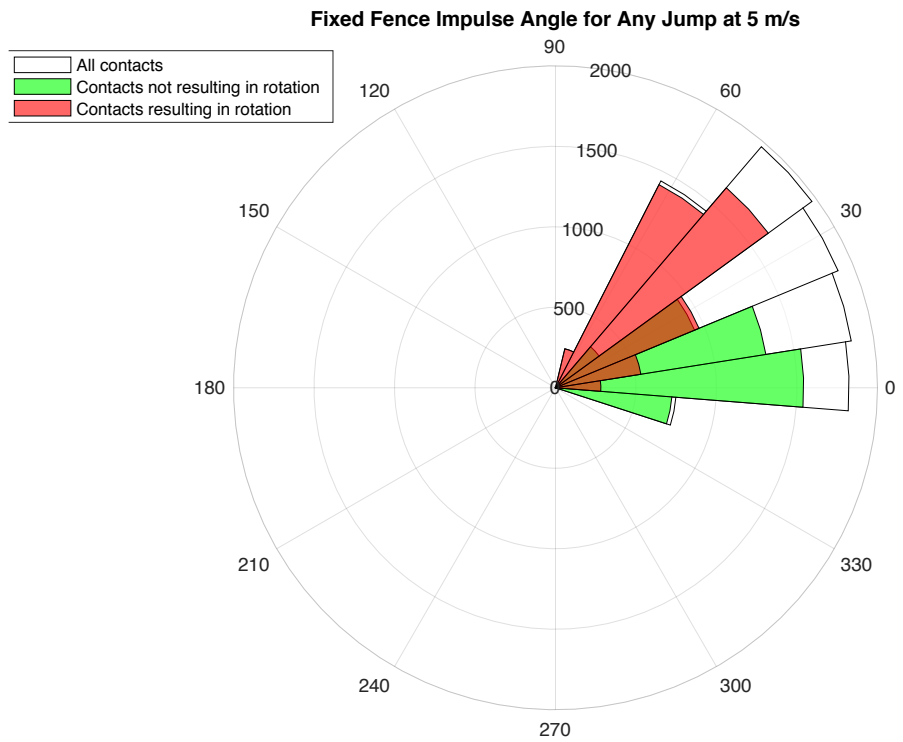
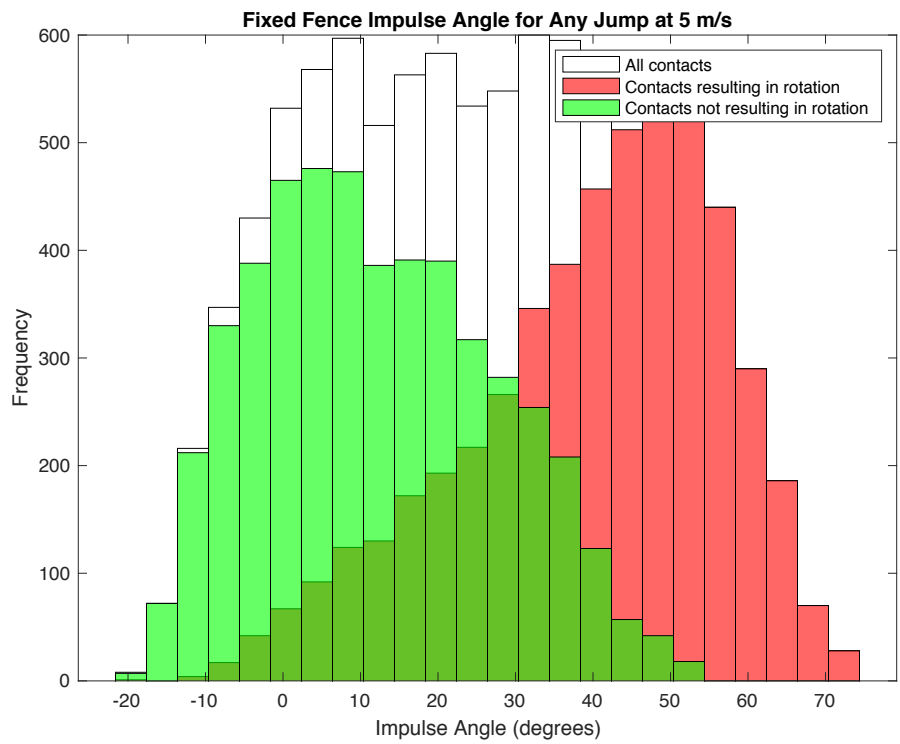


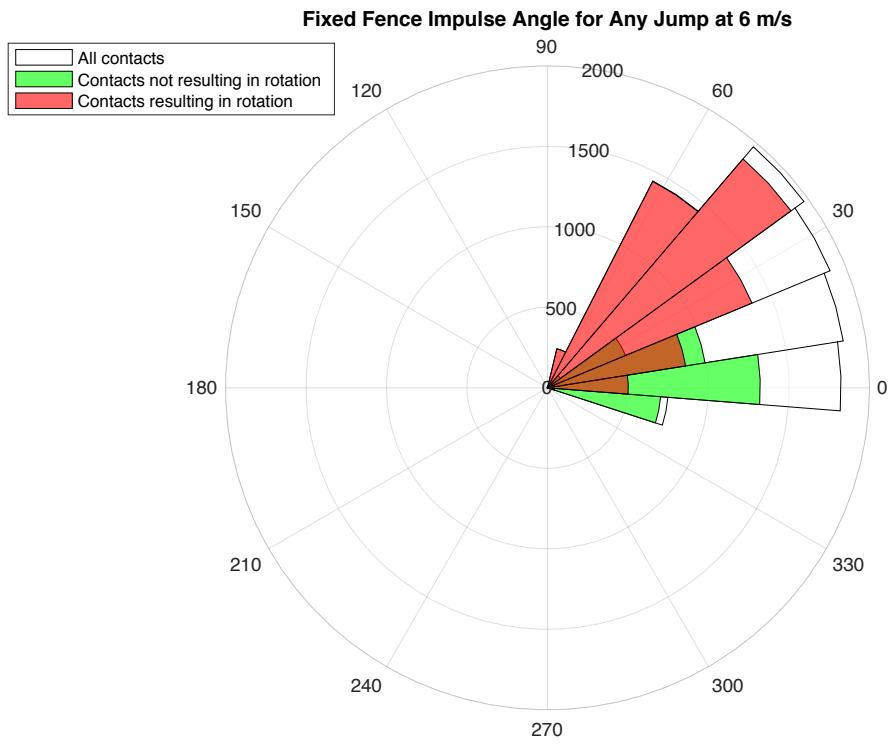
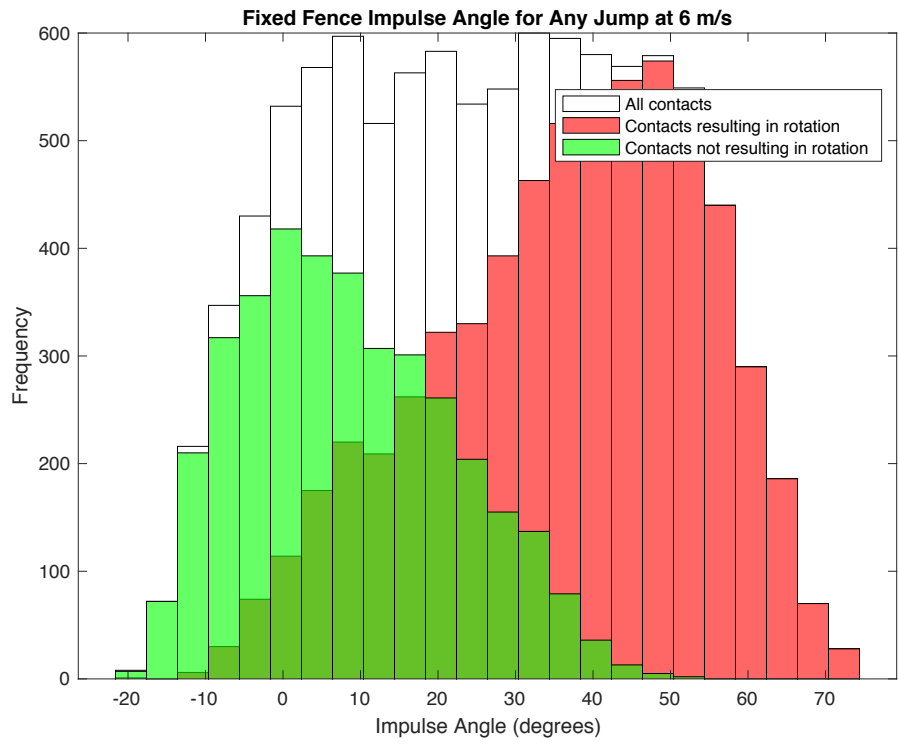


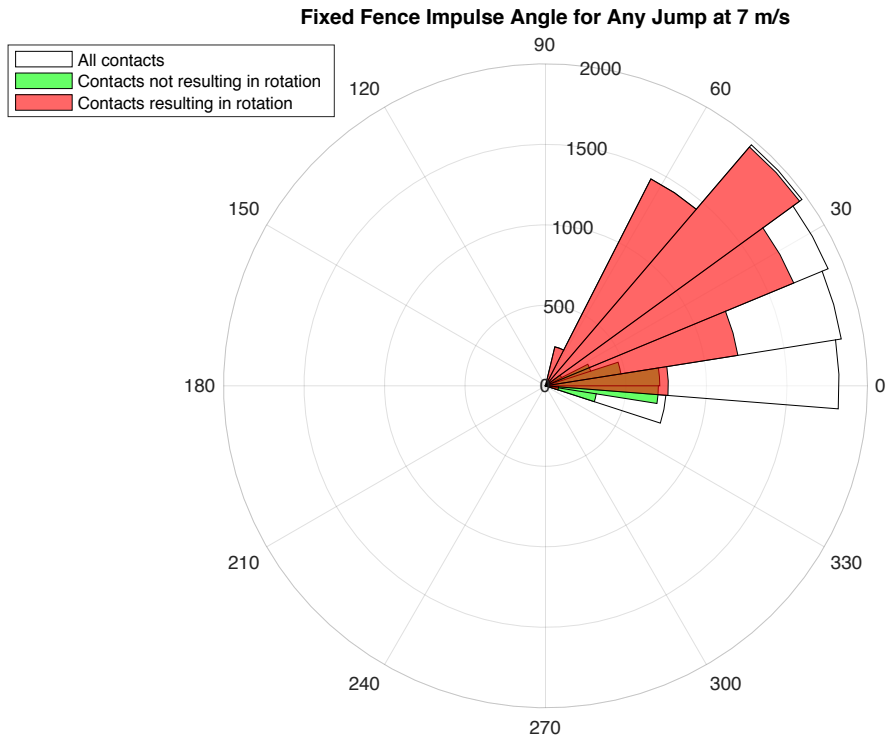
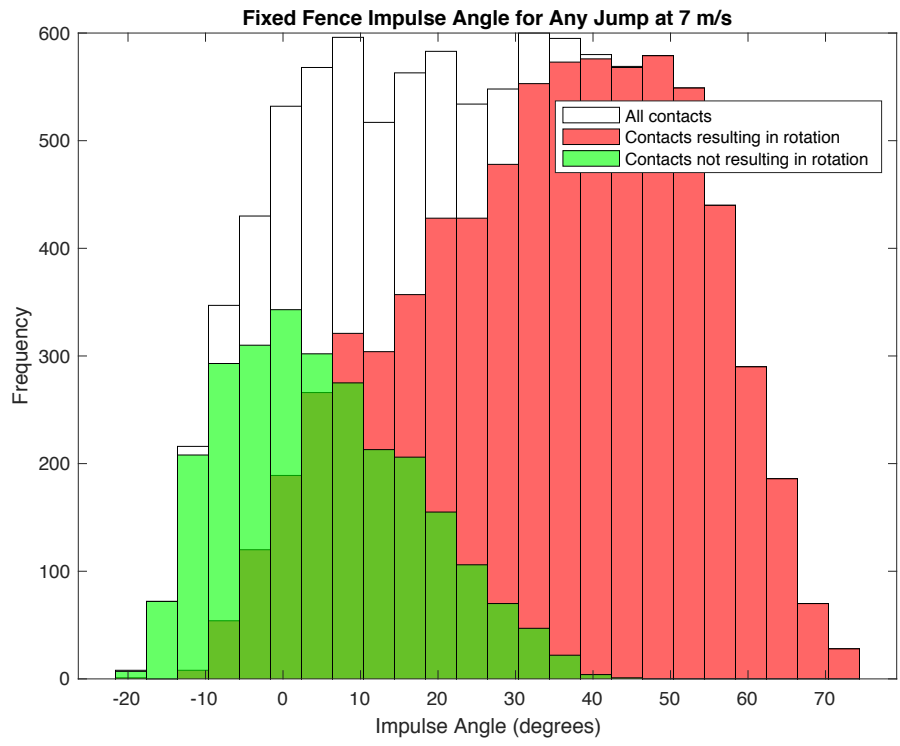
APPENDIX E: IMPULSE ANGLE HISTOGRAMS FOR LRK3DE 2018

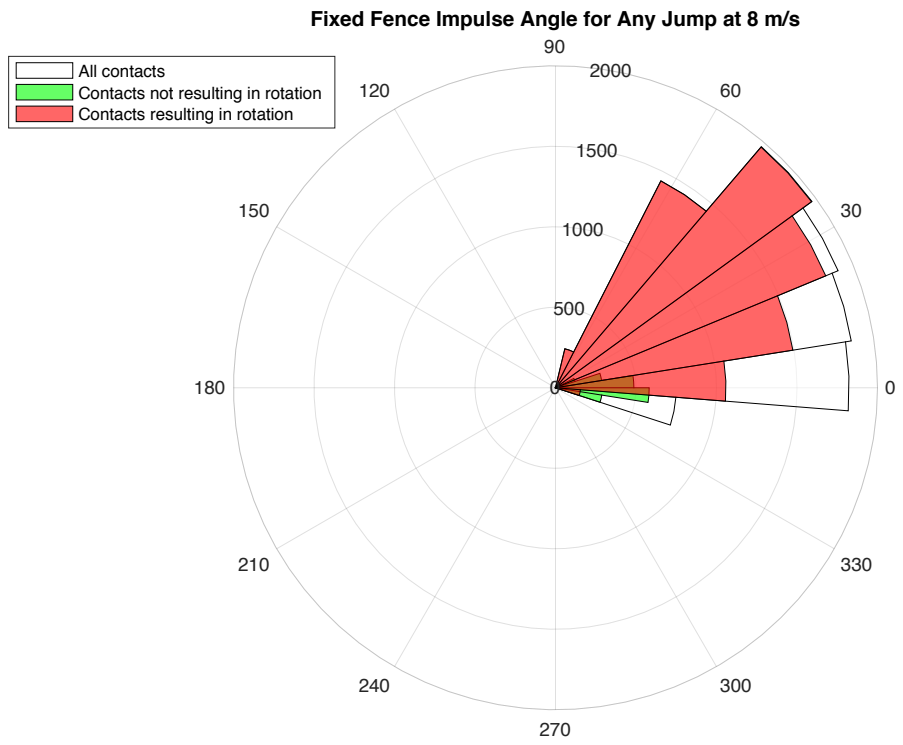
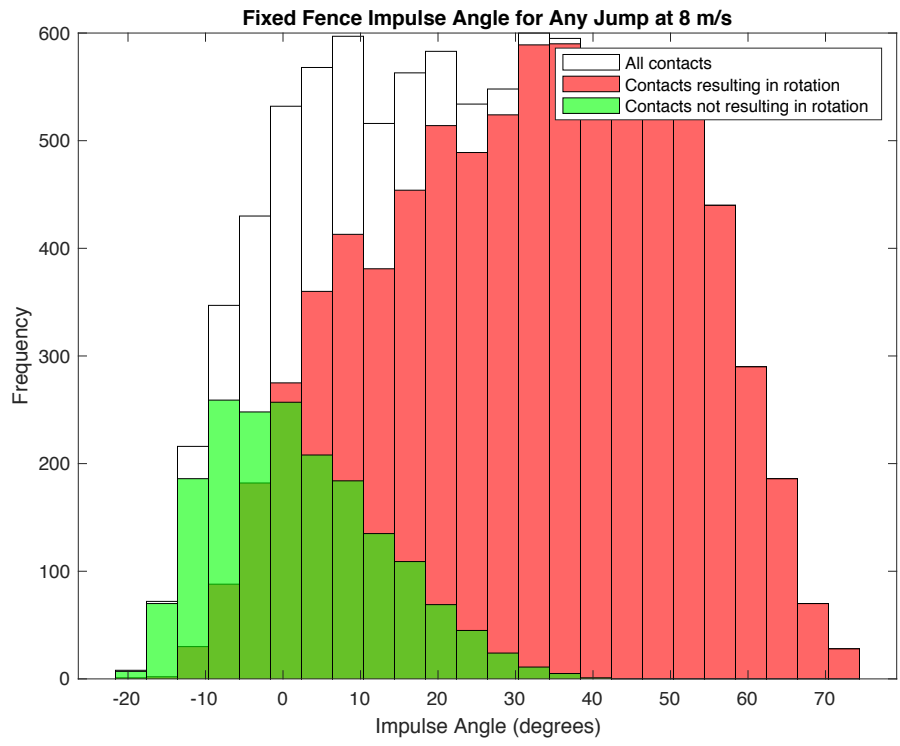


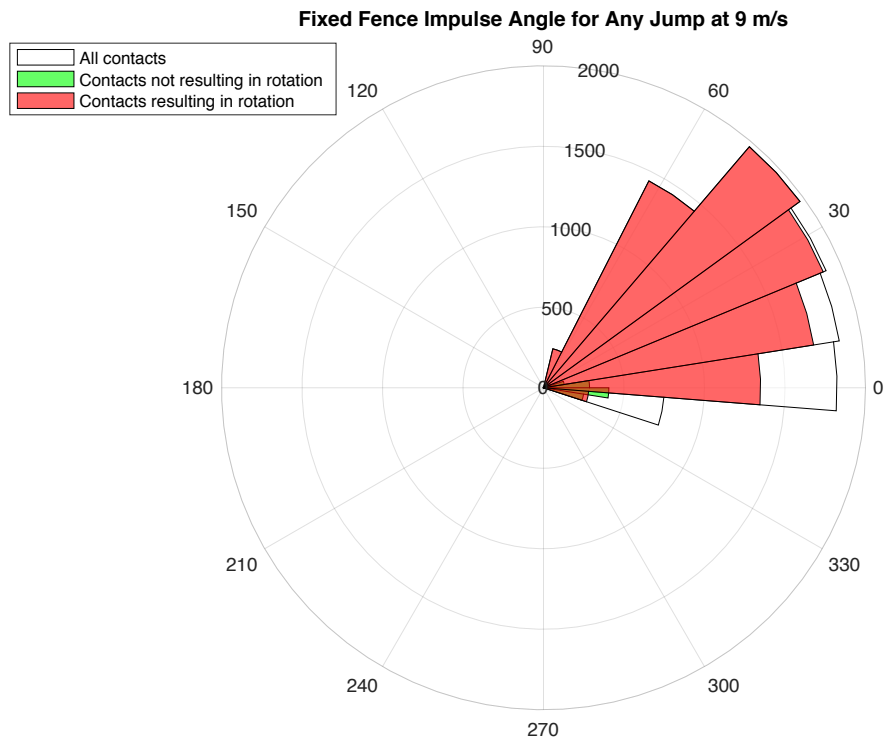
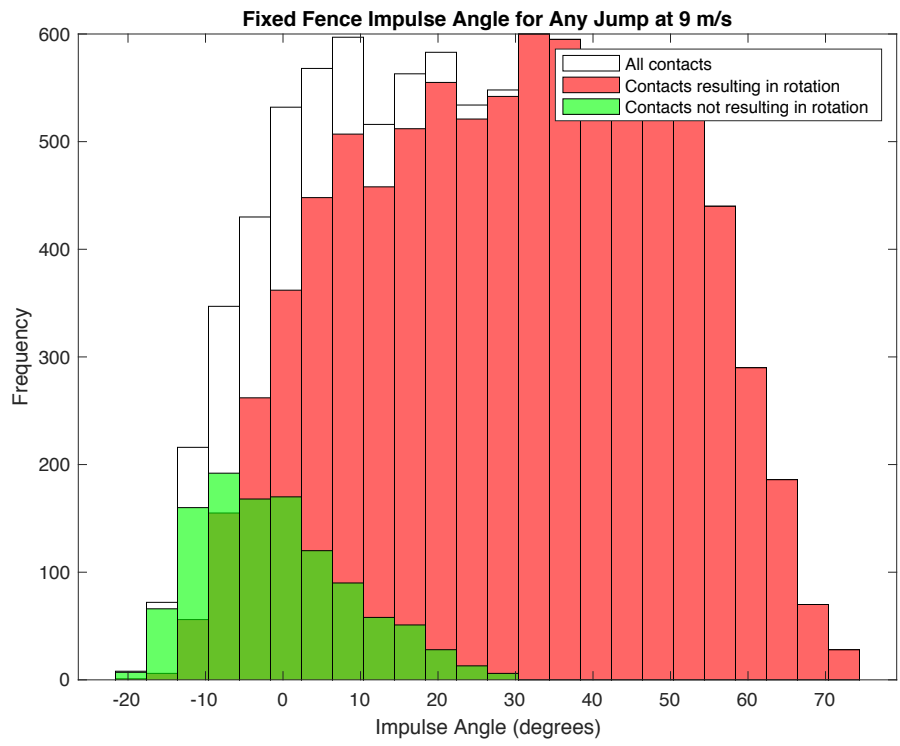












REFERENCES

- [1] J. K. Murray, “An epidemiological study of the risk factors falls horses in the of associated with and riders sport of eventing,” 2004.
- [2] A. Mellor, “Synopsis of Frangible Fence Project.”
- [3] Fédération Equestre Internationale, *Eventing rules*, no. effective 1st January 2019. 2019.
- [4] S. Kimmel-Smith, “A train wreck and the aftermath,” *Behind the Bit*, 2008.
- [5] “Grand National Fences and Course,” *GrandNation.org.uk*, 2019. [Online]. Available: <https://www.grandnational.org.uk/fences.php>.
- [6] J. Reason, “Human error : models and management,” *BMJ*, vol. 320, no. March, pp. 768–770, 2000.
- [7] Fédération Equestre Internationale, “My FEI Guide,” 2019.
- [8] United States Eventing Association, “About Us,” 2019. [Online]. Available: <https://arcticathabaskancouncil.com/wp/about-us/>.
- [9] Fédération Equestre Internationale, “Eventing rules,” *Fei*, no. December 2017, 2018.
- [10] J. Duffy, “What the *****? The New FEI Star System Explained,” pp. 1–14, 2018.
- [11] J. Autry, “ERA Urges FEI Riders to Oppose 21 Penalty Rule,” *Eventing Nation*, pp. 1–15, 2015.
- [12] J. Autry, “FEI Revises Rule to Award 11 Penalties for Breaking Frangible Pins,” *Eventing Nation*, pp. 1–15, 2015.
- [13] USEF, *Chapter EV Eventing Division*. 2019.
- [14] FEI, “Risk Management Programme Statistics 2007 – 2018 CONTENTS,” 2018.

- [15] B. R. Paix, “Rider injury rates and emergency medical services at equestrian events,” *Br. J. Sports Med.*, vol. 33, pp. 46–48, 1999.
- [16] EquiRatings, “About Us: The EquiRatings Story,” 2019. .
- [17] I. Schuhmacher, “SAP Equestrian Analytics : Making Eventing Fans Part of the Ride,” *SAP*, 2016. .
- [18] J. K. Murray, E. R. Singer, F. Saxby, and N. P. French, “Factors influencing risk of injury to horses falling during eventing,” *The Veterinary Record*, vol. 228, pp. 207–208, 2004.
- [19] R. Stevenson, “Taking a Closer Look at Safety Statistics in Eventing,” *United States Eventing Association*, pp. 1–6, 2016.
- [20] J. Newton, “A Way Forward : How Eventing Can Use Established Strategies to Improve Safety,” *Eventing Nation*, 2016.
- [21] C. Barnett, N. Huws, J. Murray, and E. Singer, “An Audit into Eventing Incorporating an Analysis of Risk Factors for Cross Country Horse Falls at FEI Eventing Competitons,” 2016.
- [22] D. O’Brien and R. Cripps, “Safety for Horses and Riders in Eventing - The SHARE database -,” 2008.
- [23] FEI, “Eventing Risk Management Programme Statistics 2006-2016,” vol. 2015, pp. 1–25, 2016.
- [24] Institut für Kraftfahrzeuge Aachen, “Test Procedure,” 2018.
- [25] Jump For Joy, “FEI Safety Cup - 20mm,” 2020. .
- [26] D. Starck and L. Starck, “An Introduction to Frangible Fences,” no. 618, 2009.
- [27] G. Naber, “Dutch Eventing – Dutch Pole Update.”

- [28] J. Thier, “Prologs at Glanusk Horse Trials,” *Eventing Nation*, 2010.
- [29] J. Melissen, P. den Hartog, and J. Venhorst, “Eventing Safety Forum January 19th 2008 Breakable Fence Pole,” 2008.
- [30] “Mimsafe NewEra Products,” 2019. .
- [31] MiMsafe NewEra, “MIMsafe New Era for safer obstacles at eventing,” 2019. .
- [32] M. (MiM C. A. Bijornetun, *Presentationm Safer Fence Maarsbergen*. 2015.
- [33] H. H. F. Buchner, H. H. C. M. Savelberg, H. C. Schamhardt, and A. Barneveld, “Inertial properties of Dutch Warmblood Horses,” *J. Biomech.*, vol. 30, no. 6, pp. 653–658, 1997.
- [34] G. R. Vega, “Simulation of Horse-Fence Interaction Affecting Rotational Falls in the Sport of Eventing,” University of Kentucky, 2017.
- [35] K. M. Kahmann, “Engineering Sport Safety: a Study of Equestrian Cross Country Eventing,” 2010.
- [36] FEI, “Standard for the minimum strength of frangible/deformable cross country fences,” vol. v. 22, pp. 1–11, 2013.
- [37] United States Eventing Association, “Kettlebell Pendulum Test Setup,” 2019.
- [38] S. Nauwelaerts, W. A. Allen, J. M. Lane, and H. M. Clayton, “Inertial properties of equine limb segments,” *J. Anat.*, vol. 218, no. 5, pp. 500–509, 2011.
- [39] K. Kubo, T. Sakai, H. Sakuraoka, and K. Ishii, “Segmental Body Weight, Volume and Mass Center in Thoroughbred Horses,” *Japan J. Equine Sci.*, vol. 3, no. 2, pp. 149–155, 1992.
- [40] P. Galloux and E. Barry, “Components of the total kinetic moment in jumping horses,” *EQUINE Vet. J.*, vol. 23, pp. 41–44, 1997.

- [41] C. E. Clauser, "Moments of Inertia and Centers of Gravity of the Living Human Body," 1963.
- [42] P. Powers and A. Harrison, "Influences of a rider on the rotation of the horse–rider system during jumping," *Equine Comp. Exerc. Physiol.*, vol. 1, no. 1, pp. 33–40, 2004.
- [43] R. F. Chandler, C. E. Clauser, J. T. McConville, H. M. Reynolds, and J. W. Young, "Investigation of inertial properties of the human body," *Natl. Highw. Traffic Saf. Adm.*, no. March, pp. 1–169, 1975.
- [44] J. T. Eckner, J. S. Kutcher, and J. K. Richardson, "Pilot evaluation of a novel clinical test of reaction time in National Collegiate Athletic Association Division I football players.," *J. Athl. Train.*, vol. 45, no. 4, pp. 327–332, 2010.
- [45] S. Wood, "Citizen Science Survey for Inertial Parameters of Live Horses and Riders for Simulating Rotational Falls in Eventing," 2017.
- [46] H. M. Clayton, "Time-motion analysis of show jumping competitions," *J. Equine Vet. Sci.*, vol. 16, no. 6, pp. 262–266, 1996.
- [47] D. Lewczuk, K. Słoniewski, and Z. Reklewski, "Repeatability of the horse's jumping parameters with and without the rider," *Livest. Sci.*, vol. 99, no. 2–3, pp. 125–130, 2006.
- [48] Clayton H.M. and D.A.Barlow, "Stride Characteristics of Four Grand Prix Jumping Horses," *Equine Exerc. Physiol.*, vol. 3, no. January 1991, pp. 151–157, 1991.
- [49] C. Fercher, "The Biomechanics of Movement of Horses Engaged in Jumping Over Different Obstacles in Competition and Training," *J. Equine Vet. Sci.*, vol. 49, pp.

69–80, 2017.

- [50] H. M. Clayton, “Effect of added weight on landing kinematics in jumping horses.,” *Equine Vet. J. Suppl.*, vol. 36, no. 23, pp. 50–53, 1997.
- [51] D. P. Moore, N. R. Deuel, S. Drevemo, and A. J. van den Bogert, “Kinematic analysis of world championship three-day event horses jumping a cross-country drop fence,” *J. Equine Vet. Sci.*, vol. 15, no. 12, pp. 527–531, 1995.
- [52] T. Kaichi *et al.*, “Image-based center of mass estimation of the human body via 3D shape and kinematic structure,” *Sport. Eng.*, vol. 22, no. 17, 2019.
- [53] T. Deans and M. Herbert, “British Eventing Safety Research,” 2010.
- [54] L. Murray, “Glanusk Junior Championships CCI* Rotational Horse Fall. Horse and Rider walked away unhurt!,” 2011. [Online]. Available: <https://www.youtube.com/watch?v=vbhDw9ELVJc>.
- [55] Dana NYB, “Tragödie um Benjamin Winter,” 2014. .
- [56] Boyd Martin, “Boyd Martin Fall At Badminton 2016.,” 2017. [Online]. Available: <https://www.youtube.com/watch?v=U69seMFNLpU>.
- [57] R. Ramsden, “Eventing in the Digital Age Updating of the FEI Eventing Fence Data.”
- [58] US Equestrian Federation, “2020 Eventing Human Accident/Injury Report Form.” 2020.
- [59] US Equestrian Federation, “2020 Equine Accident/Injury/Collapse Report Form.” .
- [60] FEI, “FEI Fall Report Form 2019.” .
- [61] A. Flogård, “Testing of Force Limitation of Obstacles within Cross Country Eventing,” 2009.

- [62] A. Flogård, “A Study of Means to Prevent Rotational Falls within Cross Country Eventing,” 2009.
- [63] United States Eventing Association and USCTA Course Design Committee, “Cross-Country Obstacle Design Guidelines.” 2018.

VITA

Shannon Wood earned a Bachelor of Science degree in Engineering Physics at Murray State University as a Presidential Fellow in 2017. Subsequently, she began the Masters of Mechanical Engineering at the University of Kentucky as a research assistant and later, a teaching assistant. Funding for Shannon was provided by the United States Eventing Association (2017-2018) and the University of Kentucky Department of Mechanical Engineering (2018-2020).